ARMY RESEARCH LABORATORY

COMBIC, Combined Obscuration Model for Battlefield Induced Contaminants:

Volume 2—Appendices

Alan Wetmore and Scarlett D. Ayres

ARL-TR-1831-2 August 2000

The findings in this report are not to be construed as an official Department of the Army position unless so designated by other authorized documents.

Citation of manufacturer's or trade names does not constitute an official endorsement or approval of the use thereof.

Destroy this report when it is no longer needed. Do not return it to the originator.

Army Research Laboratory

Adelphi, MD 20783-1197

ARL-TR-1831-2 **August 2000**

COMBIC, Combined Obscuration Model for Battlefield Induced Contaminants:

Volume 2—Appendices

Alan Wetmore
Computational and Information Sciences Directorate

Scarlett D. Ayres
Survivabilty/Lethality Analysis Directorate

Abstract

Airborne dust, smoke, and debris can significantly degrade a battlefield environment and affect electro-optical systems. The most direct effect of these combat-induced aerosols on a propagating electromagnetic signal is to remove energy (reduce transmission) through absorption and scattering. Reduced transmission through inventory smokes and dust is generally most significant at visual and infrared wavelengths and less severe at millimeter wavelengths.

Obscurant concentrations can change rapidly in a combat environment. Once generated, an aerosol cloud moves with the wind, undergoes thermally buoyant rise, and expands in the atmospheric turbulence. Thus, prevailing winds, aerosol generation factors, and the geometry of targets, observers, and aerosol clouds are important in determining transmission.

The Combined Obscuration Model for Battlefield Induced Contaminants (COMBIC) predicts time and spatial variations in transmission through dust and debris raised by high-energy explosives and by vehicular movement; smoke from phosphorus and hexachloroethane munitions; smoke from diesel oil fires; generator-disseminated fog oil and diesel fuel; and other screening aerosols from sources defined by inputs. COMBIC has been designed primarily for large scenarios where many different obscuration sources are present and where many observer-target lines of sight (LOS) must be treated simultaneously.

This document has been developed to provide both a technical description of the physics used in the COMBIC model and to serve as an operations guide for users of the COMBIC software.

Contents

Figures

Tables

Volume 2

Appendix A. Transport and Diffusion Models in COMBIC

Contents

Figures

Tables

This appendix contains detailed descriptions of the physics and computational techniques used in the COMBIC model. It will be of interest to people wishing to extract routines from COMBIC for use in other models and others wishing a deeper understanding of how physical processes influence the outputs of the COMBIC model.

The Gaussian representations of the plumes and puffs used to describe the clouds are explained, as well as the way the mass of obsurants is tracked. The appendix explores both the Phase I descriptions of the time evolution of the clouds and the calculations of transmission values for particular lines of sight (LOS's) performed in Phase II.

The links among weather conditions, terrain influences, and stability categories with the COMBIC dispersion model are explained in section A-3. Section A-4 describes the buoyancy calculations that determine how the warm plumes rise upward. Finally, section A-5 describes the process that COMBIC uses to arrive at a Pasquill stability category from the weather conditions that the user supplies.

A-1 Cloud Descriptions: The Phase I Output File

COMBIC describes obscurant clouds as combinations of subclouds. Each subcloud is defined as either a single Gaussian puff or as a continuous Gaussian plume. COMBIC further distinguishes subclouds as buoyant or nonbuoyant, depending upon whether heat is released into the cloud during the formation process.

A Gaussian puff is an ellipsoidal volume with concentration that is greatest at its center (x_c, y_c, z_c) and decreases with distance according to scaling lengths (σ_x, σ_y, σ_z). The concentration at any point (x, y, z) relative to a Gaussian puff centered on (x_c, y_c, z_c) and containing a total mass of obscurant M (Sauter and Hansen, 1990) is then

$$C(x, y, z) = \frac{M}{(2\pi)^{3/2}\sigma_x\sigma_y\sigma_z} e^{-D^2/2}, \tag{A-1}$$

where D is a dimensionless scaled distance:

$$D^2 = \left(\frac{x - x_c}{\sigma_x}\right)^2 + \left(\frac{y - y_c}{\sigma_y}\right)^2 + \left(\frac{z - z_c}{\sigma_z}\right)^2. \tag{A-2}$$

In general, COMBIC allows for a scavenging coefficient δ for the removal of mass by deposition or evaporation. Evaporation of volatiles can still result in some long-term nonvolatile component f_d of the original mass, however. Then M becomes time dependent:

$$M(t) = M[f_d + (1 - f_d)e^{-\delta t}]. \tag{A-3}$$

The Gaussian ellipsoid may also be rotated so that its principal axes no longer lie along the x, y, and z directions. This "canting" of a cloud is useful in modeling the tilted stem of a dust cloud produced by high explosive (HE). The canting rotation in COMBIC is restricted to an angle Φ about the cross-wind y-axis, tilting the ellipsoid principal z-axis toward or away from the downwind x-axis. A full description of the Gaussian puff history is thus the set of values (M, δ, Φ, x_c, y_c, z_c, σ_x, σ_y, σ_z) defined with respect to the time since the munition began to burn. Figure A-1 displays the geometric meaning of these quantities. Note that the so-called radii of the puff are between two and three times larger than the σ values, depending on definition, and are not shown.

The continuous Gaussian plume is described by a similar concentration equation:

$$C(x_c, y, z) = \frac{\dot{m}}{2\pi\sigma_y\sigma_z\mu} \exp\left[-\frac{1}{2}\left[\left(\frac{y-y_c}{\sigma_y}\right)^2 + \left(\frac{z-z_c}{\sigma_z}\right)^2\right]\right] \qquad \text{(A-4)}$$

where μ is the windspeed and $\dot{m}$ is the time rate of obscurant production that applies at the location (x_c, y_c, z_c).

Although it appears as simple as the concentration equation for the Gaussian puff, the concentration of the Gaussian plume is complicated by the fact that the variables depend on the downwind distance x_c from the source, as well as on time. Figure A-2 shows the relevant geometry of the plume parameters. In principle, the cloud history would, therefore, require a two-dimensional, space-time array of (y_c, z_c, σ_y, σ_z, μ, $\dot{m}$, δ) values for an appropriate two-parameter table of x_c and t values.

However, with the aid of simplifying assumptions, these potentially huge tables can be reduced considerably in size. First, the array of downwind table entries, or grid points, does not need to be equally spaced. In fact, the expansion and rise of the plume change more rapidly near the source and more slowly at great distances downwind.

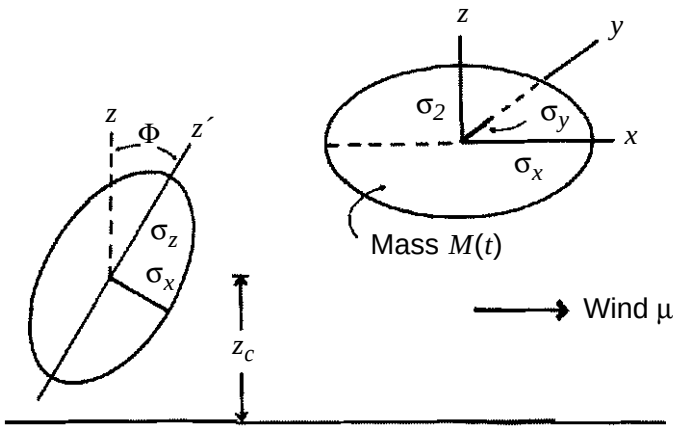

Figure A-1. Parameters that describe a Gaussian puff.

Figure A-2. Parameters that describe a Gaussian plume.

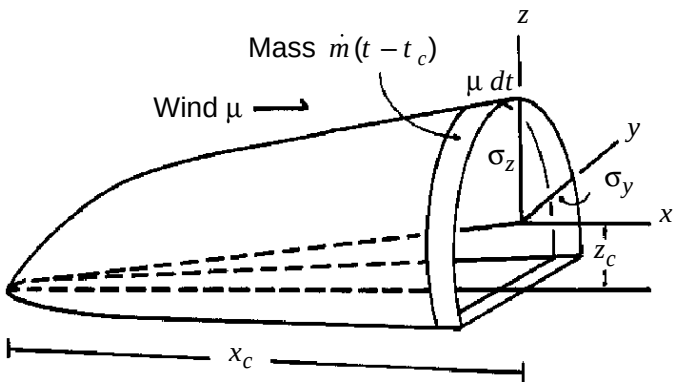

Gaussian diffusion models have been handicapped in the past by the use of empirical power laws to establish the orthogonal dispersion lengths. As discussed in more detail in section A-3, the diffusion sigmas and the vertical rise of the centerline (y_c, z_c) for puffs should not be represented in a fixed Eulerian system, but in a Lagrangian representation based upon a moving coordinate system.

The functional dependence of these quantities on x_c permits them to be written in converging Taylor series. For example, expanding σ about x_c produces

$$\begin{aligned}\sigma(x) &= \sigma(x_c) + \frac{d\sigma(x)}{dx}\bigg|_{x=x_c}(x - x_c) + \frac{d^2\sigma(x)}{dx^2}\bigg|_{x=x_c}\frac{1}{2}(x - x_c)^2 + \ldots \\ &= \sigma(x_c) + \left[1 + B\left(\frac{x - x_c}{x_c}\right) + \frac{1}{2}B(B-1)\left(\frac{x - x_c}{x_c}\right)^2 + \ldots\right]. \qquad \text{(A-5)}\end{aligned}$$

This expansion, and a similar one for z_c, represents one way to use exact values given at a series of grid points, x_c, to find approximate values between the grid points. Clearly, if x is sufficiently close to x_c, then terms higher than the first power in $(x - x_c)$ can be neglected. Specifically, assume that the absolute value of $(x - x_c)/x_c$ is kept smaller than some chosen value, say 0.06. It can be shown that linear interpolation between a grid of x_c values satisfying this condition will be quite accurate. This implies that the grid should be chosen with a spacing that increases with larger downwind distances x_c.

Previous versions of COMBIC used a downwind distance grid in which each new interval is a factor of 1.123 wider than the previous interval. That allowed the range from 50 m downwind to 5800 m downwind to be covered by just 41 grid points. Arbitrary points were chosen for the range of 0 to 50 m downwind. However, to apply the Romberg method of integration, the user must tabulate the downwind distance x in each subcloud trajectory at values such that a simple transformation of the downwind distances will

be equally spaced. The values tabulated in COMBIC (done in Phase I) satisfy this requirement for $x \geq 49.85$. The function is $x = (49.85)(1.123)^{n-10}$. But for $x < 49.85$ an exponential function will not approach zero in a finite number of steps. What is required is a power function of the form n^p that will "spline" with the exponential function at the breakpoint; that is, both the power function and its first-order derivative must agree with those of the exponential function at the breakpoint. This can best be accomplished by

$$x = n^{1.508352871} \text{ for } n < 13 . \quad \text{(A-6)}$$

$$x = (47.887223) \cdot (1.123026355)^{n-13} \text{ for } n \geq 13 . \quad \text{(A-7)}$$

The first 15 tabulated values of the downwind distance by these formulas are shown in table A-1. The breakpoint is at n = 13, where x = 47.89. This modification requires a minor change in the tabulation of subcloud trajectories from the way they are done in COMBIC87, but it promises smoothness at the breakpoint. (This smoothness is desired to prevent the Romberg integration from indicating that the integrand has some peculiarity at the breakpoint.)

The COMBIC model uses a uniform wind direction everywhere in the scenario. In the plume reference frame, x is the downwind coordinate, and y is the cross-wind coordinate. Therefore, the y value for the centerline of the plume is a constant, and y can be eliminated from the cloud tables. Similarly, the deposition or evaporation coefficient is assumed constant. Thus, only the four variables (z_c, σ_y, σ_z, $\dot{m}$) must be tabulated. Of these, the mass production rate $\dot{m}$ depends only on time and on downwind distance from the source if an average, constant thermal production rate is assumed. The scaling for variable thermal production is discussed in section A-4.

The time required for an obscurant to move from the source to each downwind grid point is tabulated in Phase I. The cumulative mass production function is stored in a separate array SNW every second for burn times <900 s from ignition to the end of obscurant production. The cumulative

Table A-1. Downwind distance grid.

Index	Downwind distances	Index	Downwind distances
1	1.00	9	27.50
2	2.84	10	32.24
3	5.24	11	37.22
4	8.09	12	42.44
5	11.33	13	47.89
6	14.92	14	53.78
7	18.82	15	60.39
8	23.02		

production function $M(t)$ is determined from the production rate $\dot{m}$ by

$$M(t) = \int_0^t \dot{m}(t')\, dt'. \tag{A-8}$$

Tabulating the mass rate table (as a function of time after ignition) so that it is incremented every second (rather than the way it was done in COMBIC87 and earlier versions) results in several advantages. No searching is required, and interpolation time is decreased by up to 50 percent over the old method.

Assuming approximately 50 tabulated points for each of four parameters for the continuous plume (z_c, σ_y, σ_z, t) and up to 900 values stored in the ($\dot{m}$) SNWD and six parameters for the Gaussian puff (z_c, σ_x, σ_y, σ_z, t, d), COMBIC Phase I output files contain about 300 to 1200 entries per subcloud, depending upon the burn time. The amount of detail or the number of physically different regions in the cloud determines the number of subclouds. Up to five subclouds per cloud can be produced by COMBIC Phase I routines and accessed by COMBIC Phase II routines. For most obscurants, one subcloud is sufficient.

A-2 Path Integration Methods: Phase II Transmission Calculations

Assume that a history file or tables describing obscurant subcloud position, dimensions, and mass distribution have been generated. Then, given observer and target pairings, the object of Phase II calculations is to determine the transmittance between each pair. In this section, we derive the formulas used to rapidly find the concentration length (CL) integral for use in equation (1) in the main body of the report, repeated here:

$$T = e^{-\alpha C L},$$

where

T = transmittance,

α = extinction coefficient,

C = aerosol concentration (in grams per meter squared), and

L = is optical path length (in meters).

A-2.1 The Path Integral through Gaussian Puffs

COMBIC uses a fast analytic solution for path integrals through Gaussian puffs. The method treats the cases of target and/or observer inside the cloud and further tests for nonintersection early in the calculation process, thus providing a built-in cloud rejection technique. First, the derivation is given. Then an interpretation of the equations is given in terms of a geometric diagram.

The target–observer LOS is defined in terms of direction cosines:

$$\alpha = \frac{x_t - x_o}{R}, \quad \beta = \frac{y_t - y_o}{R}, \quad \gamma = \frac{z_t - z_o}{R}, \tag{A-9}$$

where (x_o, y_o, z_o) and (x_t, y_t, z_t) are observer and target coordinates. R is the range of the target from the observer:

$$R = \left[(x_o - x_t)^2 + (y_o - y_t)^2 + (z_o - z_t)^2\right]^{1/2}. \tag{A-10}$$

A point on the LOS a distance r from the observer in the direction of the target thus has coordinates (x, y, z) that satisfy

$$x = x_o + \alpha r, \tag{A-11}$$
$$y = y_o + \beta r, \tag{A-12}$$
$$z = z_o + \gamma r, \tag{A-13}$$

where r can vary between 0 and R.

The CL integral (eq A-21) is derived as follows. First, all coordinates are transformed to a new frame. In the transformation, all distances in x are divided by σ_x, all distances in y are divided by σ_y, and all distances in z are divided by σ_z. Define the vectors

$$\vec{S} = \left(\frac{\alpha}{\sigma_x}\right)\hat{i} + \left(\frac{\beta}{\sigma_y}\right)\hat{j} + \left(\frac{\gamma}{\sigma_z}\right)\hat{k} \tag{A-14}$$

and

$$\vec{X} = \left(\frac{x_o - x}{\sigma_x}\right)\hat{i} + \left(\frac{y_o - y}{\sigma_y}\right)\hat{j} + \left(\frac{z_o - z}{\sigma_z}\right)\hat{k}. \tag{A-15}$$

The LOS in the new frame, from equations (A-9) through (A-13), is then

$$\vec{X} = -r\vec{S}. \tag{A-16}$$

Note that the LOS in the new frame remains a straight line, since S is a constant vector. In the new frame, the ellipsoidal Gaussian distribution has now become spherically symmetric (see fig. A-3). The vector from the puff centroid (x_c, y_c, z_c) to the observer in the new frame is

$$\vec{X}_c = \left(\frac{x_o - x_c}{\sigma_x}\right)\hat{i} + \left(\frac{y_o - y_c}{\sigma_y}\right)\hat{j} + \left(\frac{z_o - z_c}{\sigma_z}\right)\hat{k}. \tag{A-17}$$

The closest approach distance of the LOS to the puff centroid in the new frame is the vector cross-product magnitude given by

$$D = \frac{\left|\vec{X} \times \vec{X}_c\right|}{\left|\vec{X}\right|} = \frac{\left|\vec{S} \times \vec{S}_c\right|}{\left|\vec{S}\right|} \tag{A-18}$$

Figure A-3. Scaled parameters for path integration and cloud rejection.

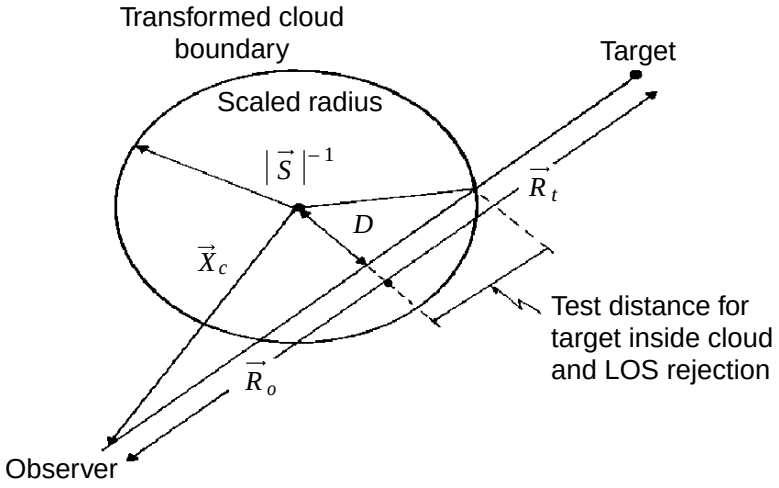

We call this the "σ-scaled closest approach distance." Similarly, the σ-scaled range from the closest point of approach to the observer is the vector dot product

$$R_o = \frac{\left|\vec{X} \cdot \vec{X_c}\right|}{\left|\vec{X}\right|} = \frac{\left|\vec{S} \cdot \vec{X_c}\right|}{\left|\vec{S}\right|}, \tag{A-19}$$

and the scaled range to the target from the closest point of approach is

$$R_t = R_o + R|\vec{S}|. \tag{A-20}$$

In terms of these quantities, the CL integral becomes the path integral from the observer point P_o to the target point P_t over the concentration (eq (A-3) and (A-4)) written in terms of the vectors just defined. However, this integral is just the well-known one-dimensional integral of a Gaussian distribution over a finite interval. The magnitude of S in the denominator of the result is due to the change of variables from the increment dr to the increment $d(rS)$:

$$\begin{aligned} \text{CL} &= \int_{P_o}^{P_t} \frac{M}{(2\pi)^{3/2}\sigma_x\sigma_y\sigma_z} e^{-\frac{1}{2}\left(\vec{X}-\vec{X_c}\right)^2} dr \\ &= \frac{M[\Phi(R_t) - \Phi(R_o)]}{(2\pi)\sigma_x\sigma_y\sigma_z|\vec{S}|} e^{-\frac{1}{2}D^2}, \end{aligned} \tag{A-21}$$

where Φ is the cumulative normal function. (The definition of Φ is given in eq (A-183).)

Although the derivation may not be obvious, a geometric interpretation is shown in figure A-3. The original Gaussian puff has an ellipsoidal shape if the sigmas are unequal ($\sigma_x \neq \sigma_y \neq \sigma_z$). The sigmas are in units of length. Define a new frame of reference in which distances along each direction x, y, z are in terms of new units (σ) found by dividing distance along those

coordinates by the appropriate σ. This new frame has two important properties. First, the Gaussian puff now has spherical symmetry. Second, the LOS remains a straight line.

The vector S has no obvious physical interpretation. The magnitude of S, however, is a scaling factor in inverse units of distance, and converts the distances in the new frame to the σ units just defined. D, found by equation (A-23), is the closest approach distance in σ units. If D is 3 or larger, the puff does not contribute to the CL because the LOS lies outside the 3σ edge, and the calculation is terminated. If D is less than 3, then the distances R_o and R_t are computed by the dot product (eq (A-19) and (A-20)). R_o and R_t are signed quantities. If R_o is less than -3, then the observer lies on the near side of the cloud. If R_o is larger than 3, then both observer and target lie on the far side of the cloud. In this case, the LOS never reaches the cloud, so the CL is 0. Similarly, if R_t is larger than 3, then the target lies on the far side of the cloud, while if it is less than -3, both the target and observer lie on the near side of the cloud. In the latter case, the CL is again 0. For R_o and / or R_t smaller than 3 in absolute value, the observer and / or target potentially lie inside the cloud. The cumulative normal distribution terms take care of the correction factors automatically in these cases.

Note to users of EOSAEL**82**: In the EOSAEL82 routine for the path integration, lines of code were suggested that users could add to find the point on the LOS closest to the cloud (Duncan, 1982). As pointed out later by a COMBIC user, the method did not work, because the suggested code change determines the point of maximum concentration on the LOS for a given cloud. This is not necessarily the geometrically closest point to the cloud center. Since these lines of code were only in the form of comments, most users were not affected. To anyone who did implement these code additions, we apologize for the misinformation.

In any case, finding the point on the LOS closest to the cloud is probably of less interest than finding the point of maximum concentration along the LOS. The distance from the observer to the point of maximum concentration is R_o / S. This distance can be used with equations (A-12) and (A-13) to find the coordinates of the point.

A-2.2 Path Integral Through Gaussian Plumes

Phase II of COMBIC deals with integrating concentration of obscurants along LOS's. Integration through the Gaussian plume is fast and simple only if the LOS is nearly crosswind. In that case, the values of the plume height z_c and the y and z components of σ are nearly constant all along the LOS. (The obscurant production rate $\dot{m}$ in eq (A-22) is evaluated as discussed in sect. A-1 and A-2.6.) The CL integral is very similar to that for the Gaussian puff:

$$\mathrm{CL} = \left(\frac{\dot{m}}{\mu}\right) \frac{[\Phi(R_t) - \Phi(R_o)]}{(2\pi)^{1/2}\sigma_y\sigma_z S} e^{-\frac{1}{2}D^2}, \qquad \text{(A-22)}$$

where

$$D = S^{-1}|(S_y\bar{X}_z - S_z\bar{X}_y)|, \quad \text{(A-23)}$$

$$R_o = S^{-1}|(S_y\bar{X}_y - S_z\bar{X}_z)|, \quad \text{(A-24)}$$

$$R_t = R_o + R|\vec{S}|. \quad \text{(A-25)}$$

Here, R is again the scalar distance between the observer and target, and the quantities S and X are defined by

$$\vec{S} = S_y\hat{j} + S_z\hat{k} = \left(\frac{\beta}{\sigma_y}\right)\hat{j} + \left(\frac{\gamma}{\sigma_z}\right)\hat{k}, \quad \text{(A-26)}$$

$$\vec{\bar{X}} = X_y\hat{j} + X_z\hat{k} = \left(\frac{y_o - \bar{y}}{\sigma_y}\right)\hat{j} + \left(\frac{z_o - \bar{z}}{\sigma_z}\right)\hat{k}, \quad \text{and} \quad \text{(A-27)}$$

$$S = (S_y^2 + S_z^2)^{1/2}. \quad \text{(A-28)}$$

The simple formula is valid for crosswind LOS's, including slant path or downward-looking paths, and, based on the power law expansions given in section A-2.1,

$$\sigma(x) = \sigma(x_c)\left[1 + B\left(\frac{x - x_c}{x_c}\right) + \ldots\right], \quad \text{(A-29)}$$

when linear and higher order terms are negligible. COMBIC assumes, for the purpose of calculation speed, that if x varies by no more than ± 5 percent of x_c (which corresponds to one downwind step in the Phase I tables) inside the cloud, then the crosswind approximation can be used. This approximation is roughly an angle within 6° of crosswind for Pasquill category A (unstable) and within 25° of crosswind for Pasquill category E (stable).

For more general LOS's, a different algorithm is required. The general CL integral for a Gaussian plume is

$$\text{CL} = \int_0^R \frac{\dot{m}/u}{2\pi\sigma_y\sigma_z} \exp\left(-1/2\left[\left(\frac{y - y_c}{\sigma_y}\right)^2 + \left(\frac{z - z_c}{\sigma_z}\right)^2\right]\right) dr. \quad \text{(A-30)}$$

If we change the variable of integration from r (the distance along the LOS) to x (the downwind distance) and evaluate $\dot{m}$ at $t - t(x)$, the CL integral becomes

$$\text{CL} = \int_{x_1}^{x_2} \frac{\dot{m}/u}{2\pi\sigma_y\sigma_z\alpha} e^{-\mathbf{X}^2/2}\, dx \quad \text{(A-31)}$$

where

$$\mathbf{X}^2 = \left[\frac{(x - x_0)\beta/\alpha + y_0 - y_c}{\sigma_y}\right]^2 + \left[\frac{(x - x_0)\gamma/\alpha + z_0 - z_c}{\sigma_z}\right]^2. \quad \text{(A-32)}$$

The cloud is assumed to have been rejected if it does not intersect the LOS. In equation (A-31) the downwind coordinates x_1 and x_2, the limits of integration, are the points of intersection of the LOS with the cloud. (For example, if the observer is inside the cloud, then $x_1 = x_0$; if the target is inside the cloud, then $x_2 = x_t$. Either x_1 or x_2 might be the downwind distance of the leading or trailing edge or of the point of intersection with the 3σ limit of the cloud.) Note that this transformation of coordinates cannot be made if $\alpha = 0$; that is, if the LOS is directly crosswind. If α is very small, equation (A-31) will be ill-conditioned because CL would then be a quotient of two small values. However, if the LOS is nearly crosswind, the CL integral is quickly and accurately approximated by the algorithms at the beginning of this section.

A-2.3 Contributions From Ground Reflection of the Plume

COMBIC92 computes the ground reflection of the Gaussian plume in a manner different from COMBIC84 and COMBIC87. The method applied is the traditional one in which the reflection cloud is assumed to have a centroid as far below (or above) ground as the centroid of the real cloud is above (or below) the ground. In COMBIC92 the amount of computation time and memory required to accomplish this modification is minimal.

If we simply replace z_c in equation (A-32) with its negative, equation (A-31) will result in the CL for the reflected cloud (assuming that 100 percent of the below-ground portion is reflected). By multiplying this by the reflection coefficient R_e and adding to equation (A-31), we get the CL for the cloud, including the reflected portion:

$$\mathrm{CL} = \int_{x_1}^{x_2} \frac{\dot{m}}{2\pi\sigma_y\sigma_z\alpha\, u}\, h(x)\, dx, \tag{A-33}$$

$$h(x) = \exp\left[\frac{1}{2\sigma_y^2}\left(\frac{(x-x_0)\beta}{\alpha} + y_0 - y_c\right)^2\right] \times \left\{\exp\left[\frac{1}{2\sigma_y^2}\left(\frac{(x-x_0)\gamma}{\alpha} + z_0 - z_c\right)^2\right] + R_e \exp\left[\frac{1}{2\sigma_y^2}\left(\frac{(x-x_0)\gamma}{\alpha} + z_0 - z_c\right)^2\right]\right\}. \tag{A-34}$$

COMBIC assumes that the reflected mass has the same above-ground distributions as the real cloud. For clouds with centroids near ground level, COMBIC92 will compute somewhat higher values for CL than COMBIC87 in the lower portions of the cloud and lower values in the higher portions.

A-2.4 Changing the Variable of Integration

COMBIC92 uses the Romberg method of integration (see sect. A-2.7) to compute the CL integral. This method requires that the integrand be defined at equally spaced values of the variable of integration. The variable

of integration is changed from the downwind distance x to the index n (see table A-1) of equation (A-6):

$$dx = \frac{(1.51) \cdot x}{\mathrm{Ind}(x)}\, dn \text{ for } n < 13, \tag{A-35}$$

$$dx = \ln(1.123) \cdot x \cdot dn \text{ for } n \geq 13\ . \tag{A-36}$$

Define, where $h(x)$ is given by equation (A-34),

$$g(x) = \frac{[\mathrm{Ind}(x_2) - \mathrm{Ind}(x_1)] \cdot x \cdot \ln(1.123) \cdot h(x)}{2\pi\sigma_y\sigma_z\alpha\, u}\ , \tag{A-37}$$

$$f(x) = \frac{(1.51)g(x)}{\ln(1.123)\mathrm{Ind}(x)} = \frac{13}{\mathrm{Ind}(x)}g(x) \text{ for } n < 13\ , \tag{A-38}$$

$$f(x) = g(x) \text{ for } n \geq 13\ . \tag{A-39}$$

Then the CL integral of equation (A-33) becomes

$$\mathrm{CL} = \int_{\mathrm{Ind}(x_1)}^{\mathrm{Ind}(x_2)} \dot{m} f(x)\, dn\ . \tag{A-40}$$

The CL integral is now set in the form $\int_a^b f(x)\ dx$. The integrands $a = \mathrm{Ind}(x_1)$ and $b = \mathrm{Ind}(x_2)$ are evenly spaced according to the requirements of the Romberg method of integration. The method iterates through certain steps, each theoretically (and in some cases, dramatically) a better approximation of the integral than the previous step. During each step, $\dot{m}$ and $f(x)$ are computed for different points along the LOS. Comparison with the previous step is used as an approximate check of the accuracy of the current step.

A-2.5 Rejecting Nonintersecting Plumes from the Path Integration

An important step in making rapid calculations in Phase II is to reject continuous plumes that do not contribute to the CL of a given LOS. This is accomplished through definition of a simple geometric volume that describes the extent of each cloud at any given simulation time. As shown in figure A-4, the volume is a (nonrectilinear) box whose vertical sides become more widely separated in the downwind direction. The top of the box is a plane that slopes upward away from the source. The volume is designed to enclose the actual plume used in the path integrations. The "corner" coordinates of the actual plume at the leading downwind edge of the cloud are (x_d, y_d, z_d). Similarly, the coordinates of the upwind corner are (x_u, y_u, z_u). The munition source is at (x_m, y_m, z_m).

Rejection of LOS's by testing for intercepts with these surfaces is straightforward. Consider the test for the ends of the box. Let s be some range between the observer and target, that is,

$$x = \alpha s + x_o. \tag{A-41}$$

Figure A-4. Boundary box for cloud.

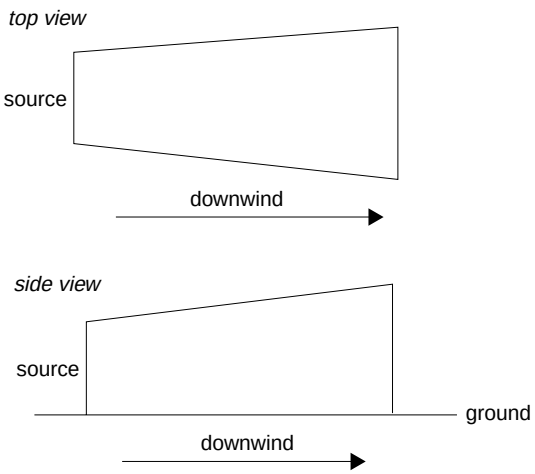

Then no intercept can occur with the downwind edge if the point of interception s_i,

$$s_i = \frac{(x_d + x_m - x_o)}{\alpha}, \tag{A-42}$$

is greater than R or less than zero. If the test is passed, then s_i is saved as a candidate for the range of entry into the cloud if s is negative (target upwind of the observer), or as a candidate for the range of exit from the cloud if s is positive. The test on x_u is similar. For the side of the box on the positive y side of the plume, the test is on the intersection of the straight lines

$$y = y'_u + y_m + (x - x_u)\left(\frac{y'_d - y'_u}{x_d - x_u}\right) \quad \text{and} \tag{A-43}$$

$$y = \beta s + y_o, \tag{A-44}$$

which results in the value for the candidate of

$$s'_i = \frac{(y'_u + y_m - y_o)(x_d - x_u) + (x_o - x_u)(y'_d - y'_u)}{\beta(x_d - x_u) - \alpha(y'_d - y'_u)}. \tag{A-45}$$

Again, the cloud is rejected if the value lies outside the interval defined by the candidate entry or exit range from the previous tests. These tests continue on the other side of the cloud, on the top, and on the bottom. If the test fails at any point, the calculation for this cloud and this LOS terminates. If all the tests are passed, the resulting entry and exit points define the range over which the CL path integral must be performed.

A-2.6 Corrections for Area Sources

Consider first the obscurant from a point source as shown in figure A-5. For any given time t, COMBIC determines the total amount of obscurant that has been transported beyond (that is, downwind of) any given point x_2:

$$M_d = M[t - t_2(x_2)], \tag{A-46}$$

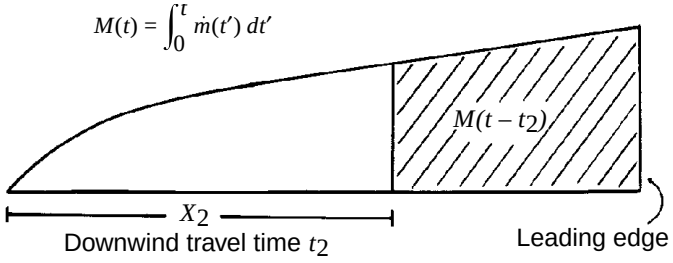

Figure A-5. Downwind obscurant mass beyond x_2 originating from a point source.

where t_2 is the time required for the obscurant to travel from the source to the point x_2, and M is the cumulative mass emitted by the source as a function of time. Figure A-5 shows this region of the plume.

The case of an extended source area is more complicated. It takes longer for obscurant from the upwind region of the source area to reach the downwind point in the plume than it does for an obscurant originating in the downwind region of the source area to reach that same point. For a Gaussian distributed source and an evaporation term of the form given in equation (A-3) for the Gaussian puff, the exact solution for the mass downwind of point x_2 (associated with a downwind time t_2 from the source) at time t is

$$M_d = \int_0^T \dot{m}(t')\phi\left[\frac{t - t_2 - t'}{\sigma_s/\mu}\right]\left[f_d + (1 - f_d)e^{-\delta(t-t')}\right]dt', \qquad \text{(A-47)}$$

where the upper limit T on the integration is*

$$T = \begin{cases} t - t_2 + 2.15\frac{\sigma_s}{\mu} & \text{for } t_2 > 2.15\frac{\sigma_s}{\mu} \\ t & \text{for } t_2 < 2.15\frac{\sigma_s}{\mu} \end{cases}. \qquad \text{(A-48)}$$

The distance σ_s is the Gaussian standard deviation for the source, and μ is the windspeed inside the source region. The integration limit separates the case of point t_2 downwind of the source region from that of t_2 inside the source region. The problem with tabulating the results of equations (A-47) and (A-48) directly is that they depend both on the current time t and the downwind time t_2. The need exists for an approximate equation in which only differences in t and t_2 appear.

Assume for the moment that the evaporation term is incorporated into the mass definition m. Integrate equation (A-47) by parts for the case of a point downwind of the source. Use the facts that $M(0)$ is 0, and the cumulative normal distribution is 1 from about $2.15\sigma_s/\mu$ to ∞ and 0 from $-\infty$ to $-2.15\sigma_s/\mu$; then

$$M_d = \int_{t-t_2-2.15\frac{\sigma_s}{\mu}}^{t-t_2+2.15\frac{\sigma_s}{\mu}} \frac{M(t')\mu}{(2\pi)^{1/2}\sigma_s}\exp\left[-\frac{1}{2}\left(\frac{t - t_2 - t'}{\frac{\sigma_s}{\mu}}\right)^2\right]dt'. \qquad \text{(A-49)}$$

*The value of 2.15 in equation (A-48) comes from $e^{-x^2/2}$ = 10 percent.

Next expand $M(t)$ in a Taylor series about $(t - t_2)$:

$$M(t') = M(t - t_2) + \frac{dM}{dt'}(t' - t + t_2) + \frac{1}{2}\frac{d^2M}{dt'^2}(t' - t + t_2)^2 + \ldots, \quad \text{(A-50)}$$

where the derivatives are evaluated at $t - t_2$. Substitute into equation (A-49) and integrate the first three terms:

$$M_d = M(t - t_2) + 0 + \left(\frac{1}{2}\frac{\sigma_s^2}{\mu^2}\right)\frac{d^2}{dt'^2}M(t - t_2) + \ldots \quad \text{(A-51)}$$

One way to approximate the second derivative is by finite differences:

$$\frac{d^2}{dt^2}M(t - t_2) = \left(\frac{\mu}{\sigma_s}\right)^2 \left[M\left(t - t_2 - \frac{\sigma_s}{\mu}\right) - 2M(t - t_2) + M\left(t - t_2 + \frac{\sigma_s}{\mu}\right)\right]. \quad \text{(A-52)}$$

Substituting into equation (A-51), we find that the amount of obscurant downwind of the point x_2 is thus

$$M_d = \frac{1}{2}\left[M\left(t - t_2 - \frac{\sigma_s}{\mu}\right) + M\left(t - t_2 + \frac{\sigma_s}{\mu}\right)\right]. \quad \text{(A-53)}$$

This can be written in an analogous way for a source with uniform mass distribution in the source region. Assume that the source region extends over a length $2\Delta L$, and the windspeed in the source area is μ. The time required for obscurant to travel from one side of the source region to the other, Δt_s, is found from

$$2\Delta t_s = \frac{2\Delta L}{\mu} = 2\frac{\sigma_s}{\mu}. \quad \text{(A-54)}$$

Taking into account this spread Δt_s, upwind and downwind of the center of the source area, the mass that is downwind of point x_2 is approximately

$$M_d = 0.5\left[M(t - t_2 + \Delta t_s) + M(t - t_2 - \Delta t_s)\right]. \quad \text{(A-55)}$$

This result applies for the case when x_2 is neither in the source area itself nor in the leading edge of the plume, as in figure A-6.

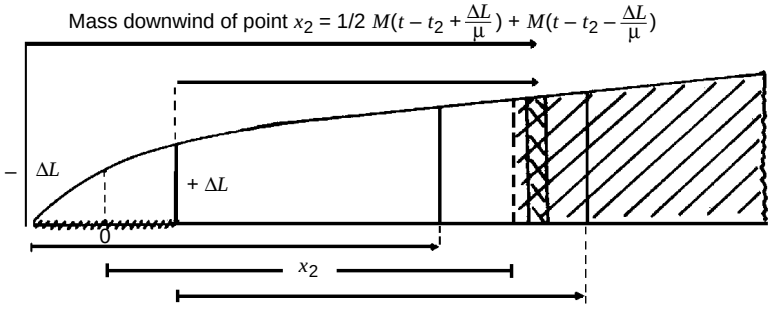

Figure A-6. Downwind mass beyond point x_2 originating from an area source.

Another way of looking at equation (A-55) is to realize that M_d is an average of the mass at $t - t_2$ for the interval $2\Delta t_s$ for a uniform source. In COMBIC92, the mass is stored every second. This is a significant change from COMBIC87, in which the mass was stored, no matter how long the burn time, in an array of 55 values. The larger array in COMBIC92 means greater accuracy in determining M and an improved run time. Thus, no searching is required, and interpolation time is decreased by about 50 percent over the old method. Furthermore, instead of M_d being computed in Phase II, it is computed and stored during Phase I.*

Equation (A-55) is a straight average at $t - t_2 - \Delta t_s$ and $t - t_2 + \Delta t_s$. A more accurate approach is to assume that the source is nonuniform and to average for every second for $2\Delta t_s$ seconds. COMBIC92 uses not only mass but also mass rate,† as was shown in equation (A-40). These data are also averaged over $2\Delta t_s$ seconds for all times when the associated downwind distance is not in the leading edge of the plume or the source region.

To better understand the approximation involved in equation (A-55), consider the different case of finding the total mass that is inside a source area at time t. Break up the source region into intervals dx. Integrate all the mass inside one interval, including any mass produced upwind at earlier times that has been transported into interval dx by time t. Then integrate over all the increments of the source region:

$$\begin{aligned} M_s &= (2\,\Delta L)^{-1} \int_0^{2\Delta L} dx \int_0^{x/\mu} dt' \dot{m}(t - t') \\ &= (2\,\Delta L)^{-1} \int_0^{2\Delta L} dx \left[M(t) - M\left(t - \frac{x}{\mu}\right) \right] \\ &= M(t) - (2\,\Delta L)^{-1} \int_0^{2\Delta L} dx M\left(t - \frac{x}{\mu}\right). \end{aligned} \tag{A-56}$$

The remaining integral depends on the form of the cumulative mass function M. COMBIC uses puffs to represent rapid obscurant releases and reserves plumes for the less abrupt, continuous releases. Thus, M is a monotonic, increasing function that is relatively smooth. We choose to approximate the second integrand by the average evaluated at its limits. The result is

$$M_s = M(t) - 0.5\,[M(t) + M(t + 2\Delta L/\mu)]\,. \tag{A-57}$$

If equation (A-57) defines the total obscurant inside the source region at time t, then the total obscurant mass downwind of the source region must be $M(t) - M_s$, or

$$M_d = 0.5\,[M(t) + M(t + 2\Delta t_s)]\,. \tag{A-58}$$

*Users who wish to use average mass data for other calculations can access these using the SNW statement function, which retrieves this information from the SMKDSS array in the SOURT common block.

†Mass rate data are also accessible; users can access these data through the SNWD statement function.

Note that this corresponds to the answer from equation (A-55) for a downwind travel time from the center of the source region of $t = \Delta$. This is by definition the downwind edge of the source region, so the answers should and do agree.

COMBIC92 uses $\dot{m}$ tables in ways quite similar to the way COMBIC87 uses m tables. Tables of m are needed for crosswind or nearly crosswind LOS's. Tables of $\dot{m}$ are needed when the Romberg method is applied. Corrections for area source for the $\dot{m}$ tables for COMBIC92 are simply the derivative of mass taken with respect to time:

$$\dot{m}_d = 0.5\left[\dot{m}(t - t_2 + \Delta t_s) + \dot{m}(t - t_2 - \Delta t_s)\right]. \tag{A-59}$$

If t_2 is greater than $t - \Delta t_s$, then the point x_2 is within the diffuse leading edge of the plume. First, equations (A-60) and (A-61) check to determine whether the source has finished burning:

$$t_d = \min\left(T_{burn} + \Delta t_s, t + \Delta t_s\right), \tag{A-60}$$

$$t_{dd} = \min\left(t_2, t_d\right). \tag{A-61}$$

T_{burn} is the total burn duration, necessary for determining the presence of the diffuse trailing edge after burnout. The mass rate $\dot{m}$ is assumed to vary linearly with $\dot{m}(\Delta t_s)$. Equation (A-62) then computes $\dot{m}_{ave}(t)$:

$$\dot{m}_{ave}(t) = \dot{m}_{ave}(\Delta t_s)\left[\frac{t_d - t_{dd}}{2\Delta t_s}\right]; \tag{A-62}$$

$\dot{m}_{ave}(t)$ is the average mass rate based upon $\dot{m}_{ave}(\Delta t_s)$ that was precomputed in Phase I (and stored in the SNWD array).

If $t_2 < \Delta t_s$ or $t_2 < t - T_{burn} + \Delta t_s$, then the point is within the area source of the plume, and $\dot{m}_{ave}(t)$ varies quadratically with $\dot{m}_{ave}(t^-)$. While the source is burning, t^- increases with time. When the source stops burning, t^- becomes fixed. Thus, t^- is defined as

$$t^- = \min(t - \Delta t_s, T_{burn} - \Delta t_s). \tag{A-63}$$

Therefore the mass rate within the source plume is

$$\dot{m}_{ave}(t) = \dot{m}_{ave}(t^-)\left[1.0 - \left(\frac{\Delta t_s - t_2}{2\Delta t_s}\right)^2\right]. \tag{A-64}$$

Again, $\dot{m}_{ave}(t^-)$ is stored in the Phase I SNWD array.

As an example, let us choose x_2, the downwind distance from the center of the source to the integration point, to be at the extreme leading edge of the plume. At this point and the current time, only the smoke from the extreme downwind edge of the source has arrived. The time from the center of the source area, t_2, to the point x_2 is $t + \Delta t_s$. From equations (A-60) to (A-62),

it can be shown that $\dot{m}(t)$ is zero, which is reasonable since the smoke has just reached that point.

As a further example, consider the case of the point x_2 at the upwind edge of the source region. In this case, $t_2 = -\Delta t_s$. It is easy to determine from equations (A-63) and (A-64) that $\dot{m}_d$ is simply zero.

Similarly, consider the case of the midpoint of the source region, where $t_2 = 0$. The result of equation (A-64) is that

$$\dot{m}_{ave} = \frac{3}{4} M(t^-). \tag{A-65}$$

For the evaporation term of equations (A-3) and (A-47) to be included in the cumulative mass function, several sets of histories must be stored in Phase I: one set for $\dot{m}$ (in addition to m stored in the SNW arrays, as in the previous versions of COMBIC), the other set for the integral in equation (A-67) (which is the same integral as in earlier versions of COMBIC, referred to as XSIG). The first is attributed to the constant f_d term, while the second is attributed to the exponential decay term. They are defined from

$$\dot{m}(t) = f_d \dot{m}(t) + (1 - f_d) e^{-\delta t} \left[\delta \int_0^t e^{+\delta t'} \dot{m}(t') dt' + e^{\delta t} \dot{m} \right], \tag{A-66}$$

which simplifies to

$$\dot{m}(t) = \dot{m}(t) - \delta (1 - f_d) e^{-\delta t} \int_0^t e^{+\delta t'} \dot{m}(t') dt'. \tag{A-67}$$

A-2.7 Romberg Integration Method

The Romberg integration method has been incorporated in COMBIC92 because it has been found to be a very efficient way of performing the integration of CL along the LOS when the LOS is not perpendicular to the wind. Details and theory of the classical Romberg integration method can be found in almost any text in numerical analysis. Its application to the CL integral is detailed in section A-2.4. The notation used here has been adapted to its ultimate application.

Unless greatly modified, the Romberg method requires that the integrand be defined at equally spaced values of the variable of integration. This equal spacing is accomplished by the indexing discussed in section A-2.4.

Three features of the Romberg method make it nicely adaptable to approximating the CL for LOS's that are not too nearly crosswind:

a. Comparison of one step of the iterative method of Romberg with the previous step will yield an approximate percentage error of the latter step from the true value of CL. This fact allows the user to specify

the maximum percentage error that can be tolerated. The number of iterations made is only the number required to achieve the necessary accuracy.

b. After as few as two iterations, the approximation might be terminated because the anticipated CL value is small enough to be below a threshold value that has been specified by the user as negligible.

c. Similarly, the approximation might be terminated if the CL is determined to be large enough to make the transmittance below some threshold value specified by the user.

The Romberg method consists of a series of steps. The initializing step is simply the trapezoidal rule for the interval $[a, b]$. It is never accepted as an accurate value.

Step 0

$$S_{0,0} = \frac{b-a}{2}[f(a) + f(b)] \; .$$

Step 1

$$\begin{aligned} S_{1,0} &= \frac{b-a}{4}\left[f(a) + 2f\left(\frac{b+a}{2}\right) + f(b)\right] \\ &= \frac{1}{2}S_{0,0} + \frac{b-a}{2}f\left(\frac{a+b}{2}\right) \\ S_{0,1} &= (4S_{1,0} - S_{0,0})/3 \end{aligned}$$

The approximation $S_{1,0}$ is the trapezoidal rule for the intervals $[a, (a+b)/2]$ and $[(a+b)/2, b]$. The approximation $S_{0,1}$ is Simpson's rule for the interval $[a, b]$; it is an extrapolation (called Richardson's extrapolation) of $S_{1,0}$ and $S_{0,0}$. If $S_{0,1}$ is smaller than a threshold value specified by the user, then the integral can be assumed negligible and further steps are not needed. Or if $S_{0,1}$ is greater than a given threshold value, further steps are not needed because the transmittance will be negligible.

Step 1 Test. Compute the absolute value of percent relative difference between $S_{0,0}$ and $S_{0,1}$:

$$100. \left[\frac{|S_{0,0} - S_{0,1}|}{S_{0,1}}\right] \; .$$

If this percentage difference is less than a user-specified value, the approximation of the integral can be terminated here. If not, step 2 is performed.

Step 2

$$\begin{aligned} S_{2,0} &= \frac{1}{2}S_{1,0} + \frac{b-a}{4}\left[f\left(\frac{3a+b}{4}\right) + f\left(\frac{a+3b}{4}\right)\right] \\ S_{1,1} &= (4S_{2,0} - S_{1,0})/3 \\ S_{0,2} &= (16S_{1,1} - S_{0,1})/15 \end{aligned}$$

Step 2 Test. Compute

$$100. \left[\frac{|S_{0,1} - S_{0,2}|}{S_{0,2}} \right]$$

and compare with the user-specified value.

Step n

$$\begin{aligned} S_{n,0} &= \frac{1}{2} S_{n-1,0} + \frac{b-a}{2^n} \sum_{i=1}^{2^{n-1}} f\left[\frac{(2^n + 1 - 2i)a + (2i-1)b}{2^n} \right] \\ S_{n-1,1} &= (4S_{n,0} - S_{n-1,0})/3 \\ S_{n-2,2} &= (16S_{n-1,1} - S_{n-2,1})/15 \\ S_{n-j,j} &= (4^j S_{n-j+1,j-1} - S_{n-j,j-1})/(4^j - 1) \quad (\text{for } j = 1 \text{ to } n) \end{aligned}$$

The sequence $S_{0,0}, S_{0,1}, S_{0,2}, \cdots, S_{0,n}, \cdots$ theoretically approaches $\int_a^b f(x)\, dx$. The only limitations are the practicability of evaluating the function $f(x)$ at a large number of values and certain requirements on the higher order derivatives of $f(x)$. In several examples using the technique, accuracy of 15 percent or better was achieved as early as step 2, which requires only five evaluations of $f(x)$. Accuracy of 1 percent is not unusual at step 3, which requires only nine evaluations of $f(x)$. To provide for rapidly changing mass production functions (such as for phosphorus-based smoke), it is suggested that coding allow up to four steps, which would require 17 evaluations.

A-2.8 Barrage Emissions

A barrage is treated as a large number of smoke or dust sources that are distributed in some Gaussian pattern of downwind standard deviation σ_b and that impact or ignite with a uniform distribution over T_{bar} seconds. The combined effect of the spatial spread due to the barrage pattern and the spatial spread of individual munitions is easily seen to remain Gaussian with a spatial variance:

$$\sigma_s^2 = \sigma_m^2 + \sigma_b^2, \tag{A-68}$$

where σ_s is the source σ for the combined effect of the barrage σ, σ_b, and the individual munition σ's, σ_m. This result follows directly if we evaluate the concentration equation when written as an expectation over impacts having Gaussian probability of igniting at x:

$$\begin{aligned} C(x) &= \int_{-\infty}^{\infty} \frac{1}{2\pi\sigma_m\sigma_b} \exp\left[-\frac{1}{2} \left(\frac{x - x'}{\sigma_m} \right)^2 \right] \exp\left[-\frac{1}{2} \left(\frac{x'}{\sigma_b} \right)^2 \right] dx' \\ &= \frac{1}{(2\pi)^{1/2} \left(\sigma_m^2 + \sigma_b^2\right)^{1/2}} \exp\left[-\frac{x^2}{2\left(\sigma_m^2 + \sigma_b^2\right)} \right]. \end{aligned} \tag{A-69}$$

The effective mass emission rate resulting from uniform impacts or ignitions over time T_{bar} of munitions with individual emission durations T_{burn} is easy to write as

$$\dot{m}(t) = \begin{cases} \frac{1}{M_m T_{bar}} \int_0^t \dot{m}_m(t')\, dt' & \text{for } 0 < t < \min(T_{bar}, T_{burn}) \\ \frac{1}{T_{bar}} & \text{for } T_{burn} < t < T_{bar} \text{ (if } T_{bar} > T_{burn}) \\ \frac{1}{M_m T_{bar}} \int_{t-T_{bar}}^{T_{burn}} \dot{m}_m\, dt^{prime} & \text{for } T_{bar} < t < T_{bar} + T_{burn}, \end{cases} \tag{A-70}$$

where M_m is the total mass of one munition, and $\dot{m}_m$ is the munition mass emission function. It should be noted that the total emission time is now $T_{bar} + T_{burn}$. If the barrage lasts longer than the individual munition burn duration, then the obscurant production is constant over the middle period of the barrage.

A-3 Diffusion Model in COMBIC

Ambient turbulence in the atmosphere causes a decrease in obscurant concentration as the puff or plume diffuses (expands) downwind. The effect of diffusion in COMBIC is contained in the parameters σ_x, σ_y, and σ_z. These are directly related to cloud dimensions. Two methodologies are used to define the σ's. The methodology used in previous versions of COMBIC is still valid for downwind travel time <30 s.

The values of the σ's for puffs, in relation to the downwind travel distance from the source $\bar{x}$, are dependent on the fractional stability category, wind speed, scaling ratio, and surface roughness length (Hansen and Pena, 1990b; Hansen and Pena, 1990a) for downwind distance greater than the distance associated with a downwind travel time of 30 s. For instantaneous Gaussian puffs, the equation for finding the longitudinal dispersion length is

$$\sigma_{x_l} = \left[\sigma_{x_o}^2 + \sigma_{x_s}^2 + \sigma_{x_t}^2\right]^{0.5}, \tag{A-71}$$

where σ_{x_o} represents the initial expansion or "source σ." The parameters σ_{x_s} and σ_{x_t} are the vertical wind shear influences and longitudinal diffusivity of a puff, respectively:

$$\sigma_{x_s} = \frac{0.012}{\sigma_z} \left\{ \left[\frac{x}{\ln 0.53 \frac{\sigma_z}{\sigma_o} + \psi_m\left(\frac{z}{L}\right)} \right]^3 \frac{\phi_M^2}{\phi_H} \right\}^{\frac{1}{2}}, \tag{A-72}$$

$$\sigma_{x_t} = \frac{3}{\bar{\mu}} \left[\ln 0.53 \frac{\sigma_z}{\sigma_o} + \psi_M \left(\frac{z}{L}\right) \right]^{-2} x, \tag{A-73}$$

where ϕ_M is the dimensionless wind shear, ϕ_H is the dimensionless lapse rate, ψ_m is the diabatic influence function for momentum, and L is the Obukhov scaling length.

The lateral dispersion length σ_y is considered to be time dependent, highly sensitive to sampling and averaging times, and responsive to changes in surface roughness length, and is represented as

$$\sigma_y = \left[\frac{z_o}{10000}\right]^{\frac{1}{3}} \left[\frac{t}{0.1}\right]^{\frac{1}{3}} \sigma_\theta f_1(x) x, \tag{A-74}$$

where σ_θ is found as a function of Pasquill stability categories, and z_o is the surface roughness length; σ_θ can be determined from table A-2:

$$\sigma_\theta = 9.714 - 4.925(P) + 0.402(P)^2 + 0.118(P)^3. \tag{A-75}$$

The function $f_1(x)$ is given by

$$f_1(x) = \left[1 + 0.308x^{0.4548}\right]^{-1} \tag{A-76}$$

for alongwind distance of 10^4 m or less. For distances greater than 10^4 m,

$$f_1(x) = 0.33(x)^{-\frac{1}{2}}. \tag{A-77}$$

The vertical dispersion length is found to be independent of alongwind travel time, but is dependent upon the surface roughness length (see table A-2), and is represented by

$$\sigma_z = \left[\frac{z_0}{0.1}\right]^{\frac{1}{3}} \sigma_\phi f_2(x) x, \tag{A-78}$$

where σ_ϕ is a function of Pasquill stability categories,

$$\sigma_\phi = 5.048 - 1.996(P) + 0.060(P)^2 + 0.056(P)^3, \tag{A-79}$$

and $f_2(x)$ for downwind distances of 5×10^3 m or less is

$$f_2(x) = \left[1 + 0.0422x^{.4548}\right]^{-1}, \tag{A-80}$$

and for distances greater than 5000 m, it is

$$f_2(x) = 0.33 \left[\frac{5000}{x}\right]^{\frac{1}{2}}. \tag{A-81}$$

We can make reliable estimates for concentration for a relatively diffusing plume by considering the trivariate (x,y,z) diffusion of a Gaussian puff. Multiple puffs may be then advected or transported along the mean wind direction to represent the plume. The resultant dispersion of gases and

Table A-2. Surface roughness lengths.

Type of surface	Surface roughness (m)
Farmland:	
Natural snow surface (farmland)	0.003
Long grass (0.6 m), crops	0.05
Few trees, summer	0.07
Hedgerows	0.10
Wheat	0.22
Alfalfa	0.0272
Corn (2.2 m)	0.74
Trees, hedges, few buildings	0.20
Agricultural areas (Asia)	0.08
Tall crops, scattered obstacles	0.25
Citrus orchards	0.35
Orchards, summer	2.00
Forest, wooded areas:	
Subtropical savannah, scattered trees	0.25
Fairly level wooded country	0.30
Forest clearings, cutover areas	0.40
Fairly level coniferous, 15–20 m trees	1.10
Rolling terrain, 20-m trees	2.00
Fir forest	2.83
Smooth open woods (pine in Connecticut)	2.83
Fir forest	2.83
Pine forest (20-m trees)	2.83
Pine forest (19-m trees) (England)	2.83
Forested plateau (crossed by small valleys, 10-m trees)	2.83
Slightly rolling terrain, forested, some buildings	2.83
Forested ridges (150–200 m high) (Tennessee)	2.83
Forested ridges, hills	3.50
Mountains, unforested:	
Rolling hills, low mountains	0.75
Plains:	
Fairly level grass, few trees, winter	0.01
Fairly level grass, few trees, summer	0.02
Closely mown grass	0.001
Short grass	0.0014
Grass (0.05–0.06 m)	0.0075
Grass (0.6–0.7 m)	0.114
Uncut grass, isolated trees	0.03
Brush, scrub growth, open	0.15
Brush, scrub growth, dense	0.25
Urban land-use:	
Villages	0.40
Towns	0.55
Light density residential	1.08
Park	1.27
Office	1.75
Airfields	0.03
Central business district	3.21
Heavy density residential	3.70

Table A-2. Surface roughness lengths (cont'd).

Type of surface	Surface roughness (m)
Other:	
Smooth mud flats	0.00001
Blacktop or concrete	0.00002
Dry lake bed	0.00003
Smooth desert	0.001
Normal sea	0.001
Tundra	0.004

aerosols will, of necessity, be less than those simulated or observed for a continuous diffusion situation. The key to successfully modeling expanding clusters of puffs may be found in correctly postulating the form of the longitudinal dispersion of a puff. For continuous Gaussian plumes, the equations are slightly different (Hansen, 1990):

$$\sigma_x = 0, \tag{A-82}$$

$$\sigma_y = \sigma_\theta f_1(x)x. \tag{A-83}$$

The dependence of these diffusive expansion coefficients on downwind travel distance from the source $\bar{x}$ for X greater than the distance the cloud reaches after 30 s is assumed to follow a power law with constants that are functions of the Pasquill category and surface roughness parameter (Hansen, 1979; Pasquill, 1974, pp 365–380). For continuous Gaussian plumes, EOSAEL82 COMBIC introduced the forms

$$\sigma_x(\bar{x}) = 0, \tag{A-84}$$

$$\sigma_y(\bar{x}) = A_i\bar{x}^{0.9}, \tag{A-85}$$

$$\sigma_z(\bar{x}) = C_{ij}\bar{x}^{D_{ij}}, \tag{A-86}$$

where i is the Pasquill category index, and j is a surface roughness index for z_o of 1, 10, or 100 cm.

Figures A-7 and A-8 illustrate how the cloud dimensions change for different Pasquill stabilities for a generic white phosphorus (WP) munition.

The values for the instantaneous Gaussian puff are

$$\sigma_x(\bar{x}) = 0.740A_i\bar{x}^{0.9}, \tag{A-87}$$

$$\sigma_y(\bar{x}) = 0.667A_i\bar{x}^{0.9}, \text{and} \tag{A-88}$$

$$\sigma_z(\bar{x}) = C_{ij}\bar{x}^{D_{ij}}. \tag{A-89}$$

Values for the constants A, C, and D used in the EOSAEL82 version of COMBIC were those of Hansen (1979), as derived from Pasquill (1974, pp 365–380), and are given in table A-3. COMBIC has retained the functional forms of these equations since EOSAEL84, but the current version uses continuous interpolating coefficients in surface roughness and Pasquill stability class. This expands the model from the specific conditions imposed by

Figure A-7. Cloud diffusive height (2.15σ) for different Pasquill categories.

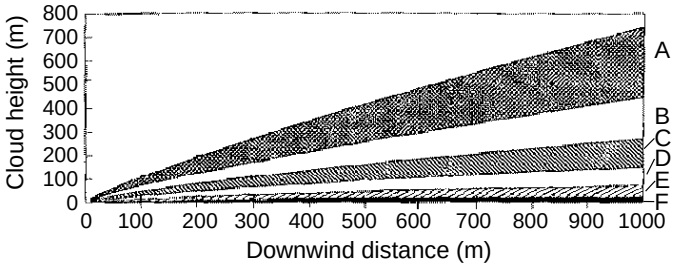

Figure A-8. Cloud diffusive width (2.15σ) for different Pasquill categories.

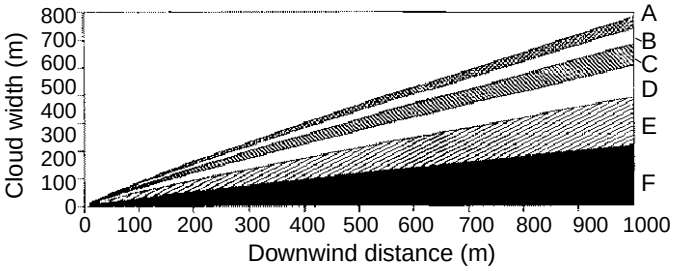

table A-3 to the general case. In addition, the σ expansion coefficients are modified by initial source terms. (Initialization is discussed in the later sections on individual obscurant types.)

It was desirable for the COMBIC84 model to allow diffusion to be computed for any surface roughness. For consistency with the boundary layer model extensions, it was further desirable to fit the dependence of the diffusion parameters on stability category so that interpolation could be performed between stability categories.

To accomplish this goal, Hansen reexamined Pasquill's original results (Hansen, 1979). Pasquill used gradient transport theory, a stability categorization similar to that in the current COMBIC boundary layer model, and observed data. He produced a table of diffusion coefficients and three graphs to extend these diffusion coefficients to other roughness lengths and to intermediate stability values.

Hansen [1979] fit Pasquill's results with interpolating functions in dependent variables P, Pasquill parameter, and surface roughness length z_o in meters. The form of the functions was somewhat determined by the boundary layer equations. For example, from equation (A-86),

$$\ln \sigma_z = \ln C(P; z_o) + D(P; z_o) \ln x, \tag{A-90}$$

while for neutral stability,

$$x = \frac{\mu t}{k} \ln \left(\frac{z}{z_o} \right). \tag{A-91}$$

Thus, it is reasonable to choose the form

$$D(P; z_o) = \delta_1(P) + \delta_2(P) \ln \left[\ln \left(\frac{z_R}{z_o} \right) \right] \tag{A-92}$$

Table A-3. Coefficients of diffusive expansion used in COMBIC82.

Index	Pasquill category	A_i	Surface roughness lengths					
			z_o = 1 cm		z_o = 10 cm		z_o = 100 cm	
			C_{i1}	D_{i1}	C_{i2}	D_{i2}	C_{i3}	D_{i3}
i = 1	A	0.40	0.154	0.94	0.279	0.90	0.615	0.83
i = 2	B	0.32	0.133	0.89	0.225	0.85	0.539	0.77
i = 3	C	0.22	0.121	0.85	0.213	0.81	0.533	0.72
i = 4	D	0.143	0.108	0.81	0.195	0.76	0.456	0.68
i = 5	E	0.102	0.078	0.78	0.139	0.73	0.348	0.65
i = 6	F	0.076	0.062	0.72	0.117	0.67	0.309	0.58

to separate the surface roughness dependence of D. A reference height of z_R of 7.5 m was chosen for consistency with the COMBIC boundary layer model. The Pasquill parameter dependence was found from Pasquill's graphs and table to be similar to a skewed hyperbolic sine curve about neutral conditions (P = 3.6). A double exponential was therefore chosen, and the resulting equations are

$$\delta_1 = 0.5629\left[1 + 0.4543e^{-0.4P} - 0.002347e^{0.75P}\right], \quad \text{(A-93)}$$

$$\delta_2 = 0.1 + 0.0084 \ln P. \quad \text{(A-94)}$$

Table A-4 shows exponents $D(P;z_o)$ from equation (A-92) at the same values for P and z_o used by Pasquill in his tabulation. Pasquill's values are also given for comparison. Agreement is good, with differences from Pasquill's two-digit precision only in categories D (z_o = 0.1 m) and E (z_o = 1.0 m). These differences produce a <4-percent difference in vertical diffusion over 1 km of downwind distance.

The multiplying coefficients for vertical diffusion $C(P,z_o)$ have similarly been fit by a product of three terms. The first term merely converts from Pasquill's units of kilometers to COMBIC's units of meters. The second terms contains the Pasquill parameter dependence. The third term contains the surface roughness dependence. Note the occurrence of the D exponent factors in the C coefficient:

$$C(P; z_o) = C_m(D)C_p(P)C_z(D; z_o), \quad \text{(A-95)}$$

with

$$C_m(D) = 1000^{[1-D(P;z_o)]}, \quad \text{(A-96)}$$

$$C_p(P) = 0.00397 + 0.193e^{-0.61P} + 0.00516P^{8.27}e^{-2.7P}, \quad \text{(A-97)}$$

$$C_z(D; z_o) = \frac{D(P; z_o)}{D(P; 0.1)}(1.2 + 0.0091 \ln z_o)^{[2.3+\ln z_o]}. \quad \text{(A-98)}$$

Table A-4. Comparison of interpolating functions for vertical diffusion exponent D with Pasquill's table.

Pasquill category	P	δ_1	δ_2	Surface roughness, z_o					
				Interpolating function			Pasquill's table		
				0.01 m	0.1 m	1. m	0.01 m	1 m	1. m
A	0.6	0.762	0.0957	0.943	0.902	0.829	0.94	0.90	0.83
B	1.6	0.693	0.1039	0.890	0.845	0.766	0.89	0.85	0.77
C	2.6	0.644	0.1080	0.848	0.802	0.720	0.85	0.80	0.72
D	3.6	0.604	0.1108	0.813	0.766	0.681	0.81	0.76	0.68
E	4.6	0.562	0.1128	0.775	0.727	0.641	0.78	0.73	0.65
F	5.6	0.502	0.1145	0.718	0.669	0.582	0.72	0.67	0.58

Table A-5 compares the C coefficients found from equations (A-95), (A-96), and (A-98), neglecting C_m to produce units of kilometers comparable to Pasquill's. Agreement is good, with some differences attributable to round-off. The results for Pasquill categories B (z_o = 0.01 m) and E (z_o = 1.0 m) show the greatest disagreement. The value for E produces 6-percent differences in vertical diffusion from Pasquill's.

Thus, the parameterized equations for C and D are good interpolators of diffusion for surface roughness and Pasquill parameter variations. The percentage differences from Pasquill's original results are not significant. Uncertainties in the choice of a surface roughness for particular terrain are at least 10 percent. Diffusion coefficients should not be extrapolated for surface roughness of 5 m or larger, however. Comparisons with Pasquill's graphs show errors increasing rapidly above this surface roughness. Similarly, comparisons for Pasquill parameters less than 0.2 show that the interpolation equations underestimate Pasquill's C coefficients by 10 to 30 percent in this region of extreme instability.

Finally, table A-6 gives the results of table A-5 for C converted to units of meters by equation (A-96). These are the values used in COMBIC. They can be compared directly with the COMBIC82 values in table A-3.

Pasquill found horizontal (crosswind) diffusion to be virtually independent of surface roughness. The coefficients A in equation (A-86) were fit, therefore, only to the Pasquill parameter based on the tabulated coefficients found in Hansen's work (1979). The result is

$$A(P) = 0.1754 - 0.018P + 0.2535e^{-0.1578P^2}. \qquad \text{(A-99)}$$

Table A-7 lists the interpolation results compared with Hansen's suggested values. The agreement is excellent.

A-4 COMBIC Model for Buoyant Rise

The rise and stabilization of warm obscurant clouds due to buoyancy (that is, the difference in air density or temperature inside and outside the

Table A-5. Comparison of interpolating functions for vertical diffusion coefficients C with Pasquill's table.

Pasquill category	P	Surface roughness, z_o					
		Interpolating function			Pasquill's table		
		0.01 m	0.1 m	1.0 m	0.01 m	0.1 m	1.0 m
A	0.6	0.103	0.138	0.193	0.102	0.140	0.190
B	1.6	0.060	0.080	0.110	0.062	0.080	0.110
C	2.6	0.042	0.056	0.076	0.043	0.056	0.077
D	3.6	0.029	0.038	0.051	0.029	0.038	0.050
E	4.6	0.017	0.022	0.029	0.017	0.023	0.031
F	5.6	0.0095	0.012	0.016	0.009	0.012	0.017

Table A-6. Comparison of interpolating functions for vertical diffusion coefficients C when X is meters.

Pasquill category	P	Surface roughness, z_o					
		EOSAEL84 COMBIC diffusion coefficient C			Pasquill's table converted to X in meters		
		0.01 m	0.1 m	1.0 m	0.01 m	0.1 m	1.0 m
A	0.6	0.153	0.272	0.629	0.154	0.279	0.615
B	1.6	0.128	0.233	0.554	0.132	0.225	0.539
C	2.6	0.120	0.220	0.526	0.121	0.223	0.532
D	3.6	0.106	0.191	0.462	0.108	0.199	0.456
E	4.6	0.080	0.145	0.346	0.078	0.149	0.348
F	5.6	0.067	0.118	0.287	0.062	0.117	0.309

Table A-7. Comparison of interpolating function and crosswind diffusion coefficients A of Hansen.

Pasquill category	P	Interpolating function $A(P)$	Hansen's suggested A coefficients
A	0.6	0.404	0.40
B	1.6	0.316	0.32
C	2.6	0.216	0.22
D	3.6	0.143	0.143
E	4.6	0.102	0.102
F	5.6	0.076	0.076

clouds) are very much influenced by the local temperature gradient and turbulent diffusivity of the atmosphere. A warm volume of air, whether natural or due to an exothermic obscurant source, will rise and expand through entrainment of ambient air. Entrainment and mixing cool the volume and make it more dense. If the volume eventually comes to equilibrium with surrounding air, it will cease to rise, perhaps overshooting the equilibrium point at first. This phenomenon is particularly prevalent at night, when the earth has cooled by radiation to a temperature below that of the air above it, and the sensible heat flux from the surface is negative (downward).

Increasing ambient air temperature with height increases the stability and produces an eventual equilibrium of a rising warm volume. The reverse is true during daylight hours, when the sensible heat flux becomes positive (upward). A volume of ambient air raised somewhat into cooler surrounding air will acquire buoyancy, thus promoting a further rise, and hence the conditions are termed unstable.

The atmosphere is not a quiescent fluid, however. Unstable conditions and low windspeeds produce warm rising columns of air near the surface. Cooler air convects to replace it. Increasing windspeed also promotes mixing (mechanical turbulence), which tends to drive the atmosphere to more neutral conditions. This turbulence produces a local eddy diffusivity that will tend to break up and halt the rise of slightly buoyant volumes.

Buoyant rise is described through a set of three differential equations and several constitutive relations. Hoock and Sutherland [1982] compared numerical solutions with analytic approximations to the differential equations with respect to the methods used in earlier EOSAEL models. The analytic solutions, attributable to Morton, Taylor, and Turner (1956), and to Briggs (1969), were found to be adequate under the assumption of a constant stability parameter (that is, constant change in air temperature with height). They were insufficient, however, to account for the early formation of dust from high explosives and for more general initial velocity conditions. Therefore, since the EOSAEL84 version, COMBIC now solves the differential equations directly. The following sections derive the equations and show the differences from the earlier version. Much of the work of this section parallels and was heavily influenced by the work of Weil (1982), which compares similar differential equations to the approximate buoyancy solutions. Weil compared plume rise from diesel fires with the database on stack effluents and found good model agreement. He also performed limited analysis of data from high-explosive dust tests.

A-4.1 Differential Equations for Rise and Advection

The rise of a warm mass of air m (in grams) at temperature T (in kelvins) in an ambient atmosphere of temperature T_a is governed by conservation of mass, momentum, and energy. We first consider energy conservation. Throughout this section, the term "thermal volume" refers to the warm mass of air, regardless of shape, for which the rise and expansion is to be found.

If an increment of ambient air dm is entrained into the thermal volume, the change in internal energy of the thermal volume is balanced by the work performed:

$$\begin{aligned} dU &= mC_V dT + (T - T_a)C_V\, dm \\ &= dQ - P\, dV, \end{aligned} \tag{A-100}$$

where C_V is the specific heat of air at constant volume, dQ is the thermal energy, P is the pressure, and dV is the volume change in the region. We assume that the expansion is adiabatic, so the change dQ is zero. The work done can be rewritten with the equation of state and the adiabatic assumption, resulting in

$$PdV = -C_V \left(\frac{\gamma - 1}{\gamma}\right) \frac{mT}{P} dP. \tag{A-101}$$

The γ factor is the ratio of specific heats of air at constant pressure to that at constant volume and is approximately 1.41. Substitution of equation (A-101) into (A-100) and collection of terms leads to a basic differential equation for temperature:

$$\left(\frac{\gamma - 1}{\gamma}\right) \frac{dP}{P} = \frac{dT}{T} + \left(1 + \frac{T_a}{T}\right) \frac{dm}{m}. \tag{A-102}$$

Although this form could be used directly, it is more convenient to eliminate the pressure term. A model used by Thompson (1982; 1979) for the rise of thermal fireballs assumes that

$$P(z) = P_o e^{-z/H_p}, \tag{A-103}$$

where H_p is a reference height, about 8400 m, specified more explicitly by

$$H_p = \left(\frac{\gamma - 1}{\gamma}\right) \frac{C_P T_a}{g}, \tag{A-104}$$

and g is acceleration due to gravity (9.8 m / s^2). With equation (A-103), the temperature equation takes on the form used by Thompson:

$$\frac{1}{T}\frac{dT}{dt} = \left(\frac{T_a}{T} - 1\right) \frac{1}{m}\frac{dm}{dt} - \left(\frac{\gamma - 1}{\gamma}\right) \frac{w}{H_p}, \tag{A-105}$$

where t is time and w is vertical velocity of the thermal volume. A still more convenient form to use with the COMBIC boundary layer model results from introducing the static stability parameter s (in units of s^{-2}). The static stability parameter should not be confused with the dynamic Pasquill stability class (Hanna and Hosker, 1982). The parameter s is defined by the temperature gradient of the atmosphere with height,

$$\begin{aligned} s &= \frac{g}{T_a}\frac{d\theta}{dz} \\ &= \frac{g}{T_a}\frac{dT_a}{dz} + \left(\frac{\gamma - 1}{\gamma}\right) \frac{g}{H_p}, \end{aligned} \tag{A-106}$$

where θ is the potential temperature and z is height. Under perfectly neutral conditions, s is identically zero. The change in temperature with height is then the natural adiabatic lapse rate of -0.0098 °C / m. In terms of s, equation (A-105) can be written in the form

$$\frac{d}{dt}\frac{T}{T_a} = \left(1 - \frac{T}{T_a}\right) \frac{1}{m}\frac{dm}{dt} - \frac{s}{g}\left(\frac{T}{T_a}\right) w. \tag{A-107}$$

An advantage of using this differential equation is the convenience of the variables' mass, vertical velocity, and the ratio of the mean temperature inside the thermal volume to that of ambient air.

The second differential equation is derived from conservation of momentum. The change in momentum of the rising thermal volume is balanced against all external forces on the volume. COMBIC includes three: buoyancy, drag, and momentum entrainment:

$$\frac{d(mw)}{dt} = m_a g - mg + w_a \frac{dm}{dt} - \frac{1}{2} C_D \rho_a A_\perp (w - w_a)|w - w_a|. \qquad \text{(A-108)}$$

The buoyant force is the difference in weight mg of the thermal volume and the weight $m_a g$ of the same volume of ambient air. The drag term includes the empirical coefficient C_D of 0.8, a value suggested by Thompson (1979) as representative for tactical high explosives. Also included are the component of the volume's area perpendicular to the motion and the density ρ_a of the ambient air. The drag term is proportional to the square of the difference in the upward velocity (w) of the thermal volume and the upward velocity (w_a) of the air outside the volume. For most applications, the latter is zero. For dust generated from a buried high explosive, however, there is a rapid upward ballistic flow of soil from the crater, up to 20 m/s and lasting 1 to 2 s. The drag term partly accounts for the momentum imparted by the soil to the thermal volume, given a model of the upward soil velocity as a function of time. The absolute value is necessary only to ensure that the drag force operates in the correct direction, opposing the motion of the thermal volume relative to outside air. The remaining term accounts for the direct entrainment (dm/dt) of outside air of nonzero velocity (if any) w_a.

A similar momentum equation is used for the horizontal component of the motion of the thermal volume:

$$\frac{d(mu)}{dt} = u_a \frac{dm}{dt} - \frac{1}{2} C_D \rho_a A_\perp (u - u_a)|u - u_a|, \qquad \text{(A-109)}$$

where u is the horizontal velocity of the thermal volume and u_a the horizontal windspeed outside the volume. This is an especially convenient way to advect the thermal volume in the ambient wind u_a.

We rewrite the momentum equations below to include the same variables as in the energy equation (A-107). The third and final equation, needed to rewrite equation (A-108) and equation (A-109), describes the mass balance. The mass of the thermal volume increases by entraining air from outside. Entrainment is fundamentally an empirical notion. The assumption, put forth by Taylor (1945), is that the rate of mass entrainment is proportional to the product of the surface area A of the thermal volume and the relative velocity between inner and outer regions:

$$\frac{dm}{dt} = \alpha \rho_a A |\vec{v} - \vec{v}_a|, \qquad \text{(A-110)}$$

where α is the entrainment coefficient. Written in terms of mass instead of area, this becomes

$$\frac{1}{m}\frac{dm}{dt} = \mu\frac{\rho_a}{\rho}\frac{|\vec{v} - \vec{v}_a|}{R}, \tag{A-111}$$

where μ is a suitably redefined entrainment coefficient in terms of α. The vector difference is between the velocity v of the thermal volume and the velocity v_a of outside air. Similarly, the ratio of densities ρ is between the outer and inner regions. The vectors $\vec{v}$ and $\vec{v}_a$ have vertical components w and w_a, and horizontal components u and u_a appearing in equations (A-108) and (A-109). The vectors can even have some crosswind components. The term $\vec{v}$ can be thought of as the wind blowing around the puff.

The equations thus far are very general. They apply equally well to instantaneous puffs and continuous plumes. The entrainment and drag terms, however, refer explicitly to surface areas in contact with outside air. Thus the geometries of puffs and plumes must be handled separately. The empirical entrainment coefficient also varies with geometry.

COMBIC models instantaneous thermal fireballs as spheroids with horizontal radius R_h and vertical radius R_z. The mass is defined by

$$m_t = \frac{4}{3}\pi R_h^2 R_z \rho, \tag{A-112}$$

where the subscript t refers to these instantaneous "thermals," the historic term given to rising spherical regions. The surface area of a spheroid is

$$A_t = 2\pi R_h^2 \begin{cases} 1 + \frac{\sin^{-1}[(1-e^2)^{1/2}]}{e(1-e^2)^{1/2}} & (0 < e < 1) \\ 2 & (e = 1) \\ 1 + \frac{\ln[e+(e^2-1)^{1/2}]}{e(e^2-1)^{1/2}} & (e > 1) \end{cases}, \tag{A-113}$$

where e is the ratio R_h / R_z, separating cases of prolate ($e > 1$) from oblate ($e < 1$) spheroids. The entrainment coefficient used in equation (A-111) for thermals is

$$\mu = 3\alpha_t, \tag{A-114}$$

where α_t is 0.25, taken from lab and field experiments (Weil, 1982; Turner, 1969). The $1/R$ term in equation (A-111) is thus one-third the area to volume ratio:

$$\frac{1}{R} = \frac{A_t}{4\pi R_h^2 R_z}. \tag{A-115}$$

A continuous plume is modeled as a sequence of disk-like regions formed by slices taken perpendicular to the plume centerline axis. The thickness of each slice is defined as

$$\triangle L = |\vec{v}|\ \triangle t, \tag{A-116}$$

where $\triangle t$ is a constant time step used in solving the differential equations; for convenience, let us say the time step is 1 s, and v is the velocity of the

plume mass at each new slice position along the plume; i.e., v is the velocity along the centerline of the plume. (Remember, not all plumes are horizontal.) For constant thermal production, then, each slice in sequence along the plume axis results from extrapolation, via the differential equations, one time step forward from the previous slice. The mass in a slice and the area of the ring in contact with outside air are

$$m_p = \pi \rho R^2 \triangle L \tag{A-117}$$

and

$$A_p = 2\pi R \triangle L. \tag{A-118}$$

The entrainment coefficient is known to vary with the angle of the plume centerline axis from the vertical. A vertical plume has

$$\mu = 2\alpha_{pv}, \tag{A-119}$$

with α_{pv} = 0.116 (Weil, 1982; Turner, 1969). A horizontal or "bent" plume (the only plume type treated in the EOSAEL82 COMBIC plume rise model) has an entrainment coefficient

$$\mu = 2\alpha_{ph}, \tag{A-120}$$

where α_{ph} = 0.60 (Briggs, 1969; Hoult *et al*, 1969). For intermediate cases, COMBIC uses an effective plume entrainment coefficient similar to that of Hoult, Fay, and Forney (1969), which is consistent with the EOSAEL FITTE fire plume model:

$$\mu = 2\left[\alpha_{pv}\left(\frac{w}{v}\right)^2 + \alpha_{ph}\left(\frac{u}{v}\right)^2\right]. \tag{A-121}$$

With these definitions and with the important assumption of pressure equilibrium between the thermal volume and the outside air,

$$\rho T = \rho_a T_a, \tag{A-122}$$

the momentum equations can be simplified to determine the velocity changes at each time step:

$$\frac{dw}{dt} = \left(\frac{T}{T_a} - 1\right) g - \frac{1.4}{m}\frac{dm}{dt}(w - w_a) \tag{A-123}$$

and

$$\frac{du}{dt} = -\frac{1.4}{m}\frac{dm}{dt}(u - u_a). \tag{A-124}$$

In summary, the COMBIC buoyancy model solves equations (A-107), (A-111), (A-123), and (A-124) for the quantities

$$\frac{d}{dt}\left(\frac{T}{T_a}\right), \quad \frac{1}{m}\frac{dm}{dt}, \quad \frac{dw}{dt}, \quad \text{and} \quad \frac{du}{dt} \tag{A-125}$$

from which T, m, w, u, z, and x are updated at each time step. The mass definitions, equations (A-112) and (A-117), are used to find the new radii at each time step. Equation (A-122) and the atmospheric boundary layer model for ambient temperature and density are used at the new height to determine the thermal volume density ρ. In all, the process is straightforward and efficient, with computation times that are very competitive with the EOSAEL82 analytic model.

A-4.2 Adjustments, Initial Conditions, and Scaling in Buoyancy Model

Adjustment can be made for the effect of obscurant mass m_a on the changes in vertical velocity w:

$$\left(\frac{dw}{dt}\right)_{corr} = \left(\frac{m}{m+m_a}\right)\frac{dw}{dt} - \left(\frac{m_a}{m+m_a}\right)g. \qquad \text{(A-126)}$$

The obscurant mass does not enter into the energy or entrainment equations. The magnitude of this aerosol correction is usually small. For example, 10 kg of obscurant initially in a sphere of radius 2 m represents only 20 percent of the total mass of obscurant plus air in the sphere. This percentage then rapidly decreases as the region grows, entraining 1.2 kg for every cubic meter of air.

The temperature used in the differential equations is the mean value for the thermal volume. It is often of interest, however, to have an estimate of the expected peak temperature. Analysis (Hoock and Sutherland, 1982) and comparison with data indicate that a reasonable estimate for the peak temperature T_{peak} in HE, WP, and diesel fire plumes in terms of the mean temperature T and the ambient air temperature T_a is given by

$$T_{peak} = \left(\frac{0.4T_a}{T_a - 0.6T}\right)T \qquad \text{(A-127)}$$

for mean temperatures less than $1.66T_a$. This is easily derived from the often used assumption that the air density defect is Gaussian about a central minimum value (Turner, 1969; Batchelor, 1954; Turner, 1962; Richards, 1963):

$$\rho(r) - \rho_a = [\rho(0) - \rho_a]e^{-(\frac{r}{b})^2}. \qquad \text{(A-128)}$$

The mean value of ρ is found by averaging over the buoyancy radius R:

$$\begin{aligned}
\rho_{ave} &= (\pi R^2)^{-1}\int_0^R 2\pi r\rho(r)\ dr \\
&= \rho_a + [\rho(0) - \rho_a](\pi R^2)^{-1}\int_0^R 2\pi r e^{-\left(\frac{r}{b}\right)^2} dr \\
&= \rho_a + \left(\frac{b}{R}\right)^2\left[1 - e^{-\left(\frac{R}{b}\right)^2}\right][\rho(0) - \rho_a]. \qquad \text{(A-129)}
\end{aligned}$$

From the pressure equilibrium condition (eq A-122),

$$\rho_{ave} T = \rho_a T_a = \rho(0) T_{peak}. \tag{A-130}$$

The mean temperature T is related to the peak temperature by substitution of equation (A-130) into equation (A-129):

$$\frac{1}{T} = \frac{1}{T_a} + \left(\frac{b}{R}\right)^2 \left[1 - e^{-\left(\frac{R}{b}\right)^2}\right] \left[\frac{1}{T_{peak}} - \frac{1}{T_a}\right]. \tag{A-131}$$

Given T_{peak}, T, and T_a, then b is determined from R. The parameter b affects only the peak temperature printed out from Phase I calculations. It does not otherwise affect internal model calculations. Equation (A-127) results from the COMBIC default value of b/R = 0.669. This ratio approximates Turner's value of 0.633 and is consistent with the 1250 K peak temperature of the FITTE modeled fire plume.

COMBIC uses default values for Q, the thermal energy per unit obscurant or explosive mass, and assumes that T is initially $1.44T_a$. This determines an initial buoyancy radius. For thermal puffs,

$$R = \left[\frac{3WQT}{4\pi\rho_a T_a C_P (T - T_a)}\right]^{1/3}. \tag{A-132}$$

For continuous plumes,

$$R = \left[\frac{\dot{m}_{obs} QT}{\upsilon\pi\rho_a T_a C_P (T - T_a)}\right]^{1/2}. \tag{A-133}$$

For model generality, the user may optionally input all but one of the values: the initial buoyancy radius R, the initial temperature T, the thermal energy Q per unit mass of obscurant or explosive, and the initial upward velocity v. Equations (A-132) and (A-133) are used to find the unknown.

Thompson (1980b) employs correction factors for the temperature dependence of the specific heat of air and modifies the entrainment coefficient for the low plume density. COMBIC assumes that these modifications are negligible, except within the first meter(s) of a large fire. In addition, COMBIC does not directly include the radiative losses of very-high-temperature plumes. Weil (1982) suggests that 50 percent of the potential diesel oil fire energy is lost to a combination of incomplete combustion and radiation near the flames. COMBIC uses this 50-percent factor to modify the buoyancy source term for diesel / motor-oil / rubber fires.

A jet is a plume injected into the atmosphere with high velocity. For nonthermal jets, the initial flux (mass of air and obscurant per unit area per unit time), the starting radius, and the initial velocity are all related. By default, COMBIC uses stored initial velocities (if any) and radii. The user may optionally provide these values.

Drag and entrainment slow and expand the jet. A vertical velocity may induce positive or negative buoyancy depending on the static stability parameter s. Models for estimating the static stability parameter are discussed in section 1.9 of the main report.

Scaling the effects of buoyancy on obscurant rise is an important function in COMBIC. The Phase I calculations are for a single thermal production value. For plumes, the thermal production rate is taken to be that of the geometric mean between the maximum rate and the rate averaged over the entire burn duration, that is,

$$\dot{Q}_m = \left(\frac{\dot{m}_{max} M_{tot}}{T_{burn}} \right)^{1/2} Q. \tag{A-134}$$

For continuous plume elements that have an actual thermal production $\dot{Q}$ different from $\dot{Q}_m$, the scaled height is then

$$z = \left(\frac{\dot{Q}}{\dot{Q}_m} \right)^{1/3} z_m, \tag{A-135}$$

where z_m is the plume height determined in Phase I from the mean production rate $\dot{Q}_m$.

Similarly, the scaled height for puff rise is

$$z = \left(\frac{Q}{Q_m} \right)^{1/4} z_m. \tag{A-136}$$

The height z_m is that associated with Phase I calculations for a total puff of thermal energy Q_m. This is used in Phase II calculations for extending Phase I histories to obscurant sources approximately one-third to three times as large as those treated in the Phase I calculation. Phase II takes such scaling into account automatically. The Q_m value is passed in the data file to Phase II.

These results are easily linked to the analytic approximation of Morton, Taylor, and Turner (1956) used in EOSAEL82 COMBIC. If we neglect drag and momentum entrainment terms, equation (A-123) can be differentiated once with time and equation (A-107) substituted for the temperature derivative:

$$\begin{aligned} \frac{d^2}{dt^2}(mw) &= mg \frac{d}{dt}\left(\frac{T}{T_a} \right) + \left(\frac{T}{T_a} - 1 \right) g \frac{dm}{dt} \\ &= -s(mw)\left(\frac{T}{T_a} \right). \end{aligned} \tag{A-137}$$

The EOSAEL82 rise model used the assumptions of Morton, Taylor, and Turner (1956) that

a. the stability parameter is constant, taken to be the average value over the region of plume rise;

b. the temperature ratio in equation (A-137) can be set to unity, which is also called the "Boussinesq approximation," and

c. the density ratio in the entrainment equation (A-111) can similarly be set to one.

With these restrictive assumptions, the solution of equation (A-137) is simply that of a harmonic oscillator. For a stable atmosphere, the parameter s, defined in equation (A-106), is positive. The result is

$$mw = m_o w_o \cos\left(s^{1/2}t\right) + \frac{F\pi\rho}{s^{1/2}} \sin\left(s^{1/2}t\right) \tag{A-138}$$

where for puffs,

$$F = \frac{MQg}{\pi C_P \rho_a T_a}, \tag{A-139}$$

and M is the mass (in grams) of obscurant in the puff producing Q cal/g. For plumes,

$$F = \frac{\dot{m}Qg}{\pi C_P \rho_a T_a}. \tag{A-140}$$

The square root of s is called the Brunt-Vaisala frequency; $\dot{m}$ is the mean production rate of obscurant (in grams per second) producing Q cal/g of heat.

F has units of m^4/s^2 for puffs and m^4/s^3 for plumes. The difference in units arises because the plume masses m and m_o (the initial mass) are for elements or slices of the plume that are moving with velocity w, that is, a mass flux.

The entrainment equation (eq (A-110)) under the above assumptions leads directly to the solution

$$r = \alpha z, \tag{A-141}$$

where $r = 0$ at $z = 0$. If we neglect the initial momentum term and substitute equation (A-138), the solution for the thermal puff is simply

$$mw = \frac{4}{3}\pi\rho\alpha_T^3 z^3 \frac{dz}{dt}. \tag{A-142}$$

This results from equation (A-138) in an expression for cloud centroid height:

$$z = \left(\frac{3MQg}{\pi\alpha_T^3 \rho_a T_a C_P s}\right)^{1/4} \left[1 - \cos\left(s^{1/2}t\right)\right]^{1/4}. \tag{A-143}$$

For bent plumes, however,

$$mw = \pi\rho\alpha_{ph}^2 z^2 u \frac{dz}{dt}. \tag{A-144}$$

This results in a somewhat different expression for cloud height:

$$z = \left(\frac{3\dot{m}_{obs} Q g}{\pi \alpha_{ph}^2 \rho_a u T_a C_P s} \right)^{1/3} \left[1 - \cos\left(s^{1/2} t \right) \right]^{1/3}. \qquad \text{(A-145)}$$

The scaling exponents, 1/3 for continuous plumes and 1/4 for puffs, which are used in COMBIC via equations (A-135) and (A-136), are thus demonstrated.

Low windspeeds and large, hot buoyancy regions are associated with plumes that are more vertical than horizontal in their motion. A plume is considered vertical in COMBIC as long as

$$\frac{dz}{dx} > 1. \qquad \text{(A-146)}$$

This assumption is equivalent to the condition that the plume axis is tilted at an angle less than 45° from the vertical. At the point where the plume bends over and no longer satisfies equation (A-146), COMBIC stores the time of rise t_c, the downwind distance x_c, the height z_c, and the sigmas σ_x, σ_y. Up to this point, the plume is considered to be Gaussian distributed in concentration perpendicular to the near-vertical plume axis. Thus, plume slices are nearly horizontal.

During the vertical rise phase, equation (A-4) is modified to describe the concentration as Gaussian distributed horizontally in x and y. The plume velocity replaces the wind velocity in equation (A-4). Obscurant from the vertical phase is assumed to act as an effective source at x_c, z_c, t_c for the "bent-plume" phase. The vertical rise phase is not applicable for obscurant clouds that never satisfy equation (A-146).

The end of puff and plume rise is determined by at least three factors. First, the thermal volume can come into buoyant equilibrium with the ambient atmosphere. This condition will occur if the atmosphere is stable, in which case the thermal region becomes less buoyant with height. Second, stabilization occurs if a strong inversion exists, creating a locally stable layer. Third, rise will cease when the rate of energy dissipation by the ambient atmosphere becomes comparable to the thermal volume kinetic energy. These conditions are given mathematically at the end of section A-5.

A-5 The COMBIC Boundary Layer Model

COMBIC requires the user to input a set of meteorological parameters at a single reference height (default 10 m). The boundary layer model then produces vertical temperature, density, and windspeed profiles that are physically consistent with the user inputs and that are necessary for transport, diffusion, and buoyancy calculations.

Required user inputs, in order of importance to transport and diffusion, are

1. windspeed u_r (in meters per second) at reference height z_r;
2. wind direction θ_w, the compass heading (in degrees), from which the wind blows;
3. Pasquill stability category, denoted on input as 1 through 7 for categories A through G;
4. temperature T_r (in kelvins) at reference height z_r;
5. pressure p_r (in millibars) used to generate a starting density;
6. relative humidity (percent), which is important for effects on obscurants but not on diffusion.

In COMBIC92, optional user inputs are allowed to better define the environmental inputs and model in terms of

1. reference height z_r (in meters, default 10 m);
2. surface roughness length z_o (in meters, default 0.1 m);
3. height of temperature inversion h_i (in meters, default to internal model);
4. choice of vertical temperature profile models: average stability parameter (i.e., constant with height), or varying stability parameter profile approaching neutral with height (default).

The user can also choose to have the Pasquill stability category computed from a set of input observations, including

1. ceiling height (in meters) of the lowest cloud layer (only two categories matter, however: above 2000 m or below);
2. cloud cover (percent) (only conditions with greater than or less than 50 percent matter to the model);
3. Julian date (1 to 365);
4. longitude of site (in degrees) with the west longitude positive;
5. time of day (local standard time in hours and fractional hours);
6. ground conditions (1 = bare ground; 2 = snow patch, $<$6 in.; 3 = snow $>$6 in. deep);
7. surface roughness length (in meters).

This widely used procedure to determine Pasquill category is documented fully elsewhere (Hansen, 1979; Pasquill, 1961). Briefly, the method uses date, longitude, and local time to determine a solar elevation angle (Woolf, 1968). Cloud cover and solar elevation determine a net radiation index

(NRI). The NRI is modified for ceiling height if the cloud cover exceeds 40 percent. Windspeed and NRI are then used in a table lookup of the Pasquill stability category.

Surface roughness z_o (in meters) became an accessible variable in COMBIC92, with a default value of 0.1 m. As shown in section A-3 (table A-3), changes in surface roughness of an order of magnitude produce significant changes in diffusion. Surface roughness also affects wind and temperature profiles with height and other meteorological quantities near ground level. A rule of thumb for estimating z_o is to take 10 to 20 percent of the highest local terrain and vegetation features upwind of the plume and over the plume path. Table A-2 gives representative examples of surface roughness values. While errors of a factor of 2 are not particularly significant in effects of z_o, factors of 10 may be significant.

The reference height z_r (in meters) is arbitrary in COMBIC92. A common height for measured winds and temperature is 10 m, the model default. The user is allowed to change that reference height, but the user should avoid a reference height that is either too high or too low (particularly one approaching the surface roughness length).

The boundary layer model for vertical temperature and winds is based on a nomogram first published by (Pasquill 1974) from the unpublished work of F. B. Smith. That nomogram, used in EOSAEL82 COMBIC, relates the Pasquill category to the sensible heat flux from the surface and to the windspeed at a 10-m height. The surface roughness was fixed at 0.1 m. Since EOSAEL84, the COMBIC model has used an extension of the nomogram, derived by Sutherland and Bach (1984) and based, in part, on more recent published results by Smith (1979). This extended nomogram allows for arbitrary surface roughness, reference height, and a variable Pasquill stability parameter.

We define the Pasquill stability class to be a continuous parameter P that differs from the user input stability category value P_c by

$$P = P_c - 0.4. \tag{A-147}$$

The user inputs a value of P_c that follows the following alphabetic sequence:

Category	Decimal representation	Meaning
A	1.	very unstable
B	2.	moderately unstable
C	3.	slightly unstable
D	4.	neutral
E	5.	slightly stable
F	6.	moderately stable

Since the Pasquill categories are now input as decimal values, users can now interpolate between categories by using fractions.

P is further related to a modified Kazanski-Monin parameter, K_m, by

$$P = 3.6e^{+K_m}. \tag{A-148}$$

The modification to K_m accounts explicitly for surface roughness z_o, sensible heat flux H (in watts per square meter, positive upward), the wind friction velocity u_* (in meters per second), the ambient air temperature T_a (in kelvins), and the air density ρ_a (in grams per cubic meter):

$$K_m = -gk^2 H \left[2\Omega_c \rho_a C_P T_a u_*^2 a \ln(b/z_o)\right]^{-1}. \tag{A-149}$$

The empirical constants a and b have been determined (Sutherland and Bach, 1984) to be 10.0 and 7.5 m, respectively. The constants Ω_c and C_P are the angular rate of rotation of the earth (7.273×10^{-5} rad / s) and the specific heat of air at constant pressure (1.013 J / g K). Von Karman's constant k is 0.4, and g is 9.8 m / s^2.

During a clear day, the sensible heat flux becomes positive (upward) and K_m becomes negative. The atmosphere is then neutral to unstable. At night, the reverse is true. The crossover point ($K_m = 0$) is at the Pasquill stability parameter P value of 3.6, within the neutral category D (3 to 4) range.

Sensible heat flux H is not easily measured and thus cannot be required as a user input. However, if H were easily measured, it would be a logical replacement for the Pasquill stability parameter in determining K_m. The wind friction velocity u_* must also be determined for equation (A-149). Both of these parameters are found from the user input windspeed and temperature as follows.

The wind friction velocity u_* is related to the input windspeed u_r at reference height z_r by (Hanna and Hosker, 1982)

$$u_* = k u_r \left[\ln\left(\frac{z_r}{z_o}\right) + f\left(\frac{z_r}{L}\right)\right]^{-1}, \tag{A-150}$$

where L is the Monin-Obukhov length (in meters). The function f is defined by Hanna et al (1982) as

$$f(z/L) = \begin{cases} 5z/L & \text{(stable, } 4 < P\text{)} \\ 0 & \text{(neutral, } 3 < P < 4\text{)} \\ -\ln\left(\frac{1+\Psi^2}{2}\right) - 2\ln\left(\frac{1+\Psi}{2}\right) + 2\tan^{-1}\Psi - \pi/2 & \text{(unstable, } P < 3\text{),} \end{cases} \tag{A-151}$$

where

$$\Psi = (1 - 15z/L)^{1/4}. \tag{A-152}$$

The Monin-Obukhov length, L, is determined from (Hanna and Hosker, 1982)

$$L = -\frac{\rho_a C_P T_a u_*^3}{gkH}. \tag{A-153}$$

Substituting from equations (A-148) and (A-149) and eliminating H, we obtain

$$L = u_* k [2\Omega_c a \ln(b/z_o) \ln(P/3.6)]^{-1}. \tag{A-154}$$

L has the same sign as K_m. The absolute value of the Monin-Obukhov length is an estimate of the depth of the mechanically mixed layer near the surface. For neutral conditions L is infinite, for stable conditions L is positive, and for unstable conditions L is negative. The sign appears through the logarithmic term in P in equation (A-154).

Since equations (A-150) and (A-154) contain only the unknowns u_* and L, they can be solved simultaneously. For unstable conditions, this is done by iteration, that is, relaxation. The starting value for L is taken to be the estimate suggested by Irwin (Hansen, 1979; Irwin, 1979):

$$L^{-1} = m z_o^n, \tag{A-155}$$

with constants m and n given by -0.114 and -0.103 for Pasquill category A; -0.038 and -0.171 for category B; and -0.008 and -0.305 for category C, respectively. The iteration rapidly converges, with u_* determined from equation (A-150) and then placed into equation (A-154) to produce a revised L for use again in equation (A-150).

For neutral conditions, L is infinite. Trivially,

$$u_* = \frac{u_r k}{\ln\left(\frac{z_r}{z_o}\right)}. \tag{A-156}$$

For stable conditions, substituting equation (A-154) into equation (A-150) produces

$$u_* = \frac{u_r k^2 - 10 z_r \Omega_c a \ln\left(\frac{b}{z_o}\right) \ln\left(\frac{P}{3.6}\right)}{k \ln\left(\frac{z_r}{z_o}\right)}. \tag{A-157}$$

The u_* from equation (A-157) is cut off at a minimum of two-thirds the neutral value from equation (A-156) for physical consistency. A final value of L is then obtained from equation (A-154).

The vertical windspeed profile for the constant values of u_* and L is then defined to be purely a function of height:

$$u = \frac{u_*}{k}\left[\ln\left(\frac{z}{z_o}\right) + f\left(\frac{z}{L}\right)\right], \tag{A-158}$$

with $f(z/L)$ determined from equations (A-151) and (A-152).

For puffs and plumes well above the surface, the puff centroid height or plume centerline height z_c is used in equation (A-158) for determining the

windspeed. But for puffs and plumes touching the surface, the larger of $1.1z_o$ and the cloud center of mass height z_{cm} is used. This height is given by

$$z_{cm} = \bar{z} + \frac{\sigma_z \exp\left[-\frac{1}{2}\left(\frac{\bar{z}}{\sigma_z}\right)^2\right]}{(2\pi)^{1/2}\Phi\left(\frac{z_c}{\sigma_z}\right)}; \tag{A-159}$$

Φ is the cumulative normal distribution.

Figure A-9, which shows the relation between u_r, P, and H, is worth studying. Higher windspeeds promote mixing and thus more neutral conditions. Higher sensible heat flux H at a given windspeed sets up greater turbulence and lower stability. The values in the region of changeover from H positive (daytime) to H negative (nighttime) are all convergent on neutral stability. However, small changes in H at very low windspeeds near the changeover point result in large stability changes, especially at night. These conditions warrant further research. At present, under these conditions, the COMBIC model can, on occasion, predict obscurant behavior poorly.

The sensible heat flux H is determined from equation (A-149) once u_* has been found. An equation suggested by Smith (1979) relates H (in watts per meter squared) to the global solar irradiance G (in watts per meter squared) during daytime as

$$H = -0.40(G - 100). \tag{A-160}$$

G typically is from 0 to 900 W / m^2. Since global irradiance is sometimes available from field measurements, it is tempting to use it as a COMBIC input to replace P. However, equation (A-160) is an estimate and as such does not include the effects of different states of terrain, wind, etc. Therefore, pending further research or a better model, global irradiance is not an alternative input to COMBIC.

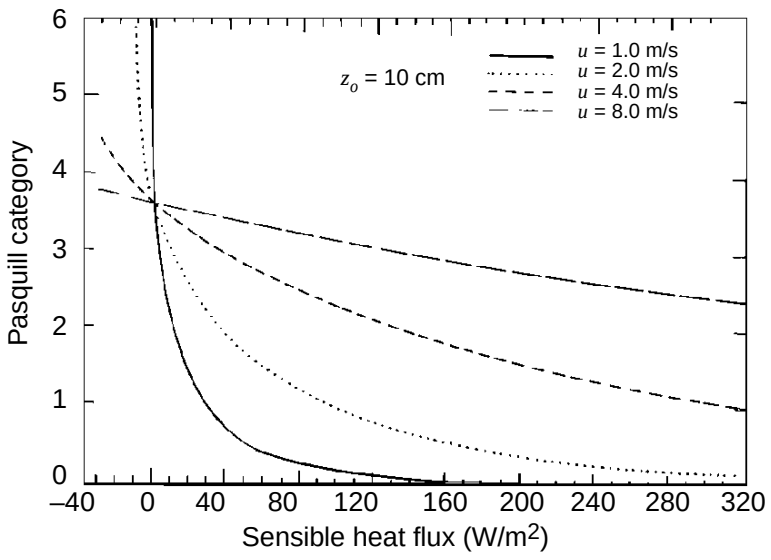

Figure A-9. Stability categories as a function of windspeed and sensible heat flux for given surface roughness.

The surface buoyancy flux is required in estimating the limiting heights of plumes and puffs. It is denoted H_b (m^2/s^3) and is computed from (Hanna and Hosker, 1982)

$$H_b = -\frac{u_*^3}{kL} = \frac{gH}{\rho_a C_p T_a}. \tag{A-161}$$

The final basic profiles are temperature and density. Temperature, found from the static stability parameter s, equation (A-106), is proportional to the Richardson number R_i (Pasquill 1974):

$$s = \frac{g}{T_a}\frac{d\theta}{dz} = R_i \left(\frac{du}{dz}\right)^2, \tag{A-162}$$

where

$$R_i = \frac{z}{L}\left(1 + \alpha\frac{z}{L}\right)^{-1} \tag{A-163}$$

and α = 0 for unstable or 5 for stable conditions. The stability parameter is 0 for neutral conditions. Taking the derivative of equation (A-158) with z, we obtain

$$\frac{du}{dz} = \frac{u_*}{k}\left(\frac{1}{z} + \frac{\alpha'}{L}\right), \tag{A-164}$$

where

$$\sigma' = \begin{cases} 5 & \text{(stable)} \\ 15/(\Psi(1+\Psi)(1+\Psi^2)) & \text{(unstable).} \end{cases} \tag{A-165}$$

Thus,

$$s_z = \frac{u_*^2}{k^2 L z}\begin{cases} (1 + 5z/L) & \text{(stable)} \\ 0 & \text{(neutral)} \\ \left[1 + \frac{15}{\Psi(1+\Psi)(1+\Psi^2)}\right]^2 & \text{(unstable).} \end{cases} \tag{A-166}$$

Both the stable and unstable values of s decrease in absolute value to zero with height. Thus, the profile and stability become increasingly neutral with height. This is a desirable property.

COMBIC includes a boundary layer model option for the definition of s. As discussed in the previous section, the analytic buoyancy solution is strictly true only if the stability parameter is constant with the height. Average values for s are, therefore, optionally computed in the COMBIC boundary layer model. The profile of s falls off by about an order of magnitude (typically between 10 and 50 m) in unstable conditions. These values were chosen as the limits (z_1 = 10 and z_2 = 50) in computing an average s. For stable conditions,

$$\begin{aligned} (\bar{s}) &= \frac{1}{z_2 - z_1}\int_{z_1}^{z_2} s(z)\, dz \\ &= \frac{u_*^2}{k^2 L}\left[\frac{\ln(z_2/z_1)}{z_2 - z_1} + \frac{5}{L}\right]. \end{aligned} \tag{A-167}$$

For unstable conditions, the integral is not trivial. The squared term in equation (A-166) ranges from about 0.25 to 1.0. We take 0.6 as typical. Using this value for unstable conditions, we estimate

$$\bar{s} = 0.60 \frac{u_*^2}{k^2 L} \left[\frac{\ln(z_2/z_1)}{z_2 - z_1} \right]. \tag{A-168}$$

The ambient temperature gradient is (in kelvins per meter)

$$\frac{dt_a}{dz} = \frac{s}{g} T_a - 0.0098. \tag{A-169}$$

This relation is used in the buoyancy model to find temperature change in the ambient atmosphere with height. For the option of a constant s,

$$T_a(z) = 0.0098 g/\bar{s} + (T_r - 0.0098 g/\bar{s})\, e^{\bar{s}(z - z_r)/g}, \tag{A-170}$$

where T_r is the temperature at reference height z_r. For near-neutral conditions, s/g is small. To lowest order in s/g, approximately

$$T_a(z) = T_r + \left(\frac{\bar{s}}{T_r} - 0.0098 \right) (z - z_r). \tag{A-171}$$

In the context of this linear change in temperature with height, a constant stability parameter is sometimes referred to as a constant lapse condition.

The ambient air density profile follows from the derivative of the equation of state. Since T_a is known at each height, a convenient equation for use by the buoyancy model is

$$\frac{d(\rho_a T_a)}{dz} = \frac{1}{R} \frac{dp}{dz} = -\frac{\rho_a G}{R} = -0.0342 \rho_a. \tag{A-172}$$

The starting density is found from the user input pressure p_r (in millibars) from

$$\rho_r = \frac{346.9 p_r}{T_r}, \tag{A-173}$$

where p_r (in grams per cubic meters) and T_r (in kelvins) are for reference height z_r. (The user actually inputs the temperature in degrees Celsius. The input is converted internally to kelvins.)

The mixing layer is usually capped by an inversion (Hanna and Hosker, 1982). This inversion is one of the possible limits on the rise of a buoyant puff or plume. Danard (1984) has reviewed nine methods for estimating the mixing layer height. None was particularly accurate for the 34 measurements used in his comparison. COMBIC now allows the user to input inversion height optionally, if that information is available. Among the best methods examined by Danard is that of Brown (1981), which was chosen for the COMBIC boundary layer model. The inversion height h_i is

$$h_i = \frac{0.3 \pi k u_*}{2 \Omega_c \left[1 + 0.15 f \left(\frac{h_i}{\pi L} \right) \right]}, \tag{A-174}$$

where f is the function defined by equations (A-151) and (A-152). The implicit dependence in equation (A-174) on h_i is weak and converges after a few iterations, with $f = 0$ the starting value. Following Danard, h_i is limited to the range of 688 to 6880 times u_*.

Under stable atmospheric conditions, puffs and plumes reach an equilibrium height at which their temperature equals that of the atmosphere, and thus their buoyancy goes to zero. The maximum rise height can be easily determined for a constant stability parameter s from equations (A-138) through (A-145). The maximum height is above the equilibrium level, however. Generally, the puff or plume overshoots the equilibrium height, then falls back, as can be seen from the equations. The often-cited semi-empirical formulas for rise in a stable atmosphere (Briggs, 1969; Weil, 1982; Hanna and Hosker, 1982) assume an average stability parameter s. For a bent plume, for example, the equilibrium height under stable conditions is

$$h_e = 2.55 \left(\frac{F}{us} \right)^{1/3}, \tag{A-175}$$

where F is from equation (A-140) and s is from equation (A-168). The windspeed u is that at 10 m, the lower height limit of the COMBIC stability parameter average. For an inclined jet, a plume with momentum but little thermal buoyancy the equilibrium height would be (in the notation of sect. A-4.2),

$$h_e = 1.5 \left(\frac{mw}{\pi \rho_a u} \right)^{1/3} s^{-1/6}, \tag{A-176}$$

where m, w, and ρ_a are initial values in the rise equation. For low windspeed, the limited rise of a buoyant vertical plume in stable conditions is

$$h_e = 5.3 F^{1/4} s^{-3/8}. \tag{A-177}$$

For the vertical jet, it would be (again in the notation of sect. A-4.2)

$$h_e = 2.44 \left(\frac{mw}{\pi \rho_a s} \right)^{1/4}. \tag{A-178}$$

The units of F and s are m^4/s^3 and s^{-2}, respectively. The units of m are grams per second by the definition of mass in each plume slice. Thus, mw/ρ is equivalent to $(Rw)^2$, where R is the slice radius. The ρ_a term in place of ρ in equations (A-176) and (A-178) accounts for density differences (Hanna and Hosker, 1982). For thermal puffs in a stable environment,

$$h_e = 2.63 \left(\frac{F}{s} \right)^{1/4}, \tag{A-179}$$

where F, given by equation (A-139), has units of m^4/s^2. These equations for limits in a stable atmosphere are used in COMBIC as estimates of where

the buoyant rise can be expected to end. The solution of the differential equations for rise, of course, comes to a temperature-stabilized equilibrium itself.

Under neutral conditions, the rise height of an inclined jet has been estimated to be (Briggs, 1969; Weil, 1982)

$$h_e = 6R\left(\frac{w}{u} - 1\right), \tag{A-180}$$

where R is the initial radius of the jet, and w and u are the initial upward plume speed and the horizontal windspeed, respectively. Under convective (unstable) atmospheric conditions, a tentative formula for buoyant plumes is (Weil, 1982; Hanna and Hosker, 1982)

$$h_e = 3\left(\frac{F}{u}\right)^{3/5} H_b^{-2/5}, \tag{A-181}$$

where F is the plume buoyancy flux defined by equation (A-140) and H_b is the surface buoyancy flux defined by equation (A-161).

A more general test for the final rise can be applied in all cases and atmospheric conditions. Briggs (1969) has suggested that ambient atmospheric turbulence dilutes plume buoyancy in its final rise stages. In this "breakup" model, the rise is terminated when the ambient eddy dissipation rate ϵ exceeds the internal dissipation rate of the plume. This condition is

$$\epsilon(z) > 1.5\frac{w^3}{z}. \tag{A-182}$$

The plume (or puff) rise velocity is w, and its height above the ground is z. The ambient eddy dissipation rate is (Hanna et al, 1982)

$$\begin{aligned} \epsilon(z) &= u_*^2\frac{du}{dz} + \frac{g}{t_a}(w_a'T_a')_{ave} \\ &= u_*^2\frac{du}{dz}\begin{cases} 0 & \text{stable, neutral)} \\ H_b & \text{unstable, } z < 0.1h_i) \\ \frac{1}{2}H_b & \text{unstable, } z > 0.1h_i). \end{cases} \end{aligned}$$

The second term contains only half the surface buoyancy flux when the eddy dissipation rate is assumed to be computed above the surface layer (0.1, h_i). This factor takes into account convective downdrafts and updrafts that contribute to the plume or puff dilution (Briggs, 1969; Weil, 1982). (The surface buoyancy term is not included, of course, for stable and neutral conditions.) The windspeed derivative is taken from equations (A-164) and (A-165).

Finally, for this section, the COMBIC model requires the cumulative normal distribution with zero mean and unit variance:

$$\Phi(x) = \frac{1}{(2\pi)^{1/2}}\int_{\infty}^{x} e^{-\frac{1}{2}(x')^2}dx'. \tag{A-183}$$

This function is approximated by the rational polynomial expression given in Abramowitz and Stegun (1964):

$$p = |x|. \tag{A-184}$$

Define

$$g = \frac{1}{2}\left[1 + a_1 p + a_2 p^2 + a_3 p^3 + a_4 p^4 + a_5 p^5 + a_6 p^6\right]^{-16}, \tag{A-185}$$

where

$$a_1 = 0.049867347, \tag{A-186}$$
$$a_2 = 0.0211410062, \tag{A-187}$$
$$a_3 = 0.0032776263, \tag{A-188}$$
$$a_4 = 0.000038003575, \tag{A-189}$$
$$a_5 = 0.000048890636, \tag{A-190}$$
$$a_6 = 0.000005382975. \tag{A-191}$$

Then,

$$\Phi(x) = \begin{cases} g & \text{if } x > 0 \\ 1 - g & \text{if } x < 0. \end{cases} \tag{A-192}$$

Note that EOSAEL82 COMBIC used a version of this approximation associated with the error function. It differed from this approximation in that the square root of two was divided into the x argument before the function was called. That division is no longer necessary and no longer occurs before each call to the routine. The square root of two factor is already contained in the approximation coefficients.

Appendix B. Smoke and Dust Models and Parameters Used in COMBIC

Contents

Figures

Tables

This appendix contains detailed descriptions of the many munition parameters that drive the obscuration models used in the COMBIC model. It will be of interest to people wishing to modify munition characteristics in COMBIC to model either modified munitions or existing or notional munitions.

Section B-1 describes the parameters used to model the source characteristics. These are used in Phase I to provide the descriptions of the cloud's creation, detailed growth, and optical properties.

The details of high-explosive impact, cratering, and dust production are described in section B-2. This section also covers the barrage option for simulating the effect of many identical munitions exploding simultaneously and the methods used to model the dust raised by moving vehicles.

B-1 The Smoke Model—Source Characteristics and Cloud Description

The smoke types modeled in COMBIC are

- bulk white phosphorus (WP),
- WP wedges, WP wicks, and plasticized white phosphorus (PWP),
- red phosphorus (RP),
- hexachloroethane (HC),
- fog oil (SGF2),
- winterized fog oil (SGF2 with kerosene),
- diesel fuel (DF) smoke (generator disseminated by vaporization and condensation),
- polyethylene glycol (PEG200),
- IR screener,
- diesel fuel, motor oil, and rubber fire mixtures.

User inputs can potentially specify other smokes. The code provides smoke extinction coefficients for anthracene, chlorosulfonic acid (FS), brass, graphite, kaolin, and titanium tetrachloride (FM), although none of the menu-specified sources in the model use these compounds as their defaults.

Any cloud can also be specified as a moving source (for example, vehicle-generated smoke). As an option for simulating barrages, COMBIC provides for a simplified treatment of many sources ignited within an extended area over an extended time period. The barrage option greatly reduces computation time, although at the expense of cloud detail. Since it is a continuous source, a barrage may also be specified to be moving. Although moving sources are restricted in COMBIC to straight-line motion at constant speed, the user can (with sufficient ingenuity) simulate a change in direction by "turning off" a moving source at some point along its path and initiating

a new source at that time and location, moving with a different speed or direction.

COMBIC also provides scaling laws, so that a basic cloud history computed in Phase I (for example, 40 gal per hour diesel oil generation) can be transformed in Phase II into the appropriate clouds produced by one or more moving generators having completely different speeds and directions.

Phase II also allows scaling of source strength; thus, the same history can be used for a range of obscurant production rates (for example, 40 gal per hour fog oil can be rescaled to 20 gal per hour).

Phase I calculations perform the following functions for smoke.

- The *total mass* of airborne aerosol is computed for the specified source.
- The *total thermal energy* released in the production process is computed.
- The *mass production* is calculated. If the source is continuous, an array of cumulative (that is, time integrated) mass production values is generated at equally spaced time intervals over the total production time. If the barrage option is specified, an effective continuous mass production profile is computed. For instantaneous sources, this is the time-averaged mass production. For continuous sources, the barrage duration is folded into the single-round mass production profile.
- Time-dependent *evaporation or deposition corrections*, if any, are made in the cumulative mass production history. (Further adjustment for evaporation or deposition, if any, is made during Phase II calculations. Besides evaporation and deposition, other mechanisms for removing aerosol are the settling velocity of the cloud and the ground reflection factor.)
- *Initial cloud dimensions*, that is, "source sigmas" (the standard deviations of the Gaussian cloud dimensions) are specified for the cloud.
- The *buoyancy radius*, which can be smaller than the obscurant cloud radius, is determined.
- Finally, a time series of *cloud positions and dimensions* is computed for the given meteorological conditions by iteration over small time steps.

The influence of the atmospheric boundary layer (presented in sect. A-5, on position and dimensions) is determined by the cloud buoyancy and diffusion models (sect. A-3 and A-4), which produce a time history for each subcloud making up the cloud.

B-1.1 Total Smoke Mass—MUNT Input Record for Smoke

Many parameters and initial conditions are required to define different obscurants and obscurant sources (munitions, generators, smoke pots). Phase I of COMBIC allows the user to user input all parameters and initial conditions to define a source fully. For most users, however, this option is far too detailed. So, at the other extreme, one can select a set of values stored internally. These values are provided from a menu of obscurant munitions and are keyed to a single number, the source type code I_s. Other intermediate levels of detail are possible through user input. The user may choose a source type I_s, for example, and then modify selected parameters stored for I_s, or the user may use default characteristics that have been assigned to the different obscurant types I_t in the code.

Source characteristics related to the total mass of smoke produced are input on a single record with the "MUNT" record. The seven parameters input on MUNT are

- X_n, total number of smoke sources,
- W_f, fill weight of individual smoke source,
- I_s, source menu code,
- I_t, smoke / obscurant type code,
- E_f, efficiency of the source,
- y_f, yield factor, and
- N_s, number of submunitions.

Input Parameter X_n

X_n is the total number of individual smoke sources detonated, ignited, generated, etc, at nearly the same point and at the same time. These smoke sources are modeled as if they form a single, combined source cloud. X_n may be input with a decimal (that is, a fractional value). It scales both the amount of smoke and the amount of heat produced in the resulting cloud. The default value is 1.0.

Input Parameter W_f

W_f is the fill weight of one individual smoke source. W_f is in pounds except for the specific liquids: SGF2, PEG200, DF, fog oil cut with kerosene, and DF / oil / rubber mixtures that produce battlefield fire smoke. These liquids have input units of gallons.

Input Parameter I_s

I_s is the source menu code number. The sources stored in COMBIC are listed in table B-1. An input of 0.0 means that the source is user defined.

Table B-1. COMBIC model default fill weights and efficiencies for various munitions types.

Type code	Munition type	Fill weight	Efficiency	Obsc. code	No. of sub-munitions
1	155-mm HC M1 canister	5.40	70	3	1
2	155-mm HC M2 canister	2.80	70	3	1
3	105-mm HC canister	1.57	70	3	1
4	155-mm HC M116B1 projectile*	19.00	70	3	4
5	105-mm HC M84A1 projectile*	4.73	70	3	3
6	Smoke pot, HC M5*	31.00	70	3	1
7	Smoke pot, HC M4A2*	27.00	70	3	1
8	60-mm WP M302A1 cartridge*	0.76	100	1	1
9	81-mm WP M375A2 cartridge*	1.60	100	1	1
10	4.2-in. WP M328A1 cartridge*	8.14	100	1	1
11	2.75-in. WP M156 rocket*	2.12	100	1	1
12	155-mm WP M110E2 projectile*	15.60	100	1	1
13	105-mm WP M60A2 cartridge*	3.83	100	1	1
14	4.2-in. PWP M328A1	8.14	60	2	1
15	5-in. PWP Zuni MK4	13.52	60	2	1
16	2.75-in. WP wedge	0.463	66	2	1
17	2.75-in. WP M259 rocket*	4.63	66	2	10
18	3-in. WP wick	0.139	71	2	1
19	6-in. WP wick	0.234	67	2	1
20	155-mm WP M825 projectile*	16.43	74	2	116
21	81-mm RP wedge	0.128	53	5	1
22	I81-mm RP XM819 cartridge*	2.834	48	5	28
23	Generator, ABC M3A3*	10.0†	100	4	1
24	Generator, vehicle engine exhaust smoke system*	11.0†	100	8	1
25	Smoke pot, fog oil M7A1*	1.7†	100	4	1
26	155-mm HE (dust)‡	14.9	—	10	1
27	105-mm HE (dust)‡	6.04	—	10	1
28	4.2-in. HE (dust)‡	7.45	—	10	1
29	10-lb C4 (dust)‡	13.4	—	10	1
30	Diesel fuel/oil/rubber fire	150.†	26	14	1
31	Muzzle blast	2.00	—	10	1
32	M76 IR grenade	2.98	60	20	1
33	L8A1/L8A3 grenade	0.794	95	5	1

*Inventory smoke sources.
†Fill weight in gallons. Note that smoke emission rate also depends on the emission or "burn duration" for this source.
‡HE munitions default to live-fire delivery casing lengths of 0.6096, 0.4064, and 0.4064 m; casing diameters of 0.1778, 0.1016, and 0.1016 m; and dip angles of 10, 10, and 60, respectively. All default charges are surface detonations.

Input Parameter I_t

I_t is the smoke/obscurant type code number. This parameter is used primarily to select the different mass extinction coefficients (optical properties) stored in the code for different obscurants. But if I_s is input as 0.0, then I_t is also used to select default models for other parameters (that is, yield factor, efficiency, initial cloud size, and so forth). If I_t is zero, then a nonzero I_s must be input to specify a type of obscurant, or all parameters must be input. The type codes are listed in table B-2.

Input Parameter E_f

E_f is the percentage efficiency of the source (0.0 to 100.0). The efficiency reduces the fill weight to provide the actual weight of smoke burned and released into the air. An efficiency below 100 percent is due to one or more

Table B-2. Smoke/obsurant type code, I_t.

Type code	Smoke type
0.	(I_t is assigned by the I_s internal table)
1.	Bulk white phosphorus (WP) munition
2.	WP wedges, WP wicks, and plasticized WP (PWP) munitions
3.	Hexachloroethane (HC) smoke pots and munitions
4.	Fog oil (SGF2) produced by generator or smoke pot
5.	Red phosphorus (RP) munition
6.	IR screener, generator disseminated
7.	IR screener, munition
8.	Diesel fuel (DF) produced by generator (vaporization, condensation)
9.	Dust, vehicular (see sect. B-2)
10.	Dust, high explosive (HE), small-particle, persistent mode (see sect. B-2)
11.	Dust, HE, large-particle mode
12.	Carbon, HE debris product
13.	Dust/soil, HE, very large ballistic soil aggregates
14.	Fire smoke from diesel fuel, oil, and rubber mix
15.	Kerosene and fog oil mixture for cold regions
16.	Polyethylene glycol (PEG200) mix of alcohols
17.	Anthracene (not used in I_s menu)
18.	Chlorosulfonic acid (FS) (not used in I_s menu)
19.	Titanium tetrachloride (FM) (not used in I_s menu)
20.	IR (M76)
21.	Brass
22.	Graphite 7525
23.	Kaolin
24.–30.	User-defined by extinction (EXTC record) and other inputs

factors, including unburned residue in the munition, screener deposited on the ground below the munition, smoke materials buried in mud or snow, and inert components in the smoke mix. Examples of inert residues are the felt or binders in WP wedges and PWP, and the components of aluminum and hydrocarbons in HC that are byproducts of the reactions producing $ZnCl_2$ smoke.

Note that COMBIC attempts to be consistent in defining fill weight and efficiency so as not to include the weight of the canister, cartridge, or other container enclosing the smoke mix. Other sources of fill weight information, including smoke munition technical manuals, often include the container weight. The efficiency must be correspondingly reduced when these data are used.

Input Parameter Y_f

Y_f is the yield factor, a dimensionless multiplier that has a value of unity for nonhygroscopic smokes. The yield factor accounts for additional weight of water condensed from the air onto the smoke droplets. Y_f depends, therefore, on relative humidity. But it also includes the weight of water formed in burning the fill to produce smoke. This is included for phosphorus-based smokes, where the reaction that forms phosphoric acid droplets produces smoke with about three times the original weight of unburned phosphorus, even at "zero" relative humidity. Like efficiency, yield factor is occasionally given other definitions in the literature.

Input Parameter N_s

N_s is the number of submunitions for the combined source of X_n individual sources, each of fill weight W_f. N_s does not affect the total amount of smoke produced. It is used to model the reduction in cloud rise that results when a single heat-producing region is separated into N_s parts. Some munitions use this technique of separating parts of a burning munition to reduce buoyancy. Cloud regions are independent when cooler ambient air can mix freely and surround each submunition.

Total Mass Calculation

In terms of the parameters just given, the total mass of airborne smoke M_a is given by

$$M_a = CX_nW_f\left(\frac{E_f}{100}\right)Y_f, \tag{B-1}$$

where C converts pounds to grams (453.6 g/lb) or gallons to grams (3785 g/gal water, 3483 g/gal fog oil, 3218 g/gal diesel fuel, 4266 g/gal PEG200) (Baer, 1984b). Table B-1 gives model defaults for various menu-selected sources. Data in the table have been accumulated from technical and field manuals, field tests, consultation with the U.S. Army Chemical Research

and Development Center, and various model analyses (Cichowicz, 1983; Baer, 1984b; Pamphlet, 1981; Manual, 1967a; Manual, 1967b; Smoke and Aerosol Working Group, 1979; Ground, 1978b; Ground 1978a; Bowman *et al*, 1979; Nelson and Farmer, 1981; Dolce and Metz, 1977; Ground, 1977; Rubel, 1983; Muhly, 1983; Yon *et al*, 1984; Pennsyle, 1982a; Ebersole, 1982; Sutherland, 1983; Pennsyle, 1982b; Matise, 1984; Baer, 1984a).

Changes Affecting MUNT Parameters in Latest Version

RP and cold-regions option. Users of EOSAEL84 COMBIC should be aware that in the latest version, RP is assigned a separate obscurant type to accommodate a "cold-regions" option. Matise (1984) determined from Smoke Week VI data that the mass of phosphorus smoke from RP fragments burning in snow is 20 percent of that produced by burning on no snow cover. The initial puff of smoke from the munition airburst is not affected. WP and felt-impregnated WP fragments, however, were observed to continue to burn after impact on snow. COMBIC therefore provides a "snow-cover" option on TERA (the terrain input record) that sets 20-percent efficiency for RP munition fragments in snow. This setting is, of course, based on limited data and should be taken as representative only of snow conditions similar to these of the Smoke Week VI test. The snow-cover input is not used for any other purpose in COMBIC at present.

New smoke sources. EOSAEL92 has three new smoke/obscurant sources as part of the default tables—muzzle blast, M76 IR grenade, and the L8A3 RP grenade. Concern has arisen that the dust produced by firing guns can attenuate transmission. The muzzle blast option has been added for those researchers who want to model these effects. Muzzle blast in COMBIC is simulated to be equivalent to the dust produced by a buried static 2-lb C-4 charge. It is modeled as an instantaneous puff of dust. The puff is treated as an instantaneous, nonbuoyant cloud of persistent dust with total cloud reflection from the ground plane. Initial cloud radius is $15 \times 10 \times 7$ m.

Battlefield fire smoke. Smoke from battlefield fire has been added to COMBIC following the EOSAEL FITTE battlefield fire model. The menu provides the source characteristics for a mixture of 150 gal of DF, 15 quarts of motor oil, and 660 lb of rubber. This mix is representative of a burning truck. Extinction coefficients, mass production, and thermal production are based on field measurements of this mixture. This DF/oil/rubber source can be used to approximate other sources, with appropriate scale factors X_n. For example, for a burning tank, an X_n scale factor of 3.33 is needed. For a burning jeep, an X_n of 0.333 is needed.

The number of gallons of diesel fuel has been chosen as the user "fill weight" input. The efficiency is assigned as 26 percent. The FITTE model uses 16-percent efficiency, but in that model the user enters all three combustible components. The COMBIC efficiency lumps all components together and relates them to the amount of diesel fuel input.

HC burn efficiency. Efficiency parameter values have been updated in COMBIC92 both to reflect further research (including field studies) and to account for differences in definitions of fill weight. Following the work of Baer (1984a) and Pennsyle (1982b), who provided burn efficiency values for HC canisters, munitions, and pots, the default HC efficiency has been changed from 77 to 70 percent in the latest version of COMBIC. The earlier, higher value was based on the theoretical maximum efficiency of HC, calculated from the contents of HC munitions: these consist of 5.5 to 9 percent Al, 45.5 to 48 percent ZnO, and 45 to 47 percent C_2C_{16} by weight (Cichowicz, 1983). Using gram molecular weights, it is easy to determine that the percentage weight of $ZnCl_2$ (smoke) per weight of original mix is 76 to 80.4 percent. Earlier versions of COMBIC accordingly used 77 percent for HC burn efficiency.

As Baer shows, however, the burn efficiency of most HC sources is 90 percent (although a value as low as 85 percent was obtained for one HC smoke pot). (This means that about 10 percent of HC fill is unburned.) The COMBIC model, therefore, uses 90 percent of the maximum possible 77 percent (that is, 70 percent) as the HC efficiency.

In Pennsyle's work, fill weight was defined to include the canister weight, along with the weight of HC inside the canister. His efficiencies are based on measured elemental zinc captured from HC smoke produced in a wind tunnel (Dugway Proving Ground, 1977). When Pennsyle's values are corrected to conform to the COMBIC definition of fill weight (which excludes the canister weight), the resulting efficiencies are 50 to 65 percent, lower values than the 70 percent derived above. This 5 to 15 percent discrepancy may be accounted for by the efficiency of the method for zinc collection, which is unknown but presumably less than 100 percent. This could account for the difference in the separate analyses.

Yield factor and relative humidity. In COMBIC the yield factor is one for all obscurants except phosphorus smoke, HC, and PEG200. These obscurants have relative-humidity-dependent yield factors. A number of laboratory measurements of yield factors and theoretical analyses have been made (Rubel, 1978; Rubel, 1981b; Tarnove, 1981; Hanel, 1976; Sutherland, 1981; Baer and Rubel, 1984). Sutherland (1981) has produced semi-empirical fits to HC and WP yield factors. Baer and Rubel (1984) have produced fits to HC, WP, and PEG200. Their PEG200 curve fit is now used in COMBIC. Figure B-1 shows the humidity-dependent yield factors used in COMBIC for these smokes.

In addition, Matise (1984) has investigated the effects of cold environment on yield factors. For temperatures below freezing comparable to those at Smoke Week VI, the absolute humidity is sharply reduced. Depletion of water vapor within HC and phosphorus clouds further reduces the effective relative humidity inside the cloud. Thus, the yield factor is smaller, particularly at ambient relative humidities above 80 percent. This effect is

shown in figure B-2. The user may specify, through a flag on the MET1 input record, that these cold-regions yield factors are to be used.

The yield factor depends on temperature and on cloud dimensions. In the current version of COMBIC, the cloud size assumed for the cold regions option has a σ of 20 m, and the effective yield factor is computed only once for each source. Corrections have not been determined for cold-regions effects on PEG200.

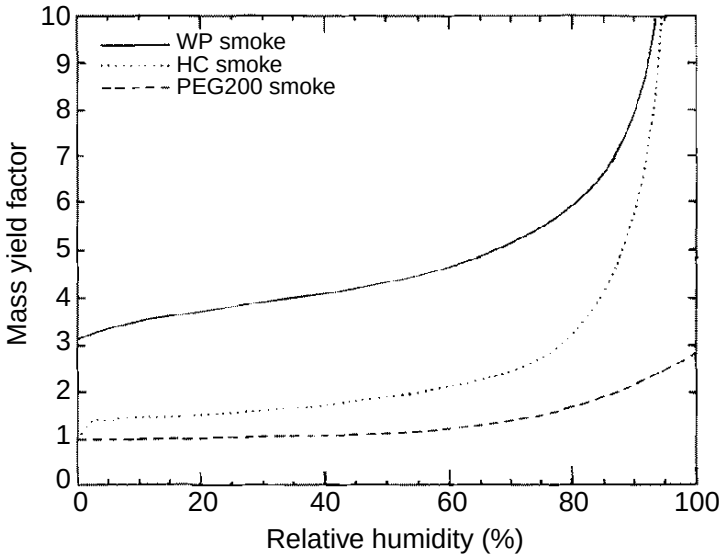

Figure B-1. Relative humidity-dependent yield factors for WP, HC, and PEG200 smokes.

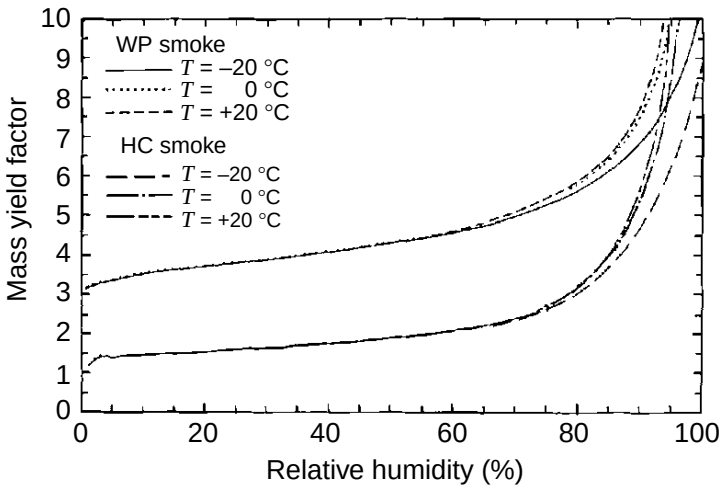

Figure B-2. Cold-regions effects on WP and HC yield factors.

B-1.2 Mass Extinction Coefficients—EXTC Input Record for Smoke

Extinction per unit mass of airborne aerosol (in meters squared per gram) depends on four factors: (1) the index of refraction of the obscurant, (2) the distribution of particle sizes, (3) shape and orientation of particles, and (4) the effect of dilution by water absorbed from the air, for example, on mass, size distribution, and effective refractive index. COMBIC assumes that the mass extinction coefficients for smoke are constant over the time intervals of interest in obscuration problems. Thus, the details of the above dependencies have been considered outside the model, and the results, which are most heavily weighted toward measurement rather than theory, are stored in the code.

The assumption of time independence is reasonable but not strictly true. Smoke size distributions and hygroscopic growth are established within a fraction of a second of release into the air. Submicrometer sizes for inventory smokes ensure that size-dependent fall velocities in the atmosphere have little, if any, effect on altering size distribution. Milham (1982), for example, measured approximately a 30-percent increase in mass extinction of WP smoke at 9 to 10 μm wavelength over a 1-hour period in a laboratory chamber.

Larger screening materials may settle more rapidly. If they are relatively monodispersed, however, their extinction per unit mass also changes slowly. Dust is a special case because of its broad size range and is, therefore, modeled with smaller size range regions. (Dust models are further discussed in sect. B-2.) Large-particle carbonaceous agglomerates from DF/oil/rubber mixtures are also known to fall out of the resulting smoke cloud. However, quantitative measurements of the effect of this fallout in changing mass extinction are lacking, and we are forced at this time to use constant extinction coefficients. Fortunately, a "rule of thumb" in estimating mass extinction is that particles that are comparable in size to the wavelength contribute most to mass extinction coefficients because of the area-to-mass ratio of the particles.

In a more complete model, the effect of evaporation on extinction in addition to the loss of mass should be included. It is not in the code at present. Turbulent fluctuations in size distributions have been studied (Huang and Frost, 1985), as well as their effect on extinction coefficients. Integrated over typical optical paths, however, these fluctuations are negligible for COMBIC applications.

Mass extinction coefficients in COMBIC are based primarily on field and laboratory measurements (Ground, 1978b; Ground, 1978a; Bowman *et al*, 1979; Nelson and Farmer, 1981; Dolce and Metz, 1977; Ground, 1977; Baer, 1984a; Milham and Anderson, 1983; Pinnick and Jennings, 1980; Shirkey, 1980; Frickel and Steubing, 1979; Maddix *et al*, 1982; Khanna and Sutherland, 1984; AMC, 1967; Bruce, 1984). Values stored are averaged over the

EOSAEL wavelength regions: 0.4 to 0.7 μm, 0.9 to 1.2 μm, 1.06 μm, 3 to 5 μm, 8 to 12 μm, 10.6 μm, and 94 GHz. Coefficients for other wavelengths or obscurants may be input to the code via the EXTC record.

The relative-humidity-dependent mass extinction values for WP and HC smokes are shown in figures B-3 and B-4. The band-averaged value over 8 to 12 μm for WP has been slightly modified from EOSAEL 82. Extinction coefficients for the other aerosols are given in table B-3. Diesel fuel, PEG200, FS, and FM coefficients are from Milham (1983). Fog oil and kerosene mixture coefficients are from Matise (1984). Millimeter wavelength (94 GHz) values are nominal upper bounds except for diesel, oil, and rubber fire smoke (private communication with C. Bruce, 1984).

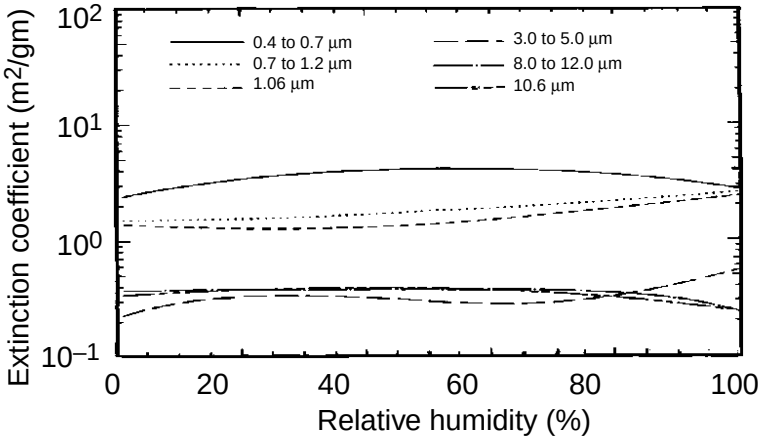

Figure B-3. Mass extinction coefficient for WP smoke.

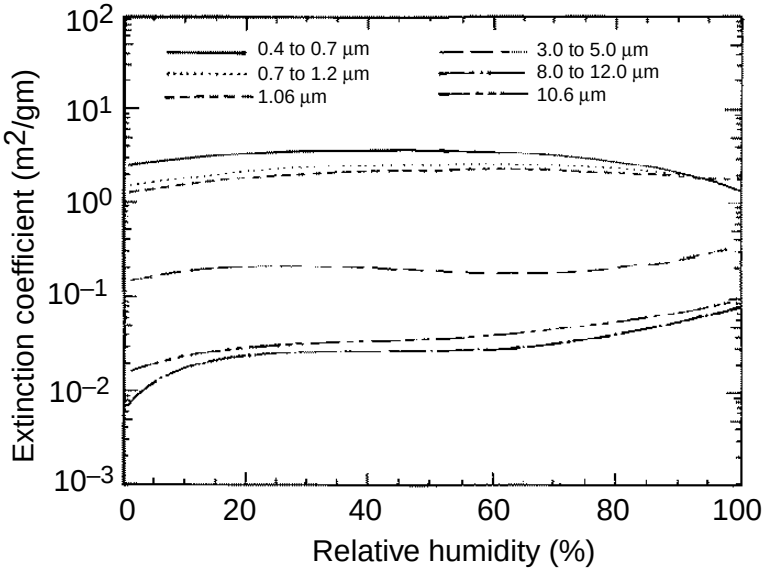

Figure B-4. Mass extinction coefficient for HC smoke.

Table B-3. Extinction coefficients for default obscurant types.

Obscurant		Wavelength (μm)						
Type	Name	0.4 to 0.7	0.7 to 1.2	1.06	3 to 5	8 to 12	10.6	94 GHz
1.	White phosphorus	(See fig. B-3)						
2.	PWP, WP wedges	(See fig. B-3)						
3.	Hexachloroethane	(See fig. B-4)						
4.	Fog oil	6.851	4.592	3.479	0.245	0.020	0.018	0.001
5.	Red phosphorus	(See fig. B-3)						
6.	IR (generator)	1.860	1.630	1.400	1.790	1.680	0.680	0.001
7.	IR (munition)	1.860	1.630	1.400	1.790	1.680	0.680	0.001
8.	Diesel fuel	5.650	4.080	3.250	0.245	0.023	0.027	0.001
9.	Vehicular dust	0.320	0.300	0.290	0.270	0.250	0.250	0.001
10.	HE dust, small	0.320	0.290	0.260	0.270	0.260	0.240	0.001
11.	HE dust, large	0.035	0.036	0.037	0.035	0.038	0.036	0.002
12.	Carbon debris	1.500	1.460	1.420	0.750	0.320	0.300	0.001
13.	HE dust, ballistic	0.001	0.001	0.001	0.001	0.001	0.001	0.0004
14.	Diesel / oil / rubber	6.100	3.750	2.94	1.350	1.010	1.000	0.002
15.	Fog oil / kerosene	6.851	4.592	1.430	0.054	0.020	0.018	0.001
16.	PEG200	5.370	2.900	2.100	0.090	0.090	0.070	0.001
17.	Anthracene	6.200	3.500	2.500	0.230	0.050	0.048	0.001
18.	FS	3.330	2.750	2.660	0.260	0.320	0.230	0.001
19.	FM	1.300	1.740	1.700	0.080	0.160	0.380	0.001
20.	IR (M76)	1.000	1.000	1.000	1.000	1.000	1.000	0.001
21.	Brass	1.300	1.400	1.400	1.400	1.400	1.400	0.001
22.	Graphite 7525	1.800	2.000	2.000	2.000	2.000	2.000	0.001
23.	Kaolin	2.000	1.000	1.000	0.100	0.400	0.400	0.001
24.–30.	User-defined	User-defined						

B-1.3 Partitioning Smoke Among Subcloud Units—CLOU and SUBA Records

The "model" for each obscurant cloud type released into the atmosphere is a mathematical representation of one or more Gaussian regions called "subclouds." Each subcloud can be an instantaneous Gaussian puff or a continuous Gaussian plume. It can also be defined as a rising (that is, buoyant) cloud, a stabilized nonrising cloud, or an instantaneous, Gaussian "stem" cloud spanning the region between two other subclouds. At the option of the user, up to five subclouds can be defined. The definition begins with the input of a "CLOU" record that contains the number of subclouds to be generated. One "SUBA" record is then input for each subcloud with the following parameters:

- S_n = subcloud designator 1 to 5.
- f_n = fraction (dimensionless 0 to 1) of the cloud mass M_a to be placed in this subcloud.

- C_n = the relative amount of debris carbon, that is, grams of carbon per gram of primary obscurant. This parameter is currently used with HE dust only. The weight of carbon is not part of the fill weight of the primary obscurant. This parameter effectively increases the mass extinction coefficient to include the extinction of C_n g of carbon per gram of primary obscurant.
- S_t = subcloud "type" flag: 1. = instantaneous, 2. = continuous.
- S_r = subcloud "rise" flag: 1. = buoyant (that is, rise calculations are performed), 2. = stabilized (that is, no rise calculation performed), or a number of the two-digit form ij (with ij from 12. to 43.) identifying the subcloud as a stem stretching from subcloud i to subcloud j.
- S_e = extinction coefficient flag 1 to 30, selecting a specific set of extinction coefficients from the I_t list in section B-1.1. This allows the model to assign different extinction coefficient sets to different subclouds. This is particularly needed for HE dust.
- S_b = "ballistic rise" model flag, used at present with HE dust. The flag is either 0. = nonballistic or 1. = ballistic.

Sources selected from the menu of munitions types (see table B-1) have the following cloud structures. For HC smoke (munition types 1 to 7), a single continuous subcloud is modeled, containing 100 percent of the HC smoke and no residual carbon. The subcloud is slightly buoyant and uses the HC extinction coefficients (I_t = 3; see table B-2). There is no ballistic rise phase.

Various materials can be used in generators to produce clouds (fog oil, generator-produced IR screener, diesel fuel, fog oil with kerosene, or PEG200; I_t = 4, 6, 8, 15, or 16). For generator-produced clouds, a single continuous subcloud is modeled. All the obscurant material is contained in this subcloud. For munition types 23 to 25 (generators and smoke pots), the fill material is selected by the I_t parameter on the MUNT card rather than on a SUBA record. The cloud is slightly buoyant; there is no residual carbon, and the cloud has no ballistic rise phase.

Diesel fire smoke (munition type 30) similarly is a single, continuous, highly buoyant cloud containing 100 percent of the obscurant material. The obscurant type is 14 (see table B-2). There is no residual carbon; carbonaceous aerosols are already included in the measured extinction coefficient, and there is no ballistic rise phase.

Bulk WP (munition types 8 to 13) contains three subclouds. The first is a highly buoyant instantaneous puff containing 51 percent of the total smoke mass. The second subcloud is a slightly buoyant, continuous cloud containing 23 percent of the smoke mass. The third subcloud is a stem connecting the buoyant puff and the leading edge of the continuous cloud. The stem contains the remaining 26 percent of the smoke mass. For the 155-mm WP cloud (I_s = 12), the instantaneous puff is assumed to contain only 23 percent

of the smoke mass, the stem contains 11 percent, and the continuous cloud contains 66 percent of the smoke mass. There is no residual carbon and no ballistic rise phase. The obscurant is bulk WP (I_t = 1) for all subclouds.

WP wicks, WP wedges, PWP munitions (types 14 to 19), and RP munitions (types 21 to 22) produce two subclouds. A small fraction of the obscurant, 7.5 percent, is placed in an instantaneous, buoyant Gaussian puff. The remainder is in a continuous, buoyant subcloud, with no stem region. The model for 155-mm M825 WP wedge munition (type 20) neglects any instantaneous puff component altogether, and thus has 100 percent of the phosphorus smoke in a single continuous, buoyant subcloud. These munitions have no residual carbon or ballistic rise phase. They burn more slowly than the bulk WP munitions and for a longer period of time. This difference is modeled through a "burn function" (see sect. B-1.1 on mass production rate).

The extinction coefficients for all phosphorus clouds are identical. The assignment of different obscurant types (I_t = 1, 2, and 5) is simply a convenient way to produce default values if the CLOU and SUBA, SUBB, and SUBC records are not input and if a menu-defined set of characteristics is not selected (I_s = 0). The default (generic) WP clouds contain three subclouds, as above, with 51, 23, and 26 percent of the smoke divided among the instantaneous puff, continuous residual cloud, and connecting stem cloud, respectively. The PWP, WP wicks and wedges, and RP generic clouds contain two subclouds as above, with 7.5 percent of the smoke in an instantaneous buoyant puff and the remaining 92.5 percent in a continuous buoyant cloud. The separate RP type code allows the efficiency to be modified for snow cover (sect. B-1.1) and does not otherwise distinguish RP from the other PWP and WP wedge munitions.

The M76 IR grenade is modeled as a nonbuoyant single puff. Diane Frederick of the Army Materiel Systems Analysis Activity (AMSAA) has determined that the extinction is 1.0 for most wavelengths (personal communication). The L8A1 grenade is modeled as three subclouds with 92.5 percent of the mass in a buoyant plume, 5 percent of the mass in a buoyant puff, and the remaining 2.5 percent in a stem connecting the two. The L8A1 burns for 658 s and does not smolder.

The default generic cloud structures for the other obscurants parallel the models above with a single, continuous subcloud for each munition. Given no detailed CLOU and SUBn record inputs, the generic subcloud structures for anthracene and FS smokes are modeled to be similar to HC, and the FM smoke cloud structures is modeled to be similar to fog-oil type sources.

B-1.4 Initial Cloud Dimensions, Thermal Production, and Evaporation/Depletion—SUBB and SUBC Input Records

Initial values are required by the transport, diffusion, and rise submodels. These are (optionally) defined on input records SUBB and SUBC. If present, these records must immediately follow the corresponding SUBA record for each subcloud. Values on the SUBB record define obscuration radii and thermal production parameters:

R_x, R_y, R_z = initial obscuration radii (in meters) in the downwind, cross-wind, and vertical directions.

R_o, T_o, q, w_o = initial buoyancy radius (in meters), initial mean temperature of the cloud (in kelvins), thermal production coefficient (calorie per gram obscurant), and initial upward velocity component of the cloud.

The Gaussian cloud dimensions are defined in terms of radius to be

$$\sigma = \frac{R}{2.15}. \tag{B-2}$$

The obscuration radii are obtained from user input, from the source menu, or from models for each generic source type. For bulk WP, the generic model for the radii of the initial burst is

$$R_x = R_y = 7.75\,(X_n W_f)^{0.3}\,, \tag{B-3}$$

and

$$R_z = 0.33 R_y. \tag{B-4}$$

These equations are the basis for Pennsyle's (1982b) suggested initial burst radii for the bulk WP in the munition menu. (This model was also used in EOSAEL82. The R_z values in that version, however, were taken to be three to five times those from eq (B-5).*) Note that the fill weight is the original value in pounds and not the converted mass from equation (B-1).

The obscuration radii for the continuous source region are taken to be the fragment dispersion radii defined by (private communication with D. Bromley (1982))

$$R_x = R_y = 16.4\,(X_n W_f)^{0.3}\,, \tag{B-5}$$

which were used in EOSAEL82 COMBIC, and, arbitrarily, the initial radius in the vertical direction is

$$R_z = 3.0. \tag{B-6}$$

WP wedges, PWP munitions, and RP munitions are more difficult to assign generic initial obscurant cloud sizes. Submunition dispersal varies depending on munition design. Approximately, however, for the instantaneous burst,

$$R_x = R_y = 7.75\,(0.075 X_n W_f)^{0.3}\,, \tag{B-7}$$

*This simplification was made so that a WP stem subcloud could be neglected.

and

$$R_z = 0.75 R_y. \tag{B-8}$$

If a value is not from the menu or is not provided by the user, COMBIC assigns dispersion radii for the continuous cloud component of

$$R_x = R_y = 19.0 \left(X_n W_f\right)^{0.3}, \tag{B-9}$$

and

$$R_z = 3.0 \tag{B-10}$$

(in meters) similar to the bulk WP radii. The error in equations (B-9) and (B-10) can be as large as 10 to 15 percent, apparently, based on the range of dispersion radii for WP wicks, WP wedges, RP rounds, and PWP rounds. If the smoke source is an individual wedge or other submunition, the COMBIC generic model uses equation (B-5), which is the same as that used for bulk phosphorus.

Table B-4 gives the initial obscuration radii for the instantaneous and continuous subclouds produced by the menu sources. HC smoke pots and canisters are assumed to produce initial obscuration radii of

$$R_x = R_y = 1.31 \left(\frac{M_a}{N_s T_b}\right)^{0.3}, \tag{B-11}$$

and

$$R_z = 1.2 R_y, \tag{B-12}$$

where M_a is from equation (B-1) and T_b is the burn duration (in seconds), discussed further in section B-1.5. Full HC munitions tend to have three or four canisters that are ejected from the munition base. The distance between canisters for a full munition is assumed to be 30 m. COMBIC further assumes that the submunitions are deployed crosswind. Thus, the radius R_y is set to 30 m, and the radius R_x uses equation (B-11). These initial values can be overridden by user input.

Generators produce clouds from small nozzles. COMBIC assigns nominal initial obscuration radii in meters:

$$R_x = R_y = R_z = 0.2. \tag{B-13}$$

Fog oil pots are also given these values. The initial value is not critical for COMBIC applications.

The obscuration radius for the continuous plume from a diesel fuel / oil / rubber fire is determined from

$$R_x = R_y = 10.7 \left(\frac{X_n W_f}{T_b}\right)^{0.5}, \tag{B-14}$$

and

$$R_z = 0.3 R_y, \tag{B-15}$$

where W_f is the diesel fuel measured in gallons. This radius is consistent with all the FITTE model source conditions.

The buoyancy radius R_o, the mean initial cloud temperature T_o, and the initial vertical velocity of the cloud w_o are inputs to the cloud rise routine. The rise of the cloud depends critically on the combination of temperature and

Table B-4. Initial obscuration radii for COMBIC menu smokes.

Munition	Type code	Radii (m)					
		Instantaneous puff			Continuous plume		
		R_x	R_y	R_z	R_x	R_y	R_z
155-mm HC M1 canister	1	—	—	—	3.1	3.1	3.7
155-mm HC M2 canister	2	—	—	—	2.8	2.8	3.4
105-mm HC canister	3	—	—	—	2.1	2.1	2.5
155-mm HC M116B1 projectile*	4	—	—	—	3.0	3.0, 30	3.6
105-mm HC M84A1 projectile*	5	—	—	—	2.1	2.1, 30	2.5
Smoke pot, HC M5*	6	—	—	—	2.6	2.6	3.2
Smoke pot, HC M4A2*	7	—	—	—	2.7	2.7	3.3
60-mm WP M302A1 cartridge*	8	7.1	7.1	2.4	15.1	15.1	3.0
81-mm WP M375A2 cartridge*	9	8.9	8.9	3.0	18.9	18.9	3.0
4.2-in. WP M328A1 cartridge*	10	14.5	14.5	4.8	30.8	30.8	3.0
2.75 in. WP M156 rocket*	11	9.7	9.7	3.2	20.5	20.5	3.0
155-mm WP M110E2 projectile*	12	17.7	17.7	5.9	37.4	37.4	3.0
105-mm WP M60A2 cartridge*	13	11.6	11.6	3.9	24.5	24.5	3.0
4.2-in. PWP M328A1	14	6.7	6.7	5.0	35.0	35.0	3.0
5-in. PWP Zuni MK4	15	7.8	7.8	5.9	41.0	41.0	3.0
2.75-in. WP wedge	16	2.8	2.8	2.0	3.8	3.8	3.0
2.75-in. WP M259 rocket*	17	5.6	5.6	4.3	34.0	34.0	3.0
3-in. WP wick	18	2.0	2.0	1.6	2.6	2.6	3.0
6-in. WP wick	19	2.3	2.3	1.8	3.1	3.1	3.0
155-mm WP M825 projectile*	20	0.0	0.0	0.0	60.0	60.0	3.0
81-mm RP wedge	21	1.9	1.9	0.6	4.2	4.2	3.0
181-mm RP XM819 cartridge*	22	4.9	4.9	1.6	17.0	17.0	3.0
Generator, ABC M3A3*	23	0.0	0.0	0.0	0.29	0.2	0.2
Generator, VEESS*	24	0.0	0.0	0.0	0.29	0.2	0.2
Smoke pot, fog oil M7A1*	25	0.0	0.0	0.0	0.29	0.2	0.2
Diesel fuel / oil / rubber fire	30	0.0	0.0	0.0	3.09	3.09	1.03
Muzzle blast	31	15	10.0	7.0	—	—	—
M76 IR grenade	32	10.8	10.8	10.8	0.0	0.0	0.0
L8A1 RP grenade	33	17.54	17.54	3.0	3.32	3.32	2.49

*Inventory smoke sources.

radius for instantaneous thermal puffs and on all three parameters for continuous buoyant plumes. This is because the combination of these factors determines the initial amount of thermal energy in the buoyant region. The constraining equations are (A-132) and (A-133). The user should be very careful that the relevant equation is satisfied if all parameters are input.

The preferred method for instantaneous puffs is to input or use model defaults for T_o and Q, the thermal production in calories per gram of obscurant. The code then determines R_o from equation (A-132). Generally, R_o is smaller than the obscurant radius, approaching zero as T_o is increased or Q is decreased. As long as equation (A-132) is satisfied, however, the actual puff rise is relatively insensitive to the assumed input temperature. For example, the analytic rise model of Morton *et al* [1956], discussed in section A-4, assumes infinite temperature and zero radius at a virtual source point $4R_o$ m below the source. The default procedure in COMBIC is to use T_o = 1.44 T_a and a Q value dependent on obscurant type. This initial mean temperature is consistent with thermal imagery of HE and WP fireballs. The model is also insensitive to initial upward velocity w_o for buoyant puffs. In a quiescent atmosphere, the drag and entrainment cooling will rapidly slow a fast-moving thermal puff. Typical rise velocities after 1 or 2 s are 2 to 3 m / s for hot thermal puffs generated from tactical smoke and HE.

For continuous buoyant plumes, the preferred method depends on whether the cloud rises at high velocities or with high temperature. The default method depends on the type of obscurant. If w_o is high (greater than 20 m / s), then the buoyancy radius R_o is set equal to the momentum radius R_m. The momentum radius is defined by

$$R_m = \left[\frac{\dot{m}_{air}}{\rho \pi v_o}\right]^{1/2}, \tag{B-16}$$

which follows from the definition of the mass of air inside the initial plume slice, as defined in section A-4. If appropriate, the velocity v_o is the total initial velocity including the vertical and horizontal components. R_o, v_o, and Q are then used in equation (A-133) to give a corresponding temperature for the region. Otherwise, if the initial velocity is not great, the preferred method to determine w_o uses T_o = 1.44 T_a (or user input); R_o equal to the source radius (or user input); and Q for the given obscurant (or user input). For diesel fuel / oil / rubber fires, w_o is typically about 2.5 m / s. For smoke generators, both R_o and R_m are small (1 to 3 cm typically), and the initial velocity is high (100 to 150 m / s). The rise equations rapidly slow this velocity with distance, however, as air entrains into the region. For continuous HC and other smokes, the velocity is small, often less than 1 m / s rise.

For phosphorus-based smoke, the thermal production coefficient defaults to

$$Q = 6600 + 580(Y_f - 3.16). \tag{B-17}$$

This value is based on 6600 cal/g produced when phosphorus burns first to P_4O_6 (5860 cal/g), and then to H_3PO_4 (740 cal/g). An additional 580 cal/g is liberated in the conversion of water vapor to liquid water. The zero humidity base value of 3.16 in the yield factor is subtracted to account for the water already included when the phosphoric acid is formed. The 3.16 value is one plus the ratio of (1) the atomic weights of three hydrogen atoms plus four oxygen atoms to (2) the atomic weight of one phosphorus atom. Other phosphorus-based acids are known to be likely constituents along with phosphoric acid. The overall value given by equation (B-18) is probably close to the true thermal production coefficient for phosphorus smoke, however.

For HC smoke munitions, the corresponding coefficient is

$$Q = 900 - 3.333T_b + 580(Y_f - 1.0). \tag{B-18}$$

Values of 300 to 940 cal/g have been reported in the literature for HC (Cichowicz, 1983). The variation is due to the amount of aluminum in the mix. For a munition with 5.5- to 9-percent aluminum, the burn duration T_b varies from 150 to 60 s (Cichowicz, 1983). Equation (B-19) is the model developed for the previous version of COMBIC to take the burn time into account. For smoke pots, a typical mix is 1 lb of fast-burning HC layered in with 30 lb of slow-burning HC. So, for smoke pots and large munitions, the limiting value is assumed to be

$$Q = 400 + 580(Y_f - 1.0). \tag{B-19}$$

For diesel fuel/oil/rubber, Q is assigned a default of 7185 cal/g diesel fuel. This value is a weighted total that includes the thermal production of motor oil and rubber, similar to the effective efficiency derived in appendix A (sect. A-4.1). It further includes a 50-percent reduction to account for thermal radiation losses (Weil, 1982). Q for anthracene is 9500 cal/g (AMC, 1967). Appropriate values for FS and FM smoke are uncertain; COMBIC uses a default of 6000 cal/g for both.

Smoke generators are usually assumed to produce a nonbuoyant cloud, despite their high exit temperatures. Model calculations tend to confirm this, but under certain conditions buoyancy may be marginally important, depending on generator design. Reports are available on generator design parameters and characteristics of the smoke vaporization-condensation process (AMC, 1967; Tarnove and Gordon, 1983). The default COMBIC model for generator production assumes two figures of merit representative of an M3A3 generator. First, a 12:1 ratio is assumed in the number of gallons of smoke produced per gallon of diesel fuel required to vaporize the smoke, S_f. Second, the smoke to air ratio, S_a, is 0.8:1 by weight. Relevant parameters for the smoke generation that are independent of the figures of merit are given in table B-5.

Table B-5. Smoke generator thermal characteristics [Tarnove and Gordon, 1983].

Obscurant	q_v (cal/g) vaporization*	q_c (cal/g) condensation	Density ratio, ρ_d/ρ_s	Boiling point, T_c (K)
Fuel (DF)	11,000†	—	—	—
Fog oil	−258	51	0.92	640
Diesel fuel	−197	58	1.00	540
PEG200	−303	59	0.75	580

*Raising smoke from 70 °F to boiling point plus 20 °F and then vaporizing it.
†Generator fuel (g) burned to vaporize smoke.

The thermal source term for the burned diesel fuel is

$$Q_s = \frac{11000}{S_f}\left(\frac{\rho_d}{\rho_s}\right) \tag{B-20}$$

in calories per gram of smoke produced. S_f is the smoke to fuel ratio, and the density ratio is given in table B-5. From the table, q_v is the value (in calories per gram of smoke) required to heat and vaporize the liquid smoke material. The internal air mixture is similarly heated. The air-vapor mixture exits the generator, entrains air, and cools to a condensation temperature. Neglecting any additional thermal terms relating particle size and vapor pressure, it can be assumed that the energy available in heating ambient air to the condensation temperature T_c and thus cooling the plume is

$$Q = Q_s - \frac{0.273}{S_a}(T_c - T_a) + q_v + q_c. \tag{B-21}$$

The value 0.273 cal/g K is the specific heat of DF combustion products (BCL, 1979). S_a is the smoke to air ratio, T_a the ambient air temperature, and T_c is taken to be the mean boiling point temperature from table B-5. Q is the thermal production value used in equation (A-133) for initial radius determination. For fog oil, diesel fuel, and PEG200, the Q values are 520, 695, and 345 cal/g smoke, respectively, at temperatures of 640, 540, and 580 K. Other generators may have significantly different characteristic ratios S_a and S_f, but equations (B-20) and (B-21) can be used with table B-5 to compute input values for Q.

These thermal production coefficients produce marginal buoyancy in a 5-m/s wind, at a 10-m reference height, and under neutral conditions, as can be seen from the following arguments. First, neglect the initial momentum of the plume. The plume is nearly horizontal, so use the windspeed for v in equation (A-145) and a very small value for s, such as 0.000001. The predicted plume rise from equation (A-145) is 7.5 m over the first 0.1 km downwind for a 36-gal/hr (35-g/s) fog oil plume. The diffusion radius of the plume for a surface roughness of 0.1 m is 15 m at 0.1 km downwind.

This calculation indicates that the plume rise can be significant even for the relatively small values of Q for fog oil compared to other smokes. However, atmospheric turbulence places a limitation on plume rise. From equation (A-156), the friction velocity is 0.29 m/s. From equations (A-158) and

(A-182), the eddy dissipation rate will halt plume rise once the plume vertical velocity falls below 0.34 m / s. For the example here, the plume rise velocity is in the range of 0.2 to 0.3 m / s. Thus, the model predicts that the rise will be limited to less than 7.5 m and the buoyancy effect is, at best, marginal.

The buoyancy radius in this example is about 3 cm. Next consider the effect of high initial plume velocity. Generator exit velocities are typically 100 to 120 m / s so that particles are the optimum size for obscuring visible wavelengths. Airflow in the above example is 44 g / s at the exit nozzle, under the assumption that parameter S_a = 0.8 and that the fog oil production rate is 35 g / s. The exit temperature, before the air-vapor mixture cools and condenses, can be estimated from

$$T_{max} = T_a + \frac{Q_s + q_v}{\frac{0.273}{S_a} + 0.58}, \tag{B-22}$$

where 0.58 is the (liquid) specific heat of fog oil in calories per gram kelvin. Values for diesel fuel and PEG200 are 0.55 and 0.72 cal / g K (Tarnove and Gordon, 1983). The exit temperature is about 960 K, which is fairly consistent with reported values for inside the nozzle. From equation (A-130) and an assumed ambient air density of 1200 g / m^3, the density of the air-vapor mixture just as it leaves the nozzle is 369 g / m^3. Assume 100 m / s velocity. Then, from equation (B-17), the momentum radius is 2 cm, not very different from the buoyancy radius when the plume has cooled to 640 K. If the nozzle is pointed upwards in the 5 m / s wind (as assumed in the example), equation (A-180) predicts that the maximum height will be 3 to 4 m. Thus, the momentum rise or "jet" action may also be marginally significant.

COMBIC allows the user to input a momentum radius on the SUBC input record. The parameters on this record are as follows:

- Z_b = burst or release height (in meters) of the obscurant above local terrain.
- v_f = terminal fall velocity (in meters per second) of particles in the cloud.
- f_d, δ = evaporation / deposition parameters defining equation (A-3):

  $$M(t) = M[f_d + (1 - f_d)e^{-\delta t}], \tag{B-23}$$

  where $M(t)$ is the time-dependent mass and M an initial mass.
- R_e = ground "reflection" coefficient (0. to 1.), required for equation (A-35). If 0, the obscurant sticks to the ground for a nonrising cloud. If 1, the obscurant is completely reflected from the ground.
- R_j = initial momentum radius (in meters) for plumes with high initial velocities, that is, "jets."

- u_o = initial horizontal velocity (in meters per second) of the plume or puff: positive with the wind, negative against the wind.

Default burst heights and fall velocities are zero for smoke. The reflection coefficient defaults to 0.55, an arbitrary value found from model comparisons with data.

The evaporation / deposition parameters that are nonzero are given in table B-6. The generator-produced smoke coefficients are fits to Rubel's data and analysis of droplet evaporation (Rubel, 1981a). Field experiments [Tarnove, 1981], however, tend to suggest that PEG200 may be as persistent as fog oil. These findings are somewhat contradictory, and further research is needed. The values in table B-6 are computed with equation (A-3); as shown, it takes 97 min to evaporate 30 percent of the initial smoke for fog oil, 3.7 min for diesel fuel, and 18.4 min for PEG200. Diesel fuel evaporates more rapidly because it contains volatiles.

For IR screener, the evaporation deposition rate has been reduced almost two orders of magnitude from that used in EOSAEL82 COMBIC. The earlier values were based on preliminary and limited observations, primarily qualitative, at smoke week tests. The current values are based on recent deposition data (Wentsel *et al*, 1984) and analysis with a modified form of the Van der Hoven method (Hanna and Hosker, 1982) for source depletion. The estimated deposition velocity from the data is 0.043 cm / s $\pm$ 0.011. This value is reasonable when compared with dry deposition theory (Hanna and Hosker, 1982) but is still rather uncertain, since only five data points were used.

Table B-6. Default evaporation / deposition parameters.

Obscurant	f_d (dimensionless)	$\delta(s^{-1})$
Fog oil (SGF2)	0.65	0.000333
Diesel fuel (DF)	0.10	0.001850
PEG200	0.25	0.000463
IR	0.00	0.000154

B-1.5 Mass Production Rate—BURN and BARG Input Records for Smoke

The SUBA, SUBB, and SUBC records will probably be little used except to input characteristics of munitions that are very different from those in the code menus. The BURN and BARG input records, however, are often used. The BURN record specifies the total length of time the source emits smoke, and the BARG record "scales up" the obscurant clouds for many sources acting over a period of time within a well-defined area.

Burn Function

The mass production rate (or "burn function") is parameterized for the specific smoke source as

$$\dot{M}(t) = \frac{1}{T_b}\left[B_1 + B_2\left(\frac{t}{T_b}\right) + B_3\left(\frac{t}{T_b}\right)^2 + B_4\left(\frac{t}{T_b}\right)^3 + B_5 B_6 T_b e^{(-B_6 t)}\right], \qquad \text{(B-24)}$$

where $\dot{M}$ is a rate (in grams per second), t is time since ignition (in seconds), and T_b is the total production time (in seconds). The user can input all six coefficients as well as a total burn duration on the BURN input record.

By integration of equation (B-25), the total mass produced between time 0 (ignition) and time t is the cumulative mass function:

$$M(t) = B_1\left(\frac{t}{T_b}\right) + \frac{1}{2}B_2\left(\frac{t}{T_b}\right)^2 + \frac{1}{3}B_3\left(\frac{t}{T_b}\right)^3 + \frac{1}{4}B_4\left(\frac{t}{T_b}\right)^4 + B_5\left(1 - e^{-B_6 t}\right). \qquad \text{(B-25)}$$

The burn durations and burn coefficients for all menu sources are given in table B-7. Users who have only EOSAEL82 should notice some changes in the table. There are additional obscurants, and some parameters are different for the values for the M825 155-mm WP round.

COMBIC tests the cumulative integral, equation (B-25), against the total mass of smoke and rescales the coefficients to ensure that 100 percent of the smoke is emitted by time T_b:

$$\dot{M}_a = \frac{M_a}{M(t_b)}\dot{M}(t). \qquad \text{(B-26)}$$

It is customary to define burn rate coefficients like B_1 through B_6 so that the total cumulative mass $M(T_b)$ is either one or the total mass. Because of the rescaling above, however, the user can apply any convenient convention.

The burn function of COMBIC was slightly modified for three munitions: XM819 RP, M825 WP, and M110 WP (Ayres and Baca, 1987). The new function allows for better modeling of the end of the burn function for some munitions. It allows the munition to smolder. The new function is

$$\begin{aligned} \dot{M}(T)^{new} &= \dot{M}(T)^{old} \qquad < T_{SMLD} \\ \dot{M}(T)^{new} &= \dot{M}(T_{SMLD})^{old} \exp\left[-\frac{C_{SMLD}}{T_{burn} - T_{SMLD}}(T - T_{SMLD})\right] \qquad T > T_{SMLD} \end{aligned} \qquad \text{(B-27)}$$

where T_{SMLD} is the time at which the munition starts to smolder and C_{SMLD} is the exponential decaying factor. Since C_{SMLD} and T_{SMLD} are zero for all other munitions, in effect the original burn function is used for these. If the user desires to use the new burn function for other munitions or change the existing parameters, it can be done through a new card record

Table B-7. COMBIC model default burn durations and coefficients.

Type code	Munition	Burn duration (s)	Production rate coefficients					
			B_1	B_2	B_3	B_4	B_5	B_6
1	155-mm HC M1 canister	100	0.537	0.476	4.779	–5.472	0.0	0.0
2	155-mm HC M2 canister	70	0.631	–0.4985	6.745	–6.52	0.0	0.0
3	105-mm HC canister	120	0.2218	3.915	–1.737	–2.400	0.0	0.0
4	155-mm HC M116B1 projectile*	100	0.537	0.476	4.779	–5.472	0.0	0.0
5	105-mm HC M84A1 projectile*	120	0.2218	3.915	–1.737	–2.400	0.0	0.0
6	Smoke pot, HC M5*	900	1.0	0.0	0.0	0.0	0.0	0.0
7	Smoke post, HC M4A2*	750	1.0	0.0	0.0	0.0	0.0	0.0
8	60-mm WP M302A1 cartridge*	45	0.6	–0.6	0.0	0.0	1.0	0.2
9	81-mm WP M375A2 cartridge*	45	0.6	–0.6	0.0	0.0	1.0	0.2
10	4.2-in. WP M328A1 cartridge*	45	0.6	–0.6	0.0	0.0	1.0	0.2
11	2.75 in. WP M156 rocket*	45	0.6	–0.6	0.0	0.0	1.0	0.2
12	155-mm WP M110E2 projectile*	240	0.2	–0.2	0.0	0.0	1.0	0.6
13	105-mm WP M60A2 cartridge*	75	0.6	–0.6	0.0	0.0	1.0	0.2
14	4.2-in. PWP M328A1	180	0.6	–0.4	0.0	0.0	0.15	0.3
15	5-in. PWP Zuni MK4	180	0.6	–0.4	0.0	0.0	0.15	0.3
16	2.75-in. WP wedge	240	0.521	2.106	–1.11	–0.748	0.0	0.0
17	2.75-in WP M259 rocket*	240	0.521	2.106	–1.11	–0.748	0.0	0.0
18	3-in. WP wick	470	1.631	0.678	–5.907	4.012	0.0	0.0
19	6-in. WP wick	390	1.8086	–2.556	2.883	–2.008	0.0	0.0
20	155-mm WP M825 projectile*	780	3.3236	–9.4664	9.5994	–3.1612	0.0	0.0
21	81-mm RP wedge	260	0.653	–3.136	15.309	–12.87	0.0	0.0
22	181-mm RP XM819 cartridge*	600	5.088	–20.268	25.938	–10.400	0.0	0.0
23	Generator, ABC M3A3*	900	1.0	0.0	0.0	0.0	0.0	0.0
24	Generator, VEESS*	900	1.0	0.0	0.0	0.0	0.0	0.0
25	Smoke pot, fog oil M7A1*	600	1.0	0.0	0.0	0.0	0.0	0.0
26	155-mm HE (dust)	1	1.0	0.0	0.0	0.0	0.0	0.0
27	105-mm HE (dust)	1	1.0	0.0	0.0	0.0	0.0	0.0
28	4.2-in. HE (dust)	1	1.0	0.0	0.0	0.0	0.0	0.0
29	10-lb C4 (dust)	1	1.0	0.0	0.0	0.0	0.0	0.0
30	Diesel fuel / oil / rubber	1800	1.0	0.0	0.0	0.0	0.0	0.0
31	Muzzle blast	0	1.0	0.0	0.0	0.0	0.0	0.0
32	M76 IR grenade	0	1.0	0.0	0.0	0.0	0.0	0.0
33	L8A1 RP grenade	658	0.0	0.0	0.0	0.0	120.0	0.0083

*Inventory smoke sources

defined in the main body (table 25). If the parameters of the records are entered as zeros, default values will be used. The user can override the new burn function for the three munitions by setting C_{SMLD} to zero, T_{SMLD} to a nonzero number, and T_{burn} back to its original value. In all situations, T_{burn} must be greater than T_{SMLD}. Table B-8 lists T_{SMLD} and C_{SMLD} for the munitions in the COMBIC source table that are believed to exhibit smoldering.

Table B-8. Production rate coefficients for three munitions to allow for smoldering.

Munition type	Burn duration (s)	Production rate coefficients							
		B_1	B_2	B_3	B_4	B_5	B_6	C_{SMLD}	T_{SMLD}
155-mm WP M110E2	240	0.2	–0.2	0.0	0.0	1.	0.6	3.0	8.
155-mm WP M825	780	3.324	–9.466	9.599	–3.161	0.	0.0	1.3	480.
I81-mm RP XM819	600	5.088	–20.268	25.938	–10.40	0.	0.0	3.0	150.

Barrage Approximation

The barrage approximation provides the means for a user to save computation time when a large number of sources ignite either at random or uniformly over a period of time within a relatively small area.

Users of EOSAEL82 COMBIC should notice some changes in the barrage option. The area is no longer in hectares. Rather, the user may now specify an area by giving its alongwind and crosswind dimensions in meters. (The constraint that the dimensions be in the alongwind and crosswind directions is, unfortunately, due to the problems associated with calculations for an arbitrary orientation.) The rate of impacts is now in terms of the number of rounds per second in the user-defined area rather than the number of rounds per hectare per minute. The barrage duration is in seconds. These changes keep the units as consistent as possible between records. Furthermore, in previous versions, setting up input records generally required the user to compute the parameters by hand from the more convenient inputs now used.

Barrage parameters are input on a BARG record. The record defines the following parameters:

$\dot{N}_B$ = a rate of impacts or ignitions (in rounds per second) in the user-defined impact region.

t_B = duration of the barrage (in seconds). This time does not include the burn duration of a single smoke round but only the time over which rounds impact or ignite.

D_x = The alongwind length of the area in which the barrage occurs (in meters). Note that this is not a radius or half width but the diameter or full width of the impact region.

D_y = The crosswind length of the area in which the barrage occurs (in meters).

The definition of a “round” is whatever obscurant mass results from a MUNT input record. Thus, if the MUNT record has a scale factor X_n of 5.0 (meaning five units of whatever is being computed in phase I), each “round” in the

barrage is actually five units. The effect of the barrage is thus equal to N_B times the number of munitions, described on the MUNT or SLOC records, becoming active each second.

The source region is actually elliptical, with the area determined from

$$A = (\pi/4) D_x D_y. \tag{B-28}$$

The barrage option does three basic things. First, it changes the total mass and the mass emission rate, combining individual rounds. Second, it modifies the initial cloud dimensions to fill the barrage impact area. Third, it combines instantaneous puffs into continuous clouds having the same rise characteristics as the puff subclouds.

The total mass of smoke produced by the barrage cloud must equal the smoke produced by individual "rounds" defined by M_a in equation (B-2). This means that the total obscurant produced is

$$M_{aB} = \dot{N}_B t_B M_a. \tag{B-29}$$

The effective barrage burn rate function (discussed in sect. A-2, eq (A-70), is computed internally by the code. Thus, the user does not need to input any special "barrage" burn function. As stated in that section, the effective smoke duration will become the total time of the barrage impacts plus the duration of a single round.

The source cloud was also discussed in section A-2, and there it was shown that the effect of combining a random impact pattern with the dimensions of a single cloud is to sum the squares of the sigmas. The sigma for the barrage region is defined to be a Gaussian region containing 95 percent of the rounds. This produces a factor of 4.47 for scaling the input "diameter" of the region:

$$\sigma_{By} = \left[\sigma_y^2 + \left(\frac{D_y}{4.470} \right)^2 \right]^{1/2} \tag{B-30}$$

and

$$\sigma_{Bx} = \left[\sigma_x^2 + \left(\frac{D_x}{4.470} \right)^2 \right]^{1/2}. \tag{B-31}$$

Barrage clouds are modeled as continuous Gaussian plumes.

Phosphorus smokes are modeled as the superposition of two clouds. The first is computed to have the same trajectory as that produced by the instantaneous puff of the basic "round."

To compute the probability that heated regions will overlap is relatively simple. Assuming a well-mixed volume of initial radius of 6 m for the heated region of a puff with mean temperature 55 K above ambient, the rise over 50 m requires about 30 s, and the average volume, including expansion, is about 8000 m^3. A 50-m-high region over a 10,000-m^2 area contains

500,000 m^3 or about 63 such cloud volumes. The probability that at least two puffs will overlap in the region is less than 53 percent for a barrage rate of 0.3 rounds per second. At a barrage rate of 0.53 rounds per second, the probability has risen to 90 percent, and at 0.73 rounds per second, it reaches 99 percent. The coupling between individual puffs, however, becomes appreciable only after a rate of 1.67 rounds per second is reached, owing to the $Q^{1/4}$ scaling of buoyant rise. By that point, the buoyancy of the average continuous cloud begins to dominate. Therefore, the barrage-produced cloud is modeled as two continuous Gaussian clouds, one with the rise trajectory of an individual round puff, and the other with the buoyant rise determined by the rate of release of heat from the effective barrage burn function computed by the code.

B-2 Model for High-Explosive and Vehicle-Generated Dust

Because of variations in the environmental sources of dust, HE and vehicle-produced dust obscuration is fundamentally more difficult to model than smoke. COMBIC models HE dust generated by static uncased, static cased, and live-fire munitions detonated at any depth or height of burst and for any angle of impact (that is, munition orientation). A model is provided to extend the crater volume prediction to include any user-defined munition and to treat various soil types. A sod depth correction has been added to reduce the computed volume of ejecta from the crater and the amount of dust accordingly.

COMBIC approaches the problem of the broad range of sizes of dust particles by dividing the cloud models into three size ranges. A very-large-particle "mode" is included that accounts for the ballistic soil and large agglomerates that remain airborne for only a few seconds. This mode was required for better modeling of dust effects at millimeter wavelengths. A large-particle mode component is included to partly address the dust size distribution from 20 to 200 μm, which falls out somewhat more slowly than the very-large-mode dust. Finally, a small-size "persistent" mode is included for dust that remains suspended for long periods and contributes the most extinction per unit mass.

Various options are available for particular scenarios. A *submunition* option allows the approximate treatment of explosive subunits that form separate craters. The *barrage* option treats large numbers of munitions impacting over a small area and relatively continuous time interval as a simplified continuous source of dust. The *vehicular* dust option models the movement of the source and provides scaling relationships for the amount of dust as a function of vehicle speed, weight, and silt content. These options are discussed in more detail in section B-2.3.

Both the submunition and barrage options deal with multiple sources, the submunition option dealing with multiple sources delivered by a simple

shell, and the barrage option dealing with many shells arriving at the same general location and time. The submunition option allows more detailed treatment of individual rounds. The barrage option accelerates calculations for many overlappling sources.

The bulk of the following discussion concentrates on the high-explosive model, giving details of its implementation.

B-2.1 High-Explosive Model Parameters

HE-generated dust clouds are treated as five subcloud components: (1) a buoyant small-particle puff, (2) a buoyant, large-particle stem that settles out with time, (3) a nonbuoyant puff that models the small-particle dust "skirt," (4) a connecting small-particle stem between the skirt and the buoyant clouds, and (5) a very-large-particle puff that follows a ballistic trajectory. Carbon particles produced during the detonation process are partitioned among the buoyant clouds and stem.

A major problem in modeling HE dust is to define the quantity of dust lofted into the atmosphere. Particle size distribution measurements (Pinnick, 1982; Pinnick *et al*, 1982) show that the size distribution is extremely broad, with an appreciable proportion of particles larger than 20 μm. Size distribution measurements performed at different locations also suggest that the airborne distributions of small particles are not as strongly correlated to the percentage of clay (less than 2 μm diam), silt (2 to 70 μm diam), and sand (greater than 70 μm diam) of the parent soil as one might expect. This imperfect correlation may be due in part to the soil analysis technique (which breaks up soil agglomerates), to the agglomeration of particles by explosive shock, and to other factors.

Defining the optical properties of dust in terms of extinction per unit mass is also made difficult by the wide range of particle sizes. Particles much larger than the wavelength of interest contribute a large part to the mass but only a small part to the extinction. They also settle out of the cloud, and thus the size distribution is time dependent. The characterization of dust clouds is, therefore, more empirical than that of smoke.

Crater volumes

Modeling begins with the prediction of the crater volume that is the source of most of the HE-generated dust. The crater volume depends on the explosive yield, which is measured in terms of the equivalent yield of TNT, the depth of burst, soil type, charge orientation, and means of delivery. To calculate crater volume, COMBIC uses a model developed by Thompson (Thompson and DeVore, 1982; Thompson, 1980a). The apparent crater volume V_{ac} is assumed to scale for any explosive yield W as

$$V_{ac} = S_{ac} W^{1.111}, \tag{B-32}$$

where W is in pounds of TNT, and V_{ac} is in meters cubed. (Bear in mind, however, that Thompson's argument in choosing 1.111 over 1 is that the charges are "small": 1000 lb or less.) The apparent crater scaling factor S_{ac} contains all other dependent factors.

Thompson developed this model from DRTRAN (Duncan, 1981), an earlier EOSAEL dust model on which some of COMBIC is based, which used polynomial fits to scaled crater depth and radius as a function of burst depth and soil conditions. Thompson found that the curves so produced could be reduced to a single representation for static uncased charges. Figure B-5 shows the resultant curve, and table B-9 presents the multiplicative scale factors for the various soil types. For equal yield, soil type, and burst depth, significant differences occur between craters formed by uncased and cased explosives and between craters formed by static explosions and by live-fire delivery. From a first principles approach, the fraction of energy carried away by the shell casing fragments, F_s, was determined (in terms of the work done by expanding combustion products) to be 37.5 percent of the total yield (Thompson and DeVore, 1982).

When the munition is assumed to be a tapered cylinder with flat ends, the quantity and energy of fragments impacting the crater region can be determined. This determination depends on the length and diameter of the casing, the depth or height of the munition, and the orientation of the munition. The model considers two limiting cases: horizontal and vertical orientation. The algorithm models F_{ch}, the fraction of energy coupled to the ground for a horizontal munition at any depth, and F_{cv}, the fraction for a vertically oriented munition at any depth. The value for any intermediate

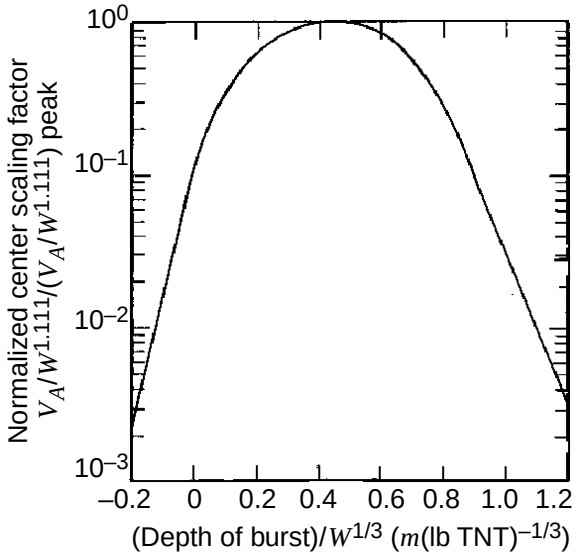

Figure B-5. Universal apparent crater volume for bare (uncased) charges.

Table B-9. Soil-dependent parameters—maximum crater scaling factors and airborne dust fractions of apparent crater volume.

Soil type and code	Peak scaled crater volume (uncased charges) $m^3 \cdot (\text{lb TNT})^{-1.111}$	Fraction of apparent crater mass in			
		Ballistic cloud	Large-particle stem	Small-particle	
				Fireball	Stem
Rock	0.0175	0.09914	0.05824	0.00029	0.00090
Dry cohesive soils	0.0218	0.05470	0.03223	0.00253	0.00734
Dry sandy soil	0.0654	0.04825	0.02844	0.00148	0.00423
Dry to moist sandy soils	0.1550	0.07204	0.04238	0.00088	0.00366
Wet sand and moist cohesive soils	0.3050	0.11842	0.07358	0.00063	0.00283
Wet cohesive soils	0.6980	0.20137	0.12163	0.00017	0.00072

*The partitioning applies to the fraction of total apparent crater mass (1500 kg / m^3) that becomes airborne.

orientation is then assumed to be

$$F_c = \left[(F_{ch} \cos\theta)^2 + (F_{cv} \sin\theta)^2 \right]^{1/2}. \tag{B-33}$$

When the apparent crater volume is assumed to be proportional to the total energy coupled into the ground, the yield coupled into the ground must be

$$W_g = [F_s F_c + (1 - F_s) F_b] W, \tag{B-34}$$

where F_b is the normalized crater scaling profile (fig. B-5) for depths above 0.45 m (lb TNT)$^{-0.33}$ and 0.947 otherwise. The model then iteratively finds the yield of the uncased charge that, at the same depth as the munition, produces the same yield W_g coupled to the ground. The apparent crater volume produced by this equivalent uncased charge must be in fact the volume produced by the cased charge, assuming that equal energy coupling into the ground lofts equal amounts of dust.

The final function of the crater model is to provide an estimate of the difference in volume between static and live-fire-delivered munitions. Based on the observed asymmetry of live-fire-produced craters and the increase in volume with inclination angle θ, the modeled dependence is

$$V_{ac}(\text{live}) = (0.4 + 0.6 \sin\theta) V_{ac}(\text{static}). \tag{B-35}$$

If the casing dimensions are for submunitions and the total yield W is distributed equally among the submunitions, then the total of the N_s crater volumes is

$$V_{ac} = N_s S_{ac} \left(\frac{W}{N_s} \right)^{1.111}. \tag{B-36}$$

The crater scaling factor S_{ac} implicitly depends on the depth, orientation, and yield of a single submunition. The internally calculated scaling factor may be overridden by the user by direct input on the MUNT input record.

COMBIC uses sod depth to correct the volume of the crater to that part of the volume that contains soil. The method parallels that used in the original EOSAEL DRTRAN2 model. The corrected volume is

$$V'_{ac} = V_{ac}\left[1 - \frac{d_{sod}}{0.38V_{ac}^{1/3}}\right]^3, \qquad \text{(B-37)}$$

where the sod thickness d_{sod} (depth) is in meters, input optionally on the TERA record.

Lofted fraction of dust

The total lofted fraction of dust from the apparent crater is only a small fraction of the apparent volume of the crater. Large detonations are reported to result in dust volumes that range from a few tenths of a percentage point to 30 percent (Gould, 1981) of the apparent crater volume. Results from measurements at a test at Fort Carson in 1983 (Long *et al*, 1984), for example, showed that the volume of airborne dust produced ranged from 0.3 to 1.7 percent of measured crater volumes. Table B-9 shows the fractions of the apparent crater volume that are assumed to be in each of the modeled dust subclouds from HE. (These are the fractions that would be input on an optional "SUBA" record, if the user were customizing a scenario.) The values were chosen partly from comparisons with data. They were also required to reproduce certain observed features in measured dust. Measured size distributions (Pinnick, 1982; Pinnick *et al*, 1982; Pinnick *et al*, 1983) are not entirely consistent, but they do tend to suggest that the mass of dust less than 10 μm in radius (the "small-particle mode") and that from 10 to 100 μm in radius (the "large-particle mode") have the trends and range of values shown in the table. These modes separate in a bimodal lognormal particle size distribution. The very-large-particle "ballistic" region of the cloud is assumed to cover the range from 100 μm to 1.0 cm. From large HE detonations, the large-particle ballistic mode tends to have a power law distribution (Seebaugh and Linnerud, 1978) with exponents of 3.75 for cohesive soils (suggesting more large particles) and 4.0 for noncohesive soils. These distributions have been matched at the 100-μm point to the large-particle mode in determining the mass in the ballistic cloud.

Besides the four subclouds shown in the table, a nonbuoyant, small-particle, surface dust cloud is modeled that is assigned a mass equal to 1.875 times the sum of the masses of the small-particle buoyant region ("fireball") and the small-particle stem.

Rise and fall velocities

The small-particle regions have 0.3 cm / s fall velocity. The large-particle cloud stem is given an average fall velocity of 0.92 m / s, that of a 75-μm particle of specific gravity 1.5. The ballistic cloud particles follow an initial cloud geometry that injects them upward into the air with a model of the form

$$\bar{z}_{vl} = -\frac{1}{4}gt^2 + \frac{1}{2}w_o t, \tag{B-38}$$

where $\bar{z}_{vl}$ is the centroid height and w_o the initial upward velocity. The model applies only over the ballistic rise time w_o/g, at which point the cloud stops rising. The upward velocity, currently modeled as nonzero only for buried charges, is given by

$$w_o = 9.9W^{1/6}. \tag{B-39}$$

Following the ballistic rise, the centroid falls back to earth with

$$\bar{z}_{vl} = \frac{1}{4}\left(\frac{w_o^2}{g}\right) - w_{fall}\left(t - \frac{w_o}{g}\right), \tag{B-40}$$

where

$$w_{fall} = \min\left[\frac{1}{4}g\left(t - \frac{w_o}{g}\right), 4.15\right], \tag{B-41}$$

where 4.15 m / s is half the terminal fall velocity of a 1050-μm particle. The bottom of the cloud remains at ground level, while the top of the cloud initially rises at twice the centroid velocity. This internal rise is the reason for the one-half factors in the equations.

Radii

The radii of the ballistic region are determined in various ways. The vertical radius of the ballistic region equals the centroid height above ground level. The horizontal radius depends on the various cases. For charges above the surface, the centroid height (discussed in sect. B-2.2) is set equal to the surface cloud vertical radius. The horizontal radius also matches the surface cloud. The ballistic cloud immediately begins to fall with the velocity in equation (B-42) (w_o is zero). For charges below the surface, however, the horizontal cloud expands with the vertical cloud rise. The horizontal radius until the end of ballistic rise is

$$R_{hvl} = \bar{z}_{vl} \cdot \max\begin{bmatrix} 1.192 - 20.5\left(\frac{D_b}{W^{1/3}}\right) - 1 \\ 0.577 \end{bmatrix} \quad ; \tag{B-42}$$

after the ballistic rise time limit, the horizontal radius remains fixed. This corresponds to the observed fallback of large dust particles but does not model the actual ballistic ejecta of rocks.

Thermal energy and rise and fall

The fraction of energy appearing as heat for thermal rise is taken to be the remainder of total energy not coupled into the ground, including the case fragments:

$$F_h = (0.53 - 0.504F_b)(1 - F_s). \tag{B-43}$$

Use of this "hydro-yield fraction" gives a total thermal energy of

$$Q = 1100CF_hW, \tag{B-44}$$

where C converts pounds to grams, and 1100 cal/g are provided by the explosive. Q provides the thermal energy for buoyant rise.

Parameter modifications

The previous discussion describes the calculation of the parameters with the default internal models. Users can modify the internal models through direct input of certain parameters.

Both the crater volume scaling factor S_{ac} and the hydro-yield fraction F_h may be input by the user on the MUNT record to override the built-in models. The data for crater volumes from field tests (Kennedy, 1980) show that a variation in crater volume of up to a factor of two is observed even in the same type of soil and for the same charge yield. Within this spread, the model provides good agreement. The spread can be attributed partly to the difficulty in measuring the precise boundaries of the crater. Subsurface soil variations are probably also a factor.

B-2.2 High-Explosive Model Application

The high-explosive model allocates matter and energy among the five subclouds described before and applies the buoyancy model to each subcloud. As a reminder, the five subclouds are (1) a buoyant fireball of small particles, (2) a surface cloud of small particles, (3) a connecting stem of small particles, (4) a stem of large particles that have 0.92 m/s fallout, and (5) an initial ballistic cloud of large particles that rapidly return to earth.

Forty percent of the available carbon from TNT (approximately 0.3 lb of carbon per pound of TNT yield) is by default divided in equal amounts among the fireball and cloud stem regions. The user may override this value by input on the SUBA record if the carbon yield is different for the type of explosive considered.

Half the total thermal energy Q is assigned to the large-particle and half to the small-particle buoyant clouds.

The vertical rise of each region is computed with the equations for Gaussian puffs given in section A-5 on the boundary layer model. Figure B-6 illustrates some of the forces that determine vertical rise. The large-particle

Figure B-6. Forces affecting rise of explosive dust.

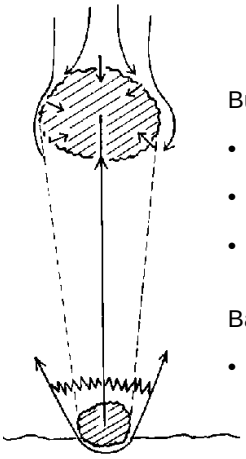

Buoyancy phase, 2 to 20 s

- Drag opposes motion
- Entrained air cools and expands fireball
- Buoyant force decreases

Ballistic rise, 0.2 to 2 s

- Momentum entrained from expelled soil

region has a height that the model computes by taking the total distance fallen over time t following the explosion and subtracting it from the height the region would have had if there were no fall velocity. The windspeed for horizontal advection is taken to be that which is appropriate to the fall velocity's adjusted height. The stem cloud centroid position is computed as the average between the small-particle buoyant region and the ground-level position that the region would have had if it were nonbuoyant. The increase in windspeed with height implies that the nonbuoyant position will lag behind the buoyant position. This shearing effect rotates or "cants" the stem through an angle whose tangent is the difference in downwind distance of the buoyant and nonbuoyant positions divided by the height of the buoyant region. The stem is an oversimplified model of the region of dust that trails the buoyant puff in real-world dust clouds. For convenience, since mass profiles are not produced and stored for Gaussian puffs, no "bleeding" of dust from the buoyant region into the stem is modeled. The storage locations used to hold the mass production profiles as a function of time for continuous Gaussian plumes are used to hold the cant angles as a function of downwind distance for Gaussian puffs.

In addition to the buoyant cloud regions, a nonbuoyant base cloud (or "skirt") is also modeled. The base cloud originates in part from the dust ejected near the edge of the crater and in part from shock and fragment-raised dust outside the crater.

The basic size for the initial clouds is determined from the largest of the following:

the buoyancy radius,

$$R_o = 1.9 \left[\frac{3q}{8\pi \rho_a C_p t_a} \right]^{1/3}, \tag{B-45}$$

the radius of a volume equal to that of the crater, and

$$R_{ac} = \left[\frac{3V_{ac}}{4\pi}\right]^{1/3} \tag{B-46}$$

the volume at which the dust density equals the air density,

$$R_d = \left[\frac{3M_a}{4\pi\rho_a}\right]^{1/3}. \tag{B-47}$$

These results are then adjusted for the observed cloud shape, which depends on burst depth. Buried charges produce higher clouds, while airbursts produce lower, wider clouds. The horizontal-to-vertical-radius ratio is taken to be a minimum of one and a maximum of four, with intermediate values between these limits given by

$$S_h = 2.25N_s^{1/3} - \frac{10.4D_b}{W^{1/3}}. \tag{B-48}$$

The source sigmas are then specified in terms of the basic values

$$\sigma_z = \frac{R}{2.15S_h^{1/3}} \tag{B-49}$$

and

$$\sigma_x = \sigma_y = S_h\sigma_z. \tag{B-50}$$

The sigmas for the buoyant small-particle region and buoyant large-particle region are, therefore, initially equal to the basic values. For the base cloud, the values are

$$\sigma_{0z} = 1.8\sigma_z, \tag{B-51}$$

$$\sigma_{0x} = \sigma_{0y} = 1.5\sigma_x, \tag{B-52}$$

and for the cloud stem,

$$\sigma_{0z} = 1.25\sigma_z, \tag{B-53}$$

$$\sigma_{0x} = \sigma_{0y} = 1.25\sigma_x. \tag{B-54}$$

B-2.3 Model Options

Submunition option

If the submunition option is selected by the SUBM parameter being set to a number larger than 1.0 on the MUNT record, then the casing dimensions on a corresponding DUST record should refer to the dimensions of the submunitions. This will allow proper calculation (by eq (B-36)) of the total crater volume producing obscurants.

Barrage option

For the barrage approximation, the dust production model is similar to that for WP smoke. Two continuous Gaussian clouds are produced, buoyant and nonbuoyant. The buoyant cloud has the vertical rise trajectory of a single small-particle buoyant region for an individual munition. For both clouds, the mass production is assumed to be uniform over the barrage period. The buoyant cloud is given the total mass of the small-particle buoyant clouds and stem, and 5 percent of the mass of the large-particle region; it is also given 83 percent of the carbon. The buoyant cloud is assumed to have zero fall velocity. The nonbuoyant cloud is given the mass of the base cloud plus 5 percent of the mass of the large-particle region and 17 percent of the carbon. Both clouds are assumed to be small-particle mode. Since the large-particle mode has only 10 percent of the mass extinction of the small mode, the 5-percent rather than 50-percent mass fractions are partitioned to represent the large particles. The barrage source sigmas are computed as they are for smoke.

Table B-3 gives the mass extinction coefficients for the small-particle and large-particle modes. The small-mode mass extinction values are based on field tests [Duncan, 1981; Bowman *et al*, 1979, Ground, 1978b; Maddix *et al*, 1982; Nelson and Farmer, 1981]. The large-particle mode values are based on Mie calculations. These values should not be taken out of the context of the COMBIC dust model. As mentioned in section B-1.2, mass extinction for large particles is not in fact a constant when applied to a size distribution of finite width that varies in both space and time, as in real-world clouds. The carbon mass extinction values are those of the DRTRAN model (Duncan, 1981) and represent small particles of mean radius of about 0.2 μm. The millimeter-wave values are based on a study by Alexander, Brown, and Mott (1984). The appropriate scaling to the ballistic sizes has also been performed with Mie calculations.

Vehicular dust option

Vehicular dust is modeled as a nonbuoyant, continuous Gaussian plume. The source terms are those of the DRTRAN vehicular dust model (Duncan, 1981; Dyck and Stukel, 1976). (DRTRAN is an earlier EOSAEL dust model on which some of COMBIC is based; it is no longer used.) The production rate of dust is determined by

$$\dot{M}(t) = aNS_nM_vu_v^2, \tag{B-55}$$

where $\dot{M}$ is the constant dust production rate in grams per second, N is an arbitrary dimensionless scale factor (it may be input by the user, but normally it has a default value of one), S_n is the percentage of silt, M_v is the vehicle weight in tons, and u_v is the vehicle speed in meters per second. The scale factor was derived for DRTRAN based on the analysis of Smoke

Week II vehicle dust trials (Ground, 1978a):

$$a = \begin{cases} 0.00345 & \text{for wheeled vehicles} \\ 0.00460 & \text{for tracked vehicles.} \end{cases} \tag{B-56}$$

The source sigmas are taken as

$$\sigma_{0x} = 0, \tag{B-57}$$
$$\sigma_{0y} = 0.233 W_v (1 + u_v/20), \text{and} \tag{B-58}$$
$$\sigma_{0z} = 0.15 W_v, \tag{B-59}$$

where W_v is the vehicle width in meters. The height of the source is assumed to be 25 percent of its width.

Scaling laws for changing the total obscurant mass and for accounting for locally warm, buoyant regions in the clouds have been discussed in various sections. However, for clouds produced by moving sources, a special set of scaling laws is applied. The cloud produced by a moving source has an apparent direction that is different from that produced by a source at rest; this direction is the vector difference of the wind and source velocities (fig. B-7). The downwind transport and diffusion, however, are dependent on the distance over which the cloud has traveled in relation to the position at which that portion of the cloud was generated. Note that it does not depend on the present position of the vehicle or source but rather on its earlier position. This fact is used to allow the cloud history computed for a stationary source in Phase I to be used in Phase II for sources moving at any constant speed and direction. The model assumes that the cloud extends from the current source position to a leading edge along a straight line. The leading edge position is determined by the current time and the position of the source at ignition time (that is, the starting time and position when production began). The assumption that the effective plume lies along a straight line is not quite accurate, since a windspeed that is changing with height moves the leading edge downwind at a different speed than portions of the cloud near the source. But for the nonbuoyant or slightly buoyant source, the resulting curvature of the plume centerline is small.

All table lookup and LOS intersections for the continuous plume produced by a moving source are computed in the rotated frame in which the centerline of the plume is the x-axis. This computation is accomplished by the relations

$$C_x = (x_d - x_{os} - x_s + x_{os})/L_e, \tag{B-60}$$
$$C_y = -(y_s + y_{os})/L_e, \tag{B-61}$$
$$L_e = \left[(x_d - x_s)^2 + (y_{os} - y_s)^2)\right]^{1/2}, \tag{B-62}$$
$$x_e = C_x x_w + C_y y_w, \tag{B-63}$$
$$y_e = -C_y x_w + C_x y_w, \tag{B-64}$$

Figure B-7. Vehicular source dependence on vehicle speed and windspeed.

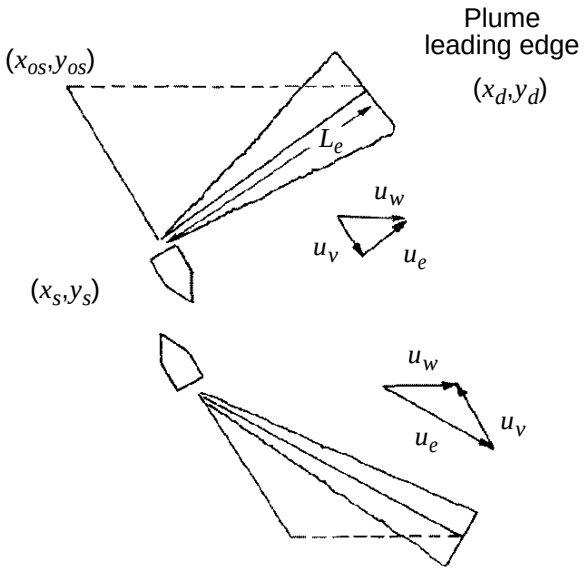

which transform any coordinates in the Phase II wind-rotated system into the effective plume system. L_e is the length of the effective plume; x_{os}, y_{os} are the coordinates of the source at ignition time, that is, its starting position in the original wind-rotated system; x_s, y_s are the current source coordinates in the wind-rotated system; and x_d, y_d are the current downwind coordinates of the leading edge of the plume in the wind-rotated system.

A linear scaling of distances along the effective plume is used to provide values for table lookup. A correction factor is

$$S_t = \frac{x_d - x_{os}}{x_{de} - x_{se}} = \frac{x_d - x_{os}}{L_e}, \tag{B-65}$$

where $x_d - x_{os}$ is the distance between the leading edge and the initial source position in the wind-rotated frame, and $x_{de} - x_{se}$ is the distance of the leading edge from the current source position in the effective plume coordinate system, L_e. Thus, to look up the cloud dimensions at 15 m down the axis of the effective plume in relation to the moving source, one simply uses $15S_t$ in the stored cloud tables. Similarly, when one finds the average mass per unit downwind concentration, the average mass per unit distance in the effective plume is simply that value multiplied by S_t.

Vehicular dust sources are scaled in Phase II if the vehicle speed differs from that of Phase I. The scaling follows the assumed model for dust production:

$$\dot{M}(t)_{II} = \frac{v_{II}^2}{v_I^2}\dot{M}(t)_I, \tag{B-66}$$

where v_I and $\dot{M}_I$ are the vehicle speed and dust production rates input in Phase I, and v_{II} and $\dot{M}_{II}$ are the Phase II inputs.

Appendix C. Munitions Default Parameters

Tables

The tables in this appendix give the default parameters for the 33 munitions modeled by COMBIC. These are included to aid the user in creating new smoke munitions and new high explosives (HE). Although extinction values are not listed, they may be found in the previous appendices.

In the following tables, yield factors are listed for a relative humidity of 90 percent. The initial cloud temperature is for an ambient temperature of 27 °C. The initial cloud temperature is determined from how much air is entrained into the cloud with a volume defined by the initial obscurant radii.

Table C-1. Defaults for 155-mm HC M1 canister, source No. 1.

Parameter	Value
Fill weight (lb)	5.4
Obscurant type code	3.0
Efficiency (%)	70.0
Yield factor	5.725
No. of submunitions	1.0
Burn duration (s)	100.0
Burn rate coefficients:	
B_1	0.5370
B_2	0.4760
B_3	4.779
B_4	–5.472
B_5	0.0
B_6	0.0
Smoldering time (s)	0.0
Smoldering coefficient	0.0

	Subcloud No.				
Parameter	1	2	3	4	5
Mass fraction	1.0				
Debris carbon (g carbon per g obscurant)	0.0				
Plume flag (1 = puff, 2 = plume)	2.0				
Rise flag (1 = rise, 2 = no rise, >3 = stem)	1.0				
Extinction coefficient code	3.0				
Ballistic flag (1 = yes, 0 = no)	0.0				
Initial obscurant radii (m):					
Downwind	3.1				
Crosswind	3.1				
Vertical	3.7				
Buoyancy radius (m)	2.29				
Initial cloud temperature (K)	312.07				
Thermal production coefficient (cal / g)	3307.09				
Upward velocity (m / s)	0.94				
Height of burst (m)	0.0				
Fall velocity (m / s)	0.0				
Evaporation / deposition:					
F_δ (long-term)	1.0				
δ (s^{-1})	0.0				
Reflection coefficient	0.55				
Momentum radius (m)	0.0				
Horizontal velocity (m / s)	0.85				

Table C-2. Defaults for 155-mm HC M2 canister, source No. 2.

Parameter	Value
Fill weight (lb)	2.8
Obscurant type code	3.0
Efficiency (%)	70.0
Yield factor	5.725
No. of submunitions	1.0
Burn duration (s)	70.0
Burn rate coefficients:	
B_1	0.631
B_2	–0.4985
B_3	6.745
B_4	–6.52
B_5	0.0
B_6	0.0
Smoldering time (s)	0.0
Smoldering coefficient	0.0

	Subcloud No.				
Parameter	1	2	3	4	5
Mass fraction	1.0				
Debris carbon (g carbon per g obscurant)	0.0				
Plume flag (1 = puff, 2 = plume)	2.0				
Rise flag (1 = rise, 2 = no rise, >3 = stem)	1.0				
Extinction coefficient code	3.0				
Ballistic flag (1 = yes, 0 = no)	0.0				
Initial obscurant radii (m):					
Downwind	2.8				
Crosswind	2.8				
Vertical	3.4				
Buoyancy radius (m)	2.07				
Initial cloud temperature (K)	311.66				
Thermal production coefficient (cal / g)	340.08				
Upward velocity (m / s)	0.91				
Height of burst (m)	0.0				
Fall velocity (m / s)	0.0				
Evaporation / deposition:					
F_δ (long-term)	1.0				
δ (s^{-1})	0.0				
Reflection coefficient	0.55				
Momentum radius (m)	0.0				
Horizontal velocity (m / s)	0.83				

Table C-3. Defaults for 105-mm HC canister, source No. 3.

Parameter	Value
Fill weight (lb)	1.52
Obscurant type code	3.0
Efficiency (%)	70.0
Yield factor	5.725
No. of submunitions	1.0
Burn duration (s)	120.0
Burn rate coefficients:	
B_1	0.2218
B_2	3.915
B_3	–1.7368
B_4	–2.3995
B_5	0.0
B_6	0.0
Smoldering time (s)	0.0
Smoldering coefficient	0.0

	Subcloud No.				
Parameter	1	2	3	4	5
Mass fraction	1.0				
Debris carbon (g carbon per g obscurant)	0.0				
Plume flag (1 = puff, 2 = plume)	2.0				
Rise flag (1 = rise, 2 = no rise, >3 = stem)	1.0				
Extinction coefficient code	3.0				
Ballistic flag (1 = yes, 0 = no)	0.0				
Initial obscurant radii (m):					
Downwind	2.1				
Crosswind	2.1				
Vertical	2.5				
Buoyancy radius (m)	1.55				
Initial cloud temperature (K)	307.32				
Thermal production coefficient (cal / g)	3240.43				
Upward velocity (m / s)	0.80				
Height of burst (m)	0.0				
Fall velocity (m / s)	0.0				
Evaporation / deposition:					
F_δ (long-term)	1.0				
δ (s^{-1})	0.0				
Reflection coefficient	0.55				
Momentum radius (m)	0.0				
Horizontal velocity (m / s)	0.73				

Table C-4. Defaults for 155-mm HC M116B1 projectile, source No. 4.

Parameter	Value
Fill weight (lb)	19.0
Obscurant type code	3.0
Efficiency (%)	70.0
Yield factor	5.725
No. of submunitions	4.0
Burn duration (s)	100.0
Burn rate coefficients:	
B_1	0.537
B_2	0.476
B_3	4.779
B_4	–5.472
B_5	0.0
B_6	0.0
Smoldering time (s)	0.0
Smoldering coefficient	0.0

	Subcloud No.				
Parameter	1	2	3	4	5
Mass fraction	1.0				
Debris carbon (g carbon per g obscurant)	0.0				
Plume flag (1 = puff, 2 = plume)	2.0				
Rise flag (1 = rise, 2 = no rise, >3 = stem)	1.0				
Extinction coefficient code	3.0				
Ballistic flag (1 = yes, 0 = no)	0.0				
Initial obscurant radii (m):					
Downwind	3.0				
Crosswind	30.0				
Vertical	3.6				
Buoyancy radius (m)	4.74				
Initial cloud temperature (K)	302.63				
Thermal production coefficient (cal / g)	3307.09				
Upward velocity (m / s)	0.93				
Height of burst (m)	0.0				
Fall velocity (m / s)	0.0				
Evaporation / deposition:					
F_δ (long-term)	1.0				
δ (s^{-1})	0.0				
Reflection coefficient	0.55				
Momentum radius (m)	0.0				
Horizontal velocity (m / s)	0.84				

Table C-5. Defaults for 105-mm HC M84A1 projectile, source No. 5.

Parameter	Value
Fill weight (lb)	4.73
Obscurant type code	3.0
Efficiency (%)	70.0
Yield factor	5.725
No. of submunitions	3.0
Burn duration (s)	120.0
Burn rate coefficients:	
B_1	0.2218
B_2	3.915
B_3	–1.7368
B_4	–2.3995
B_5	0.0
B_6	0.0
Smoldering time (s)	0.0
Smoldering coefficient	0.0

	Subcloud No.				
Parameter	1	2	3	4	5
Mass fraction	1.0				
Debris carbon (g carbon per g obscurant)	0.0				
Plume flag (1 = puff, 2 = plume)	2.0				
Rise flag (1 = rise, 2 = no rise, >3 = stem)	1.0				
Extinction coefficient code	3.0				
Ballistic flag (1 = yes, 0 = no)	0.0				
Initial obscurant radii (m):					
Downwind	2.1				
Crosswind	30.0				
Vertical	2.5				
Buoyancy radius (m)	2.7				
Initial cloud temperature (K)	302.63				
Thermal production coefficient (cal / g)	3240.43				
Upward velocity (m / s)	0.80				
Height of burst (m)	0.0				
Fall velocity (m / s)	0.0				
Evaporation / deposition:					
F_δ (long-term)	1.0				
δ (s^{-1})	0.0				
Reflection coefficient	0.55				
Momentum radius (m)	0.0				
Horizontal velocity (m / s)	0.73				

Table C-6. Defaults for smoke pot, HC M5, source No. 6.

Parameter	Value
Fill weight (lb)	31.0
Obscurant type code	3.0
Efficiency (%)	70.0
Yield factor	5.725
No. of submunitions	1.0
Burn duration (s)	900.0
Burn rate coefficients:	
B_1	1.0
B_2	0.0
B_3	0.0
B_4	0.0
B_5	0.0
B_6	0.0
Smoldering time (s)	0.0
Smoldering coefficient	0.0

	Subcloud No.				
Parameter	1	2	3	4	5
Mass fraction	1.0				
Debris carbon (g carbon per g obscurant)	0.0				
Plume flag (1 = puff, 2 = plume)	2.0				
Rise flag (1 = rise, 2 = no rise, >3 = stem)	1.0				
Extinction coefficient code	3.0				
Ballistic flag (1 = yes, 0 = no)	0.0				
Initial obscurant radii (m):					
Downwind	2.6				
Crosswind	2.6				
Vertical	3.2				
Buoyancy radius (m)	1.92				
Initial cloud temperature (K)	309.39				
Thermal production coefficient (cal / g)	3140.39				
Upward velocity (m / s)	0.89				
Height of burst (m)	0.0				
Fall velocity (m / s)	0.0				
Evaporation / deposition:					
F_δ (long-term)	1.0				
δ (s^{-1})	0.0				
Reflection coefficient	0.55				
Momentum radius (m)	0.0				
Horizontal velocity (m / s)	0.81				

Table C-7. Defaults for smoke pot, HC M4A2, source No. 7.

Parameter	Value
Fill weight (lb)	27.0
Obscurant type code	3.0
Efficiency (%)	70.0
Yield factor	5.725
No. of submunitions	1.0
Burn duration (s)	750.0
Burn rate coefficients:	
B_1	1.0
B_2	0.0
B_3	0.0
B_4	0.0
B_5	0.0
B_6	0.0
Smoldering time (s)	0.0
Smoldering coefficient	0.0

	Subcloud No.				
Parameter	1	2	3	4	5
Mass fraction	1.0				
Debris carbon (g carbon per g obscurant)	0.0				
Plume flag (1 = puff, 2 = plume)	2.0				
Rise flag (1 = rise, 2 = no rise, >3 = stem)	1.0				
Extinction coefficient code	3.0				
Ballistic flag (1 = yes, 0 = no)	0.0				
Initial obscurant radii (m):					
Downwind	2.7				
Crosswind	2.7				
Vertical	3.3				
Buoyancy radius (m)	2.0				
Initial cloud temperature (K)	308.99				
Thermal production coefficient (cal / g)	3140.39				
Upward velocity (m / s)	0.90				
Height of burst (m)	0.0				
Fall velocity (m / s)	0.0				
Evaporation / deposition:					
F_δ (long-term)	1.0				
δ (s^{-1})	0.0				
Reflection coefficient	0.55				
Momentum radius (m)	0.0				
Horizontal velocity (m / s)	0.82				

Table C-8. Defaults for 60-mm WP M302A1 cartridge, source No. 8.

Parameter	Value
Fill weight (lb)	0.76
Obscurant type code	1.0
Efficiency (%)	100.0
Yield factor	7.847
No. of submunitions	1.0
Burn duration (s)	45.0
Burn rate coefficients:	
B_1	0.6
B_2	–0.6
B_3	0.0
B_4	0.0
B_5	1.0
B_6	0.2
Smoldering time (s)	0.0
Smoldering coefficient	0.0

	Subcloud No.				
Parameter	1	2	3	4	5
Mass fraction	0.23	0.51	0.26		
Debris carbon (g carbon per g obscurant)	0.0	0.0	0.0		
Plume flag (1 = puff, 2 = plume)	2.0	1.0	1.0		
Rise flag (1 = rise, 2 = no rise, >3 = stem)	1.0	1.0	12.0		
Extinction coefficient code	1.0	1.0	1.0		
Ballistic flag (1 = yes, 0 = no)	0.0	0.0	0.0		
Initial obscurant radii (m):					
Downwind	15.1	7.1	11.1		
Crosswind	15.1	7.1	11.1		
Vertical	3.0	2.4	2.7		
Buoyancy radius (m)	3.95	2.48	0.0		
Initial cloud temperature (K)	302.62	432.56	0.0		
Thermal production coefficient (cal / g)	9318.31	9318.31	9318.31		
Upward velocity (m / s)	0.99	1.62	0.0		
Height of burst (m)	1.0	1.0	1.0		
Fall velocity (m / s)	0.0	0.0	0.0		
Evaporation / deposition:					
F_δ (long-term)	1.0	1.0	1.0		
δ (s^{-1})	0.0	0.0	0.0		
Reflection coefficient	0.55	0.55	0.55		
Momentum radius (m)	0.0	0.0	0.0		
Horizontal velocity (m / s)	0.90	0.85	0.0		

Table C-9. Defaults for 81-mm WP M375A2 cartridge, source No. 9.

Parameter	Value
Fill weight (lb)	1.6
Obscurant type code	1.0
Efficiency (%)	100.0
Yield factor	7.847
No. of submunitions	1.0
Burn duration (s)	45.0
Burn rate coefficients:	
B_1	0.6
B_2	–0.6
B_3	0.0
B_4	0.0
B_5	1.0
B_6	0.2
Smoldering time (s)	0.0
Smoldering coefficient	0.0

	Subcloud No.				
Parameter	1	2	3	4	5
Mass fraction	0.23	0.51	0.26		
Debris carbon (g carbon per g obscurant)	0.0	0.0	0.0		
Plume flag (1 = puff, 2 = plume)	2.0	1.0	1.0		
Rise flag (1 = rise, 2 = no rise, >3 = stem)	1.0	1.0	12.0		
Extinction coefficient code	1.0	1.0	1.0		
Ballistic flag (1 = yes, 0 = no)	0.0	0.0	0.0		
Initial obscurant radii (m):					
Downwind	18.9	8.9	13.9		
Crosswind	18.9	8.9	13.9		
Vertical	3.0	3.0	3.0		
Buoyancy radius (m)	5.71	3.18	0.0		
Initial cloud temperature (K)	302.62	432.56	0.0		
Thermal production coefficient (cal / g)	9318.31	9318.31	9318.31		
Upward velocity (m / s)	0.99	1.62	0.0		
Height of burst (m)	1.0	1.0	1.0		
Fall velocity (m / s)	0.0	0.0	0.0		
Evaporation / deposition:					
F_δ (long-term)	1.0	1.0	1.0		
δ (s^{-1})	0.0	0.0	0.0		
Reflection coefficient	0.55	0.55	0.55		
Momentum radius (m)	0.0	0.0	0.0		
Horizontal velocity (m / s)	0.90	0.90	0.0		

Table C-10. Defaults for 4.2-in. WP M328A1 cartridge, source No. 10.

Parameter	Value
Fill weight (lb)	8.14
Obscurant type code	1.0
Efficiency (%)	100.0
Yield factor	7.847
No. of submunitions	1.0
Burn duration (s)	45.0
Burn rate coefficients:	
B_1	0.6
B_2	–0.6
B_3	0.0
B_4	0.0
B_5	1.0
B_6	0.2
Smoldering time (s)	0.0
Smoldering coefficient	0.0

	Subcloud No.				
Parameter	1	2	3	4	5
Mass fraction	0.23	0.51	0.26		
Debris carbon (g carbon per g obscurant)	0.0	0.0	0.0		
Plume flag (1 = puff, 2 = plume)	2.0	1.0	1.0		
Rise flag (1 = rise, 2 = no rise, >3 = stem)	1.0	1.0	12.0		
Extinction coefficient code	1.0	1.0	1.0		
Ballistic flag (1 = yes, 0 = no)	0.0	0.0	0.0		
Initial obscurant radii (m):					
Downwind	30.8	14.5	22.7		
Crosswind	30.8	14.5	22.7		
Vertical	3.0	4.8	3.9		
Buoyancy radius (m)	12.87	5.47	0.0		
Initial cloud temperature (K)	302.62	432.55	0.0		
Thermal production coefficient (cal / g)	9318.31	9318.31	9318.31		
Upward velocity (m / s)	0.99	1.62	0.0		
Height of burst (m)	1.0	1.0	1.0		
Fall velocity (m / s)	0.0	0.0	0.0		
Evaporation / deposition:					
F_δ (long-term)	1.0	1.0	1.0		
δ (s^{-1})	0.0	0.0	0.0		
Reflection coefficient	0.55	0.55	0.55		
Momentum radius (m)	0.0	0.0	0.0		
Horizontal velocity (m / s)	0.90	1.01	0.0		

Table C-11. Defaults for 2.75-in. WP M156 rocket, source No. 11.

Parameter	Value
Fill weight (lb)	2.12
Obscurant type code	1.0
Efficiency (%)	100.0
Yield factor	7.847
No. of submunitions	1.0
Burn duration (s)	45.0
Burn rate coefficients:	
B_1	0.6
B_2	–0.6
B_3	0.0
B_4	0.0
B_5	1.0
B_6	0.2
Smoldering time (s)	0.0
Smoldering coefficient	0.0

	Subcloud No.				
Parameter	1	2	3	4	5
Mass fraction	0.23	0.51	0.26		
Debris carbon (g carbon per g obscurant)	0.0	0.0	0.0		
Plume flag (1 = puff, 2 = plume)	2.0	1.0	1.0		
Rise flag (1 = rise, 2 = no rise, >3 = Stem)	1.0	1.0	12.0		
Extinction coefficient code	1.0	1.0	1.0		
Ballistic flag (1 = yes, 0 = no)	0.0	0.0	0.0		
Initial obscurant radii (m):					
Downwind	20.5	9.7	15.1		
Crosswind	20.5	9.7	15.1		
Vertical	3.0	3.2	3.1		
Buoyancy radius (m)	6.57	3.5	0.0		
Initial cloud temperature (K)	302.62	432.56	0.0		
Thermal production coefficient (cal / g)	9318.31	9318.31	9318.31		
Upward velocity (m / s)	0.99	1.62	0.0		
Height of burst (m)	1.0	1.0	1.0		
Fall velocity (m / s)	0.0	0.0	0.0		
Evaporation / deposition:					
F_δ (long-term)	1.0	1.0	1.0		
δ (s^{-1})	0.0	0.0	0.0		
Reflection coefficient	0.55	0.55	0.55		
Momentum radius (m)	0.0	0.0	0.0		
Horizontal velocity (m / s)	0.90	0.91	0.0		

Table C-12. Defaults for 155-mm WP M110E2 projectile, source No. 12.

Parameter	Value
Fill weight (lb)	15.6
Obscurant type code	1.0
Efficiency (%)	100.0
Yield factor	7.847
No. of submunitions	1.0
Burn duration (s)	240.0
Burn rate coefficients:	
B_1	0.2
B_2	-0.2
B_3	0.0
B_4	0.0
B_5	1.0
B_6	0.6
Smoldering time (s)	8.0
Smoldering coefficient	3.0

	Subcloud No.				
Parameter	1	2	3	4	5
Mass fraction	0.66	0.23	0.11		
Debris carbon (g carbon per g obscurant)	0.0	0.0	0.0		
Plume flag (1 = puff, 2 = plume)	2.0	1.0	1.0		
Rise flag (1 = rise, 2 = no rise, >3 = stem)	1.0	1.0	12.0		
Extinction coefficient code	1.0	1.0	1.0		
Ballistic flag (1 = yes, 0 = no)	0.0	0.0	0.0		
Initial obscurant radii (m):					
Downwind	37.4	17.7	27.6		
Crosswind	37.4	17.7	27.6		
Vertical	3.0	5.9	4.5		
Buoyancy radius (m)	23.99	5.21	0.0		
Initial cloud temperature (K)	302.62	432.55	0.0		
Thermal production coefficient (cal / g)	9318.31	9318.31	9318.31		
Upward velocity (m / s)	0.99	1.62	0.0		
Height of burst (m)	1.0	1.0	1.0		
Fall velocity (m / s)	0.0	0.0	0.0		
Evaporation / deposition:					
F_δ (long-term)	1.0	1.0	1.0		
δ (s^{-1})	0.0	0.0	0.0		
Reflection coefficient	0.55	0.55	0.55		
Momentum radius (m)	0.0	0.0	0.0		
Horizontal velocity (m / s)	0.90	1.06	0.0		

Table C-13. Defaults for 105-mm WP M60A2 cartridge, source No. 13.

Parameter	Value
Fill weight (lb)	3.83
Obscurant type code	1.0
Efficiency (%)	100.0
Yield factor	7.847
No. of submunitions	1.0
Burn duration (s)	75.0
Burn rate coefficients:	
B_1	0.6
B_2	–0.6
B_3	0.0
B_4	0.0
B_5	1.0
B_6	0.2
Smoldering time (s)	8.0
Smoldering coefficient	3.0

	Subcloud No.				
Parameter	1	2	3	4	5
Mass fraction	0.23	0.51	0.26		
Debris carbon (g carbon per g obscurant)	0.0	0.0	0.0		
Plume flag (1 = puff, 2 = plume)	2.0	1.0	1.0		
Rise flag (1 = rise, 2 = no rise, >3 = stem)	1.0	1.0	12.0		
Extinction coefficient code	1.0	1.0	1.0		
Ballistic flag (1 = yes, 0 = no)	0.0	0.0	0.0		
Initial obscurant radii (m):					
Downwind	24.5	11.6	18.0		
Crosswind	24.5	11.6	18.0		
Vertical	3.0	3.9	3.5		
Buoyancy radius (m)	7.05	4.26	0.0		
Initial cloud temperature (K)	302.62	432.56	0.0		
Thermal production coefficient (cal / g)	9318.31	9318.31	9318.31		
Upward velocity (m / s)	0.99	1.62	0.0		
Height of burst (m)	1.0	1.0	1.0		
Fall velocity (m / s)	0.0	0.0	0.0		
Evaporation / deposition:					
F_δ (long-term)	1.0	1.0	1.0		
δ (s^{-1})	0.0	0.0	0.0		
Reflection coefficient	0.55	0.55	0.55		
Momentum radius (m)	0.0	0.0	0.0		
Horizontal velocity (m / s)	0.90	0.96	0.0		

Table C-14. Defaults for 4.2-in. PWP M328A1, source No. 14.

Parameter	Value
Fill weight (lb)	8.14
Obscurant type code	2.0
Efficiency (%)	60.0
Yield factor	7.847
No. of submunitions	1.0
Burn duration (s)	180.0
Burn rate coefficients:	
B_1	0.6
B_2	–0.4
B_3	0.0
B_4	0.0
B_5	0.15
B_6	0.3
Smoldering time (s)	8.0
Smoldering coefficient	3.0

	Subcloud No.				
Parameter	1	2	3	4	5
Mass fraction	0.925	0.075			
Debris carbon (g carbon per g obscurant)	0.0	0.0			
Plume flag (1 = puff, 2 = plume)	2.0	1.0			
Rise flag (1 = rise, 2 = no rise, >3 = stem)	1.0	1.0			
Extinction coefficient code	2.0	2.0			
Ballistic flag (1 = yes, 0 = no)	0.0	0.0			
Initial obscurant radii (m):					
Downwind	35.0	6.7			
Crosswind	35.0	6.7			
Vertical	3.0	5.0			
Buoyancy radius (m)	11.91	2.44			
Initial cloud temperature (K)	302.62	432.55			
Thermal production coefficient (cal / g)	9318.31	9318.31			
Upward velocity (m / s)	0.99	1.62			
Height of burst (m)	1.0	1.0			
Fall velocity (m / s)	0.0	0.0			
Evaporation / deposition:					
F_δ (long-term)	1.0	1.0			
δ (s^{-1})	0.0	0.0			
Reflection coefficient	0.55	0.55			
Momentum radius (m)	0.0	0.0			
Horizontal velocity (m / s)	0.90	1.02			

Table C-15. Defaults for 5-in. PWP Zuni MK4, source No. 15.

Parameter	Value
Fill weight (lb)	13.52
Obscurant type code	2.0
Efficiency (%)	60.0
Yield factor	7.847
No. of submunitions	1.0
Burn duration (s)	180.0
Burn rate coefficients:	
B_1	0.6
B_2	–0.4
B_3	0.0
B_4	0.0
B_5	0.15
B_6	0.3
Smoldering time (s)	8.0
Smoldering coefficient	3.0

	Subcloud No.				
Parameter	1	2	3	4	5
Mass fraction	0.925	0.075			
Debris carbon (g carbon per g obscurant)	0.0	0.0			
Plume flag (1 = puff, 2 = plume)	2.0	1.0			
Rise flag (1 = rise, 2 = no rise, >3 = stem)	1.0	1.0			
Extinction coefficient code	2.0	2.0			
Ballistic flag (1 = yes, 0 = no)	0.0	0.0			
Initial obscurant radii (m):					
Downwind	41.0	7.8			
Crosswind	41.0	7.8			
Vertical	3.0	5.9			
Buoyancy radius (m)	15.34	2.89			
Initial cloud temperature (K)	302.62	432.55			
Thermal production coefficient (cal / g)	9318.31	9318.31			
Upward velocity (m / s)	0.99	1.62			
Height of burst (m)	1.0	1.0			
Fall velocity (m / s)	0.0	0.0			
Evaporation / deposition:					
F_δ (long-term)	1.0	1.0			
δ (s^{-1})	0.0	0.0			
Reflection coefficient	0.55	0.55			
Momentum radius (m)	0.0	0.0			
Horizontal velocity (m / s)	0.90	1.06			

Table C-16. Defaults for 2.75-in. WP wedge, source No. 16.

Parameter	Value
Fill weight (lb)	0.463
Obscurant type code	2.0
Efficiency (%)	66.0
Yield factor	7.847
No. of submunitions	1.0
Burn duration (s)	240.0
Burn rate coefficients:	
B_1	0.521
B_2	2.106
B_3	–1.110
B_4	–0.748
B_5	0.0
B_6	0.0
Smoldering time (s)	8.0
Smoldering coefficient	3.0

	Subcloud No.				
Parameter	1	2	3	4	5
Mass fraction	0.925	0.075			
Debris carbon (g carbon per g obscurant)	0.0	0.0			
Plume flag (1 = puff, 2 = plume)	2.0	1.0			
Rise flag (1 = rise, 2 = no rise, >3 = stem)	1.0	1.0			
Extinction coefficient code	2.0	2.0			
Ballistic flag (1 = yes, 0 = no)	0.0	0.0			
Initial obscurant radii (m):					
Downwind	3.8	2.8			
Crosswind	3.8	2.8			
Vertical	3.0	2.0			
Buoyancy radius (m)	1.76	0.97			
Initial cloud temperature (K)	302.62	432.56			
Thermal production coefficient (cal / g)	9318.31	9318.31			
Upward velocity (m / s)	0.99	1.62			
Height of burst (m)	1.0	1.0			
Fall velocity (m / s)	0.0	0.0			
Evaporation / deposition:					
F_δ (long-term)	1.0	1.0			
δ (s^{-1})	0.0	0.0			
Reflection coefficient	0.55	0.55			
Momentum radius (m)	0.0	0.0			
Horizontal velocity (m / s)	0.90	0.82			

Table C-17. Defaults for 2.75-in. WP M259 rocket, source No. 17.

Parameter	Value
Fill weight (lb)	4.63
Obscurant type code	2.0
Efficiency (%)	66.0
Yield factor	7.847
No. of submunitions	1.0
Burn duration (s)	240.0
Burn rate coefficients:	
B_1	0.521
B_2	2.106
B_3	–1.110
B_4	–0.748
B_5	0.0
B_6	0.0
Smoldering time (s)	8.0
Smoldering coefficient	3.0

	Subcloud No.				
Parameter	1	2	3	4	5
Mass fraction	0.925	0.075			
Debris carbon (g carbon per g obscurant)	0.0	0.0			
Plume flag (1 = puff, 2 = plume)	2.0	1.0			
Rise flag (1 = rise, 2 = no rise, >3 = stem)	1.0	1.0			
Extinction coefficient code	2.0	2.0			
Ballistic flag (1 = yes, 0 = no)	0.0	0.0			
Initial obscurant radii (m):					
Downwind	34.0	5.6			
Crosswind	34.0	5.6			
Vertical	3.0	4.3			
Buoyancy radius (m)	1.76	0.97			
Initial cloud temperature (K)	302.62	432.55			
Thermal production coefficient (cal / g)	9318.31	9318.31			
Upward velocity (m / s)	0.99	1.62			
Height of burst (m)	1.0	1.0			
Fall velocity (m / s)	0.0	0.0			
Evaporation / deposition:					
F_δ (long-term)	1.0	1.0			
δ (s^{-1})	0.0	0.0			
Reflection coefficient	0.55	0.55			
Momentum radius (m)	0.0	0.0			
Horizontal velocity (m / s)	0.90	0.98			

Table C-18. Defaults for 3-in. WP wick, source No. 18.

Parameter	Value
Fill weight (lb)	0.139
Obscurant type code	2.0
Efficiency (%)	71.0
Yield factor	7.847
No. of submunitions	1.0
Burn duration (s)	470.0
Burn rate coefficients:	
B_1	1.631
B_2	0.678
B_3	–5.907
B_4	4.012
B_5	0.0
B_6	0.0
Smoldering time (s)	0.0
Smoldering coefficient	0.0

	Subcloud No.				
Parameter	1	2	3	4	5
Mass fraction	0.925	0.075			
Debris carbon (g carbon per g obscurant)	0.0	0.0			
Plume flag (1 = puff, 2 = plume)	2.0	1.0			
Rise flag (1 = rise, 2 = no rise, >3 = stem)	1.0	1.0			
Extinction coefficient code	2.0	2.0			
Ballistic flag (1 = yes, 0 = no)	0.0	0.0			
Initial obscurant radii (m):					
Downwind	2.6	2.0			
Crosswind	2.6	2.0			
Vertical	3.0	1.6			
Buoyancy radius (m)	0.72	0.66			
Initial cloud temperature (K)	302.62	432.57			
Thermal production coefficient (cal / g)	9318.31	9318.31			
Upward velocity (m / s)	0.99	1.62			
Height of burst (m)	1.0	1.0			
Fall velocity (m / s)	0.0	0.0			
Evaporation / deposition:					
F_δ (long-term)	1.0	1.0			
δ (s^{-1})	0.0	1.0			
Reflection coefficient	0.55	0.55			
Momentum radius (m)	0.0	0.0			
Horizontal velocity (m / s)	0.90	0.79			

Table C-19. Defaults for 6-in. WP wick, source No. 19.

Parameter	Value
Fill weight (lb)	0.234
Obscurant type code	2.0
Efficiency (%)	67.0
Yield factor	7.847
No. of submunitions	1.0
Burn duration (s)	390.0
Burn rate coefficients:	
B_1	1.808
B_2	–2.556
B_3	2.883
B_4	2.008
B_5	0.0
B_6	0.0
Smoldering time (s)	8.0
Smoldering coefficient	3.0

	Subcloud No.				
Parameter	1	2	3	4	5
Mass fraction	0.925	0.075			
Debris carbon (g carbon per g obscurant)	0.0	0.0			
Plume flag (1 = puff, 2 = plume)	2.0	1.0			
Rise flag (1 = rise, 2 = no rise, >3 = stem)	1.0	1.0			
Extinction coefficient code	2.0	2.0			
Ballistic flag (1 = yes, 0 = no)	0.0	0.0			
Initial obscurant radii (m):					
Downwind	3.1	2.3			
Crosswind	3.1	2.3			
Vertical	3.0	1.8			
Buoyancy radius (m)	1.0	0.78			
Initial cloud temperature (K)	302.62	432.57			
Thermal production coefficient (cal / g)	9318.31	9318.31			
Upward velocity (m / s)	0.99	1.62			
Height of burst (m)	1.0	1.0			
Fall velocity (m / s)	0.0	0.0			
Evaporation / deposition:					
F_δ (long-term)	1.0	1.0			
δ (s^{-1})	0.0	0.0			
Reflection coefficient	0.55	0.55			
Momentum radius (m)	0.0	0.0			
Horizontal velocity (m / s)	0.90	0.81			

Table C-20. Defaults for 155-mm WP M825 projectile, source No. 20.

Parameter	Value
Fill weight (lb)	16.43
Obscurant type code	2.0
Efficiency (%)	74.0
Yield factor	7.847
No. of submunitions	116.0
Burn duration (s)	780.0
Burn rate coefficients:	
B_1	3.3236
B_2	–9.4664
B_3	9.5994
B_4	–3.1612
B_5	0.0
B_6	0.0
Smoldering time (s)	8.0
Smoldering coefficient	3.0

	Subcloud No.				
Parameter	1	2	3	4	5
Mass fraction	1.0				
Debris carbon (g carbon per g obscurant)	0.0				
Plume flag (1 = puff, 2 = plume)	2.0				
Rise flag (1 = rise, 2 = no rise, >3 = stem)	1.0				
Extinction coefficient code	2.0				
Ballistic flag (1 = yes, 0 = no)	0.0				
Initial obscurant radii (m):					
Downwind	37.0				
Crosswind	37.0				
Vertical	3.0				
Buoyancy radius (m)	0.61				
Initial cloud temperature (K)	302.62				
Thermal production coefficient (cal / g)	9318.31				
Upward velocity (m / s)	0.99				
Height of burst (m)	1.0				
Fall velocity (m / s)	0.0				
Evaporation / deposition:					
F_δ (long-term)	1.0				
δ (s^{-1})	0.0				
Reflection coefficient	0.55				
Momentum radius (m)	0.0				
Horizontal velocity (m / s)	0.90				

Table C-21. Defaults for 81-mm RP wedge, source No. 21.

Parameter	Value
Fill weight (lb)	0.128
Obscurant type code	5.0
Efficiency (%)	53.0
Yield factor	7.847
No. of submunitions	1.0
Burn duration (s)	260.0
Burn rate coefficients:	
B_1	0.653
B_2	–3.136
B_3	15.309
B_4	–12.872
B_5	0.0
B_6	0.0
Smoldering time (s)	8.0
Smoldering coefficient	3.0

	Subcloud No.				
Parameter	1	2	3	4	5
Mass fraction	0.925	0.075			
Debris carbon (g carbon per g obscurant)	0.0	0.0			
Plume flag (1 = puff, 2 = plume)	2.0	1.0			
Rise flag (1 = rise, 2 = no rise, >3 = stem)	1.0	1.0			
Extinction coefficient code	5.0	5.0			
Ballistic flag (1 = yes, 0 = no)	0.0	0.0			
Initial obscurant radii (m):					
Downwind	4.2	1.9			
Crosswind	4.2	1.9			
Vertical	3.0	0.6			
Buoyancy radius (m)	0.82	0.59			
Initial cloud temperature (K)	302.62	432.57			
Thermal production coefficient (cal / g)	9318.31	9318.31			
Upward velocity (m / s)	0.99	1.62			
Height of burst (m)	1.0	1.0			
Fall velocity (m / s)	0.0	0.0			
Evaporation / deposition:					
F_δ (long-term)	10	1.0			
δ (s^{-1})	0.0	0.0			
Reflection coefficient	0.55	0.55			
Momentum radius (m)	0.0	0.0			
Horizontal velocity (m / s)	0.90	0.75			

Table C-22. Defaults for I81-mm RP XM819 cartridge, source No. 22.

Parameter	Value
Fill weight (gal)	2.834
Obscurant type code	5.0
Efficiency (%)	48.0
Yield factor	7.847
No. of submunitions	28.0
Burn duration (s)	600.0
Burn rate coefficients:	
B_1	5.088
B_2	–20.268
B_3	25.938
B_4	–10.400
B_5	0.0
B_6	0.0
Smoldering time (s)	8.0
Smoldering coefficient	3.0

	Subcloud No.				
Parameter	1	2	3	4	5
Mass fraction	0.925	0.075			
Debris carbon (g carbon per g obscurant)	0.0	0.0			
Plume flag (1 = puff, 2 = plume)	2.0	1.0			
Rise flag (1 = rise, 2 = no rise, >3 = stem)	1.0	1.0			
Extinction coefficient code	5.0	5.0			
Ballistic flag (1 = yes, 0 = no)	0.0	0.0			
Initial obscurant radii (m):					
Downwind	17.0	4.9			
Crosswind	17.0	4.9			
Vertical	3.0	1.6			
Buoyancy radius (m)	0.45	0.52			
Initial cloud temperature (K)	302.62	432.57			
Thermal production coefficient (cal / g)	9318.31	9318.31			
Upward velocity (m / s)	0.99	1.62			
Height of burst (m)	1.0	1.0			
Fall velocity (m / s)	0.0	0.0			
Evaporation / deposition:					
F_δ (long-term)	1.0	1.0			
δ (s^{-1})	0.0	0.0			
Reflection coefficient	0.55	0.55			
Momentum radius (m)	0.0	0.0			
Horizontal velocity (m / s)	0.90	0.79			

Table C-23. Defaults for generator, ABC M3A3, source No. 23.

Parameter	Value
Fill weight (gal)	10.0
Obscurant type code	4.0
Efficiency (%)	100.0
Yield factor	1.0
No. of submunitions	1.0
Burn duration (s)	900.0
Burn rate coefficients:	
B_1	1.0
B_2	0.0
B_3	0.0
B_4	0.0
B_5	0.0
B_6	0.0
Smoldering time (s)	8.0
Smoldering coefficient	3.0

	Subcloud No.				
Parameter	1	2	3	4	5
Mass fraction	1.0				
Debris carbon (g carbon per g obscurant)	0.0				
Plume flag (1 = puff, 2 = plume)	2.0				
Rise flag (1 = rise, 2 = no rise, >3 = stem)	1.0				
Extinction coefficient code	4.0				
Ballistic flag (1 = yes, 0 = no)	0.0				
Initial obscurant radii (m):					
Downwind	0.2				
Crosswind	0.2				
Vertical	0.2				
Buoyancy radius (m)	0.04				
Initial cloud temperature (K)	640.0				
Thermal production coefficient (cal / g)	523.95				
Upward velocity (m / s)	31.89				
Height of burst (m)	1.0				
Fall velocity (m / s)	0.0				
Evaporation / deposition:					
F_δ (long-term)	0.65				
δ (s^{-1})	0.000333				
Reflection coefficient	0.55				
Momentum radius (m)	0.03				
Horizontal velocity (m / s)	55.24				

Table C-24. Defaults for generator, VEESS, source No. 24.

Parameter	Value
Fill weight (gal)	11.0
Obscurant type code	8.0
Efficiency (%)	100.0
Yield factor	1.0
No. of submunitions	1.0
Burn duration (s)	900.0
Burn rate coefficients:	
B_1	1.0
B_2	0.0
B_3	0.0
B_4	0.0
B_5	0.0
B_6	0.0
Smoldering time (s)	8.0
Smoldering coefficient	3.0

	Subcloud No.				
Parameter	1	2	3	4	5
Mass fraction	1.0				
Debris carbon (g carbon per g obscurant)	0.0				
Plume flag (1 = puff, 2 = plume)	2.0				
Rise flag (1 = rise, 2 = no rise, >3 = stem)	1.0				
Extinction coefficient code	8.0				
Ballistic flag (1 = yes, 0 = no)	0.0				
Initial obscurant radii (m):					
Downwind	0.2				
Crosswind	0.2				
Vertical	0.2				
Buoyancy radius (m)	0.06				
Initial cloud temperature (K)	540.0				
Thermal production coefficient (cal / g)	695.82				
Upward velocity (m / s)	17.82				
Height of burst (m)	1.0				
Fall velocity (m / s)	0.0				
Evaporation / deposition:					
F_δ (long-term)	0.1				
δ (s^{-1})	0.00185				
Reflection coefficient	0.55				
Momentum radius (m)	0.06				
Horizontal velocity (m / s)	30.86				

Table C-25. Defaults for smoke pot, fog oil M7A1, source No. 25.

Parameter	Value
Fill weight (lb)	1.7
Obscurant type code	4.0
Efficiency (%)	100.0
Yield factor	1.0
No. of submunitions	1.0
Burn time (s)	600.0
Burn rate coefficients:	
B_1	1.0
B_2	0.0
B_3	0.0
B_4	0.0
B_5	0.0
B_6	0.0
Smoldering time (s)	0.0
Smoldering coefficient	0.0

	Subcloud No.				
Parameter	1	2	3	4	5
Mass fraction	1.0				
Debris carbon (g carbon per g obscurant)	0.0				
Plume flag (1 = puff, 2 = plume)	2.0				
Rise flag (1 = rise, 2 = no rise, >3 = stem)	1.0				
Extinction coefficient code	4.0				
Ballistic flag (1 = yes, 0 = no)	0.0				
Initial obscurant radii (m):					
Downwind	0.2				
Crosswind	0.2				
Vertical	0.2				
Buoyancy radius (m)	0.02				
Initial cloud temp (K)	640.0				
Thermal production coefficient (cal / g)	532.95				
Upward velocity (m / s)	31.89				
Height of burst (m)	1.0				
Fall velocity (m / s)	0.0				
Evaporation / deposition:					
F_δ (long-term)	0.65				
δ (s^{-1})	0.000333				
Reflection coefficient	0.0				
Momentum radius (m)	0.02				
Horizontal velocity (m / s)	55.24				

Table C-26. Defaults for 155-mm HE (dust), source No. 26.

Parameter	Value
Fill weight (lb)	14.9
Obscurant type code	10.0
Efficiency (%)	31.2
Yield factor	0.027
No. of submunitions	1.0
Depth of burst (m)	–0.06
Munition delivery:	
(1 = uncased charge, 2 = static, 3 = live)	3.0
Casing length (m)	0.61
Casing diam. (m)	0.178
Impact angle (°)	10.0

	Subcloud No.				
Parameter	1	2	3	4	5
Mass fraction	0.03555	0.5842	0.005075	0.021725	0.35345
Debris carbon (g carbon per g obscurant)	0.0	0.003	1.784	0.092	0.006
Plume flag (1 = puff, 2 = plume)	1.0	1.0	1.0	1.0	1.0
Rise flag (1 = rise, 2 = no rise, >3 = stem)	2.0	2.0	1.0	13.0	13.0
Extinction coefficient code	10.0	13.0	10.0	10.0	11.0
Ballistic flag (1 = yes, 0 = no)	0.0	1.0	1.0	0.0	0.0
Initial obscurant radii (m):					
Downwind	11.37	9.48	7.58	9.48	9.48
Crosswind	11.37	9.48	7.58	9.48	9.48
Vertical	5.45	5.45	3.03	4.24	4.24
Buoyancy radius (m)	0.0	0.0	2.59	0.0	0.0
Initial cloud temp (K)	0.0	0.0	432.57	0.0	0.0
Thermal production coefficient (cal / g)	0.0	0.0	173399.0	5063.29	311.22
Upward velocity (m / s)	0.0	0.0	1.62	0.0	0.0
Height of burst (m)	0.0	0.05	0.1	0.0	0.0
Fall velocity (m / s)	0.003	4.15	0.003	0.003	0.92
Evaporation / deposition:					
F_δ (long-term)	1.0	1.0	1.0	1.0	1.0
δ (s^{-1})	0.0	0.0	0.0	0.0	0.0
Reflection coefficient	0.1	0.1	0.1	0.1	0.1
Momentum radius (m)	0.0	0.0	0.0	0.0	0.0
Horizontal velocity (m / s)	0.0	0.0	0.79	0.0	0.0

Table C-27. Defaults for 105-mm HE (dust), source No. 27.

Parameter	Value
Fill weight (lb)	6.04
Obscurant type code	10.0
Efficiency (%)	31.5
Yield factor	0.029
No. of submunitions	1.0
Depth of burst (m)	–0.06
Munition delivery:	
(1 = uncased charge, 2 = static, 3 = live)	3.0
Casing length (m)	0.406
Casing diam. (m)	0.102
Impact angle (°)	10.0

	Subcloud No.				
Parameter	1	2	3	4	5
Mass fraction	0.03555	0.5842	0.005075	0.021725	0.35345
Debris carbon (g carbon per g obscurant)	0.0	0.003	1.797	0.093	0.006
Plume flag (1 = puff, 2 = plume)	1.0	1.0	1.0	1.0	1.0
Rise flag (1 = rise, 2 = no rise, >3 = stem)	2.0	2.0	1.0	13.0	13.0
Extinction coefficient code	10.0	13.0	10.0	10.0	11.0
Ballistic flag (1 = yes, 0 = no)	0.0	1.0	1.0	0.0	0.0
Initial obscurant radii (m):					
Downwind	8.7	7.25	5.8	7.25	7.25
Crosswind	8.7	7.25	5.8	7.25	7.25
Vertical	4.03	4.03	2.24	3.13	3.13
Buoyancy radius (m)	0.0	0.0	1.92	0.0	0.0
Initial cloud temp (K)	0.0	0.0	432.57	0.0	0.0
Thermal production coefficient (cal / g)	0.0	0.0	173399.0	5063.29	311.22
Upward velocity (m / s)	0.0	0.0	1.62	0.0	0.0
Height of burst (m)	0.0	0.0	0.1	0.0	0.0
Fall velocity (m / s)	0.003	4.15	0.003	0.003	0.92
Evaporation / deposition:					
F_δ (long-term)	1.0	1.0	1.0	1.0	1.0
δ (s^{-1})	0.0	0.0	0.0	0.0	0.0
Reflection coefficient	0.1	0.1	0.1	0.1	0.1
Momentum radius (m)	0.0	0.0	0.0	0.0	0.0
Horizontal velocity (m / s)	0.0	0.0	0.70	0.0	0.0

Table C-28. Defaults for 4.2-in. HE (dust), source No. 28.

Parameter	Value
Fill weight (gal)	7.45
Obscurant type code	10.0
Efficiency (%)	31.4
Yield factor	0.039
No. of submunitions	1.0
Depth of burst (m)	–0.6
Munition delivery:	
(1 = uncased charge, 2 = static, 3 = live)	3.0
Casing length (m)	0.46
Casing diam. (m)	0.102
Impact angle (°)	60.0

	Subcloud No.				
Parameter	1	2	3	4	5
Mass fraction	0.03555	0.5842	0.005075	0.021725	0.35345
Debris carbon (g carbon per g obscurant)	0.0	0.003	1.321	0.068	0.004
Plume flag (1 = puff, 2 = plume)	1.0	1.0	1.0	1.0	1.0
Rise flag (1 = rise, 2 = no rise, >3 = stem)	2.0	2.0	1.0	13.0	13.0
Extinction coefficient code	10.0	13.0	10.0	10.0	11.0
Ballistic flag (1 = yes, 0 = no)	0.0	1.0	1.0	0.0	0.0
Initial obscurant radii (m):					
Downwind	10.24	8.54	6.83	8.54	8.54
Crosswind	10.24	8.54	6.83	8.54	8.54
Vertical	4.78	4.78	2.66	3.72	3.72
Buoyancy radius (m)	0.0	0.0	2.06	0.0	0.0
Initial cloud temperature (K)	0.0	0.0	432.57	0.0	0.0
Thermal production coefficient (cal / g)	0.0	0.0	173399.0	5063.29	311.22
Upward velocity (m / s)	0.0	0.0	1.62	0.0	0.0
Height of burst (m)	0.0	0.0	0.1	0.0	0.0
Fall velocity (m / s)	0.003	4.15	0.003	0.003	0.92
Evaporation / deposition:					
F_δ (long-term)	1.0	1.0	1.0	1.0	1.0
δ (s^{-1})	0.0	0.0	0.0	0.0	0.0
Reflection coefficient	0.1	0.1	0.1	0.1	0.1
Momentum radius (m)	0.0	0.0	0.0	0.0	0.0
Horizontal velocity (m / s)	0.0	0.0	0.75	0.0	0.0

Table C-29. Defaults for 10-lb C4 HE (dust), source No. 29.

Parameter	Value
Fill weight (gal)	13.4
Obscurant type code	10.0
Efficiency (%)	49.9
Yield factor	0.015
No. of submunitions	1.0
Depth of burst (m)	–0.06
Munition delivery:	
(1 = uncased charge, 2 = static, 3 = live)	1.0
Casing length (m)	0.606
Casing diam. (m)	0.178
Impact angle (°)	0.0

	Subcloud No.				
Parameter	1	2	3	4	5
Mass fraction	0.03555	0.5842	0.005075	0.021725	0.35345
Debris carbon (g carbon per g obscurant)	0.0	0.006	3.256	0.168	0.01
Plume flag (1 = puff, 2 = plume)	1.0	1.0	1.0	1.0	1.0
Rise flag (1 = rise, 2 = no rise, >3 = stem)	2.0	2.0	1.0	13.0	13.0
Extinction coefficient code	10.0	13.0	10.0	10.0	11.0
Ballistic flag (1 = yes, 0 = no)	0.0	1.0	1.0	0.0	0.0
Initial obscurant radii (m):					
Downwind	11.02	9.18	7.35	9.18	9.18
Crosswind	11.02	9.18	7.35	9.18	9.18
Vertical	5.26	5.26	2.92	4.09.	4.09
Buoyancy radius (m)	0.0	0.0	2.92	0.0	0.0
Initial cloud temperature (K)	0.0	0.0	432.57	0.0	0.0
Thermal production coefficient (cal / g)	0.0	0.0	173399.0	5063.29	311.22
Upward velocity (m / s)	0.0	0.0	1.62	0.0	0.0
Height of burst (m)	0.0	0.0	0.1	0.0	0.0
Fall velocity (m / s)	0.003	4.15	0.003	0.003	0.92
Evaporation / deposition:					
F_δ (long-term)	1.0	1.0	1.0	1.0	1.0
δ (s^{-1})	0.0	0.0	0.0	0.0	0.0
Reflection coefficient	0.1	0.1	0.1	0.1	0.1
Momentum radius (m)	0.0	0.0	0.0	0.0	0.0
Horizontal velocity (m / s)	0.0	0.0	0.78	0.0	0.0

Table C-30. Defaults for diesel fuel / oil / rubber fire, source No. 30.

Parameter	Value
Fill weight (lb)	150.0
Obscurant type code	14.0
Efficiency (%)	26.0
Yield factor	1.0
No. of subclouds	1.0
Burn duration (s)	1800.0
Burn rate coefficients:	
B_1	1.0
B_2	0.0
B_3	0.0
B_4	0.0
B_5	0.0
B_6	0.0
Smoldering time (s)	0.0
Smoldering coefficient	0.0

	Subcloud No.				
Parameter	1	2	3	4	5
Mass fraction	1.0				
Debris carbon (g carbon per g obscurant)	0.0				
Plume flag (1 = puff, 2 = plume)	2.0				
Rise flag (1 = rise, 2 = no rise, >3 = stem)	1.0				
Extinction coefficient code	14.0				
Ballistic flag (1 = yes, 0 = no)	.0				
Initial obscurant radii (m):					
Downwind	3.09				
Crosswind	3.09				
Vertical	1.03				
Buoyancy radius (m)	2.96				
Initial cloud temperature (K)	349.59				
Thermal production coefficient (cal / g)	7185.0				
Upward velocity (m / s)	1.48				
Height of burst (m)	.0				
Fall velocity (m / s)	.0				
Evaporation / deposition:					
F_δ (long-term)	.1				
δ (s^{-1})	0.0				
Reflection coefficient	.55				
Momentum radius (m)	.0				
Horizontal velocity (m / s)	.44				

Table C-31. Defaults for muzzle blast smoke, source No. 31.

Parameter	Value
Fill weight (lb)	2.0
Obscurant type code	10.0
Efficiency (%)	5.0
Yield factor	0.01
No. of subclouds	1.0
Depth of burst (m)	–0.06
Munition delivery:	
(1 = uncased charge, 2 = static, 3 = live)	1.0
Casing length (m)	0.606
Casing diam. (m)	0.178
Impact angle (°)	0.0

	Subcloud No.				
Parameter	1	2	3	4	5
Mass fraction	1.0				
Debris carbon (g carbon per g obscurant)	0.0				
Plume flag (1 = puff, 2 = plume)	1.0				
Rise flag (1 = rise, 2 = no rise, >3 = stem)	2.0				
Extinction coefficient code	10.0				
Ballistic flag (1 = yes, 0 = no)	0.0				
Initial obscurant radii (m):					
Downwind	15.0				
Crosswind	10.0				
Vertical	7.0				
Buoyancy radius (m)	0.0				
Initial cloud temperature (K)	0.0				
Thermal production coefficient (cal / g)	0.0				
Upward velocity (m / s)	0.0				
Height of burst (m)	0.0				
Fall velocity (m / s)	0.0				
Evaporation / deposition:					
F_δ (long-term)	1.0				
δ (s^{-1})	0.0				
Reflection coefficient	0.0				
Momentum radius (m)	1.0				
Horizontal velocity (m / s)	0.0				

Table C-32. Defaults for M76 IR grenade, source No. 32.

Parameter	Value
Fill weight (lb)	2.98
Obscurant type code	20.0
Efficiency (%)	60.0
Yield factor	1.0
No. of subclouds	1.0
Burn duration (s)	0.0
Burn rate coefficients:	
B_1	1.0
B_2	0.0
B_3	0.0
B_4	0.0
B_5	0.0
B_6	0.0
Smoldering time (s)	0.0
Smoldering coefficient	0.0

	Subcloud No.				
Parameter	1	2	3	4	5
Mass fraction	1.0				
Debris carbon (g carbon per g obscurant)	0.0				
Plume flag (1 = puff, 2 = plume)	1.0				
Rise flag (1 = rise, 2 = no rise, >3 = stem)	2				
Extinction coefficient code	20.0				
Ballistic flag (1 = yes, 0 = no)	0.0				
Initial obscurant radii (m):					
Downwind	10.8				
Crosswind	10.8				
Vertical	16.8				
Buoyancy radius (m)	.0				
Initial cloud temperature (K)	.0				
Thermal production coefficient (cal / g)	.0				
Upward velocity (m / s)	.0				
Height of burst (m)	10.0				
Fall velocity (m / s)	0.0				
Evaporation / deposition:					
F_δ (long-term)	1.0				
δ (s^{-1})	0.0				
Reflection coefficient	1.0				
Momentum radius (m)	0.0				
Horizontal velocity (m / s)	0.0				

Table C-33. Defaults for L8A1 / L8A3 RP grenade, source No. 33.

Parameter	Value
Fill weight (lb)	0.794
Obscurant type code	5.0
Efficiency (%)	95.0
Yield factor	7.847
No. of subclouds	1.0
Burn duration (s)	658.0
Burn rate coefficients:	
B_1	0.0
B_2	0.0
B_3	0.0
B_4	0.0
B_5	120.0
B_6	0.0083
Smoldering time (s)	0.0
Smoldering coefficient	0.0

	Subcloud No.				
Parameter	1	2	3	4	5
Mass fraction	0.925	0.05	0.025		
Debris carbon (g carbon per g obscurant)	0.0	0.0	0.0		
Plume flag (1 = puff, 2 = plume)	2.0	1.0	1.0		
Rise flag (1 = rise, 2 = no rise, >3 = stem)	1.0	1.0	12.0		
Extinction coefficient code	5.0	5.0	5.0		
Ballistic flag (1 = yes, 0 = no)	0.0	0.0	0.0		
Initial obscurant radii (m):					
Downwind	17.54	3.32	3.32		
Crosswind	17.54	3.32	3.32		
Vertical	3.0	2.4	2.49		
Buoyancy radius (m)	2.09	1.14	0.0		
Initial cloud temperature (K)	302.63	432.41	0.0		
Thermal production coefficient (cal / g)	9318.31	9318.31	0.0		
Upward velocity (m / s)	.86	1.62	0.0		
Height of burst (m)	0.0	.0	0.0		
Fall velocity (m / s)	0.0	0.0	0.0		
Evaporation / deposition:					
F_δ (long-term)	1.0	1.0	1.0		
δ (s^{-1})	0.0	0.0	0.0		
Reflection coefficient	1.0	1.0	1.0		
Momentum radius (m)	0.0	0.0	0.0		
Horizontal velocity (m / s)	0.78	1.56	0.0		

Appendix D. Sample Outputs

Contents

The three samples in this appendix provide the complete output files for the first three samples discussed in section 5 of the main report. (For the other two samples, whose output is less voluminous, the output is provided in sect. 5.)

D-1 Example 1: Simple HC Scenario

The following example is discussed in detail in section 5.2 in the main body of the report.

D-1.1 Input

The following inputs exhibit the most basic COMBIC Phase I run.

```
WAVL      1.06
COMBIC
PHAS            1.0       5.0       6.0       0.0       9.0       0.0       0.0
FILE          9.0  h.history
NAME            0.
  SAMPLE ONLY
MET1           50.0      2.20       3.      27.50     962.5    202.40      0.00
MUNT            0.0       0.0       1.0       0.0       0.0       0.0       0.0
DONE            0.0
END
STOP
```

D-1.2 Output

```
*************************************************************************
  WARNING - THIS LIBRARY CONTAINS TECHNICAL DATA WHOSE EXPORT IS RESTRICTED
  BY THE ARMS EXPORT CONTROL ACT (TITLE 22, U.S.C., SEC 2751 ET SEQ.) OR
  EXECUTIVE ORDER 12470.  VIOLATION OF THESE EXPORT LAWS ARE SUBJECT TO
                  SEVERE CRIMINAL PENALTIES.
*************************************************************************


1




                  *********************************
                  *                               *
                  *    ELECTRO-OPTICAL SYSTEMS    *
                  *                               *
                  *  ATMOSPHERIC EFFECTS LIBRARY  *
                  *                               *
                  *    NOT FOR OPERATIONAL USE    *
                  *                               *
                  * EOSAEL87 REV 2.1   02/23/90   *
                  *                               *
                  *********************************



WAVL      1.06
 NOTE: THAT THE ABOVE CARD WAS MODIFIED FOR CONSISTENCY TO:
WAVL       .1060E+01 .1060E+01 .0000E+00



                                     BEGINNING           ENDING

            WAVENUMBER (CM**-1)       9433.963           9433.963

            WAVELENGTH (MICROMETERS)     1.060              1.060

            FREQUENCY (GHZ)         283018.875         283018.875



         **** EOSAEL WARNING ****
 VISIBILITY AND EXTINCTION = 0.0, VISIBILITY CHANGED TO 10.0 KM
```

VISIBILITY
10.00 KM

1

```
*********************************
*                               *
*        C O M B I C            *
*                               *
*COMBINED OBSCURATION MODEL FOR*
* BATTLEFIELD-INDUCED AEROSOLS *
*   NOT FOR OPERATIONAL USE     *
*                               *
* EOSAEL92 REV 1.0   12/12/90  *
*                               *
*********************************
```

1

```
*****************
*               *
*    COMBIC     *
*    PHASE 1    *
*               *
*****************
```

COMBIC WARNING: FILE(h.history   )
WILL BE OVER WRITTEN

COMBIC CLOUD HISTORY ON UNIT 9 OPENED TO: h.history

1

METEOROLOGICAL CONDITIONS

REFERENCE HEIGHT	10.00	METERS	WIND SPEED	2.20	METERS/SEC
SURFACE ROUGHNESS	.10000	METERS	WIND DIRECTION	202.4	DEG WRT NORTH
INVERSION HEIGHT	824.	METERS	TEMPERATURE	27.49	DEG CELCIUS
PRESSURE	963.	MB	RELATIVE HUMIDITY	50.0	%
PASQUILL CATEGORY	3				

BOUNDARY LAYER PARAMETERS

FRICTION VELOCITY	.214 M/SEC	PASQUILL CLASS	2.60
KAZANSKI-MONIN	-.3254	OMEGA	.853
COLD REGION FLAG	0	SBAR MODEL FLAG	0
AIR DENSITY	1110.4 G/M**3	1/MONIN-OBUKHOV LENGTH	-.02386 M**-1
SENSIBLE HEAT FLUX	20.2 WATT/M**2	SURFACE BUOYANCY FLUX	.0006 M**2/S**3
MEAN STATIC SBAR (10-50M)	-.000165 SEC**-2		

DIFFUSION COEFFICIENTS

A COEFFICIENT	B COEFFICIENT	C COEFFICIENT	D COEFFICIENT
.216	.900	.220	.802

SURFACE CONDITIONS

SNOW COVER FLAG	0	SILT CONTENT	50.0 %	SOD DEPTH	.000 METERS

1 VERTICAL PROFILE MODEL

HEIGHT (M)	WINDSPEED (M/S)	ATMOSPHERIC TEMPERATURE CONSTANT SBAR MODEL (DEG K)	VARIABLE S MODEL (DEG K)	S, STATIC STABILITY PARAMETER	EDDY DISSIPATION RATE (M**2/S**3)
1.0	1.19	300.78	301.05	-.00586841	.02165
2.0	1.52	300.77	300.91	-.00261031	.00996
3.0	1.71	300.75	300.83	-.00158293	.00627
4.0	1.84	300.74	300.78	-.00109635	.00452
5.0	1.93	300.72	300.74	-.00081889	.00353
6.0	2.00	300.71	300.71	-.00064244	.00289
7.0	2.06	300.69	300.68	-.00052179	.00246
8.0	2.12	300.68	300.65	-.00043491	.00215
9.0	2.16	300.66	300.63	-.00036983	.00191
10.0	2.20	300.65	300.61	-.00031958	.00173
15.0	2.34	300.58	300.52	-.00018065	.00123
20.0	2.44	300.50	300.45	-.00011971	.00102
25.0	2.51	300.43	300.38	-.00008673	.00090
30.0	2.56	300.35	300.32	-.00006654	.00082
35.0	2.60	300.28	300.26	-.00005313	.00078
40.0	2.64	300.20	300.21	-.00004368	.00074
45.0	2.67	300.13	300.15	-.00003674	.00072
50.0	2.70	300.06	300.10	-.00003146	.00070
55.0	2.72	299.98	300.04	-.00002734	.00068
60.0	2.74	299.91	299.99	-.00002404	.00067
65.0	2.76	299.83	299.94	-.00002136	.00066
70.0	2.78	299.76	299.89	-.00001914	.00065
75.0	2.80	299.68	299.83	-.00001728	.00065
80.0	2.81	299.61	299.78	-.00001570	.00064
85.0	2.83	299.54	299.73	-.00001435	.00034
90.0	2.84	299.46	299.68	-.00001318	.00034
95.0	2.85	299.39	299.63	-.00001217	.00034
100.0	2.86	299.31	299.58	-.00001127	.00033
125.0	2.91	298.94	299.33	-.00000809	.00032
150.0	2.95	298.57	299.08	-.00000617	.00032
175.0	2.98	298.20	298.83	-.00000490	.00031
200.0	3.00	297.83	298.58	-.00000401	.00031
225.0	3.02	297.46	298.33	-.00000337	.00030
250.0	3.04	297.09	298.08	-.00000288	.00030
275.0	3.06	296.72	297.84	-.00000249	.00030
300.0	3.07	296.35	297.59	-.00000219	.00030
325.0	3.09	295.98	297.34	-.00000194	.00030
350.0	3.10	295.61	297.10	-.00000174	.00030
375.0	3.11	295.24	296.85	-.00000157	.00030
400.0	3.12	294.87	296.60	-.00000142	.00030
450.0	3.14	294.13	296.11	-.00000119	.00030
500.0	3.15	293.40	295.62	-.00000102	.00030
550.0	3.17	292.66	295.13	-.00000088	.00030

600.0	3.18	291.92	294.64	-.00000078	.00030
650.0	3.19	291.19	294.15	-.00000069	.00030
700.0	3.20	290.45	293.65	-.00000062	.00030
750.0	3.21	289.72	293.16	-.00000056	.00029
800.0	3.22	288.98	292.67	-.00000050	.00029
850.0	3.22	288.25	292.18	-.00000046	.00029
900.0	3.23	287.52	291.69	-.00000042	.00029
950.0	3.24	286.79	291.20	-.00000039	.00029
1000.0	3.24	286.06	290.71	-.00000036	.00029

1

MASS EXTINCTION COEFFICIENTS (M**2/GRAM)

OBSCURANT	WAVELENGTH (MICROMETERS)						
CODE	.4-.7	.7-1.2	1.06	3.-5.	8.-12.	10.6	94 GHZ
1	4.0790	1.7699	1.3742	.2939	.3756	.3800	.0010
2	4.0790	1.7699	1.3742	.2939	.3756	.3800	.0010
3	3.6618	2.6693	2.2810	.1897	.0280	.0377	.0010
4	6.8510	4.5920	3.4970	.2450	.0200	.0180	.0010
5	4.0790	1.7699	1.3742	.2939	.3756	.3800	.0010
6	1.8600	1.6300	1.4000	1.7900	1.6800	1.6800	.0010
7	1.8600	1.6300	1.4000	1.7900	1.6800	1.6800	.0010
8	5.6500	4.0800	3.2500	.2450	.0230	.0270	.0010
9	.3200	.3000	.2900	.2700	.2500	.2500	.0010
10	.3200	.2900	.2600	.2700	.2600	.2400	.0010
11	.0350	.0360	.0370	.0350	.0380	.0360	.0010
12	1.5000	1.4600	1.4200	.7500	.3200	.3000	.0010
13	.0010	.0010	.0010	.0010	.0010	.0010	.0004
14	6.1000	3.7500	2.9400	1.3500	1.0100	1.0000	.0020
15	6.8510	4.5920	1.4300	.0540	.0200	.0180	.0010
16	5.3700	2.9000	2.1000	.0900	.0900	.0700	.0010
17	6.2000	3.5000	2.5000	.2300	.0500	.0480	.0010
18	3.3300	2.7500	2.6600	.2600	.3200	.2300	.0010
19	1.3000	1.7400	1.7000	.0800	.1600	.3800	.0010
20	2.0000	2.0000	2.0000	1.6000	2.0000	.0000	.0000
21	2.0000	2.0000	1.0000	.1000	.4000	.0000	.0000
22	.0000	.0000	.0000	.0000	.0000	.0000	.0000
23	.0000	.0000	.0000	.0000	.0000	.0000	.0000
24	.0000	.0000	.0000	.0000	.0000	.0000	.0000
25	.0000	.0000	.0000	.0000	.0000	.0000	.0000
26	.0000	.0000	.0000	.0000	.0000	.0000	.0000
27	.0000	.0000	.0000	.0000	.0000	.0000	.0000
28	.0000	.0000	.0000	.0000	.0000	.0000	.0000
29	.0000	.0000	.0000	.0000	.0000	.0000	.0000
30	.0000	.0000	.0000	.0000	.0000	.0000	.0000

1

CLOUD HISTORY, FILE NAME = COMHIS

HISTORY FILE SOURCE # 1 CONTAINS 1 SUBCLOUDS, TOTAL 3242.71 GRAMS OBSCURANT

XN NO. OF SOURCES	FILL WEIGHT (LB, GAL OR LB TNT)	MENU SELECTION TYPE	OBSCURANT TYPE CODE	EFFICIENCY (PERCENT)	YIELD FACTOR	NUMBER OF SUBMUNITIONS
1.00	5.400	1.	3.	70.0	1.891	1.00

BURN DURATION (SEC)	BURN RATE COEFFICIENTS B1	B2	B3	B4	B5	B6
100.00	.5370	.4760	4.7790	-5.4720	.0000	.0000

SMOULDERING TIME (SEC)	SMOULDERING COEFFICIENT CSMLD
.00	.0000

1

PROCESSING SUBCLOUD 1

SUBCLOUD # 1 HISTORY FILE SOURCE # 1

MASS FRACTION	DEBRIS CARBON (G/G OBSC)	PLUME (1=PUFF, 2=PLUME)	CLOUD RISE MODEL (1=RISE, 2= NO RISE, >2=STEM)	EXTINCTION COEFFICIENT CODE	BALLISTIC SUBCLOUD (1=Y, 0=N)
1.000000	.000	2.	1.	3.	0.

INITIAL THERMAL UPWARD

INITIAL OBSCURANT RADII (M)			BUOYANCY	CLOUD	PRODUCTION	VELOCITY
DOWNWIND	CROSSWIND	VERTICAL	RADIUS(M)	TEMP(DEG K)	COEF (CAL/G)	(M/S)
3.10	3.10	3.70	2.29	306.01	1083.63	.74

	FALL	EVAPORATION/DEPOSITION			MOMENTUM	HORIZONTAL
HEIGHT OF	VELOCITY	FD	DELTA	REFL.	RADIUS	VELOCITY
BURST (M)	(M/S)	(LONG-TERM)	(S**-1)	COEF.	(M)	(M/S)
.0	.000	1.000000	.00000	.5500	.00	.67

MASS PRODUCTION PROFILE

TIME T AFTER IGNITION (SEC)	MASS PRODUCED UP UNTIL TIME T (G)	MASS STILL AIRBORNE BY TIME T (G)	MDOT
1.000	17.5	17.5	17.5880
2.000	35.2	35.2	17.6902
3.000	53.1	53.1	17.9040
4.000	71.2	71.2	18.1461
5.000	89.6	89.6	18.4154
6.000	108.3	108.3	18.7110
7.000	127.3	127.3	19.0317
8.000	146.7	146.7	19.3765
9.000	166.4	166.4	19.7443
10.000	186.6	186.6	20.1340
11.000	207.1	207.1	20.5446
12.000	228.1	228.1	20.9751
13.000	249.5	249.5	21.4242
14.000	271.4	271.4	21.8911
15.000	293.8	293.8	22.3746
16.000	316.6	316.6	22.8736
17.000	340.0	340.0	23.3872
18.000	363.9	363.9	23.9141
19.000	388.4	388.4	24.4535
20.000	413.4	413.4	25.0041
21.000	438.9	438.9	25.5649
22.000	465.1	465.1	26.1350
23.000	491.8	491.8	26.7131
24.000	519.1	519.1	27.2983
25.000	547.0	547.0	27.8894
26.000	575.4	575.4	28.4855
27.000	604.5	604.5	29.0854

28.000	634.2	634.2	29.6880
29.000	664.5	664.5	30.2924
30.000	695.4	695.4	30.8975
31.000	726.9	726.9	31.5021
32.000	759.0	759.0	32.1053
33.000	791.7	791.7	32.7059
34.000	825.0	825.0	33.3029
35.000	858.9	858.9	33.8953
36.000	893.4	893.4	34.4818
37.000	928.5	928.5	35.0616
38.000	964.1	964.1	35.6335
39.000	1000.3	1000.3	36.1966
40.000	1037.1	1037.1	36.7496
41.000	1074.4	1074.4	37.2915
42.000	1112.2	1112.2	37.8213
43.000	1150.5	1150.5	38.3379
44.000	1189.4	1189.4	38.8403
45.000	1228.7	1228.7	39.3274
46.000	1268.5	1268.5	39.7981
47.000	1308.8	1308.8	40.2513
48.000	1349.5	1349.5	40.6861
49.000	1390.6	1390.6	41.1012
50.000	1432.1	1432.1	41.4956
51.000	1473.9	1473.9	41.8684
52.000	1516.2	1516.2	42.2184
53.000	1558.7	1558.7	42.5447
54.000	1601.6	1601.6	42.8460
55.000	1644.7	1644.7	43.1213
56.000	1688.1	1688.1	43.3695
57.000	1731.7	1731.7	43.5897
58.000	1775.5	1775.5	43.7807
59.000	1819.4	1819.4	43.9416
60.000	1863.5	1863.5	44.0712
61.000	1907.7	1907.7	44.1684
62.000	1951.9	1951.9	44.2321
63.000	1996.2	1996.2	44.2613
64.000	2040.5	2040.5	44.2550
65.000	2084.7	2084.7	44.2122
66.000	2128.8	2128.8	44.1316
67.000	2172.9	2172.9	44.0124
68.000	2216.7	2216.7	43.8532
69.000	2260.4	2260.4	43.6532
70.000	2303.8	2303.8	43.4114
71.000	2347.0	2347.0	43.1265
72.000	2389.8	2389.8	42.7975
73.000	2432.2	2432.2	42.4233
74.000	2474.2	2474.2	42.0030
75.000	2515.8	2515.8	41.5354

76.000	2556.8	2556.8	41.0197
77.000	2597.3	2597.3	40.4543
78.000	2637.2	2637.2	39.8389
79.000	2676.3	2676.3	39.1716
80.000	2714.8	2714.8	38.4517
81.000	2752.5	2752.5	37.6781
82.000	2789.4	2789.4	36.8499
83.000	2825.4	2825.4	35.9661
84.000	2860.4	2860.4	35.0253
85.000	2894.4	2894.4	34.0268
86.000	2927.4	2927.4	32.9690
87.000	2959.3	2959.3	31.8513
88.000	2990.0	2990.0	30.6725
89.000	3019.5	3019.5	29.4315
90.000	3047.6	3047.6	28.1274
91.000	3074.4	3074.4	26.7589
92.000	3099.7	3099.7	25.3252
93.000	3123.6	3123.6	23.8248
94.000	3145.9	3145.9	22.2571
95.000	3166.5	3166.5	20.6208
96.000	3185.4	3185.4	18.9150
97.000	3202.6	3202.6	17.1383
98.000	3217.9	3217.9	15.2900
99.000	3231.3	3231.3	13.0912
100.000	3242.7	3242.7	7.6571

SUBCLOUD TRAJECTORY

DOWNWIND DISTANCE (M)	TIME (SEC)	CENTROID HEIGHT (M)	GAUSSIAN CLOUD STD. DEVIATIONS (M) SIGMAX	SIGMAY	SIGMAZ	PEAK CLOUD TEMP. (DEG K)	MEAN CLOUD TEMP. (DEG K)	AIR TEMP. (DEG K)	AIR DENSITY (G/M**3)	CENTROID OR CM VELOCITY VERT. (M/S)	HOR. (M/S)	CM HEIGHT (M)	EFFECTIVE BUOYANCY RADIUS (M)
1.00	1.20	.78	1.44	1.59	2.22	309.88	304.44	300.92	1110.46	.57	.99	2.1	2.567
2.84	2.80	1.56	1.44	1.87	2.60	306.76	303.20	300.87	1110.56	.43	1.27	2.8	2.911
5.24	4.56	2.24	1.44	2.29	2.87	305.06	302.51	300.83	1110.61	.35	1.44	3.3	3.268
8.09	6.45	2.87	1.44	2.84	3.13	304.02	302.08	300.81	1110.64	.31	1.56	3.9	3.628
11.33	8.47	3.47	1.44	3.50	3.41	303.32	301.79	300.78	1110.65	.29	1.64	4.5	3.988
14.92	10.61	4.06	1.44	4.26	3.71	302.83	301.58	300.76	1110.66	.27	1.71	5.0	4.350
18.82	12.85	4.63	1.44	5.08	4.05	302.46	301.42	300.74	1110.66	.25	1.77	5.7	4.713
23.02	15.18	5.20	1.44	5.98	4.41	302.18	301.30	300.72	1110.65	.24	1.82	6.4	5.077
27.50	17.61	5.76	1.44	6.93	4.80	301.95	301.20	300.70	1110.64	.23	1.87	6.8	5.442
32.24	20.08	5.99	1.44	7.70	5.20	301.32	300.93	300.70	1110.63	.09	1.94	7.2	5.596
37.22	22.60	5.99	1.44	8.35	5.59	301.01	300.81	300.70	1110.63	.10	1.98	7.5	5.596

42.44	25.19	5.99	1.44	9.03	6.00	300.85	300.75	300.69	1110.62	.10	2.01	7.7	5.596
47.89	27.86	5.99	1.44	9.72	6.42	300.77	300.72	300.68	1110.61	.11	2.04	8.0	5.596
53.78	30.72	5.99	1.44	10.47	6.87	300.72	300.70	300.68	1110.60	.11	2.06	8.3	5.596
60.39	33.89	5.99	1.44	11.30	7.37	300.69	300.68	300.67	1110.58	.11	2.08	8.7	5.596
67.82	37.42	5.99	1.44	12.22	7.91	300.68	300.67	300.66	1110.57	.11	2.10	9.0	5.596
76.17	41.36	5.99	1.44	13.25	8.51	300.67	300.66	300.65	1110.55	.11	2.12	9.5	5.596
85.54	45.74	5.99	1.44	14.40	9.17	300.65	300.65	300.64	1110.53	.11	2.14	10.0	5.596
96.06	50.62	5.99	1.44	15.68	9.90	300.64	300.64	300.63	1110.51	.11	2.16	10.5	5.596
107.88	56.05	5.99	1.44	17.10	10.71	300.63	300.63	300.62	1110.48	.11	2.18	11.1	5.596
121.15	62.10	5.99	1.44	18.67	11.60	300.62	300.62	300.61	1110.44	.11	2.19	11.8	5.596
136.06	68.84	5.99	1.44	20.43	12.57	300.61	300.61	300.60	1110.40	.11	2.21	12.5	5.596
152.80	76.33	5.99	1.44	22.38	13.65	300.60	300.60	300.59	1110.36	.11	2.23	13.4	5.596
171.60	84.67	5.99	1.44	24.55	14.83	300.58	300.58	300.57	1110.30	.11	2.25	14.3	5.596
192.71	93.94	5.99	1.44	26.96	16.13	300.57	300.57	300.56	1110.24	.11	2.28	15.3	5.596
216.42	104.26	5.99	1.44	29.64	17.56	300.56	300.56	300.54	1110.17	.11	2.30	16.4	5.596
243.04	115.73	5.99	1.44	32.62	19.13	300.54	300.54	300.52	1110.10	.11	2.32	17.7	5.596
272.94	128.49	5.99	1.44	35.92	20.86	300.52	300.52	300.51	1110.01	.11	2.34	19.0	5.596
306.52	142.68	5.99	1.44	39.60	22.76	300.50	300.50	300.49	1109.91	.11	2.37	20.5	5.596
344.23	158.46	5.99	1.44	43.68	24.85	300.49	300.49	300.47	1109.79	.10	2.39	22.2	5.596
386.58	176.00	5.99	1.44	48.22	27.14	300.46	300.46	300.44	1109.67	.10	2.41	24.0	5.596
434.14	195.52	5.99	1.44	53.25	29.67	300.44	300.44	300.42	1109.53	.10	2.44	26.0	5.596
487.55	217.22	5.99	1.44	58.85	32.44	300.42	300.42	300.39	1109.37	.10	2.46	28.2	5.596
547.53	241.35	5.99	1.44	65.06	35.48	300.39	300.39	300.37	1109.19	.10	2.49	30.6	5.596
614.89	268.20	5.99	1.44	71.96	38.82	300.37	300.37	300.34	1108.99	.10	2.51	33.3	5.596
690.54	298.06	5.99	1.44	79.62	42.49	300.34	300.34	300.31	1108.77	.10	2.53	36.2	5.596
775.49	331.29	5.99	1.44	88.13	46.53	300.31	300.31	300.27	1108.53	.10	2.56	39.4	5.596
870.90	368.26	5.99	1.44	97.58	50.95	300.27	300.27	300.24	1108.26	.10	2.58	42.9	5.596
978.04	409.41	5.99	1.44	108.07	55.82	300.23	300.23	300.20	1107.96	.09	2.60	46.8	5.596
1098.37	455.20	5.99	1.44	119.72	61.15	300.20	300.20	300.16	1107.63	.09	2.63	51.0	5.596
1233.50	506.19	5.99	1.44	132.65	67.01	300.15	300.15	300.11	1107.26	.09	2.65	55.7	5.596
1385.25	562.96	5.99	1.44	147.01	73.45	300.11	300.11	300.06	1106.86	.09	2.67	60.8	5.596
1555.67	626.19	5.99	1.44	162.95	80.51	300.06	300.06	300.00	1106.41	.09	2.70	66.5	5.596
1747.06	696.61	5.99	1.44	180.65	88.27	300.00	300.00	299.95	1105.92	.09	2.72	72.7	5.596
1962.00	775.07	5.99	1.44	200.30	96.79	299.94	299.94	299.88	1105.38	.09	2.74	79.4	5.596
2203.37	862.49	5.99	1.44	222.12	106.13	299.88	299.88	299.81	1104.79	.09	2.76	86.9	5.596
2474.45	959.92	5.99	1.44	246.34	116.39	299.80	299.80	299.73	1104.13	.08	2.78	95.1	5.596
2778.87	1068.53	5.99	1.44	273.23	127.66	299.73	299.73	299.65	1103.41	.08	2.80	104.1	5.596
3120.74	1189.61	5.99	1.44	303.09	140.02	299.64	299.64	299.56	1102.62	.08	2.82	113.9	5.596
3504.68	1324.62	5.99	1.44	336.23	153.59	299.55	299.55	299.46	1101.74	.08	2.84	124.8	5.596
3935.85	1475.20	5.99	1.44	373.02	168.49	299.45	299.45	299.35	1100.78	.08	2.86	136.6	5.596
4420.06	1643.17	5.99	1.44	413.86	184.84	299.34	299.34	299.23	1099.73	.08	2.88	149.7	5.596
4963.84	1830.56	5.99	1.44	459.20	202.79	299.22	299.22	299.10	1098.57	.08	2.90	164.0	5.596
5574.53	2039.66	5.99	1.44	509.54	222.49	299.09	299.09	298.96	1097.30	.08	2.92	179.7	5.596
6260.34	2273.03	5.99	1.44	565.41	244.11	298.94	298.94	298.80	1095.91	.07	2.94	197.0	5.596
7030.53	2533.52	5.99	1.44	627.44	267.84	298.79	298.79	298.63	1094.37	.07	2.96	215.9	5.596
7895.47	2824.33	5.99	1.44	696.30	293.89	298.61	298.61	298.44	1092.69	.07	2.97	236.7	5.596
8866.82	3149.04	5.99	1.44	772.75	322.48	298.42	298.42	298.23	1090.85	.07	2.99	259.5	5.596
9957.67	3511.65	5.99	1.44	857.61	353.87	298.22	298.22	298.01	1088.82	.07	3.01	284.5	5.596

```
 11182.73  3916.66     5.99    1.44  951.81  388.31   297.99   297.99   297.76  1086.60    .07   3.02  312.0   5.596

              TOTAL TRANMITANCE FOR ALL SOURCES IS:  .0000E+00



                                 END EOSAEL RUN
STOP 000
```

D-2 Example 2: Phases I and II: Vehicle Dust and HC Scenario

The following example is discussed in detail in section 5.3 in the main body of the report.

D-2.1 Input

```
WAVL      1.06
COMBIC
PHAS            1.0       5.0       6.0       0.0       9.0       0.0       0.0
FILE          9.0  h.vehc-hc
NAME            0.
  SAMPLE INPUT SHOWING VEHICULAR DUST AND HC
MET1           90.0      5.00       3.      27.50     962.5    202.40      0.00
MUNT            0.0       0.0       1.0       0.0       0.0       0.0       0.0
GO
MUNT            0.0       0.0       0.0       9.0       0.0       0.0       0.0
VEHC            4.0       3.0      60.0       1.0      90.0
DONE            0.0
END
CONTINUE
WAVL      1.06
COMBIC
PHAS            2.0       5.0       6.0       0.0       9.0       0.0       0.0
FILE          9.0  h.vehc-hc
NAME            0.
  SAMPLE INPUT SHOWING VEHICULAR DUST AND HC
ORIG            0.0       0.0       0.0      31.0     155.0
LIST            1.0       0.0     120.0       5.0
NAME            0.
123456789 123456789 123456789 123456789 123456789 123456789 123456789 123456789
NAME
        Four munition at {90., 80., 0.,) starting at T=20.
SLOC            1.0       4.0      20.0     300.0      90.0      80.0     0.0
NAME
        One vehicle {50., 218., 0.,) starting at T=20.
NAME
        Traveling 7.6m/s at 82 degrees wrt North
VEH1            2.0       1.0      20.0      50.0     300.0
VEH2           50.0     218.0       0.0      82.0       7.6
OLOC            1.0      50.0     130.0       3.0      20.0     100.0
TLOC            1.0     250.0     150.0      15.0       1.0
TLOC            1.0     220.0     100.0       3.0       2.0
DONE            0.0
END
STOP
```

D-2.2 Output

```
*************************************************************************
  WARNING - THIS LIBRARY CONTAINS TECHNICAL DATA WHOSE EXPORT IS RESTRICTED
  BY THE ARMS EXPORT CONTROL ACT (TITLE 22, U.S.C., SEC 2751 ET SEQ.) OR
  EXECUTIVE ORDER 12470.  VIOLATION OF THESE EXPORT LAWS ARE SUBJECT TO
                  SEVERE CRIMINAL PENALTIES.
*************************************************************************


1




                  *********************************
                  *                               *
                  *    ELECTRO-OPTICAL SYSTEMS    *
                  *                               *
                  *  ATMOSPHERIC EFFECTS LIBRARY  *
                  *                               *
                  *    NOT FOR OPERATIONAL USE    *
                  *                               *
                  * EOSAEL87 REV 2.1   02/23/90   *
                  *                               *
                  *********************************



WAVL      1.06
 NOTE: THAT THE ABOVE CARD WAS MODIFIED FOR CONSISTENCY TO:
WAVL       .1060E+01 .1060E+01 .0000E+00



                                     BEGINNING           ENDING

            WAVENUMBER (CM**-1)       9433.963           9433.963

            WAVELENGTH (MICROMETERS)     1.060              1.060

            FREQUENCY (GHZ)         283018.875         283018.875



         **** EOSAEL WARNING ****
 VISIBILITY AND EXTINCTION = 0.0, VISIBILITY CHANGED TO 10.0 KM
```

VISIBILITY
10.00 KM

1

```
*********************************
*                               *
*        C O M B I C            *
*                               *
*COMBINED OBSCURATION MODEL FOR*
* BATTLEFIELD-INDUCED AEROSOLS *
*   NOT FOR OPERATIONAL USE     *
*                               *
* EOSAEL92 REV 1.0   12/12/90  *
*                               *
*********************************
```

1

```
*****************
*               *
*    COMBIC     *
*    PHASE 1    *
*               *
*****************
```

COMBIC WARNING: FILE(h.vehc-hc)
WILL BE OVER WRITTEN

COMBIC CLOUD HISTORY ON UNIT 9 OPENED TO: h.vehc-hc

1

METEOROLOGICAL CONDITIONS

REFERENCE HEIGHT	10.00	METERS	WIND SPEED	5.00	METERS/SEC
SURFACE ROUGHNESS	.10000	METERS	WIND DIRECTION	202.4	DEG WRT NORTH
INVERSION HEIGHT	1783.	METERS	TEMPERATURE	27.49	DEG CELCIUS
PRESSURE	963.	MB	RELATIVE HUMIDITY	90.0	%
PASQUILL CATEGORY	3				

BOUNDARY LAYER PARAMETERS

FRICTION VELOCITY	.464 M/SEC	PASQUILL CLASS	2.60
KAZANSKI-MONIN	-.3254	OMEGA	.853
COLD REGION FLAG	0	SBAR MODEL FLAG	0
AIR DENSITY	1110.4 G/M**3	1/MONIN-OBUKHOV LENGTH	-.01102 M**-1
SENSIBLE HEAT FLUX	94.7 WATT/M**2	SURFACE BUOYANCY FLUX	.0027 M**2/S**3
MEAN STATIC SBAR (10-50M)	-.000357 SEC**-2		

DIFFUSION COEFFICIENTS

A COEFFICIENT	B COEFFICIENT	C COEFFICIENT	D COEFFICIENT
.216	.900	.220	.802

SURFACE CONDITIONS

SNOW COVER FLAG	0	SILT CONTENT	50.0 %	SOD DEPTH	.000 METERS

1 VERTICAL PROFILE MODEL

HEIGHT (M)	WINDSPEED (M/S)	ATMOSPHERIC TEMPERATURE CONSTANT SBAR MODEL (DEG K)	VARIABLE S MODEL (DEG K)	S, STATIC STABILITY PARAMETER	EDDY DISSIPATION RATE (M**2/S**3)
1.0	2.62	300.84	301.53	-.01371238	.23342
2.0	3.38	300.82	301.21	-.00641614	.11068
3.0	3.82	300.80	301.03	-.00403414	.07061
4.0	4.11	300.77	300.91	-.00287111	.05104
5.0	4.34	300.75	300.82	-.00219048	.03959
6.0	4.52	300.73	300.75	-.00174800	.03215
7.0	4.67	300.71	300.69	-.00143973	.02696
8.0	4.79	300.69	300.64	-.00121410	.02317
9.0	4.90	300.67	300.60	-.00104273	.02029
10.0	5.00	300.65	300.56	-.00090875	.01803
15.0	5.36	300.55	300.39	-.00052900	.01164
20.0	5.59	300.44	300.27	-.00035665	.00874
25.0	5.77	300.34	300.18	-.00026134	.00714
30.0	5.91	300.23	300.09	-.00020211	.00614
35.0	6.02	300.13	300.01	-.00016235	.00548
40.0	6.11	300.03	299.94	-.00013412	.00500
45.0	6.20	299.92	299.87	-.00011323	.00465
50.0	6.27	299.82	299.81	-.00009725	.00438
55.0	6.33	299.72	299.75	-.00008471	.00417
60.0	6.39	299.61	299.68	-.00007466	.00400
65.0	6.44	299.51	299.62	-.00006645	.00386
70.0	6.48	299.41	299.57	-.00005964	.00375
75.0	6.52	299.30	299.51	-.00005392	.00365
80.0	6.56	299.20	299.45	-.00004906	.00357
85.0	6.60	299.09	299.39	-.00004489	.00350
90.0	6.63	298.99	299.34	-.00004127	.00344
95.0	6.66	298.89	299.28	-.00003812	.00339
100.0	6.69	298.78	299.23	-.00003535	.00334
125.0	6.82	298.27	298.96	-.00002544	.00317
150.0	6.91	297.75	298.70	-.00001943	.00307
175.0	6.99	297.23	298.44	-.00001546	.00300
200.0	7.05	296.72	298.18	-.00001268	.00159
225.0	7.11	296.20	297.93	-.00001064	.00155
250.0	7.16	295.69	297.68	-.00000910	.00153
275.0	7.20	295.17	297.43	-.00000790	.00151
300.0	7.24	294.66	297.17	-.00000694	.00149
325.0	7.27	294.15	296.92	-.00000616	.00148
350.0	7.31	293.63	296.67	-.00000551	.00147
375.0	7.33	293.12	296.43	-.00000497	.00146
400.0	7.36	292.61	296.18	-.00000452	.00145
450.0	7.41	291.59	295.68	-.00000379	.00144
500.0	7.45	290.57	295.19	-.00000324	.00143
550.0	7.48	289.55	294.69	-.00000281	.00142

600.0	7.52	288.53	294.20	-.00000246	.00141
650.0	7.55	287.52	293.70	-.00000219	.00141
700.0	7.57	286.50	293.21	-.00000196	.00141
750.0	7.60	285.49	292.72	-.00000177	.00140
800.0	7.62	284.48	292.22	-.00000160	.00140
850.0	7.64	283.47	291.73	-.00000146	.00140
900.0	7.66	282.47	291.24	-.00000134	.00139
950.0	7.68	281.46	290.75	-.00000124	.00139
1000.0	7.69	280.46	290.26	-.00000115	.00139

1

MASS EXTINCTION COEFFICIENTS (M**2/GRAM)

OBSCURANT	WAVELENGTH (MICROMETERS)						
CODE	.4-.7	.7-1.2	1.06	3.-5.	8.-12.	10.6	94 GHZ
1	3.2280	2.3638	2.1094	.4127	.3043	.2792	.0010
2	3.2280	2.3638	2.1094	.4127	.3043	.2792	.0010
3	2.1520	2.1368	2.0302	.2668	.0601	.0750	.0010
4	6.8510	4.5920	3.4970	.2450	.0200	.0180	.0010
5	3.2280	2.3638	2.1094	.4127	.3043	.2792	.0010
6	1.8600	1.6300	1.4000	1.7900	1.6800	1.6800	.0010
7	1.8600	1.6300	1.4000	1.7900	1.6800	1.6800	.0010
8	5.6500	4.0800	3.2500	.2450	.0230	.0270	.0010
9	.3200	.3000	.2900	.2700	.2500	.2500	.0010
10	.3200	.2900	.2600	.2700	.2600	.2400	.0010
11	.0350	.0360	.0370	.0350	.0380	.0360	.0010
12	1.5000	1.4600	1.4200	.7500	.3200	.3000	.0010
13	.0010	.0010	.0010	.0010	.0010	.0010	.0004
14	6.1000	3.7500	2.9400	1.3500	1.0100	1.0000	.0020
15	6.8510	4.5920	1.4300	.0540	.0200	.0180	.0010
16	5.3700	2.9000	2.1000	.0900	.0900	.0700	.0010
17	6.2000	3.5000	2.5000	.2300	.0500	.0480	.0010
18	3.3300	2.7500	2.6600	.2600	.3200	.2300	.0010
19	1.3000	1.7400	1.7000	.0800	.1600	.3800	.0010
20	2.0000	2.0000	2.0000	1.6000	2.0000	.0000	.0000
21	2.0000	2.0000	1.0000	.1000	.4000	.0000	.0000
22	.0000	.0000	.0000	.0000	.0000	.0000	.0000
23	.0000	.0000	.0000	.0000	.0000	.0000	.0000
24	.0000	.0000	.0000	.0000	.0000	.0000	.0000
25	.0000	.0000	.0000	.0000	.0000	.0000	.0000
26	.0000	.0000	.0000	.0000	.0000	.0000	.0000
27	.0000	.0000	.0000	.0000	.0000	.0000	.0000
28	.0000	.0000	.0000	.0000	.0000	.0000	.0000
29	.0000	.0000	.0000	.0000	.0000	.0000	.0000
30	.0000	.0000	.0000	.0000	.0000	.0000	.0000

1

CLOUD HISTORY, FILE NAME = COMHIS

HISTORY FILE SOURCE # 1 CONTAINS 1 SUBCLOUDS, TOTAL 9815.65 GRAMS OBSCURANT

XN NO. OF SOURCES	FILL WEIGHT (LB, GAL OR LB TNT)	MENU SELECTION TYPE	OBSCURANT TYPE CODE	EFFICIENCY (PERCENT)	YIELD FACTOR	NUMBER OF SUBMUNITIONS
1.00	5.400	1.	3.	70.0	5.725	1.00

BURN DURATION (SEC)	BURN RATE COEFFICIENTS B1	B2	B3	B4	B5	B6
100.00	.5370	.4760	4.7790	-5.4720	.0000	.0000

SMOULDERING TIME (SEC)	SMOULDERING COEFFICIENT CSMLD
.00	.0000

1

PROCESSING SUBCLOUD 1

SUBCLOUD # 1 HISTORY FILE SOURCE # 1

MASS FRACTION	DEBRIS CARBON (G/G OBSC)	PLUME (1=PUFF, 2=PLUME)	CLOUD RISE MODEL (1=RISE, 2= NO RISE, >2=STEM)	EXTINCTION COEFFICIENT CODE	BALLISTIC SUBCLOUD (1=Y, 0=N)
1.000000	.000	2.	1.	3.	0.

INITIAL THERMAL UPWARD

INITIAL OBSCURANT RADII (M)			BUOYANCY	CLOUD	PRODUCTION	VELOCITY
DOWNWIND	CROSSWIND	VERTICAL	RADIUS(M)	TEMP(DEG K)	COEF (CAL/G)	(M/S)
3.10	3.10	3.70	2.29	308.38	3307.09	1.64

	FALL	EVAPORATION/DEPOSITION			MOMENTUM	HORIZONTAL
HEIGHT OF	VELOCITY	FD	DELTA	REFL.	RADIUS	VELOCITY
BURST (M)	(M/S)	(LONG-TERM)	(S**-1)	COEF.	(M)	(M/S)
.0	.000	1.000000	.00000	.5500	.00	1.49

MASS PRODUCTION PROFILE

TIME T AFTER IGNITION (SEC)	MASS PRODUCED UP UNTIL TIME T (G)	MASS STILL AIRBORNE BY TIME T (G)	MDOT
1.000	53.0	53.0	52.9591
2.000	106.5	106.5	53.5183
3.000	160.6	160.6	54.1665
4.000	215.5	215.5	54.9004
5.000	271.3	271.3	55.7168
6.000	327.9	327.9	56.6126
7.000	385.5	385.5	57.5844
8.000	444.1	444.1	58.6291
9.000	503.8	503.8	59.7436
10.000	564.8	564.8	60.9243
11.000	626.9	626.9	62.1683
12.000	690.4	690.4	63.4723
13.000	755.2	755.2	64.8331
14.000	821.5	821.5	66.2473
15.000	889.2	889.2	67.7120
16.000	958.4	958.4	69.2236
17.000	1029.2	1029.2	70.7791
18.000	1101.6	1101.6	72.3754
19.000	1175.6	1175.6	74.0088
20.000	1251.3	1251.3	75.6768
21.000	1328.6	1328.6	77.3755
22.000	1407.7	1407.7	79.1021
23.000	1488.6	1488.6	80.8531
24.000	1571.2	1571.2	82.6255
25.000	1655.6	1655.6	84.4159
26.000	1741.8	1741.8	86.2212
27.000	1829.9	1829.9	88.0385

28.000	1919.7	1919.7	89.8634
29.000	2011.4	2011.4	91.6940
30.000	2105.0	2105.0	93.5269
31.000	2200.3	2200.3	95.3579
32.000	2297.5	2297.5	97.1848
33.000	2396.5	2396.5	99.0042
34.000	2497.3	2497.3	100.8120
35.000	2599.9	2599.9	102.6062
36.000	2704.3	2704.3	104.3833
37.000	2810.5	2810.5	106.1387
38.000	2918.3	2918.3	107.8711
39.000	3027.9	3027.9	109.5764
40.000	3139.2	3139.2	111.2520
41.000	3252.0	3252.0	112.8931
42.000	3366.5	3366.5	114.4978
43.000	3482.6	3482.6	116.0630
44.000	3600.2	3600.2	117.5845
45.000	3719.3	3719.3	119.0603
46.000	3839.7	3839.7	120.4856
47.000	3961.6	3961.6	121.8589
48.000	4084.8	4084.8	123.1758
49.000	4209.2	4209.2	124.4336
50.000	4334.8	4334.8	125.6289
51.000	4461.6	4461.6	126.7578
52.000	4589.4	4589.4	127.8184
53.000	4718.2	4718.2	128.8076
54.000	4847.9	4847.9	129.7207
55.000	4978.5	4978.5	130.5547
56.000	5109.8	5109.8	131.3076
57.000	5241.8	5241.8	131.9751
58.000	5374.3	5374.3	132.5537
59.000	5507.4	5507.4	133.0420
60.000	5640.8	5640.8	133.4360
61.000	5774.5	5774.5	133.7310
62.000	5908.5	5908.5	133.9243
63.000	6042.5	6042.5	134.0142
64.000	6176.5	6176.5	133.9966
65.000	6310.3	6310.3	133.8677
66.000	6444.0	6444.0	133.6255
67.000	6577.2	6577.2	133.2646
68.000	6710.0	6710.0	132.7842
69.000	6842.2	6842.2	132.1802
70.000	6973.6	6973.6	131.4487
71.000	7104.2	7104.2	130.5879
72.000	7233.8	7233.8	129.5933
73.000	7362.3	7362.3	128.4614
74.000	7489.5	7489.5	127.1899
75.000	7615.3	7615.3	125.7764

76.000	7739.5	7739.5	124.2153
77.000	7862.0	7862.0	122.5063
78.000	7982.6	7982.6	120.6426
79.000	8101.2	8101.2	118.6260
80.000	8217.7	8217.7	116.4463
81.000	8331.8	8331.8	114.1064
82.000	8443.4	8443.4	111.6006
83.000	8552.3	8552.3	108.9248
84.000	8658.4	8658.4	106.0811
85.000	8761.5	8761.5	103.0576
86.000	8861.3	8861.3	99.8574
87.000	8957.8	8957.8	96.4746
88.000	9050.7	9050.7	92.9082
89.000	9139.9	9139.9	89.1533
90.000	9225.1	9225.1	85.2051
91.000	9306.1	9306.1	81.0654
92.000	9382.9	9382.9	76.7256
93.000	9455.0	9455.0	72.1855
94.000	9522.5	9522.5	67.4404
95.000	9585.0	9585.0	62.4893
96.000	9642.3	9642.3	57.3271
97.000	9694.2	9694.2	51.9502
98.000	9740.6	9740.6	46.3555
99.000	9781.1	9781.1	40.5430
100.000	9815.6	9815.6	34.5039

SUBCLOUD TRAJECTORY

DOWNWIND		CENTROID	GAUSSIAN CLOUD			PEAK CLOUD	MEAN CLOUD	AIR	AIR	CENTROID OR CM VELOCITY		CM	EFFECTIVE BUOYANCY
DISTANCE	TIME	HEIGHT	STD. DEVIATIONS (M)			TEMP.	TEMP.	TEMP.	DENSITY	VERT.	HOR.	HEIGHT	RADIUS
(M)	(SEC)	(M)	SIGMAX	SIGMAY	SIGMAZ	(DEG K)	(DEG K)	(DEG K)	(G/M**3)	(M/S)	(M/S)	(M)	(M)
1.00	.54	.71	1.44	1.60	2.33	313.80	306.12	301.21	1109.38	1.03	2.21	2.2	2.594
2.84	1.26	1.30	1.44	1.86	2.66	309.67	304.48	301.12	1109.64	.66	2.81	2.7	2.896
5.24	2.06	1.75	1.44	2.26	2.88	307.46	303.59	301.06	1109.80	.49	3.15	3.1	3.196
8.09	2.94	2.14	1.44	2.79	3.10	306.08	303.02	301.02	1109.91	.40	3.37	3.4	3.490
11.33	3.87	2.49	1.44	3.44	3.35	305.14	302.63	300.98	1110.02	.35	3.53	3.8	3.779
14.92	4.87	2.81	1.44	4.18	3.62	304.44	302.33	300.94	1110.10	.31	3.67	4.2	4.066
18.82	5.92	3.12	1.44	5.00	3.93	303.90	302.09	300.90	1110.20	.28	3.78	4.6	4.352
23.02	7.01	3.42	1.44	5.89	4.26	303.47	301.90	300.87	1110.27	.26	3.89	5.1	4.639
27.50	8.15	3.71	1.44	6.83	4.63	303.12	301.74	300.83	1110.34	.25	3.98	5.5	4.928
32.24	9.33	3.99	1.44	7.82	5.02	302.82	301.61	300.80	1110.39	.23	4.06	5.9	5.220
37.22	10.53	4.15	1.44	8.69	5.43	301.81	301.16	300.79	1110.41	.24	4.24	6.2	5.390

42.44	11.73	4.15	1.44	9.36	5.84	301.29	300.97	300.78	1110.42	.25	4.33	6.5	5.390
47.89	12.97	4.15	1.44	10.06	6.26	301.03	300.87	300.77	1110.45	.25	4.41	6.8	5.390
53.78	14.28	4.15	1.44	10.80	6.71	300.89	300.81	300.75	1110.48	.25	4.48	7.2	5.390
60.39	15.74	4.15	1.44	11.63	7.21	300.81	300.77	300.73	1110.50	.26	4.54	7.5	5.390
67.82	17.35	4.15	1.44	12.55	7.76	300.76	300.74	300.71	1110.53	.26	4.60	8.0	5.390
76.17	19.14	4.15	1.44	13.58	8.36	300.72	300.71	300.69	1110.55	.26	4.66	8.4	5.390
85.54	21.13	4.15	1.44	14.72	9.03	300.70	300.69	300.67	1110.58	.26	4.71	8.9	5.390
96.06	23.34	4.15	1.44	16.00	9.76	300.67	300.67	300.64	1110.60	.26	4.77	9.5	5.390
107.88	25.79	4.15	1.44	17.41	10.57	300.65	300.64	300.62	1110.61	.26	4.82	10.1	5.390
121.15	28.51	4.15	1.44	18.99	11.46	300.62	300.62	300.60	1110.63	.26	4.88	10.8	5.390
136.06	31.53	4.15	1.44	20.74	12.43	300.60	300.59	300.57	1110.63	.25	4.94	11.6	5.390
152.80	34.88	4.15	1.44	22.69	13.51	300.57	300.57	300.54	1110.64	.25	5.00	12.4	5.390
171.60	38.60	4.15	1.44	24.85	14.70	300.54	300.54	300.52	1110.63	.25	5.06	13.4	5.390
192.71	42.72	4.15	1.44	27.26	16.00	300.51	300.51	300.49	1110.62	.25	5.12	14.4	5.390
216.42	47.30	4.15	1.44	29.94	17.43	300.49	300.49	300.46	1110.60	.25	5.18	15.5	5.390
243.04	52.38	4.15	1.44	32.91	19.01	300.46	300.46	300.43	1110.57	.25	5.24	16.8	5.390
272.94	58.02	4.15	1.44	36.22	20.74	300.43	300.43	300.40	1110.53	.24	5.30	18.1	5.390
306.52	64.28	4.15	1.44	39.89	22.64	300.39	300.39	300.36	1110.47	.24	5.37	19.7	5.390
344.23	71.22	4.15	1.44	43.97	24.73	300.36	300.36	300.33	1110.41	.24	5.43	21.3	5.390
386.58	78.93	4.15	1.44	48.50	27.03	300.33	300.33	300.29	1110.33	.24	5.50	23.1	5.390
434.14	87.48	4.15	1.44	53.53	29.56	300.29	300.29	300.26	1110.23	.23	5.56	25.2	5.390
487.55	96.98	4.15	1.44	59.12	32.33	300.26	300.26	300.22	1110.12	.23	5.62	27.4	5.390
547.53	107.52	4.15	1.44	65.33	35.37	300.22	300.22	300.18	1109.98	.23	5.69	29.8	5.390
614.89	119.23	4.15	1.44	72.23	38.72	300.18	300.18	300.14	1109.83	.23	5.75	32.5	5.390
690.54	132.24	4.15	1.44	79.89	42.39	300.14	300.14	300.10	1109.65	.23	5.82	35.4	5.390
775.49	146.69	4.15	1.44	88.39	46.43	300.10	300.10	300.05	1109.45	.22	5.88	38.6	5.390
870.90	162.74	4.15	1.44	97.84	50.86	300.05	300.05	300.01	1109.21	.22	5.94	42.1	5.390
978.04	180.59	4.15	1.44	108.33	55.72	300.00	300.00	299.96	1108.95	.22	6.00	46.0	5.390
1098.37	200.42	4.15	1.44	119.97	61.06	299.95	299.95	299.90	1108.66	.21	6.07	50.3	5.390
1233.50	222.47	4.15	1.44	132.90	66.92	299.90	299.90	299.85	1108.33	.21	6.13	54.9	5.390
1385.25	247.00	4.15	1.44	147.26	73.36	299.84	299.84	299.79	1107.96	.21	6.19	60.1	5.390
1555.67	274.28	4.15	1.44	163.20	80.43	299.78	299.78	299.72	1107.54	.21	6.25	65.7	5.390
1747.06	304.63	4.15	1.44	180.90	88.19	299.72	299.72	299.66	1107.08	.20	6.31	71.9	5.390
1962.00	338.41	4.15	1.44	200.55	96.70	299.65	299.65	299.58	1106.57	.20	6.36	78.7	5.390
2203.37	376.00	4.15	1.44	222.36	106.05	299.58	299.58	299.50	1106.01	.20	6.42	86.1	5.390
2474.45	417.86	4.15	1.44	246.58	116.31	299.50	299.50	299.42	1105.38	.20	6.48	94.3	5.390
2778.87	464.47	4.15	1.44	273.47	127.58	299.41	299.41	299.33	1104.68	.19	6.53	103.3	5.390
3120.74	516.39	4.15	1.44	303.31	139.94	299.32	299.32	299.23	1103.91	.19	6.58	113.2	5.390
3504.68	574.23	4.15	1.44	336.45	153.52	299.22	299.22	299.12	1103.06	.19	6.64	124.0	5.390
3935.85	638.68	4.15	1.44	373.24	168.42	299.11	299.11	299.01	1102.13	.18	6.69	135.9	5.390
4420.06	710.52	4.15	1.44	414.08	184.77	299.00	299.00	298.88	1101.10	.18	6.74	148.9	5.390
4963.84	790.59	4.15	1.44	459.42	202.72	298.87	298.87	298.74	1099.96	.18	6.79	163.3	5.390
5574.53	879.88	4.15	1.44	509.75	222.42	298.73	298.73	298.60	1098.70	.18	6.84	179.0	5.390
6260.34	979.44	4.15	1.44	565.63	244.04	298.58	298.58	298.43	1097.33	.17	6.89	196.2	5.390
7030.53	1090.50	4.15	1.44	627.66	267.78	298.42	298.42	298.26	1095.81	.17	6.94	215.2	5.390
7895.47	1214.40	4.15	1.44	696.51	293.83	298.24	298.24	298.06	1094.14	.17	6.98	236.0	5.390
8866.82	1352.64	4.15	1.44	772.95	322.42	298.05	298.05	297.85	1092.31	.17	7.03	258.8	5.390
9957.67	1506.92	4.15	1.44	857.81	353.81	297.83	297.83	297.62	1090.29	.16	7.07	283.8	5.390

```
  11182.73  1679.12     4.15    1.44  952.01  388.25   297.60   297.60   297.37  1088.08    .16   7.11  311.3   5.390
1

                  CLOUD HISTORY, FILE NAME = COMHIS

 HISTORY FILE SOURCE #  2 CONTAINS 1 SUBCLOUDS, TOTAL  198720.00 GRAMS OBSCURANT
```

XN NO. OF SOURCES	FILL WEIGHT (LB, GAL OR LB TNT)	MENU SELECTION TYPE	OBSCURANT TYPE CODE	EFFICIENCY (PERCENT)	YIELD FACTOR	NUMBER OF SUBMUNITIONS
1.00	438.103	0.	9.	100.0	1.000	1.00

BURN DURATION (SEC)	BURN RATE COEFFICIENTS B1	B2	B3	B4	B5	B6
900.00	1.0000	.0000	.0000	.0000	.0000	.0000

SMOULDERING TIME (SEC)	SMOULDERING COEFFICIENT CSMLD
.00	.0000

MOVING SOURCE OR VEHICLE DUST

VEHICLE SPEED (M/S)	VEHICLE WIDTH (M)	VEHICLE WEIGHT (TONS)	VEHICLE TYPE (0=WHEELED, 1=TRACKED)	VEHICLE DIRECTION (DEG)
4.0	3.0	60.0	1.	90.0

```
1

          PROCESSING SUBCLOUD  1

         SUBCLOUD # 1        HISTORY FILE SOURCE #  2
```

MASS FRACTION	DEBRIS CARBON (G/G OBSC)	PLUME (1=PUFF, 2=PLUME)	CLOUD RISE MODEL (1=RISE, 2= NO RISE, >2=STEM)	EXTINCTION COEFFICIENT CODE	BALLISTIC SUBCLOUD (1=Y, 0=N)
1.000000	.000	2.	2.	9.	0.

INITIAL OBSCURANT RADII (M)			BUOYANCY	INITIAL CLOUD	THERMAL PRODUCTION	UPWARD VELOCITY
DOWNWIND	CROSSWIND	VERTICAL	RADIUS(M)	TEMP(DEG K)	COEF (CAL/G)	(M/S)
2.70	2.70	1.20	.00	.00	.00	.00

HEIGHT OF BURST (M)	FALL VELOCITY (M/S)	EVAPORATION/DEPOSITION FD (LONG-TERM)	DELTA (S**-1)	REFL. COEF.	MOMENTUM RADIUS (M)	HORIZONTAL VELOCITY (M/S)
.0	.000	1.000000	.00000	.5500	.00	.00

MASS PRODUCTION PROFILE

TIME T AFTER IGNITION (SEC)	MASS PRODUCED UP UNTIL TIME T (G)	MASS STILL AIRBORNE BY TIME T (G)	MDOT
1.000	220.8	220.8	220.8000
2.000	441.6	441.6	220.8000
3.000	662.4	662.4	220.8000
4.000	883.2	883.2	220.8000
5.000	1104.0	1104.0	220.8000
6.000	1324.8	1324.8	220.8000
7.000	1545.6	1545.6	220.8000
8.000	1766.4	1766.4	220.7999
9.000	1987.2	1987.2	220.7999
10.000	2208.0	2208.0	220.8000
11.000	2428.8	2428.8	220.8000
12.000	2649.6	2649.6	220.8000
13.000	2870.4	2870.4	220.7998
14.000	3091.2	3091.2	220.8003
15.000	3312.0	3312.0	220.8000
16.000	3532.8	3532.8	220.7998
17.000	3753.6	3753.6	220.8000

18.000	3974.4	3974.4	220.7998
19.000	4195.2	4195.2	220.7998
20.000	4416.0	4416.0	220.8003
21.000	4636.8	4636.8	220.7998
22.000	4857.6	4857.6	220.8003
23.000	5078.4	5078.4	220.7998
24.000	5299.2	5299.2	220.8003
25.000	5520.0	5520.0	220.7998
26.000	5740.8	5740.8	220.7998
27.000	5961.6	5961.6	220.8003
28.000	6182.4	6182.4	220.8003
29.000	6403.2	6403.2	220.7998
30.000	6624.0	6624.0	220.8003
31.000	6844.8	6844.8	220.7993
32.000	7065.6	7065.6	220.8003
33.000	7286.4	7286.4	220.7998
34.000	7507.2	7507.2	220.8003
35.000	7728.0	7728.0	220.8003
36.000	7948.8	7948.8	220.7993
37.000	8169.6	8169.6	220.8003
38.000	8390.4	8390.4	220.7993
39.000	8611.2	8611.2	220.8008
40.000	8832.0	8832.0	220.7998
41.000	9052.8	9052.8	220.7998
42.000	9273.6	9273.6	220.7998
43.000	9494.4	9494.4	220.8008
44.000	9715.2	9715.2	220.7998
45.000	9936.0	9936.0	220.7998
46.000	10156.8	10156.8	220.7998
47.000	10377.6	10377.6	220.7998
48.000	10598.4	10598.4	220.8008
49.000	10819.2	10819.2	220.7998
50.000	11040.0	11040.0	220.7998
51.000	11260.8	11260.8	220.8008
52.000	11481.6	11481.6	220.7988
53.000	11702.4	11702.4	220.8008
54.000	11923.2	11923.2	220.7998
55.000	12144.0	12144.0	220.7998
56.000	12364.8	12364.8	220.8008
57.000	12585.6	12585.6	220.7988
58.000	12806.4	12806.4	220.8008
59.000	13027.2	13027.2	220.7998
60.000	13248.0	13248.0	220.8008
61.000	13468.8	13468.8	220.7988
62.000	13689.6	13689.6	220.7998
63.000	13910.4	13910.4	220.8008
64.000	14131.2	14131.2	220.7998
65.000	14352.0	14352.0	220.8008

66.000	14572.8	14572.8	220.7988
67.000	14793.6	14793.6	220.7998
68.000	15014.4	15014.4	220.8008
69.000	15235.2	15235.2	220.7998
70.000	15456.0	15456.0	220.8008
71.000	15676.8	15676.8	220.7988
72.000	15897.6	15897.6	220.7998
73.000	16118.4	16118.4	220.8008
74.000	16339.2	16339.2	220.7998
75.000	16560.0	16560.0	220.7998
76.000	16780.8	16780.8	220.7988
77.000	17001.6	17001.6	220.8008
78.000	17222.4	17222.4	220.8008
79.000	17443.2	17443.2	220.7988
80.000	17664.0	17664.0	220.8008
81.000	17884.8	17884.8	220.8008
82.000	18105.6	18105.6	220.7988
83.000	18326.4	18326.4	220.8008
84.000	18547.2	18547.2	220.7988
85.000	18768.0	18768.0	220.8008
86.000	18988.8	18988.8	220.8008
87.000	19209.6	19209.6	220.7988
88.000	19430.4	19430.4	220.8008
89.000	19651.2	19651.2	220.7988
90.000	19872.0	19872.0	220.8008
91.000	20092.8	20092.8	220.8008
92.000	20313.6	20313.6	220.7988
93.000	20534.4	20534.4	220.8008
94.000	20755.2	20755.2	220.7988
95.000	20976.0	20976.0	220.8008
96.000	21196.8	21196.8	220.8008
97.000	21417.6	21417.6	220.7988
98.000	21638.4	21638.4	220.8008
99.000	21859.2	21859.2	220.7988
100.000	22080.0	22080.0	220.8008
101.000	22300.8	22300.8	220.8008
102.000	22521.6	22521.6	220.8008
103.000	22742.4	22742.4	220.7988
104.000	22963.2	22963.2	220.7988
105.000	23184.0	23184.0	220.8008
106.000	23404.8	23404.8	220.8008
107.000	23625.6	23625.6	220.8008
108.000	23846.4	23846.4	220.7988
109.000	24067.2	24067.2	220.7988
110.000	24288.0	24288.0	220.8008
111.000	24508.8	24508.8	220.8008
112.000	24729.6	24729.6	220.8008
113.000	24950.4	24950.4	220.7988

114.000	25171.2	25171.2	220.7988
115.000	25392.0	25392.0	220.8027
116.000	25612.8	25612.8	220.7988
117.000	25833.6	25833.6	220.7988
118.000	26054.4	26054.4	220.8008
119.000	26275.2	26275.2	220.7988
120.000	26496.0	26496.0	220.8027
121.000	26716.8	26716.8	220.7988
122.000	26937.6	26937.6	220.7988
123.000	27158.4	27158.4	220.8008
124.000	27379.2	27379.2	220.7988
125.000	27600.0	27600.0	220.8027
126.000	27820.8	27820.8	220.7988
127.000	28041.6	28041.6	220.7988
128.000	28262.4	28262.4	220.8008
129.000	28483.2	28483.2	220.7988
130.000	28704.0	28704.0	220.8027
131.000	28924.8	28924.8	220.7988
132.000	29145.6	29145.6	220.7988
133.000	29366.4	29366.4	220.8008
134.000	29587.2	29587.2	220.7988
135.000	29808.0	29808.0	220.8027
136.000	30028.8	30028.8	220.7988
137.000	30249.6	30249.6	220.7988
138.000	30470.4	30470.4	220.8008
139.000	30691.2	30691.2	220.7988
140.000	30912.0	30912.0	220.8027
141.000	31132.8	31132.8	220.7988
142.000	31353.6	31353.6	220.7988
143.000	31574.4	31574.4	220.8008
144.000	31795.2	31795.2	220.7988
145.000	32016.0	32016.0	220.8027
146.000	32236.8	32236.8	220.7988
147.000	32457.6	32457.6	220.7988
148.000	32678.4	32678.4	220.8008
149.000	32899.2	32899.2	220.7988
150.000	33120.0	33120.0	220.8008
151.000	33340.8	33340.8	220.8008
152.000	33561.6	33561.6	220.7969
153.000	33782.4	33782.4	220.8008
154.000	34003.2	34003.2	220.8008
155.000	34224.0	34224.0	220.8008
156.000	34444.8	34444.8	220.8008
157.000	34665.6	34665.6	220.7969
158.000	34886.4	34886.4	220.8008
159.000	35107.2	35107.2	220.8008
160.000	35328.0	35328.0	220.8008
161.000	35548.8	35548.8	220.8008

162.000	35769.6	35769.6	220.8008
163.000	35990.4	35990.4	220.7969
164.000	36211.2	36211.2	220.8008
165.000	36432.0	36432.0	220.8008
166.000	36652.8	36652.8	220.8008
167.000	36873.6	36873.6	220.8008
168.000	37094.4	37094.4	220.7969
169.000	37315.2	37315.2	220.8008
170.000	37536.0	37536.0	220.8008
171.000	37756.8	37756.8	220.8008
172.000	37977.6	37977.6	220.8008
173.000	38198.4	38198.4	220.7969
174.000	38419.2	38419.2	220.8008
175.000	38640.0	38640.0	220.8008
176.000	38860.8	38860.8	220.8008
177.000	39081.6	39081.6	220.8008
178.000	39302.4	39302.4	220.7969
179.000	39523.2	39523.2	220.8008
180.000	39744.0	39744.0	220.8008
181.000	39964.8	39964.8	220.8008
182.000	40185.6	40185.6	220.8008
183.000	40406.4	40406.4	220.7969
184.000	40627.2	40627.2	220.8008
185.000	40848.0	40848.0	220.8008
186.000	41068.8	41068.8	220.8008
187.000	41289.6	41289.6	220.8008
188.000	41510.4	41510.4	220.7969
189.000	41731.2	41731.2	220.8008
190.000	41952.0	41952.0	220.8008
191.000	42172.8	42172.8	220.8008
192.000	42393.6	42393.6	220.8008
193.000	42614.4	42614.4	220.7969
194.000	42835.2	42835.2	220.8008
195.000	43056.0	43056.0	220.8008
196.000	43276.8	43276.8	220.8008
197.000	43497.6	43497.6	220.8008
198.000	43718.4	43718.4	220.7969
199.000	43939.2	43939.2	220.8008
200.000	44160.0	44160.0	220.8008
201.000	44380.8	44380.8	220.8008
202.000	44601.6	44601.6	220.8008
203.000	44822.4	44822.4	220.7969
204.000	45043.2	45043.2	220.8047
205.000	45264.0	45264.0	220.7969
206.000	45484.8	45484.8	220.8008
207.000	45705.6	45705.6	220.8008
208.000	45926.4	45926.4	220.7969
209.000	46147.2	46147.2	220.8047

210.000	46368.0	46368.0	220.7969
211.000	46588.8	46588.8	220.8008
212.000	46809.6	46809.6	220.8008
213.000	47030.4	47030.4	220.7969
214.000	47251.2	47251.2	220.8047
215.000	47472.0	47472.0	220.7969
216.000	47692.8	47692.8	220.8008
217.000	47913.6	47913.6	220.8008
218.000	48134.4	48134.4	220.7969
219.000	48355.2	48355.2	220.8047
220.000	48576.0	48576.0	220.7969
221.000	48796.8	48796.8	220.8008
222.000	49017.6	49017.6	220.8008
223.000	49238.4	49238.4	220.7969
224.000	49459.2	49459.2	220.8047
225.000	49680.0	49680.0	220.7969
226.000	49900.8	49900.8	220.8008
227.000	50121.6	50121.6	220.7969
228.000	50342.4	50342.4	220.8008
229.000	50563.2	50563.2	220.8008
230.000	50784.0	50784.0	220.8047
231.000	51004.8	51004.8	220.7930
232.000	51225.6	51225.6	220.8047
233.000	51446.4	51446.4	220.8008
234.000	51667.2	51667.2	220.7969
235.000	51888.0	51888.0	220.8008
236.000	52108.8	52108.8	220.8008
237.000	52329.6	52329.6	220.7969
238.000	52550.4	52550.4	220.8008
239.000	52771.2	52771.2	220.8008
240.000	52992.0	52992.0	220.8047
241.000	53212.8	53212.8	220.7930
242.000	53433.6	53433.6	220.8047
243.000	53654.4	53654.4	220.8008
244.000	53875.2	53875.2	220.7969
245.000	54096.0	54096.0	220.8008
246.000	54316.8	54316.8	220.8008
247.000	54537.6	54537.6	220.7969
248.000	54758.4	54758.4	220.8008
249.000	54979.2	54979.2	220.8008
250.000	55200.0	55200.0	220.8047
251.000	55420.8	55420.8	220.7930
252.000	55641.6	55641.6	220.8047
253.000	55862.4	55862.4	220.8008
254.000	56083.2	56083.2	220.7969
255.000	56304.0	56304.0	220.8008
256.000	56524.8	56524.8	220.8008
257.000	56745.6	56745.6	220.7969

258.000	56966.4	56966.4	220.8008
259.000	57187.2	57187.2	220.8008
260.000	57408.0	57408.0	220.8047
261.000	57628.8	57628.8	220.7930
262.000	57849.6	57849.6	220.8047
263.000	58070.4	58070.4	220.8008
264.000	58291.2	58291.2	220.7969
265.000	58512.0	58512.0	220.8008
266.000	58732.8	58732.8	220.8008
267.000	58953.6	58953.6	220.7969
268.000	59174.4	59174.4	220.8008
269.000	59395.2	59395.2	220.8008
270.000	59616.0	59616.0	220.8047
271.000	59836.8	59836.8	220.7930
272.000	60057.6	60057.6	220.8047
273.000	60278.4	60278.4	220.8008
274.000	60499.2	60499.2	220.7969
275.000	60720.0	60720.0	220.8008
276.000	60940.8	60940.8	220.8008
277.000	61161.6	61161.6	220.8008
278.000	61382.4	61382.4	220.7969
279.000	61603.2	61603.2	220.8008
280.000	61824.0	61824.0	220.8047
281.000	62044.8	62044.8	220.7930
282.000	62265.6	62265.6	220.8047
283.000	62486.4	62486.4	220.8008
284.000	62707.2	62707.2	220.7969
285.000	62928.0	62928.0	220.8008
286.000	63148.8	63148.8	220.8008
287.000	63369.6	63369.6	220.8008
288.000	63590.4	63590.4	220.7969
289.000	63811.2	63811.2	220.8008
290.000	64032.0	64032.0	220.8047
291.000	64252.8	64252.8	220.7930
292.000	64473.6	64473.6	220.8047
293.000	64694.4	64694.4	220.8008
294.000	64915.2	64915.2	220.7969
295.000	65136.0	65136.0	220.8008
296.000	65356.8	65356.8	220.8008
297.000	65577.6	65577.6	220.8008
298.000	65798.4	65798.4	220.7969
299.000	66019.2	66019.2	220.8047
300.000	66240.0	66240.0	220.7969
301.000	66460.8	66460.8	220.7969
302.000	66681.6	66681.6	220.8047
303.000	66902.4	66902.4	220.7969
304.000	67123.2	67123.2	220.7969
305.000	67344.0	67344.0	220.8047

306.000	67564.8	67564.8	220.7969
307.000	67785.6	67785.6	220.8047
308.000	68006.4	68006.4	220.7969
309.000	68227.2	68227.2	220.8047
310.000	68448.0	68448.0	220.7969
311.000	68668.8	68668.8	220.7969
312.000	68889.6	68889.6	220.8047
313.000	69110.4	69110.4	220.7969
314.000	69331.2	69331.2	220.7969
315.000	69552.0	69552.0	220.8047
316.000	69772.8	69772.8	220.7969
317.000	69993.6	69993.6	220.8047
318.000	70214.4	70214.4	220.7969
319.000	70435.2	70435.2	220.8047
320.000	70656.0	70656.0	220.7969
321.000	70876.8	70876.8	220.7969
322.000	71097.6	71097.6	220.8047
323.000	71318.4	71318.4	220.7969
324.000	71539.2	71539.2	220.8047
325.000	71760.0	71760.0	220.7969
326.000	71980.8	71980.8	220.7969
327.000	72201.6	72201.6	220.8047
328.000	72422.4	72422.4	220.7969
329.000	72643.2	72643.2	220.8047
330.000	72864.0	72864.0	220.7969
331.000	73084.8	73084.8	220.7969
332.000	73305.6	73305.6	220.8047
333.000	73526.4	73526.4	220.7969
334.000	73747.2	73747.2	220.8047
335.000	73968.0	73968.0	220.7969
336.000	74188.8	74188.8	220.7969
337.000	74409.6	74409.6	220.8047
338.000	74630.4	74630.4	220.7969
339.000	74851.2	74851.2	220.8047
340.000	75072.0	75072.0	220.7969
341.000	75292.8	75292.8	220.7969
342.000	75513.6	75513.6	220.8047
343.000	75734.4	75734.4	220.7969
344.000	75955.2	75955.2	220.8047
345.000	76176.0	76176.0	220.7969
346.000	76396.8	76396.8	220.7969
347.000	76617.6	76617.6	220.8047
348.000	76838.4	76838.4	220.7969
349.000	77059.2	77059.2	220.8047
350.000	77280.0	77280.0	220.7969
351.000	77500.8	77500.8	220.7969
352.000	77721.6	77721.6	220.8047
353.000	77942.4	77942.4	220.7969

354.000	78163.2	78163.2	220.8047
355.000	78384.0	78384.0	220.7969
356.000	78604.8	78604.8	220.7969
357.000	78825.6	78825.6	220.8047
358.000	79046.4	79046.4	220.7969
359.000	79267.2	79267.2	220.8047
360.000	79488.0	79488.0	220.7969
361.000	79708.8	79708.8	220.8047
362.000	79929.6	79929.6	220.7969
363.000	80150.4	80150.4	220.7969
364.000	80371.2	80371.2	220.8047
365.000	80592.0	80592.0	220.7969
366.000	80812.8	80812.8	220.7969
367.000	81033.6	81033.6	220.8047
368.000	81254.4	81254.4	220.7969
369.000	81475.2	81475.2	220.8047
370.000	81696.0	81696.0	220.7969
371.000	81916.8	81916.8	220.8047
372.000	82137.6	82137.6	220.7969
373.000	82358.4	82358.4	220.7969
374.000	82579.2	82579.2	220.8047
375.000	82800.0	82800.0	220.7969
376.000	83020.8	83020.8	220.7969
377.000	83241.6	83241.6	220.8047
378.000	83462.4	83462.4	220.7969
379.000	83683.2	83683.2	220.7969
380.000	83904.0	83904.0	220.8047
381.000	84124.8	84124.8	220.8047
382.000	84345.6	84345.6	220.7969
383.000	84566.4	84566.4	220.7969
384.000	84787.2	84787.2	220.8047
385.000	85008.0	85008.0	220.7969
386.000	85228.8	85228.8	220.7969
387.000	85449.6	85449.6	220.8047
388.000	85670.4	85670.4	220.7969
389.000	85891.2	85891.2	220.7969
390.000	86112.0	86112.0	220.8047
391.000	86332.8	86332.8	220.8047
392.000	86553.6	86553.6	220.7969
393.000	86774.4	86774.4	220.7969
394.000	86995.2	86995.2	220.8047
395.000	87216.0	87216.0	220.7969
396.000	87436.8	87436.8	220.7969
397.000	87657.6	87657.6	220.8047
398.000	87878.4	87878.4	220.7969
399.000	88099.2	88099.2	220.7969
400.000	88320.0	88320.0	220.8047
401.000	88540.8	88540.8	220.8047

402.000	88761.6	88761.6	220.7969
403.000	88982.4	88982.4	220.7969
404.000	89203.2	89203.2	220.8047
405.000	89424.0	89424.0	220.7969
406.000	89644.8	89644.8	220.7969
407.000	89865.6	89865.6	220.8047
408.000	90086.4	90086.4	220.8047
409.000	90307.2	90307.2	220.7891
410.000	90528.0	90528.0	220.8047
411.000	90748.8	90748.8	220.8047
412.000	90969.6	90969.6	220.7969
413.000	91190.4	91190.4	220.7969
414.000	91411.2	91411.2	220.8047
415.000	91632.0	91632.0	220.7969
416.000	91852.8	91852.8	220.7969
417.000	92073.6	92073.6	220.8047
418.000	92294.4	92294.4	220.8047
419.000	92515.2	92515.2	220.7891
420.000	92736.0	92736.0	220.8047
421.000	92956.8	92956.8	220.8047
422.000	93177.6	93177.6	220.7969
423.000	93398.4	93398.4	220.7969
424.000	93619.2	93619.2	220.8047
425.000	93840.0	93840.0	220.7969
426.000	94060.8	94060.8	220.7969
427.000	94281.6	94281.6	220.8047
428.000	94502.4	94502.4	220.8047
429.000	94723.2	94723.2	220.7891
430.000	94944.0	94944.0	220.8047
431.000	95164.8	95164.8	220.8047
432.000	95385.6	95385.6	220.7969
433.000	95606.4	95606.4	220.7969
434.000	95827.2	95827.2	220.8047
435.000	96048.0	96048.0	220.7969
436.000	96268.8	96268.8	220.7969
437.000	96489.6	96489.6	220.8047
438.000	96710.4	96710.4	220.8047
439.000	96931.2	96931.2	220.7891
440.000	97152.0	97152.0	220.8047
441.000	97372.8	97372.8	220.8047
442.000	97593.6	97593.6	220.7969
443.000	97814.4	97814.4	220.7969
444.000	98035.2	98035.2	220.8047
445.000	98256.0	98256.0	220.7969
446.000	98476.8	98476.8	220.7969
447.000	98697.6	98697.6	220.8047
448.000	98918.4	98918.4	220.8047
449.000	99139.2	99139.2	220.7891

450.000	99360.0	99360.0	220.8047
451.000	99580.8	99580.8	220.7969
452.000	99801.6	99801.6	220.8047
453.000	100022.4	100022.4	220.7969
454.000	100243.2	100243.2	220.7969
455.000	100464.0	100464.0	220.8047
456.000	100684.8	100684.8	220.7969
457.000	100905.6	100905.6	220.7969
458.000	101126.4	101126.4	220.8047
459.000	101347.2	101347.2	220.7969
460.000	101568.0	101568.0	220.8125
461.000	101788.8	101788.8	220.7969
462.000	102009.6	102009.6	220.7891
463.000	102230.4	102230.4	220.8125
464.000	102451.2	102451.2	220.7969
465.000	102672.0	102672.0	220.7969
466.000	102892.8	102892.8	220.8047
467.000	103113.6	103113.6	220.7969
468.000	103334.4	103334.4	220.7969
469.000	103555.2	103555.2	220.8047
470.000	103776.0	103776.0	220.7969
471.000	103996.8	103996.8	220.7969
472.000	104217.6	104217.6	220.8047
473.000	104438.4	104438.4	220.7969
474.000	104659.2	104659.2	220.7969
475.000	104880.0	104880.0	220.8047
476.000	105100.8	105100.8	220.7969
477.000	105321.6	105321.6	220.7969
478.000	105542.4	105542.4	220.8047
479.000	105763.2	105763.2	220.7969
480.000	105984.0	105984.0	220.8125
481.000	106204.8	106204.8	220.7969
482.000	106425.6	106425.6	220.7891
483.000	106646.4	106646.4	220.8125
484.000	106867.2	106867.2	220.7969
485.000	107088.0	107088.0	220.7969
486.000	107308.8	107308.8	220.8047
487.000	107529.6	107529.6	220.7969
488.000	107750.4	107750.4	220.7969
489.000	107971.2	107971.2	220.8047
490.000	108192.0	108192.0	220.7969
491.000	108412.8	108412.8	220.7969
492.000	108633.6	108633.6	220.8047
493.000	108854.4	108854.4	220.7969
494.000	109075.2	109075.2	220.7969
495.000	109296.0	109296.0	220.8047
496.000	109516.8	109516.8	220.7969
497.000	109737.6	109737.6	220.8125

498.000	109958.4	109958.4	220.7891
499.000	110179.2	110179.2	220.7969
500.000	110400.0	110400.0	220.8125
501.000	110620.8	110620.8	220.7969
502.000	110841.6	110841.6	220.7891
503.000	111062.4	111062.4	220.8125
504.000	111283.2	111283.2	220.7969
505.000	111504.0	111504.0	220.7969
506.000	111724.8	111724.8	220.8047
507.000	111945.6	111945.6	220.7969
508.000	112166.4	112166.4	220.7969
509.000	112387.2	112387.2	220.8047
510.000	112608.0	112608.0	220.7969
511.000	112828.8	112828.8	220.7969
512.000	113049.6	113049.6	220.8047
513.000	113270.4	113270.4	220.7969
514.000	113491.2	113491.2	220.7969
515.000	113712.0	113712.0	220.8047
516.000	113932.8	113932.8	220.7969
517.000	114153.6	114153.6	220.8125
518.000	114374.4	114374.4	220.7891
519.000	114595.2	114595.2	220.7969
520.000	114816.0	114816.0	220.8125
521.000	115036.8	115036.8	220.7969
522.000	115257.6	115257.6	220.7891
523.000	115478.4	115478.4	220.8125
524.000	115699.2	115699.2	220.7969
525.000	115920.0	115920.0	220.7891
526.000	116140.8	116140.8	220.8125
527.000	116361.6	116361.6	220.7969
528.000	116582.4	116582.4	220.7969
529.000	116803.2	116803.2	220.8047
530.000	117024.0	117024.0	220.7969
531.000	117244.8	117244.8	220.7969
532.000	117465.6	117465.6	220.8047
533.000	117686.4	117686.4	220.7969
534.000	117907.2	117907.2	220.7969
535.000	118128.0	118128.0	220.8047
536.000	118348.8	118348.8	220.7969
537.000	118569.6	118569.6	220.8047
538.000	118790.4	118790.4	220.7969
539.000	119011.2	119011.2	220.7969
540.000	119232.0	119232.0	220.8125
541.000	119452.8	119452.8	220.7891
542.000	119673.6	119673.6	220.7969
543.000	119894.4	119894.4	220.8125
544.000	120115.2	120115.2	220.7969
545.000	120336.0	120336.0	220.7891

546.000	120556.8	120556.8	220.8125
547.000	120777.6	120777.6	220.7969
548.000	120998.4	120998.4	220.7969
549.000	121219.2	121219.2	220.8047
550.000	121440.0	121440.0	220.7969
551.000	121660.8	121660.8	220.7969
552.000	121881.6	121881.6	220.8047
553.000	122102.4	122102.4	220.7969
554.000	122323.2	122323.2	220.8047
555.000	122544.0	122544.0	220.7969
556.000	122764.8	122764.8	220.7969
557.000	122985.6	122985.6	220.8047
558.000	123206.4	123206.4	220.7969
559.000	123427.2	123427.2	220.7969
560.000	123648.0	123648.0	220.8125
561.000	123868.8	123868.8	220.7891
562.000	124089.6	124089.6	220.7969
563.000	124310.4	124310.4	220.8125
564.000	124531.2	124531.2	220.7969
565.000	124752.0	124752.0	220.7891
566.000	124972.8	124972.8	220.8125
567.000	125193.6	125193.6	220.7969
568.000	125414.4	125414.4	220.7969
569.000	125635.2	125635.2	220.8047
570.000	125856.0	125856.0	220.7969
571.000	126076.8	126076.8	220.7969
572.000	126297.6	126297.6	220.8047
573.000	126518.4	126518.4	220.7969
574.000	126739.2	126739.2	220.8047
575.000	126960.0	126960.0	220.7969
576.000	127180.8	127180.8	220.7969
577.000	127401.6	127401.6	220.8047
578.000	127622.4	127622.4	220.7969
579.000	127843.2	127843.2	220.7969
580.000	128064.0	128064.0	220.8125
581.000	128284.8	128284.8	220.7891
582.000	128505.6	128505.6	220.7969
583.000	128726.4	128726.4	220.8125
584.000	128947.2	128947.2	220.7969
585.000	129168.0	129168.0	220.7891
586.000	129388.8	129388.8	220.8125
587.000	129609.6	129609.6	220.7969
588.000	129830.4	129830.4	220.7969
589.000	130051.2	130051.2	220.8047
590.000	130272.0	130272.0	220.7969
591.000	130492.8	130492.8	220.8047
592.000	130713.6	130713.6	220.7969
593.000	130934.4	130934.4	220.7969

594.000	131155.2	131155.2	220.8047
595.000	131376.0	131376.0	220.7969
596.000	131596.8	131596.8	220.7969
597.000	131817.6	131817.6	220.8125
598.000	132038.4	132038.4	220.7969
599.000	132259.2	132259.2	220.7969
600.000	132480.0	132480.0	220.7969
601.000	132700.8	132700.8	220.7969
602.000	132921.6	132921.6	220.7969
603.000	133142.4	133142.4	220.8125
604.000	133363.2	133363.2	220.7969
605.000	133584.0	133584.0	220.7969
606.000	133804.8	133804.8	220.7969
607.000	134025.6	134025.6	220.7969
608.000	134246.4	134246.4	220.7969
609.000	134467.2	134467.2	220.8125
610.000	134688.0	134688.0	220.7969
611.000	134908.8	134908.8	220.8125
612.000	135129.6	135129.6	220.7813
613.000	135350.4	135350.4	220.7969
614.000	135571.2	135571.2	220.8125
615.000	135792.0	135792.0	220.7969
616.000	136012.8	136012.8	220.7969
617.000	136233.6	136233.6	220.8125
618.000	136454.4	136454.4	220.7969
619.000	136675.2	136675.2	220.7969
620.000	136896.0	136896.0	220.7969
621.000	137116.8	137116.8	220.7969
622.000	137337.6	137337.6	220.7969
623.000	137558.4	137558.4	220.8125
624.000	137779.2	137779.2	220.7969
625.000	138000.0	138000.0	220.7969
626.000	138220.8	138220.8	220.7969
627.000	138441.6	138441.6	220.7969
628.000	138662.4	138662.4	220.7969
629.000	138883.2	138883.2	220.8125
630.000	139104.0	139104.0	220.7969
631.000	139324.8	139324.8	220.8125
632.000	139545.6	139545.6	220.7813
633.000	139766.4	139766.4	220.7969
634.000	139987.2	139987.2	220.8125
635.000	140208.0	140208.0	220.7969
636.000	140428.8	140428.8	220.7969
637.000	140649.6	140649.6	220.8125
638.000	140870.4	140870.4	220.7969
639.000	141091.2	141091.2	220.7969
640.000	141312.0	141312.0	220.7969
641.000	141532.8	141532.8	220.7969

642.000	141753.6	141753.6	220.7969
643.000	141974.4	141974.4	220.8125
644.000	142195.2	142195.2	220.7969
645.000	142416.0	142416.0	220.7969
646.000	142636.8	142636.8	220.7969
647.000	142857.6	142857.6	220.7969
648.000	143078.4	143078.4	220.8125
649.000	143299.2	143299.2	220.7969
650.000	143520.0	143520.0	220.7969
651.000	143740.8	143740.8	220.8125
652.000	143961.6	143961.6	220.7813
653.000	144182.4	144182.4	220.7969
654.000	144403.2	144403.2	220.8125
655.000	144624.0	144624.0	220.7969
656.000	144844.8	144844.8	220.7969
657.000	145065.6	145065.6	220.8125
658.000	145286.4	145286.4	220.7969
659.000	145507.2	145507.2	220.7969
660.000	145728.0	145728.0	220.7969
661.000	145948.8	145948.8	220.7969
662.000	146169.6	146169.6	220.7969
663.000	146390.4	146390.4	220.8125
664.000	146611.2	146611.2	220.7969
665.000	146832.0	146832.0	220.7969
666.000	147052.8	147052.8	220.7969
667.000	147273.6	147273.6	220.7969
668.000	147494.4	147494.4	220.8125
669.000	147715.2	147715.2	220.7969
670.000	147936.0	147936.0	220.7969
671.000	148156.8	148156.8	220.8125
672.000	148377.6	148377.6	220.7813
673.000	148598.4	148598.4	220.7969
674.000	148819.2	148819.2	220.8125
675.000	149040.0	149040.0	220.7969
676.000	149260.8	149260.8	220.7969
677.000	149481.6	149481.6	220.8125
678.000	149702.4	149702.4	220.7969
679.000	149923.2	149923.2	220.7813
680.000	150144.0	150144.0	220.8125
681.000	150364.8	150364.8	220.7969
682.000	150585.6	150585.6	220.7969
683.000	150806.4	150806.4	220.8125
684.000	151027.2	151027.2	220.7969
685.000	151248.0	151248.0	220.7969
686.000	151468.8	151468.8	220.7969
687.000	151689.6	151689.6	220.7969
688.000	151910.4	151910.4	220.8125
689.000	152131.2	152131.2	220.7969

690.000	152352.0	152352.0	220.7969
691.000	152572.8	152572.8	220.7969
692.000	152793.6	152793.6	220.7969
693.000	153014.4	153014.4	220.7969
694.000	153235.2	153235.2	220.8125
695.000	153456.0	153456.0	220.7969
696.000	153676.8	153676.8	220.7969
697.000	153897.6	153897.6	220.8125
698.000	154118.4	154118.4	220.7969
699.000	154339.2	154339.2	220.7813
700.000	154560.0	154560.0	220.8125
701.000	154780.8	154780.8	220.7969
702.000	155001.6	155001.6	220.7969
703.000	155222.4	155222.4	220.8125
704.000	155443.2	155443.2	220.7969
705.000	155664.0	155664.0	220.7969
706.000	155884.8	155884.8	220.7969
707.000	156105.6	156105.6	220.7969
708.000	156326.4	156326.4	220.8125
709.000	156547.2	156547.2	220.7969
710.000	156768.0	156768.0	220.7969
711.000	156988.8	156988.8	220.7969
712.000	157209.6	157209.6	220.7969
713.000	157430.4	157430.4	220.7969
714.000	157651.2	157651.2	220.8125
715.000	157872.0	157872.0	220.7969
716.000	158092.8	158092.8	220.7969
717.000	158313.6	158313.6	220.8125
718.000	158534.4	158534.4	220.7969
719.000	158755.2	158755.2	220.7813
720.000	158976.0	158976.0	220.8125
721.000	159196.8	159196.8	220.7969
722.000	159417.6	159417.6	220.8125
723.000	159638.4	159638.4	220.7969
724.000	159859.2	159859.2	220.7969
725.000	160080.0	160080.0	220.7969
726.000	160300.8	160300.8	220.7969
727.000	160521.6	160521.6	220.7969
728.000	160742.4	160742.4	220.8125
729.000	160963.2	160963.2	220.7969
730.000	161184.0	161184.0	220.7969
731.000	161404.8	161404.8	220.7969
732.000	161625.6	161625.6	220.7969
733.000	161846.4	161846.4	220.7969
734.000	162067.2	162067.2	220.8125
735.000	162288.0	162288.0	220.7969
736.000	162508.8	162508.8	220.7969
737.000	162729.6	162729.6	220.8125

738.000	162950.4	162950.4	220.7969
739.000	163171.2	163171.2	220.7813
740.000	163392.0	163392.0	220.8125
741.000	163612.8	163612.8	220.7969
742.000	163833.6	163833.6	220.8125
743.000	164054.4	164054.4	220.7969
744.000	164275.2	164275.2	220.7969
745.000	164496.0	164496.0	220.7969
746.000	164716.8	164716.8	220.7969
747.000	164937.6	164937.6	220.7969
748.000	165158.4	165158.4	220.8125
749.000	165379.2	165379.2	220.7969
750.000	165600.0	165600.0	220.7969
751.000	165820.8	165820.8	220.7969
752.000	166041.6	166041.6	220.7969
753.000	166262.4	166262.4	220.7969
754.000	166483.2	166483.2	220.8125
755.000	166704.0	166704.0	220.7969
756.000	166924.8	166924.8	220.7969
757.000	167145.6	167145.6	220.8125
758.000	167366.4	167366.4	220.7813
759.000	167587.2	167587.2	220.7969
760.000	167808.0	167808.0	220.8125
761.000	168028.8	168028.8	220.7969
762.000	168249.6	168249.6	220.8125
763.000	168470.4	168470.4	220.7969
764.000	168691.2	168691.2	220.7969
765.000	168912.0	168912.0	220.7969
766.000	169132.8	169132.8	220.7969
767.000	169353.6	169353.6	220.7969
768.000	169574.4	169574.4	220.8125
769.000	169795.2	169795.2	220.7969
770.000	170016.0	170016.0	220.7969
771.000	170236.8	170236.8	220.7969
772.000	170457.6	170457.6	220.7969
773.000	170678.4	170678.4	220.7969
774.000	170899.2	170899.2	220.8125
775.000	171120.0	171120.0	220.7969
776.000	171340.8	171340.8	220.7969
777.000	171561.6	171561.6	220.8125
778.000	171782.4	171782.4	220.7813
779.000	172003.2	172003.2	220.8125
780.000	172224.0	172224.0	220.7969
781.000	172444.8	172444.8	220.7969
782.000	172665.6	172665.6	220.8125
783.000	172886.4	172886.4	220.7969
784.000	173107.2	173107.2	220.7969
785.000	173328.0	173328.0	220.7969

786.000	173548.8	173548.8	220.7969
787.000	173769.6	173769.6	220.7969
788.000	173990.4	173990.4	220.8125
789.000	174211.2	174211.2	220.7969
790.000	174432.0	174432.0	220.7969
791.000	174652.8	174652.8	220.7969
792.000	174873.6	174873.6	220.7969
793.000	175094.4	175094.4	220.7969
794.000	175315.2	175315.2	220.8125
795.000	175536.0	175536.0	220.7969
796.000	175756.8	175756.8	220.7969
797.000	175977.6	175977.6	220.8125
798.000	176198.4	176198.4	220.7813
799.000	176419.2	176419.2	220.8125
800.000	176640.0	176640.0	220.7969
801.000	176860.8	176860.8	220.7969
802.000	177081.6	177081.6	220.8125
803.000	177302.4	177302.4	220.7969
804.000	177523.2	177523.2	220.7969
805.000	177744.0	177744.0	220.7969
806.000	177964.8	177964.8	220.7969
807.000	178185.6	178185.6	220.7969
808.000	178406.4	178406.4	220.8125
809.000	178627.2	178627.2	220.7969
810.000	178848.0	178848.0	220.7969
811.000	179068.8	179068.8	220.7969
812.000	179289.6	179289.6	220.7969
813.000	179510.4	179510.4	220.7969
814.000	179731.2	179731.2	220.8125
815.000	179952.0	179952.0	220.7969
816.000	180172.8	180172.8	220.8125
817.000	180393.6	180393.6	220.7969
818.000	180614.4	180614.4	220.7813
819.000	180835.2	180835.2	220.8125
820.000	181056.0	181056.0	220.7969
821.000	181276.8	181276.8	220.7969
822.000	181497.6	181497.6	220.8125
823.000	181718.4	181718.4	220.7969
824.000	181939.2	181939.2	220.7969
825.000	182160.0	182160.0	220.7969
826.000	182380.8	182380.8	220.7969
827.000	182601.6	182601.6	220.7969
828.000	182822.4	182822.4	220.8125
829.000	183043.2	183043.2	220.7969
830.000	183264.0	183264.0	220.7969
831.000	183484.8	183484.8	220.7969
832.000	183705.6	183705.6	220.7969
833.000	183926.4	183926.4	220.7969

834.000	184147.2	184147.2	220.8125
835.000	184368.0	184368.0	220.7969
836.000	184588.8	184588.8	220.8125
837.000	184809.6	184809.6	220.7813
838.000	185030.4	185030.4	220.7969
839.000	185251.2	185251.2	220.8125
840.000	185472.0	185472.0	220.7969
841.000	185692.8	185692.8	220.7969
842.000	185913.6	185913.6	220.8125
843.000	186134.4	186134.4	220.7969
844.000	186355.2	186355.2	220.7969
845.000	186576.0	186576.0	220.7969
846.000	186796.8	186796.8	220.7969
847.000	187017.6	187017.6	220.7969
848.000	187238.4	187238.4	220.8125
849.000	187459.2	187459.2	220.7969
850.000	187680.0	187680.0	220.7969
851.000	187900.8	187900.8	220.7969
852.000	188121.6	188121.6	220.7969
853.000	188342.4	188342.4	220.7969
854.000	188563.2	188563.2	220.8125
855.000	188784.0	188784.0	220.7969
856.000	189004.8	189004.8	220.8125
857.000	189225.6	189225.6	220.7813
858.000	189446.4	189446.4	220.7969
859.000	189667.2	189667.2	220.8125
860.000	189888.0	189888.0	220.7969
861.000	190108.8	190108.8	220.7969
862.000	190329.6	190329.6	220.8125
863.000	190550.4	190550.4	220.7969
864.000	190771.2	190771.2	220.7969
865.000	190992.0	190992.0	220.7969
866.000	191212.8	191212.8	220.7969
867.000	191433.6	191433.6	220.7969
868.000	191654.4	191654.4	220.8125
869.000	191875.2	191875.2	220.7969
870.000	192096.0	192096.0	220.7969
871.000	192316.8	192316.8	220.7969
872.000	192537.6	192537.6	220.7969
873.000	192758.4	192758.4	220.8125
874.000	192979.2	192979.2	220.7969
875.000	193200.0	193200.0	220.7969
876.000	193420.8	193420.8	220.8125
877.000	193641.6	193641.6	220.7813
878.000	193862.4	193862.4	220.7969
879.000	194083.2	194083.2	220.8125
880.000	194304.0	194304.0	220.7969
881.000	194524.8	194524.8	220.7969

882.000	194745.6	194745.6	220.8125
883.000	194966.4	194966.4	220.7969
884.000	195187.2	195187.2	220.7969
885.000	195408.0	195408.0	220.7969
886.000	195628.8	195628.8	220.7969
887.000	195849.6	195849.6	220.7969
888.000	196070.4	196070.4	220.8125
889.000	196291.2	196291.2	220.7969
890.000	196512.0	196512.0	220.7969
891.000	196732.8	196732.8	220.7969
892.000	196953.6	196953.6	220.7969
893.000	197174.4	197174.4	220.8125
894.000	197395.2	197395.2	220.7969
895.000	197616.0	197616.0	220.7969
896.000	197836.8	197836.8	220.8125
897.000	198057.6	198057.6	220.7813
898.000	198278.4	198278.4	220.7969
899.000	198499.2	198499.2	220.8125
900.000	198720.0	198720.0	220.7969

SUBCLOUD TRAJECTORY

DOWNWIND		CENTROID	GAUSSIAN CLOUD			PEAK CLOUD	MEAN CLOUD	AIR	AIR	CENTROID OR CM VELOCITY		CM	EFFECTIVE BUOYANCY
DISTANCE	TIME	HEIGHT	STD. DEVIATIONS (M)			TEMP.	TEMP.	TEMP.	DENSITY	VERT.	HOR.	HEIGHT	RADIUS
(M)	(SEC)	(M)	SIGMAX	SIGMAY	SIGMAZ	(DEG K)	(DEG K)	(DEG K)	(G/M**3)	(M/S)	(M/S)	(M)	(M)
1.00	.58	.00	1.26	1.41	.69	301.82	301.82	301.82	1107.32	.19	1.71	.6	.000
2.84	1.62	.00	1.26	1.70	.93	301.77	301.77	301.71	1107.71	.18	1.78	.7	.000
5.24	2.86	.00	1.26	2.07	1.22	301.67	301.67	301.56	1108.24	.18	1.94	1.0	.000
8.09	4.19	.00	1.26	2.49	1.53	301.55	301.55	301.43	1108.70	.19	2.13	1.2	.000
11.33	5.58	.00	1.26	2.97	1.88	301.43	301.43	301.32	1109.09	.20	2.35	1.5	.000
14.92	6.97	.00	1.26	3.49	2.24	301.33	301.33	301.22	1109.40	.21	2.56	1.8	.000
18.82	8.38	.00	1.26	4.04	2.62	301.23	301.23	301.14	1109.67	.22	2.77	2.1	.000
23.02	9.80	.00	1.26	4.62	3.02	301.15	301.15	301.07	1109.89	.22	2.97	2.4	.000
27.50	11.21	.00	1.26	5.24	3.42	301.08	301.08	301.01	1110.08	.23	3.15	2.7	.000
32.24	12.64	.00	1.26	5.88	3.84	301.02	301.02	300.95	1110.24	.23	3.32	3.1	.000
37.22	14.07	.00	1.26	6.54	4.27	300.96	300.96	300.90	1110.38	.24	3.48	3.4	.000
42.44	15.52	.00	1.26	7.23	4.70	300.91	300.91	300.86	1110.50	.24	3.62	3.8	.000
47.89	16.97	.00	1.26	7.95	5.15	300.86	300.86	300.82	1110.61	.24	3.75	4.1	.000
53.78	18.49	.00	1.26	8.71	5.62	300.82	300.82	300.78	1110.70	.25	3.87	4.5	.000
60.39	20.16	.00	1.26	9.56	6.14	300.78	300.78	300.74	1110.79	.25	3.97	4.9	.000
67.82	21.98	.00	1.26	10.50	6.71	300.75	300.75	300.71	1110.87	.25	4.08	5.4	.000
76.17	23.98	.00	1.26	11.55	7.33	300.71	300.71	300.67	1110.94	.25	4.18	5.8	.000

85.54	26.17	.00	1.26	12.71	8.02	300.67	300.67	300.64	1111.01	.25	4.27	6.4	.000
96.06	28.58	.00	1.26	14.00	8.77	300.64	300.64	300.60	1111.07	.25	4.36	7.0	.000
107.88	31.24	.00	1.26	15.44	9.60	300.60	300.60	300.57	1111.13	.25	4.46	7.7	.000
121.15	34.16	.00	1.26	17.03	10.51	300.57	300.57	300.53	1111.18	.25	4.54	8.4	.000
136.06	37.37	.00	1.26	18.81	11.51	300.53	300.53	300.49	1111.22	.25	4.63	9.2	.000
152.80	40.92	.00	1.26	20.77	12.60	300.49	300.49	300.46	1111.25	.25	4.72	10.1	.000
171.60	44.83	.00	1.26	22.96	13.81	300.46	300.46	300.42	1111.27	.25	4.81	11.0	.000
192.71	49.15	.00	1.26	25.39	15.13	300.42	300.42	300.39	1111.28	.24	4.89	12.1	.000
216.42	53.92	.00	1.26	28.08	16.58	300.39	300.39	300.35	1111.28	.24	4.97	13.2	.000
243.04	59.18	.00	1.26	31.08	18.18	300.35	300.35	300.31	1111.27	.24	5.06	14.5	.000
272.94	65.00	.00	1.26	34.40	19.93	300.31	300.31	300.28	1111.25	.24	5.14	15.9	.000
306.52	71.44	.00	1.26	38.09	21.85	300.28	300.28	300.24	1111.21	.24	5.22	17.4	.000
344.23	78.56	.00	1.26	42.19	23.96	300.24	300.24	300.20	1111.16	.24	5.30	19.1	.000
386.58	86.44	.00	1.26	46.74	26.27	300.20	300.20	300.16	1111.09	.23	5.38	21.0	.000
434.14	95.16	.00	1.26	51.80	28.81	300.16	300.16	300.12	1111.00	.23	5.45	23.0	.000
487.55	104.82	.00	1.26	57.41	31.60	300.12	300.12	300.08	1110.89	.23	5.53	25.2	.000
547.53	115.53	.00	1.26	63.64	34.66	300.08	300.08	300.04	1110.77	.23	5.60	27.7	.000
614.89	127.40	.00	1.26	70.55	38.02	300.04	300.04	300.00	1110.62	.23	5.68	30.3	.000
690.54	140.56	.00	1.26	78.23	41.71	300.00	300.00	299.95	1110.45	.22	5.75	33.3	.000
775.49	155.16	.00	1.26	86.76	45.76	299.95	299.95	299.91	1110.25	.22	5.82	36.5	.000
870.90	171.36	.00	1.26	96.22	50.21	299.90	299.90	299.86	1110.02	.22	5.89	40.1	.000
978.04	189.35	.00	1.26	106.73	55.08	299.86	299.86	299.81	1109.76	.22	5.96	44.0	.000
1098.37	209.33	.00	1.26	118.39	60.44	299.80	299.80	299.75	1109.47	.21	6.02	48.2	.000
1233.50	231.52	.00	1.26	131.34	66.32	299.75	299.75	299.69	1109.14	.21	6.09	52.9	.000
1385.25	256.18	.00	1.26	145.71	72.77	299.69	299.69	299.63	1108.77	.21	6.15	58.1	.000
1555.67	283.60	.00	1.26	161.67	79.85	299.63	299.63	299.57	1108.36	.21	6.22	63.7	.000
1747.06	314.08	.00	1.26	179.38	87.62	299.57	299.57	299.50	1107.90	.20	6.28	69.9	.000
1962.00	347.99	.00	1.26	199.05	96.15	299.50	299.50	299.43	1107.39	.20	6.34	76.7	.000
2203.37	385.71	.00	1.26	220.88	105.51	299.42	299.42	299.35	1106.82	.20	6.40	84.2	.000
2474.45	427.69	.00	1.26	245.12	115.78	299.34	299.34	299.26	1106.20	.20	6.46	92.4	.000
2778.87	474.43	.00	1.26	272.02	127.06	299.26	299.26	299.17	1105.50	.19	6.51	101.4	.000
3120.74	526.46	.00	1.26	301.89	139.44	299.16	299.16	299.07	1104.73	.19	6.57	111.3	.000
3504.68	584.42	.00	1.26	335.04	153.02	299.06	299.06	298.96	1103.88	.19	6.62	122.1	.000
3935.85	648.99	.00	1.26	371.85	167.93	298.96	298.96	298.85	1102.94	.18	6.68	134.0	.000
4420.06	720.93	.00	1.26	412.70	184.30	298.84	298.84	298.72	1101.91	.18	6.73	147.0	.000
4963.84	801.12	.00	1.26	458.06	202.26	298.71	298.71	298.59	1100.77	.18	6.78	161.4	.000
5574.53	890.51	.00	1.26	508.41	221.97	298.57	298.57	298.44	1099.51	.18	6.83	177.1	.000
6260.34	990.19	.00	1.26	564.30	243.60	298.42	298.42	298.27	1098.13	.17	6.88	194.4	.000
7030.53	1101.35	.00	1.26	626.34	267.35	298.26	298.26	298.10	1096.61	.17	6.93	213.3	.000
7895.47	1225.35	.00	1.26	695.21	293.41	298.08	298.08	297.90	1094.94	.17	6.98	234.1	.000
8866.82	1363.69	.00	1.26	771.67	322.01	297.89	297.89	297.69	1093.11	.16	7.02	256.9	.000
9957.67	1518.07	.00	1.26	856.54	353.40	297.67	297.67	297.46	1091.09	.16	7.07	282.0	.000
11182.73	1690.37	.00	1.26	950.75	387.86	297.44	297.44	297.21	1088.88	.16	7.11	309.5	.000

TOTAL TRANMITANCE FOR ALL SOURCES IS: .0000E+00

```
WAVL      1.06
 NOTE: THAT THE ABOVE CARD WAS MODIFIED FOR CONSISTENCY TO:
WAVL       .1060E+01 .1060E+01 .0000E+00
```

	BEGINNING	ENDING
WAVENUMBER (CM**-1)	9433.963	9433.963
WAVELENGTH (MICROMETERS)	1.060	1.060
FREQUENCY (GHZ)	283018.875	283018.875

```
         **** EOSAEL WARNING ****
 VISIBILITY AND EXTINCTION = 0.0, VISIBILITY CHANGED TO 10.0 KM
```

VISIBILITY
10.00 KM

RUN NUMBER 2

```
1
```

****

```
                    *             *
                    *   COMBIC    *
                    *   PHASE 2   *
                    *             *
                    *****************
```

COMBIC CLOUD HISTORY ON UNIT 9 OPENED TO: h.vehc-hc
1

METEOROLOGICAL CONDITIONS FROM HISTORY FILE

WINDSPEED (10 M) =	5.0 M/S	WIND DIRECTION =	202.4 DEG WRT N
RELATIVE HUMIDITY =	90.0 PERCENT	PASQUILL CATEGORY =	C (2.60)
AIR TEMPERATURE =	300.6 DEG K	AIR PRESSURE =	963. MB
SURFACE ROUGHNESS =	.1000 M	AIR DENSITY =	1110. G/M**3

MASS EXTINCTION COEFFICIENTS FROM HISTORY FILE (M**2/GRAM)

OBSCURANT	WAVELENGTH (MICROMETERS)						
CODE	.4-.7	.7-1.2	1.06	3.-5.	8.-12.	10.6	94 GHZ
1	3.2280	2.3638	2.1094	.4127	.3043	.2792	.0010
2	3.2280	2.3638	2.1094	.4127	.3043	.2792	.0010
3	2.1520	2.1368	2.0302	.2668	.0601	.0750	.0010
4	6.8510	4.5920	3.4970	.2450	.0200	.0180	.0010
5	3.2280	2.3638	2.1094	.4127	.3043	.2792	.0010
6	1.8600	1.6300	1.4000	1.7900	1.6800	1.6800	.0010
7	1.8600	1.6300	1.4000	1.7900	1.6800	1.6800	.0010
8	5.6500	4.0800	3.2500	.2450	.0230	.0270	.0010
9	.3200	.3000	.2900	.2700	.2500	.2500	.0010
10	.3200	.2900	.2600	.2700	.2600	.2400	.0010
11	.0350	.0360	.0370	.0350	.0380	.0360	.0010
12	1.5000	1.4600	1.4200	.7500	.3200	.3000	.0010
13	.0010	.0010	.0010	.0010	.0010	.0010	.0004
14	6.1000	3.7500	2.9400	1.3500	1.0100	1.0000	.0020
15	6.8510	4.5920	1.4300	.0540	.0200	.0180	.0010
16	5.3700	2.9000	2.1000	.0900	.0900	.0700	.0010
17	6.2000	3.5000	2.5000	.2300	.0500	.0480	.0010
18	3.3300	2.7500	2.6600	.2600	.3200	.2300	.0010
19	1.3000	1.7400	1.7000	.0800	.1600	.3800	.0010
20	2.0000	2.0000	2.0000	1.6000	2.0000	.0000	.0000
21	2.0000	2.0000	1.0000	.1000	.4000	.0000	.0000

22	.0000	.0000	.0000	.0000	.0000	.0000	.0000
23	.0000	.0000	.0000	.0000	.0000	.0000	.0000
24	.0000	.0000	.0000	.0000	.0000	.0000	.0000
25	.0000	.0000	.0000	.0000	.0000	.0000	.0000
26	.0000	.0000	.0000	.0000	.0000	.0000	.0000
27	.0000	.0000	.0000	.0000	.0000	.0000	.0000
28	.0000	.0000	.0000	.0000	.0000	.0000	.0000
29	.0000	.0000	.0000	.0000	.0000	.0000	.0000
30	.0000	.0000	.0000	.0000	.0000	.0000	.0000

1

HISTORY FILE CONTAINS INFORMATION ON 2 SOURCES

SOURCE ID	NUMBER OF SUBCLOUDS	XN SCALE FACTOR	FILL WEIGHT	MENU NUMBER	OBSC TYPE	EFFICIENCY PERCENT	YIELD FACTOR	NUMBER OF SUB-MUNITIONS
1	1	1.00	5.40	1.	3.	70.00	5.72	1.00
2	1	1.00	438.10	0.	9.	100.00	1.00	1.00

SOURCE ID	BURN DURATION (SEC)	VEHICLE SPEED (M/S)	VEHICLE DIRECTION DEG	BARRAGE ROUNDS PER SEC	BARRAGE DURATION (SEC)	BARRAGE IMPACT X (M)	BARRAGE REGION Y (M)	HIGH-EXP SOIL TYPE	HIGH-EXP DOB (M)
1	100.	.0	0.	.0	0.	0.	0.	.0	.00
2	900.	4.0	90.	.0	0.	0.	0.	.0	.00

WIND DIRECTION ALTERED TO 155.0 DEG WRT N

3.13.1

SOURCES ADDED

SOURCE UNIT	ID	XN SCALING	ACTIVE TIME LIMIT BEGIN	END	POSITION (ORIGINAL SYSTEM) X	Y	Z	POSITION (ROTATED SYSTEM) X	Y	Z	MOVING SOURCE SPEED	DIRECTION
1	1	4.000	20.00	300.00	90.0	80.0	.0	116.7	-29.9	.0	.00	-359.8

2.72.7

2	2	1.000	20.00	300.00	50.0	218.0	.0	172.4	-142.4	.0	7.60	82.0

NEW OR ALTERED LINES OF SIGHT

		ORIGINAL SYSTEM						ROTATED SYSTEM							
OBS	TGT	OBSERVER (M)			TARGET (M)			OBSERVER (M)			TARGET (M)			TIME (SEC)	
NO.	NO.	X	Y	Z	X	Y	Z	X	Y	Z	X	Y	Z	START	END
1	1	50.0	130.0	3.0	250.0	150.0	15.0	135.7	31.2	3.0	264.2	-123.4	15.0	20.0	100.0
1	2	50.0	130.0	3.0	220.0	100.0	3.0	135.7	31.2	3.0	205.9	-126.5	3.0	20.0	100.0

1

TIME (SEC)	OBS NO.	TARG NO.	TOTAL NUMBER CL (G/M**2)	OF CLOUDS	TRANSMISSION .4-.7	.7-1.2	1.06	3.-5.	8.-12.	10.6	94 GHZ
I, NCHAR, TYP,TVAL,RMMDOT,ROMX,ROMT =	1	1	L		10.00	47.38	32.77	9.46			
I, NCHAR, TYP,TVAL,RMMDOT,ROMX,ROMT =	2	1	L		10.00	11.97	36.59	10.38			
I, NCHAR, TYP,TVAL,RMMDOT,ROMX,ROMT =	3	1	L		10.00	29.68	34.68	9.92			
I,ROMFX1, ROMFX2, ROMFX3 =	1	.000	.004	.002							
CLCON,CLCONN=	.002	.000									
30.0	1	2	.002	1	.996	.996	.996	1.000	1.000	1.000	1.000
I, NCHAR, TYP,TVAL,RMMDOT,ROMX,ROMT =	1	3	M		15.00	54.17	41.87	11.60			
I, NCHAR, TYP,TVAL,RMMDOT,ROMX,ROMT =	2	1	L		15.00	12.72	58.66	15.36			
I, NCHAR, TYP,TVAL,RMMDOT,ROMX,ROMT =	3	1	M		15.00	52.96	49.74	13.38			
I,ROMFX1, ROMFX2, ROMFX3 =	1	.000	.093	.045							
CLCON,CLCONN=	.045	.000									
35.0	1	1	.045	1	.907	.908	.912	.988	.997	.997	1.000
I, NCHAR, TYP,TVAL,RMMDOT,ROMX,ROMT =	1	5	M		15.00	55.72	33.73	9.69			
I, NCHAR, TYP,TVAL,RMMDOT,ROMX,ROMT =	2	1	L		15.00	12.72	58.66	15.36			
I, NCHAR, TYP,TVAL,RMMDOT,ROMX,ROMT =	3	2	M		15.00	53.52	45.27	12.37			
I,ROMFX1, ROMFX2, ROMFX3 =	1	.004	.027	1.460							
I, NCHAR, TYP,TVAL,RMMDOT,ROMX,ROMT =	4	3	M		15.00	54.17	39.36	11.02			
I, NCHAR, TYP,TVAL,RMMDOT,ROMX,ROMT =	5	1	M		15.00	52.96	51.59	13.79			
I,K,ROMFXK=	2	4	.351								
I,K,ROMFXK=	2	5	.784								
I, NCHAR, TYP,TVAL,RMMDOT,ROMX,ROMT =	6	4	M		15.00	54.90	36.49	10.35			
I, NCHAR, TYP,TVAL,RMMDOT,ROMX,ROMT =	7	3	M		15.00	54.17	42.25	11.69			
I, NCHAR, TYP,TVAL,RMMDOT,ROMX,ROMT =	8	1	M		15.00	52.96	48.32	13.07			
I, NCHAR, TYP,TVAL,RMMDOT,ROMX,ROMT =	9	1	L		15.00	43.81	54.99	14.55			
I,K,ROMFXK=	3	6	.064								
I,K,ROMFXK=	3	7	.980								
I,K,ROMFXK=	3	8	1.307								
I,K,ROMFXK=	3	9	.269								
CLCON,CLCONN=	.657	.000									
35.0	1	2	.657	1	.243	.246	.263	.839	.961	.952	.999
I, NCHAR, TYP,TVAL,RMMDOT,ROMX,ROMT =	1	8	M		20.00	58.63	43.00	11.86			
I, NCHAR, TYP,TVAL,RMMDOT,ROMX,ROMT =	2	1	L		20.00	12.76	81.89	20.36			
I, NCHAR, TYP,TVAL,RMMDOT,ROMX,ROMT =	3	4	M		20.00	54.90	59.45	15.53			

```
I,ROMFX1, ROMFX2, ROMFX3 =   1   .004   .180   .791
I, NCHAR, TYP,TVAL,RMMDOT,ROMX,ROMT =  4 6 M      20.00   56.61   50.71   13.60
I, NCHAR, TYP,TVAL,RMMDOT,ROMX,ROMT =  5 2 M      20.00   53.52   69.77   17.77
I,K,ROMFXK=   2  4   .127
I,K,ROMFXK=   2  5  1.342
I, NCHAR, TYP,TVAL,RMMDOT,ROMX,ROMT =  6 7 M      20.00   57.58   46.75   12.71
I, NCHAR, TYP,TVAL,RMMDOT,ROMX,ROMT =  7 5 M      20.00   55.72   54.89   14.53
I, NCHAR, TYP,TVAL,RMMDOT,ROMX,ROMT =  8 3 M      20.00   54.17   64.44   16.62
I, NCHAR, TYP,TVAL,RMMDOT,ROMX,ROMT =  9 0 M      20.00     .00   75.52   19.00
I,K,ROMFXK=   3  6   .029
I,K,ROMFXK=   3  7   .372
I,K,ROMFXK=   3  8  1.203
I,K,ROMFXK=   3  9   .000
I, NCHAR, TYP,TVAL,RMMDOT,ROMX,ROMT = 10 7 M      20.00   57.58   44.88   12.29
I, NCHAR, TYP,TVAL,RMMDOT,ROMX,ROMT = 11 6 M      20.00   56.61   48.69   13.15
I, NCHAR, TYP,TVAL,RMMDOT,ROMX,ROMT = 12 5 M      20.00   55.72   52.74   14.05
I, NCHAR, TYP,TVAL,RMMDOT,ROMX,ROMT = 13 4 M      20.00   54.90   57.17   15.03
I, NCHAR, TYP,TVAL,RMMDOT,ROMX,ROMT = 14 3 M      20.00   54.17   61.89   16.06
I, NCHAR, TYP,TVAL,RMMDOT,ROMX,ROMT = 15 2 M      20.00   53.52   67.00   17.17
I, NCHAR, TYP,TVAL,RMMDOT,ROMX,ROMT = 16 1 M      20.00   52.96   72.64   18.39
I, NCHAR, TYP,TVAL,RMMDOT,ROMX,ROMT = 17 1 L      20.00   39.10   78.66   19.67
I,K,ROMFXK=   4 10   .012
I,K,ROMFXK=   4 11   .062
I,K,ROMFXK=   4 12   .226
I,K,ROMFXK=   4 13   .566
I,K,ROMFXK=   4 14  1.002
I,K,ROMFXK=   4 15  1.317
I,K,ROMFXK=   4 16  1.277
I,K,ROMFXK=   4 17   .711
I, NCHAR, TYP,TVAL,RMMDOT,ROMX,ROMT =  113 M      20.00  266.36   14.26    6.72
I, NCHAR, TYP,TVAL,RMMDOT,ROMX,ROMT =  213 M      20.00  266.36   14.76    6.91
I, NCHAR, TYP,TVAL,RMMDOT,ROMX,ROMT =  313 M      20.00  266.36   14.51    6.81
I,ROMFX1, ROMFX2, ROMFX3 =   1   .666   .469   .580
CLCON,CLCONN=   .576   .000
    40.0   1   1    1.183     2     .225  .230  .246  .728  .835  .827  .999
I, NCHAR, TYP,TVAL,RMMDOT,ROMX,ROMT =  110 M      20.00   60.92   34.32    9.83
I, NCHAR, TYP,TVAL,RMMDOT,ROMX,ROMT =  2 2 M      20.00   53.52   67.41   17.26
I, NCHAR, TYP,TVAL,RMMDOT,ROMX,ROMT =  3 6 M      20.00   56.61   48.95   13.21
I,ROMFX1, ROMFX2, ROMFX3 =   1   .011   .000  1.583
I, NCHAR, TYP,TVAL,RMMDOT,ROMX,ROMT =  4 8 M      20.00   58.63   41.39   11.49
I, NCHAR, TYP,TVAL,RMMDOT,ROMX,ROMT =  5 4 M      20.00   54.90   57.50   15.10
I,K,ROMFXK=   2  4  1.001
I,K,ROMFXK=   2  5   .159
```

```
I, NCHAR, TYP,TVAL,RMMDOT,ROMX,ROMT =  6 9 M      20.00   59.74   37.79   10.66
I, NCHAR, TYP,TVAL,RMMDOT,ROMX,ROMT =  7 7 M      20.00   57.58   45.11   12.34
I, NCHAR, TYP,TVAL,RMMDOT,ROMX,ROMT =  8 5 M      20.00   55.72   53.02   14.11
I, NCHAR, TYP,TVAL,RMMDOT,ROMX,ROMT =  9 3 M      20.00   54.17   62.28   16.15
I,K,ROMFXK=   3  6    .192
I,K,ROMFXK=   3  7   1.872
I,K,ROMFXK=   3  8    .710
I,K,ROMFXK=   3  9    .020
I, NCHAR, TYP,TVAL,RMMDOT,ROMX,ROMT = 10 9 M      20.00   59.74   36.04   10.25
I, NCHAR, TYP,TVAL,RMMDOT,ROMX,ROMT = 11 8 M      20.00   58.63   39.59   11.08
I, NCHAR, TYP,TVAL,RMMDOT,ROMX,ROMT = 12 8 M      20.00   58.63   43.23   11.91
I, NCHAR, TYP,TVAL,RMMDOT,ROMX,ROMT = 13 7 M      20.00   57.58   46.99   12.77
I, NCHAR, TYP,TVAL,RMMDOT,ROMX,ROMT = 14 6 M      20.00   56.61   50.99   13.66
I, NCHAR, TYP,TVAL,RMMDOT,ROMX,ROMT = 15 5 M      20.00   55.72   55.22   14.60
I, NCHAR, TYP,TVAL,RMMDOT,ROMX,ROMT = 16 4 M      20.00   54.90   59.79   15.60
I, NCHAR, TYP,TVAL,RMMDOT,ROMX,ROMT = 17 3 M      20.00   54.17   64.84   16.71
I,K,ROMFXK=   4 10    .057
I,K,ROMFXK=   4 11    .505
I,K,ROMFXK=   4 12   1.514
I,K,ROMFXK=   4 13   1.905
I,K,ROMFXK=   4 14   1.149
I,K,ROMFXK=   4 15    .362
I,K,ROMFXK=   4 16    .062
I,K,ROMFXK=   4 17    .006
CLCON,CLCONN=   .694   .000
I, NCHAR, TYP,TVAL,RMMDOT,ROMX,ROMT =  117 M      20.00  266.36    3.82    2.12
I, NCHAR, TYP,TVAL,RMMDOT,ROMX,ROMT =  216 M      20.00  266.36    6.71    3.54
I, NCHAR, TYP,TVAL,RMMDOT,ROMX,ROMT =  317 M      20.00  266.36    5.15    2.81
I,ROMFX1, ROMFX2, ROMFX3 =   1   .791  2.698  3.525
I, NCHAR, TYP,TVAL,RMMDOT,ROMX,ROMT =  417 M      20.00  266.36    4.49    2.47
I, NCHAR, TYP,TVAL,RMMDOT,ROMX,ROMT =  516 M      20.00  266.36    5.92    3.18
I,K,ROMFXK=   2  4  2.156
I,K,ROMFXK=   2  5  3.538
CLCON,CLCONN=  2.766   .000
    40.0   1   2    3.460     2     .093  .099  .110  .394  .480  .475  .997
I, NCHAR, TYP,TVAL,RMMDOT,ROMX,ROMT =  112 M      25.00   63.47   43.76   12.03
I, NCHAR, TYP,TVAL,RMMDOT,ROMX,ROMT =  2 1 L      25.00   13.29  105.73   25.34
I, NCHAR, TYP,TVAL,RMMDOT,ROMX,ROMT =  3 7 M      25.00   57.58   68.08   17.41
I,ROMFX1, ROMFX2, ROMFX3 =   1   .010   .015  1.953
I, NCHAR, TYP,TVAL,RMMDOT,ROMX,ROMT =  410 M      25.00   60.92   54.68   14.48
I, NCHAR, TYP,TVAL,RMMDOT,ROMX,ROMT =  5 4 M      25.00   54.90   84.83   20.98
I,K,ROMFXK=   2  4    .525
I,K,ROMFXK=   2  5    .831
```

```
I, NCHAR, TYP,TVAL,RMMDOT,ROMX,ROMT =  611 M      25.00   62.17   49.00   13.22
I, NCHAR, TYP,TVAL,RMMDOT,ROMX,ROMT =  7 9 M      25.00   59.74   61.01   15.87
I, NCHAR, TYP,TVAL,RMMDOT,ROMX,ROMT =  8 5 M      25.00   55.72   75.98   19.10
I, NCHAR, TYP,TVAL,RMMDOT,ROMX,ROMT =  9 1 M      25.00   52.96   94.71   23.05
I,K,ROMFXK=   3  6   .104
I,K,ROMFXK=   3  7  1.380
I,K,ROMFXK=   3  8  1.624
I,K,ROMFXK=   3  9   .271
I, NCHAR, TYP,TVAL,RMMDOT,ROMX,ROMT = 1012 M      25.00   63.47   46.34   12.62
I, NCHAR, TYP,TVAL,RMMDOT,ROMX,ROMT = 1111 M      25.00   62.17   51.79   13.84
I, NCHAR, TYP,TVAL,RMMDOT,ROMX,ROMT = 12 9 M      25.00   59.74   57.81   15.17
I, NCHAR, TYP,TVAL,RMMDOT,ROMX,ROMT = 13 8 M      25.00   58.63   64.53   16.64
I, NCHAR, TYP,TVAL,RMMDOT,ROMX,ROMT = 14 6 M      25.00   56.61   72.03   18.25
I, NCHAR, TYP,TVAL,RMMDOT,ROMX,ROMT = 15 4 M      25.00   54.90   80.39   20.04
I, NCHAR, TYP,TVAL,RMMDOT,ROMX,ROMT = 16 2 M      25.00   53.52   89.72   22.01
I, NCHAR, TYP,TVAL,RMMDOT,ROMX,ROMT = 17 0 M      25.00     .00  100.14   24.18
I,K,ROMFXK=   4 10   .036
I,K,ROMFXK=   4 11   .260
I,K,ROMFXK=   4 12   .928
I,K,ROMFXK=   4 13  1.784
I,K,ROMFXK=   4 14  1.896
I,K,ROMFXK=   4 15  1.204
I,K,ROMFXK=   4 16   .487
I,K,ROMFXK=   4 17   .000
CLCON,CLCONN=   .828   .000
I, NCHAR, TYP,TVAL,RMMDOT,ROMX,ROMT =  114 M      25.00  282.78   24.52   10.27
I, NCHAR, TYP,TVAL,RMMDOT,ROMX,ROMT =  213 M      25.00  282.78   27.65   11.26
I, NCHAR, TYP,TVAL,RMMDOT,ROMX,ROMT =  314 M      25.00  282.78   26.08   10.76
I,ROMFX1, ROMFX2, ROMFX3 =   1  1.958  2.758  5.686
I, NCHAR, TYP,TVAL,RMMDOT,ROMX,ROMT =  414 M      25.00  282.78   25.30   10.52
I, NCHAR, TYP,TVAL,RMMDOT,ROMX,ROMT =  513 M      25.00  282.78   26.86   11.01
I,K,ROMFXK=   2  4  4.262
I,K,ROMFXK=   2  5  4.931
CLCON,CLCONN=  4.394   .000
    45.0   1   1    5.222     2     .041  .046  .052  .245  .317  .313  .995
I, NCHAR, TYP,TVAL,RMMDOT,ROMX,ROMT =  115 M      25.00   67.71   34.70    9.92
I, NCHAR, TYP,TVAL,RMMDOT,ROMX,ROMT =  2 7 M      25.00   57.58   66.21   17.00
I, NCHAR, TYP,TVAL,RMMDOT,ROMX,ROMT =  311 M      25.00   62.17   48.70   13.15
I,ROMFX1, ROMFX2, ROMFX3 =   1   .016   .000  1.636
I, NCHAR, TYP,TVAL,RMMDOT,ROMX,ROMT =  413 M      25.00   64.83   41.48   11.51
I, NCHAR, TYP,TVAL,RMMDOT,ROMX,ROMT =  510 M      25.00   60.92   56.83   14.95
I,K,ROMFXK=   2  4  1.030
I,K,ROMFXK=   2  5   .208
```

```
I, NCHAR, TYP,TVAL,RMMDOT,ROMX,ROMT =  614 M      25.00   66.25   38.03   10.72
I, NCHAR, TYP,TVAL,RMMDOT,ROMX,ROMT =  712 M      25.00   63.47   45.04   12.32
I, NCHAR, TYP,TVAL,RMMDOT,ROMX,ROMT =  810 M      25.00   60.92   52.60   14.02
I, NCHAR, TYP,TVAL,RMMDOT,ROMX,ROMT =  9 9 M      25.00   59.74   61.30   15.94
I,K,ROMFXK=   3  6    .223
I,K,ROMFXK=   3  7   1.871
I,K,ROMFXK=   3  8    .798
I,K,ROMFXK=   3  9    .032
CLCON,CLCONN=   .731    .000
I, NCHAR, TYP,TVAL,RMMDOT,ROMX,ROMT =  118 M      25.00  282.78   13.17    6.29
I, NCHAR, TYP,TVAL,RMMDOT,ROMX,ROMT =  216 M      25.00  282.78   18.30    8.19
I, NCHAR, TYP,TVAL,RMMDOT,ROMX,ROMT =  317 M      25.00  282.78   15.66    7.24
I,ROMFX1, ROMFX2, ROMFX3 =   1  6.489  6.014 13.749
I, NCHAR, TYP,TVAL,RMMDOT,ROMX,ROMT =  418 M      25.00  282.78   14.38    6.77
I, NCHAR, TYP,TVAL,RMMDOT,ROMX,ROMT =  517 M      25.00  282.78   16.98    7.72
I,K,ROMFXK=   2  4 12.616
I,K,ROMFXK=   2  5 10.663
CLCON,CLCONN= 11.083    .000
    45.0   1   2   11.814     2     .006  .008  .009  .041  .060  .059  .988
I, NCHAR, TYP,TVAL,RMMDOT,ROMX,ROMT =  117 M      30.00   70.78   44.31   12.16
I, NCHAR, TYP,TVAL,RMMDOT,ROMX,ROMT =  2 1 L      30.00   12.79  130.28   30.36
I, NCHAR, TYP,TVAL,RMMDOT,ROMX,ROMT =  310 M      30.00   60.92   75.98   19.10
I,ROMFX1, ROMFX2, ROMFX3 =   1   .017   .000  2.161
I, NCHAR, TYP,TVAL,RMMDOT,ROMX,ROMT =  414 M      30.00   66.25   58.14   15.24
I, NCHAR, TYP,TVAL,RMMDOT,ROMX,ROMT =  5 5 M      30.00   55.72   99.55   24.06
I,K,ROMFXK=   2  4  1.301
I,K,ROMFXK=   2  5   .188
I, NCHAR, TYP,TVAL,RMMDOT,ROMX,ROMT =  616 M      30.00   69.22   50.84   13.63
I, NCHAR, TYP,TVAL,RMMDOT,ROMX,ROMT =  712 M      30.00   63.47   66.48   17.06
I, NCHAR, TYP,TVAL,RMMDOT,ROMX,ROMT =  8 8 M      30.00   58.63   86.97   21.43
I, NCHAR, TYP,TVAL,RMMDOT,ROMX,ROMT =  9 2 M      30.00   53.52  113.90   27.02
I,K,ROMFXK=   3  6    .258
I,K,ROMFXK=   3  7  2.545
I,K,ROMFXK=   3  8    .870
I,K,ROMFXK=   3  9    .025
I, NCHAR, TYP,TVAL,RMMDOT,ROMX,ROMT = 1017 M      30.00   70.78   47.46   12.87
I, NCHAR, TYP,TVAL,RMMDOT,ROMX,ROMT = 1115 M      30.00   67.71   54.31   14.40
I, NCHAR, TYP,TVAL,RMMDOT,ROMX,ROMT = 1213 M      30.00   64.83   62.17   16.12
I, NCHAR, TYP,TVAL,RMMDOT,ROMX,ROMT = 1311 M      30.00   62.17   71.14   18.07
I, NCHAR, TYP,TVAL,RMMDOT,ROMX,ROMT = 14 9 M      30.00   59.74   81.38   20.25
I, NCHAR, TYP,TVAL,RMMDOT,ROMX,ROMT = 15 7 M      30.00   57.58   93.07   22.71
I, NCHAR, TYP,TVAL,RMMDOT,ROMX,ROMT = 16 4 M      30.00   54.90  106.39   25.48
I, NCHAR, TYP,TVAL,RMMDOT,ROMX,ROMT = 17 1 M      30.00   52.96  121.64   28.61
```

```
I,K,ROMFXK=   4 10   .077
I,K,ROMFXK=   4 11   .643
I,K,ROMFXK=   4 12  2.019
I,K,ROMFXK=   4 13  2.565
I,K,ROMFXK=   4 14  1.482
I,K,ROMFXK=   4 15   .439
I,K,ROMFXK=   4 16   .074
I,K,ROMFXK=   4 17   .008
CLCON,CLCONN=   .915   .000
I, NCHAR, TYP,TVAL,RMMDOT,ROMX,ROMT =  115 M      30.00  295.78   37.17   14.06
I, NCHAR, TYP,TVAL,RMMDOT,ROMX,ROMT =  214 M      30.00  295.78   41.35   15.22
I, NCHAR, TYP,TVAL,RMMDOT,ROMX,ROMT =  315 M      30.00  295.78   39.26   14.64
I,ROMFX1, ROMFX2, ROMFX3 =   1  2.054  2.629  6.073
I, NCHAR, TYP,TVAL,RMMDOT,ROMX,ROMT =  415 M      30.00  295.78   38.21   14.35
I, NCHAR, TYP,TVAL,RMMDOT,ROMX,ROMT =  515 M      30.00  295.78   40.31   14.93
I,K,ROMFXK=   2  4  4.558
I,K,ROMFXK=   2  5  4.962
CLCON,CLCONN=  4.558   .000
    50.0   1   1    5.473     2     .032  .036  .042  .229  .303  .299  .995
I, NCHAR, TYP,TVAL,RMMDOT,ROMX,ROMT =  120 M      30.00   75.68   34.97    9.99
I, NCHAR, TYP,TVAL,RMMDOT,ROMX,ROMT =  213 M      30.00   64.83   65.38   16.82
I, NCHAR, TYP,TVAL,RMMDOT,ROMX,ROMT =  316 M      30.00   69.22   48.54   13.11
I,ROMFX1, ROMFX2, ROMFX3 =   1   .021   .000  1.699
I, NCHAR, TYP,TVAL,RMMDOT,ROMX,ROMT =  418 M      30.00   72.38   41.55   11.53
I, NCHAR, TYP,TVAL,RMMDOT,ROMX,ROMT =  515 M      30.00   67.71   56.36   14.85
I,K,ROMFXK=   2  4  1.064
I,K,ROMFXK=   2  5   .253
I, NCHAR, TYP,TVAL,RMMDOT,ROMX,ROMT =  619 M      30.00   74.01   38.21   10.76
I, NCHAR, TYP,TVAL,RMMDOT,ROMX,ROMT =  717 M      30.00   70.78   45.00   12.31
I, NCHAR, TYP,TVAL,RMMDOT,ROMX,ROMT =  816 M      30.00   69.22   52.31   13.95
I, NCHAR, TYP,TVAL,RMMDOT,ROMX,ROMT =  914 M      30.00   66.25   60.62   15.79
I,K,ROMFXK=   3  6   .249
I,K,ROMFXK=   3  7  1.898
I,K,ROMFXK=   3  8   .889
I,K,ROMFXK=   3  9   .044
CLCON,CLCONN=   .769   .000
I, NCHAR, TYP,TVAL,RMMDOT,ROMX,ROMT =  120 M      30.00  295.78   23.15    9.84
I, NCHAR, TYP,TVAL,RMMDOT,ROMX,ROMT =  217 M      30.00  295.78   30.65   12.16
I, NCHAR, TYP,TVAL,RMMDOT,ROMX,ROMT =  319 M      30.00  295.78   26.81   11.00
I,ROMFX1, ROMFX2, ROMFX3 =   1  6.175  4.894 14.126
I, NCHAR, TYP,TVAL,RMMDOT,ROMX,ROMT =  419 M      30.00  295.78   24.98   10.42
I, NCHAR, TYP,TVAL,RMMDOT,ROMX,ROMT =  518 M      30.00  295.78   28.71   11.58
I,K,ROMFXK=   2  4 12.490
```

```
I,K,ROMFXK=   2  5  9.691
CLCON,CLCONN= 10.631   .000
    50.0   1   2   11.400     2     .006  .008  .010  .046  .067  .066  .989
I, NCHAR, TYP,TVAL,RMMDOT,ROMX,ROMT =  122 M      35.00   79.10   44.72   12.25
I, NCHAR, TYP,TVAL,RMMDOT,ROMX,ROMT =  2 3 M      35.00   54.17  137.50   31.82
I, NCHAR, TYP,TVAL,RMMDOT,ROMX,ROMT =  315 M      35.00   67.71   78.54   19.65
I,ROMFX1, ROMFX2, ROMFX3 =   1   .024   .000  2.127
I, NCHAR, TYP,TVAL,RMMDOT,ROMX,ROMT =  419 M      35.00   74.01   59.31   15.50
I, NCHAR, TYP,TVAL,RMMDOT,ROMX,ROMT =  510 M      35.00   60.92  103.98   24.98
I,K,ROMFXK=   2  4  1.749
I,K,ROMFXK=   2  5   .119
I, NCHAR, TYP,TVAL,RMMDOT,ROMX,ROMT =  621 M      35.00   77.38   51.58   13.79
I, NCHAR, TYP,TVAL,RMMDOT,ROMX,ROMT =  717 M      35.00   70.78   68.19   17.43
I, NCHAR, TYP,TVAL,RMMDOT,ROMX,ROMT =  812 M      35.00   63.47   90.39   22.15
I, NCHAR, TYP,TVAL,RMMDOT,ROMX,ROMT =  9 6 M      35.00   56.61  119.53   28.18
I,K,ROMFXK=   3  6   .368
I,K,ROMFXK=   3  7  2.997
I,K,ROMFXK=   3  8   .683
I,K,ROMFXK=   3  9   .012
CLCON,CLCONN=  1.014   .000
I, NCHAR, TYP,TVAL,RMMDOT,ROMX,ROMT =  117 M      35.00  306.40   50.46   17.63
I, NCHAR, TYP,TVAL,RMMDOT,ROMX,ROMT =  216 M      35.00  306.40   55.75   18.99
I, NCHAR, TYP,TVAL,RMMDOT,ROMX,ROMT =  316 M      35.00  306.40   53.00   18.29
I,ROMFX1, ROMFX2, ROMFX3 =   1  1.834  2.149  6.086
I, NCHAR, TYP,TVAL,RMMDOT,ROMX,ROMT =  417 M      35.00  306.40   51.73   17.96
I, NCHAR, TYP,TVAL,RMMDOT,ROMX,ROMT =  516 M      35.00  306.40   54.32   18.63
I,K,ROMFXK=   2  4  4.454
I,K,ROMFXK=   2  5  4.741
CLCON,CLCONN=  4.391   .000
    55.0   1   1    5.404     2     .028  .031  .036  .233  .314  .309  .995
I, NCHAR, TYP,TVAL,RMMDOT,ROMX,ROMT =  124 M      35.00   82.63   35.18   10.04
I, NCHAR, TYP,TVAL,RMMDOT,ROMX,ROMT =  218 M      35.00   72.38   64.76   16.69
I, NCHAR, TYP,TVAL,RMMDOT,ROMX,ROMT =  321 M      35.00   77.38   48.41   13.09
I,ROMFX1, ROMFX2, ROMFX3 =   1   .026   .006  1.763
I, NCHAR, TYP,TVAL,RMMDOT,ROMX,ROMT =  423 M      35.00   80.85   41.60   11.54
I, NCHAR, TYP,TVAL,RMMDOT,ROMX,ROMT =  520 M      35.00   75.68   56.02   14.78
I,K,ROMFXK=   2  4  1.096
I,K,ROMFXK=   2  5   .296
I, NCHAR, TYP,TVAL,RMMDOT,ROMX,ROMT =  624 M      35.00   82.63   38.34   10.79
I, NCHAR, TYP,TVAL,RMMDOT,ROMX,ROMT =  722 M      35.00   79.10   44.97   12.31
I, NCHAR, TYP,TVAL,RMMDOT,ROMX,ROMT =  821 M      35.00   77.38   52.09   13.91
I, NCHAR, TYP,TVAL,RMMDOT,ROMX,ROMT =  919 M      35.00   74.01   60.15   15.69
I,K,ROMFXK=   3  6   .271
```

```
I,K,ROMFXK=   3  7  1.932
I,K,ROMFXK=   3  8   .964
I,K,ROMFXK=   3  9   .058
CLCON,CLCONN=   .805   .000
I, NCHAR, TYP,TVAL,RMMDOT,ROMX,ROMT =  122 M      35.00  306.40   33.42   12.98
I, NCHAR, TYP,TVAL,RMMDOT,ROMX,ROMT =  219 M      35.00  306.40   43.74   15.86
I, NCHAR, TYP,TVAL,RMMDOT,ROMX,ROMT =  320 M      35.00  306.40   38.46   14.42
I,ROMFX1, ROMFX2, ROMFX3 =   1  4.946  3.634 12.522
I, NCHAR, TYP,TVAL,RMMDOT,ROMX,ROMT =  421 M      35.00  306.40   35.92   13.70
I, NCHAR, TYP,TVAL,RMMDOT,ROMX,ROMT =  519 M      35.00  306.40   41.08   15.14
I,K,ROMFXK=   2  4 11.282
I,K,ROMFXK=   2  5  8.468
CLCON,CLCONN=  9.359   .000
    55.0   1   2   10.165     2     .009  .011  .013  .064  .092  .091  .990
I, NCHAR, TYP,TVAL,RMMDOT,ROMX,ROMT =  127 M      40.00   88.04   45.06   12.33
I, NCHAR, TYP,TVAL,RMMDOT,ROMX,ROMT =  2 8 M      40.00   58.63  134.84   31.28
I, NCHAR, TYP,TVAL,RMMDOT,ROMX,ROMT =  320 M      40.00   75.68   78.04   19.54
I,ROMFX1, ROMFX2, ROMFX3 =   1   .030   .000  2.371
I, NCHAR, TYP,TVAL,RMMDOT,ROMX,ROMT =  424 M      40.00   82.63   59.34   15.51
I, NCHAR, TYP,TVAL,RMMDOT,ROMX,ROMT =  515 M      40.00   67.71  102.67   24.71
I,K,ROMFXK=   2  4  1.869
I,K,ROMFXK=   2  5   .154
I, NCHAR, TYP,TVAL,RMMDOT,ROMX,ROMT =  626 M      40.00   86.22   51.78   13.84
I, NCHAR, TYP,TVAL,RMMDOT,ROMX,ROMT =  722 M      40.00   79.10   67.99   17.39
I, NCHAR, TYP,TVAL,RMMDOT,ROMX,ROMT =  818 M      40.00   72.38   89.53   21.97
I, NCHAR, TYP,TVAL,RMMDOT,ROMX,ROMT =  912 M      40.00   63.47  117.68   27.80
I,K,ROMFXK=   3  6   .410
I,K,ROMFXK=   3  7  3.208
I,K,ROMFXK=   3  8   .832
I,K,ROMFXK=   3  9   .017
CLCON,CLCONN=  1.116   .000
I, NCHAR, TYP,TVAL,RMMDOT,ROMX,ROMT =  118 M      40.00  315.30   64.21   21.09
I, NCHAR, TYP,TVAL,RMMDOT,ROMX,ROMT =  217 M      40.00  315.30   70.50   22.62
I, NCHAR, TYP,TVAL,RMMDOT,ROMX,ROMT =  318 M      40.00  315.30   67.21   21.83
I,ROMFX1, ROMFX2, ROMFX3 =   1  1.619  1.798  5.721
I, NCHAR, TYP,TVAL,RMMDOT,ROMX,ROMT =  418 M      40.00  315.30   65.71   21.46
I, NCHAR, TYP,TVAL,RMMDOT,ROMX,ROMT =  517 M      40.00  315.30   68.82   22.22
I,K,ROMFXK=   2  4  4.134
I,K,ROMFXK=   2  5  4.308
CLCON,CLCONN=  4.030   .000
    60.0   1   1    5.146     2     .025  .028  .032  .250  .341  .336  .995
I, NCHAR, TYP,TVAL,RMMDOT,ROMX,ROMT =  129 M      40.00   91.69   35.35   10.08
I, NCHAR, TYP,TVAL,RMMDOT,ROMX,ROMT =  223 M      40.00   80.85   64.27   16.58
```

```
I, NCHAR, TYP,TVAL,RMMDOT,ROMX,ROMT =  326 M      40.00   86.22   48.32   13.06
I,ROMFX1, ROMFX2, ROMFX3 =   1   .031   .008  1.819
I, NCHAR, TYP,TVAL,RMMDOT,ROMX,ROMT =  428 M      40.00   89.86   41.65   11.55
I, NCHAR, TYP,TVAL,RMMDOT,ROMX,ROMT =  525 M      40.00   84.42   55.75   14.72
I,K,ROMFXK=   2  4  1.124
I,K,ROMFXK=   2  5   .336
I, NCHAR, TYP,TVAL,RMMDOT,ROMX,ROMT =  629 M      40.00   91.69   38.45   10.81
I, NCHAR, TYP,TVAL,RMMDOT,ROMX,ROMT =  727 M      40.00   88.04   44.95   12.30
I, NCHAR, TYP,TVAL,RMMDOT,ROMX,ROMT =  826 M      40.00   86.22   51.92   13.87
I, NCHAR, TYP,TVAL,RMMDOT,ROMX,ROMT =  924 M      40.00   82.63   59.80   15.61
I,K,ROMFXK=   3  6   .289
I,K,ROMFXK=   3  7  1.963
I,K,ROMFXK=   3  8  1.030
I,K,ROMFXK=   3  9   .070
CLCON,CLCONN=   .837   .000
I, NCHAR, TYP,TVAL,RMMDOT,ROMX,ROMT =  123 M      40.00  315.30   47.23   16.79
I, NCHAR, TYP,TVAL,RMMDOT,ROMX,ROMT =  220 M      40.00  315.30   57.16   19.35
I, NCHAR, TYP,TVAL,RMMDOT,ROMX,ROMT =  321 M      40.00  315.30   51.99   18.03
I,ROMFX1, ROMFX2, ROMFX3 =   1  6.896  2.268  7.288
I, NCHAR, TYP,TVAL,RMMDOT,ROMX,ROMT =  422 M      40.00  315.30   49.58   17.41
I, NCHAR, TYP,TVAL,RMMDOT,ROMX,ROMT =  521 M      40.00  315.30   54.46   18.67
I,K,ROMFXK=   2  4  8.239
I,K,ROMFXK=   2  5  4.664
CLCON,CLCONN=  6.272   .000
    60.0   1   2    7.110     2     .022  .025  .030  .147  .198  .196  .993
I, NCHAR, TYP,TVAL,RMMDOT,ROMX,ROMT =  132 M      45.00   97.18   45.34   12.39
I, NCHAR, TYP,TVAL,RMMDOT,ROMX,ROMT =  214 M      45.00   66.25  132.82   30.87
I, NCHAR, TYP,TVAL,RMMDOT,ROMX,ROMT =  325 M      45.00   84.42   77.65   19.46
I,ROMFX1, ROMFX2, ROMFX3 =   1   .036   .000  2.625
I, NCHAR, TYP,TVAL,RMMDOT,ROMX,ROMT =  429 M      45.00   91.69   59.37   15.51
I, NCHAR, TYP,TVAL,RMMDOT,ROMX,ROMT =  520 M      45.00   75.68  101.62   24.49
I,K,ROMFXK=   2  4  1.991
I,K,ROMFXK=   2  5   .193
I, NCHAR, TYP,TVAL,RMMDOT,ROMX,ROMT =  631 M      45.00   95.36   51.95   13.87
I, NCHAR, TYP,TVAL,RMMDOT,ROMX,ROMT =  727 M      45.00   88.04   67.84   17.36
I, NCHAR, TYP,TVAL,RMMDOT,ROMX,ROMT =  823 M      45.00   80.85   88.84   21.82
I, NCHAR, TYP,TVAL,RMMDOT,ROMX,ROMT =  917 M      45.00   70.78  116.19   27.49
I,K,ROMFXK=   3  6   .451
I,K,ROMFXK=   3  7  3.429
I,K,ROMFXK=   3  8   .975
I,K,ROMFXK=   3  9   .023
CLCON,CLCONN=  1.220   .000
I, NCHAR, TYP,TVAL,RMMDOT,ROMX,ROMT =  120 M      45.00  322.87   78.76   24.58
```

```
I, NCHAR, TYP,TVAL,RMMDOT,ROMX,ROMT =  218 M      45.00  322.87   85.45   26.15
I, NCHAR, TYP,TVAL,RMMDOT,ROMX,ROMT =  319 M      45.00  322.87   82.11   25.37
I,ROMFX1, ROMFX2, ROMFX3 =   1  1.786  1.564  4.944
I, NCHAR, TYP,TVAL,RMMDOT,ROMX,ROMT =  420 M      45.00  322.87   80.43   24.98
I, NCHAR, TYP,TVAL,RMMDOT,ROMX,ROMT =  519 M      45.00  322.87   83.78   25.76
I,K,ROMFXK=   2  4  4.009
I,K,ROMFXK=   2  5  3.550
CLCON,CLCONN=  3.607   .000
    65.0   1   1    4.827     2     .023  .025  .030  .273  .377  .370  .995
I, NCHAR, TYP,TVAL,RMMDOT,ROMX,ROMT =  134 M      45.00  100.81   35.48   10.11
I, NCHAR, TYP,TVAL,RMMDOT,ROMX,ROMT =  228 M      45.00   89.86   63.87   16.49
I, NCHAR, TYP,TVAL,RMMDOT,ROMX,ROMT =  331 M      45.00   95.36   48.24   13.05
I,ROMFX1, ROMFX2, ROMFX3 =   1   .035   .011  1.865
I, NCHAR, TYP,TVAL,RMMDOT,ROMX,ROMT =  433 M      45.00   99.00   41.69   11.56
I, NCHAR, TYP,TVAL,RMMDOT,ROMX,ROMT =  530 M      45.00   93.53   55.53   14.67
I,K,ROMFXK=   2  4  1.144
I,K,ROMFXK=   2  5   .373
I, NCHAR, TYP,TVAL,RMMDOT,ROMX,ROMT =  634 M      45.00  100.81   38.54   10.84
I, NCHAR, TYP,TVAL,RMMDOT,ROMX,ROMT =  732 M      45.00   97.18   44.93   12.30
I, NCHAR, TYP,TVAL,RMMDOT,ROMX,ROMT =  831 M      45.00   95.36   51.79   13.84
I, NCHAR, TYP,TVAL,RMMDOT,ROMX,ROMT =  929 M      45.00   91.69   59.51   15.54
I,K,ROMFXK=   3  6   .305
I,K,ROMFXK=   3  7  1.986
I,K,ROMFXK=   3  8  1.087
I,K,ROMFXK=   3  9   .082
CLCON,CLCONN=   .864   .000
I, NCHAR, TYP,TVAL,RMMDOT,ROMX,ROMT =  124 M      45.00  322.87   62.69   20.72
I, NCHAR, TYP,TVAL,RMMDOT,ROMX,ROMT =  222 M      45.00  322.87   70.81   22.69
I, NCHAR, TYP,TVAL,RMMDOT,ROMX,ROMT =  323 M      45.00  322.87   66.58   21.68
I,ROMFX1, ROMFX2, ROMFX3 =   1  4.818  1.222  3.244
CLCON,CLCONN=  3.169   .000
    65.0   1   2    4.033     2     .056  .061  .069  .338  .430  .424  .996
I, NCHAR, TYP,TVAL,RMMDOT,ROMX,ROMT =  137 M      50.00  106.14   45.58   12.45
I, NCHAR, TYP,TVAL,RMMDOT,ROMX,ROMT =  219 M      50.00   74.01  131.14   30.53
I, NCHAR, TYP,TVAL,RMMDOT,ROMX,ROMT =  330 M      50.00   93.53   77.32   19.39
I,ROMFX1, ROMFX2, ROMFX3 =   1   .041   .000  2.876
I, NCHAR, TYP,TVAL,RMMDOT,ROMX,ROMT =  434 M      50.00  100.81   59.40   15.52
I, NCHAR, TYP,TVAL,RMMDOT,ROMX,ROMT =  525 M      50.00   84.42  100.75   24.31
I,K,ROMFXK=   2  4  2.107
I,K,ROMFXK=   2  5   .237
I, NCHAR, TYP,TVAL,RMMDOT,ROMX,ROMT =  636 M      50.00  104.38   52.09   13.91
I, NCHAR, TYP,TVAL,RMMDOT,ROMX,ROMT =  732 M      50.00   97.18   67.72   17.33
I, NCHAR, TYP,TVAL,RMMDOT,ROMX,ROMT =  828 M      50.00   89.86   88.27   21.71
```

```
I, NCHAR, TYP,TVAL,RMMDOT,ROMX,ROMT =  922 M      50.00   79.10  114.96   27.24
I,K,ROMFXK=   3  6   .489
I,K,ROMFXK=   3  7  3.698
I,K,ROMFXK=   3  8  1.122
I,K,ROMFXK=   3  9   .031
CLCON,CLCONN=  1.333   .000
    70.0   1   1    2.962     2     .034  .036  .042  .451  .614  .602  .997
I, NCHAR, TYP,TVAL,RMMDOT,ROMX,ROMT =  139 M      50.00  109.58   35.60   10.14
I, NCHAR, TYP,TVAL,RMMDOT,ROMX,ROMT =  233 M      50.00   99.00   63.54   16.42
I, NCHAR, TYP,TVAL,RMMDOT,ROMX,ROMT =  336 M      50.00  104.38   48.18   13.03
I,ROMFX1, ROMFX2, ROMFX3 =   1   .039   .013  1.899
I, NCHAR, TYP,TVAL,RMMDOT,ROMX,ROMT =  438 M      50.00  107.87   41.72   11.57
I, NCHAR, TYP,TVAL,RMMDOT,ROMX,ROMT =  535 M      50.00  102.61   55.34   14.63
I,K,ROMFXK=   2  4  1.157
I,K,ROMFXK=   2  5   .405
I, NCHAR, TYP,TVAL,RMMDOT,ROMX,ROMT =  639 M      50.00  109.58   38.62   10.85
I, NCHAR, TYP,TVAL,RMMDOT,ROMX,ROMT =  737 M      50.00  106.14   44.92   12.30
I, NCHAR, TYP,TVAL,RMMDOT,ROMX,ROMT =  836 M      50.00  104.38   51.67   13.81
I, NCHAR, TYP,TVAL,RMMDOT,ROMX,ROMT =  934 M      50.00  100.81   59.27   15.49
I,K,ROMFXK=   3  6   .317
I,K,ROMFXK=   3  7  1.999
I,K,ROMFXK=   3  8  1.135
I,K,ROMFXK=   3  9   .093
CLCON,CLCONN=   .885   .000
I, NCHAR, TYP,TVAL,RMMDOT,ROMX,ROMT =  125 M      50.00  329.51   78.40   24.50
I, NCHAR, TYP,TVAL,RMMDOT,ROMX,ROMT =  224 M      50.00  329.51   84.60   25.95
I, NCHAR, TYP,TVAL,RMMDOT,ROMX,ROMT =  324 M      50.00  329.51   81.50   25.23
I,ROMFX1, ROMFX2, ROMFX3 =   1  2.205   .683  1.360
CLCON,CLCONN=  1.388   .000
    70.0   1   2    2.273     2     .096  .100  .111  .543  .670  .661  .998
I, NCHAR, TYP,TVAL,RMMDOT,ROMX,ROMT =  142 M      55.00  114.50   45.86   12.51
I, NCHAR, TYP,TVAL,RMMDOT,ROMX,ROMT =  224 M      55.00   82.63  129.21   30.14
I, NCHAR, TYP,TVAL,RMMDOT,ROMX,ROMT =  335 M      55.00  102.61   76.96   19.31
I,ROMFX1, ROMFX2, ROMFX3 =   1   .048   .000  3.114
I, NCHAR, TYP,TVAL,RMMDOT,ROMX,ROMT =  439 M      55.00  109.58   59.44   15.53
I, NCHAR, TYP,TVAL,RMMDOT,ROMX,ROMT =  530 M      55.00   93.53   99.76   24.10
I,K,ROMFXK=   2  4  2.202
I,K,ROMFXK=   2  5   .292
I, NCHAR, TYP,TVAL,RMMDOT,ROMX,ROMT =  641 M      55.00  112.89   52.26   13.94
I, NCHAR, TYP,TVAL,RMMDOT,ROMX,ROMT =  737 M      55.00  106.14   67.60   17.30
I, NCHAR, TYP,TVAL,RMMDOT,ROMX,ROMT =  833 M      55.00   99.00   87.63   21.57
I, NCHAR, TYP,TVAL,RMMDOT,ROMX,ROMT =  928 M      55.00   89.86  113.54   26.95
I,K,ROMFXK=   3  6   .528
```

```
I,K,ROMFXK=   3  7  3.877
I,K,ROMFXK=   3  8  1.285
I,K,ROMFXK=   3  9   .042
CLCON,CLCONN=  1.431   .000
    75.0   1   1    2.570     2     .032  .033  .039  .502  .690  .676  .997
I, NCHAR, TYP,TVAL,RMMDOT,ROMX,ROMT =  144 M      55.00  117.58   35.74   10.17
I, NCHAR, TYP,TVAL,RMMDOT,ROMX,ROMT =  238 M      55.00  107.87   63.15   16.34
I, NCHAR, TYP,TVAL,RMMDOT,ROMX,ROMT =  341 M      55.00  112.89   48.10   13.02
I,ROMFX1, ROMFX2, ROMFX3 =   1   .043   .016  1.916
I, NCHAR, TYP,TVAL,RMMDOT,ROMX,ROMT =  443 M      55.00  116.06   41.76   11.58
I, NCHAR, TYP,TVAL,RMMDOT,ROMX,ROMT =  540 M      55.00  111.25   55.13   14.58
I,K,ROMFXK=   2  4  1.163
I,K,ROMFXK=   2  5   .439
I, NCHAR, TYP,TVAL,RMMDOT,ROMX,ROMT =  644 M      55.00  117.58   38.71   10.87
I, NCHAR, TYP,TVAL,RMMDOT,ROMX,ROMT =  742 M      55.00  114.50   44.91   12.29
I, NCHAR, TYP,TVAL,RMMDOT,ROMX,ROMT =  841 M      55.00  112.89   51.54   13.78
I, NCHAR, TYP,TVAL,RMMDOT,ROMX,ROMT =  939 M      55.00  109.58   58.99   15.43
I,K,ROMFXK=   3  6   .329
I,K,ROMFXK=   3  7  1.994
I,K,ROMFXK=   3  8  1.175
I,K,ROMFXK=   3  9   .106
CLCON,CLCONN=   .900   .000
I, NCHAR, TYP,TVAL,RMMDOT,ROMX,ROMT =  126 M      55.00  336.80   94.71   28.27
I, NCHAR, TYP,TVAL,RMMDOT,ROMX,ROMT =  225 M      55.00  336.80   99.14   29.27
I, NCHAR, TYP,TVAL,RMMDOT,ROMX,ROMT =  326 M      55.00  336.80   96.84   28.76
I,ROMFX1, ROMFX2, ROMFX3 =   1   .819   .330   .544
CLCON,CLCONN=   .554   .000
    75.0   1   2    1.454     2     .121  .124  .137  .677  .825  .814  .999
I, NCHAR, TYP,TVAL,RMMDOT,ROMX,ROMT =  147 M      60.00  121.86   46.04   12.55
I, NCHAR, TYP,TVAL,RMMDOT,ROMX,ROMT =  230 M      60.00   93.53  128.03   29.90
I, NCHAR, TYP,TVAL,RMMDOT,ROMX,ROMT =  340 M      60.00  111.25   76.74   19.26
I,ROMFX1, ROMFX2, ROMFX3 =   1   .053   .000  3.329
I, NCHAR, TYP,TVAL,RMMDOT,ROMX,ROMT =  444 M      60.00  117.58   59.47   15.54
I, NCHAR, TYP,TVAL,RMMDOT,ROMX,ROMT =  536 M      60.00  104.38   99.15   23.98
I,K,ROMFXK=   2  4  2.291
I,K,ROMFXK=   2  5   .347
I, NCHAR, TYP,TVAL,RMMDOT,ROMX,ROMT =  646 M      60.00  120.49   52.37   13.97
I, NCHAR, TYP,TVAL,RMMDOT,ROMX,ROMT =  742 M      60.00  114.50   67.53   17.29
I, NCHAR, TYP,TVAL,RMMDOT,ROMX,ROMT =  838 M      60.00  107.87   87.23   21.49
I, NCHAR, TYP,TVAL,RMMDOT,ROMX,ROMT =  933 M      60.00   99.00  112.68   26.77
I,K,ROMFXK=   3  6   .558
I,K,ROMFXK=   3  7  4.052
I,K,ROMFXK=   3  8  1.426
```

```
I,K,ROMFXK=   3  9    .052
CLCON,CLCONN=  1.521    .000
    80.0    1    1    2.010      2      .032   .033   .040   .584   .808   .790   .998
I, NCHAR, TYP,TVAL,RMMDOT,ROMX,ROMT =  149 M      60.00  124.43   35.82   10.19
I, NCHAR, TYP,TVAL,RMMDOT,ROMX,ROMT =  243 M      60.00  116.06   62.91   16.29
I, NCHAR, TYP,TVAL,RMMDOT,ROMX,ROMT =  346 M      60.00  120.49   48.06   13.01
I,ROMFX1, ROMFX2, ROMFX3 =   1    .046    .018  1.928
I, NCHAR, TYP,TVAL,RMMDOT,ROMX,ROMT =  448 M      60.00  123.18   41.78   11.58
I, NCHAR, TYP,TVAL,RMMDOT,ROMX,ROMT =  545 M      60.00  119.06   55.00   14.55
I,K,ROMFXK=   2  4  1.166
I,K,ROMFXK=   2  5    .463
I, NCHAR, TYP,TVAL,RMMDOT,ROMX,ROMT =  649 M      60.00  124.43   38.77   10.89
I, NCHAR, TYP,TVAL,RMMDOT,ROMX,ROMT =  747 M      60.00  121.86   44.90   12.29
I, NCHAR, TYP,TVAL,RMMDOT,ROMX,ROMT =  846 M      60.00  120.49   51.46   13.77
I, NCHAR, TYP,TVAL,RMMDOT,ROMX,ROMT =  944 M      60.00  117.58   58.82   15.39
I,K,ROMFXK=   3  6    .336
I,K,ROMFXK=   3  7  1.992
I,K,ROMFXK=   3  8  1.204
I,K,ROMFXK=   3  9    .116
CLCON,CLCONN=    .911    .000
I, NCHAR, TYP,TVAL,RMMDOT,ROMX,ROMT =  128 M      60.00  341.82  110.95   31.91
I, NCHAR, TYP,TVAL,RMMDOT,ROMX,ROMT =  227 M      60.00  341.82  113.39   32.45
I, NCHAR, TYP,TVAL,RMMDOT,ROMX,ROMT =  327 M      60.00  341.82  112.17   32.18
I,ROMFX1, ROMFX2, ROMFX3 =   1    .226    .138    .178
CLCON,CLCONN=    .179    .000
    80.0    1    2    1.090      2      .133   .135   .149   .747   .905   .893   .999
I, NCHAR, TYP,TVAL,RMMDOT,ROMX,ROMT =  152 M      65.00  127.82   46.19   12.58
I, NCHAR, TYP,TVAL,RMMDOT,ROMX,ROMT =  235 M      65.00  102.61  127.00   29.69
I, NCHAR, TYP,TVAL,RMMDOT,ROMX,ROMT =  345 M      65.00  119.06   76.55   19.22
I,ROMFX1, ROMFX2, ROMFX3 =   1    .058    .007  3.515
I, NCHAR, TYP,TVAL,RMMDOT,ROMX,ROMT =  449 M      65.00  124.43   59.50   15.54
I, NCHAR, TYP,TVAL,RMMDOT,ROMX,ROMT =  541 M      65.00  112.89   98.62   23.87
I,K,ROMFXK=   2  4  2.360
I,K,ROMFXK=   2  5    .395
I, NCHAR, TYP,TVAL,RMMDOT,ROMX,ROMT =  651 M      65.00  126.76   52.46   13.99
I, NCHAR, TYP,TVAL,RMMDOT,ROMX,ROMT =  747 M      65.00  121.86   67.47   17.28
I, NCHAR, TYP,TVAL,RMMDOT,ROMX,ROMT =  843 M      65.00  116.06   86.89   21.41
I, NCHAR, TYP,TVAL,RMMDOT,ROMX,ROMT =  938 M      65.00  107.87  111.92   26.62
I,K,ROMFXK=   3  6    .583
I,K,ROMFXK=   3  7  4.193
I,K,ROMFXK=   3  8  1.557
I,K,ROMFXK=   3  9    .062
CLCON,CLCONN=  1.599    .000
```

```
    85.0   1   1    1.741     2     .031  .031  .037  .628  .876  .856  .998
I, NCHAR, TYP,TVAL,RMMDOT,ROMX,ROMT =  154 M      65.00  129.72   35.90   10.21
I, NCHAR, TYP,TVAL,RMMDOT,ROMX,ROMT =  248 M      65.00  123.18   62.70   16.24
I, NCHAR, TYP,TVAL,RMMDOT,ROMX,ROMT =  352 M      65.00  127.82   48.02   13.00
I,ROMFX1, ROMFX2, ROMFX3 =   1   .049   .021  1.936
I, NCHAR, TYP,TVAL,RMMDOT,ROMX,ROMT =  453 M      65.00  128.81   41.81   11.59
I, NCHAR, TYP,TVAL,RMMDOT,ROMX,ROMT =  550 M      65.00  125.63   54.88   14.53
I,K,ROMFXK=   2  4  1.166
I,K,ROMFXK=   2  5   .483
I, NCHAR, TYP,TVAL,RMMDOT,ROMX,ROMT =  654 M      65.00  129.72   38.82   10.90
I, NCHAR, TYP,TVAL,RMMDOT,ROMX,ROMT =  752 M      65.00  127.82   44.89   12.29
I, NCHAR, TYP,TVAL,RMMDOT,ROMX,ROMT =  851 M      65.00  126.76   51.39   13.75
I, NCHAR, TYP,TVAL,RMMDOT,ROMX,ROMT =  949 M      65.00  124.43   58.67   15.36
I,K,ROMFXK=   3  6   .342
I,K,ROMFXK=   3  7  1.984
I,K,ROMFXK=   3  8  1.225
I,K,ROMFXK=   3  9   .124
CLCON,CLCONN=   .918   .000
I, NCHAR, TYP,TVAL,RMMDOT,ROMX,ROMT =  129 U      65.00  335.51  127.36   35.50
I, NCHAR, TYP,TVAL,RMMDOT,ROMX,ROMT =  229 U      65.00  340.99  127.74   35.58
I, NCHAR, TYP,TVAL,RMMDOT,ROMX,ROMT =  329 U      65.00  338.49  127.55   35.54
I,ROMFX1, ROMFX2, ROMFX3 =   1   .018   .017   .017
CLCON,CLCONN=   .017   .000
    85.0   1   2     .935     2     .138  .140  .154  .779  .942  .930  .999
I, NCHAR, TYP,TVAL,RMMDOT,ROMX,ROMT =  157 M      70.00  131.98   46.33   12.62
I, NCHAR, TYP,TVAL,RMMDOT,ROMX,ROMT =  240 M      70.00  111.25  126.07   29.50
I, NCHAR, TYP,TVAL,RMMDOT,ROMX,ROMT =  350 M      70.00  125.63   76.38   19.19
I,ROMFX1, ROMFX2, ROMFX3 =   1   .062   .008  3.664
I, NCHAR, TYP,TVAL,RMMDOT,ROMX,ROMT =  454 M      70.00  129.72   59.52   15.55
I, NCHAR, TYP,TVAL,RMMDOT,ROMX,ROMT =  546 M      70.00  120.49   98.14   23.77
I,K,ROMFXK=   2  4  2.407
I,K,ROMFXK=   2  5   .441
I, NCHAR, TYP,TVAL,RMMDOT,ROMX,ROMT =  655 M      70.00  130.55   52.55   14.01
I, NCHAR, TYP,TVAL,RMMDOT,ROMX,ROMT =  752 M      70.00  127.82   67.42   17.26
I, NCHAR, TYP,TVAL,RMMDOT,ROMX,ROMT =  848 M      70.00  123.18   86.58   21.35
I, NCHAR, TYP,TVAL,RMMDOT,ROMX,ROMT =  943 M      70.00  116.06  111.24   26.48
I,K,ROMFXK=   3  6   .601
I,K,ROMFXK=   3  7  4.292
I,K,ROMFXK=   3  8  1.673
I,K,ROMFXK=   3  9   .072
CLCON,CLCONN=  1.660   .000
    90.0   1   1    1.693     2     .028  .029  .034  .636  .898  .876  .998
I, NCHAR, TYP,TVAL,RMMDOT,ROMX,ROMT =  159 M      70.00  133.04   35.97   10.23
```

```
I, NCHAR, TYP,TVAL,RMMDOT,ROMX,ROMT =  253 M      70.00  128.81   62.51   16.20
I, NCHAR, TYP,TVAL,RMMDOT,ROMX,ROMT =  357 M      70.00  131.98   47.99   12.99
I,ROMFX1, ROMFX2, ROMFX3 =   1   .051   .023  1.933
I, NCHAR, TYP,TVAL,RMMDOT,ROMX,ROMT =  458 M      70.00  132.55   41.83   11.59
I, NCHAR, TYP,TVAL,RMMDOT,ROMX,ROMT =  555 M      70.00  130.55   54.78   14.50
I,K,ROMFXK=   2  4  1.165
I,K,ROMFXK=   2  5   .500
I, NCHAR, TYP,TVAL,RMMDOT,ROMX,ROMT =  659 M      70.00  133.04   38.87   10.91
I, NCHAR, TYP,TVAL,RMMDOT,ROMX,ROMT =  757 M      70.00  131.98   44.89   12.29
I, NCHAR, TYP,TVAL,RMMDOT,ROMX,ROMT =  856 M      70.00  131.31   51.33   13.74
I, NCHAR, TYP,TVAL,RMMDOT,ROMX,ROMT =  954 M      70.00  129.72   58.53   15.33
I,K,ROMFXK=   3  6   .347
I,K,ROMFXK=   3  7  1.973
I,K,ROMFXK=   3  8  1.239
I,K,ROMFXK=   3  9   .132
CLCON,CLCONN=   .921   .000
    90.0   1   2     .921     1     .138  .140  .154  .782  .946  .933  .999
I, NCHAR, TYP,TVAL,RMMDOT,ROMX,ROMT =  162 M      75.00  133.92   46.46   12.65
I, NCHAR, TYP,TVAL,RMMDOT,ROMX,ROMT =  245 M      75.00  119.06  125.22   29.33
I, NCHAR, TYP,TVAL,RMMDOT,ROMX,ROMT =  355 M      75.00  130.55   76.22   19.16
I,ROMFX1, ROMFX2, ROMFX3 =   1   .066   .010  3.770
I, NCHAR, TYP,TVAL,RMMDOT,ROMX,ROMT =  459 M      75.00  133.04   59.55   15.55
I, NCHAR, TYP,TVAL,RMMDOT,ROMX,ROMT =  551 M      75.00  126.76   97.71   23.68
I,K,ROMFXK=   2  4  2.431
I,K,ROMFXK=   2  5   .483
I, NCHAR, TYP,TVAL,RMMDOT,ROMX,ROMT =  660 M      75.00  133.44   52.63   14.03
I, NCHAR, TYP,TVAL,RMMDOT,ROMX,ROMT =  757 M      75.00  131.98   67.37   17.25
I, NCHAR, TYP,TVAL,RMMDOT,ROMX,ROMT =  853 M      75.00  128.81   86.30   21.29
I, NCHAR, TYP,TVAL,RMMDOT,ROMX,ROMT =  948 M      75.00  123.18  110.62   26.35
I,K,ROMFXK=   3  6   .616
I,K,ROMFXK=   3  7  4.346
I,K,ROMFXK=   3  8  1.769
I,K,ROMFXK=   3  9   .083
CLCON,CLCONN=  1.704   .000
    95.0   1   1    1.711     2     .025  .026  .031  .633  .901  .879  .998
I, NCHAR, TYP,TVAL,RMMDOT,ROMX,ROMT =  164 M      75.00  134.00   36.03   10.24
I, NCHAR, TYP,TVAL,RMMDOT,ROMX,ROMT =  258 M      75.00  132.55   62.34   16.16
I, NCHAR, TYP,TVAL,RMMDOT,ROMX,ROMT =  362 M      75.00  133.92   47.95   12.98
I,ROMFX1, ROMFX2, ROMFX3 =   1   .054   .025  1.925
I, NCHAR, TYP,TVAL,RMMDOT,ROMX,ROMT =  463 M      75.00  134.01   41.85   11.60
I, NCHAR, TYP,TVAL,RMMDOT,ROMX,ROMT =  560 M      75.00  133.44   54.68   14.48
I,K,ROMFXK=   2  4  1.162
I,K,ROMFXK=   2  5   .514
```

```
I, NCHAR, TYP,TVAL,RMMDOT,ROMX,ROMT =  664 M      75.00  134.00   38.91   10.92
I, NCHAR, TYP,TVAL,RMMDOT,ROMX,ROMT =  762 M      75.00  133.92   44.88   12.29
I, NCHAR, TYP,TVAL,RMMDOT,ROMX,ROMT =  861 M      75.00  133.73   51.27   13.72
I, NCHAR, TYP,TVAL,RMMDOT,ROMX,ROMT =  959 M      75.00  133.04   58.40   15.30
I,K,ROMFXK=   3  6   .352
I,K,ROMFXK=   3  7  1.959
I,K,ROMFXK=   3  8  1.248
I,K,ROMFXK=   3  9   .138
CLCON,CLCONN=   .923   .000
    95.0   1   2     .923     1     .137  .139  .154  .782  .946  .933  .999
I, NCHAR, TYP,TVAL,RMMDOT,ROMX,ROMT =  167 M      80.00  133.26   46.58   12.67
I, NCHAR, TYP,TVAL,RMMDOT,ROMX,ROMT =  250 M      80.00  125.63  124.47   29.18
I, NCHAR, TYP,TVAL,RMMDOT,ROMX,ROMT =  360 M      80.00  133.44   76.10   19.13
I,ROMFX1, ROMFX2, ROMFX3 =   1   .069   .011  3.880
I, NCHAR, TYP,TVAL,RMMDOT,ROMX,ROMT =  464 M      80.00  134.00   59.57   15.56
I, NCHAR, TYP,TVAL,RMMDOT,ROMX,ROMT =  556 M      80.00  131.31   97.33   23.60
I,K,ROMFXK=   2  4  2.429
I,K,ROMFXK=   2  5   .519
I, NCHAR, TYP,TVAL,RMMDOT,ROMX,ROMT =  665 M      80.00  133.87   52.71   14.04
I, NCHAR, TYP,TVAL,RMMDOT,ROMX,ROMT =  762 M      80.00  133.92   67.33   17.25
I, NCHAR, TYP,TVAL,RMMDOT,ROMX,ROMT =  858 M      80.00  132.55   86.06   21.24
I, NCHAR, TYP,TVAL,RMMDOT,ROMX,ROMT =  953 M      80.00  128.81  110.07   26.24
I,K,ROMFXK=   3  6   .625
I,K,ROMFXK=   3  7  4.350
I,K,ROMFXK=   3  8  1.841
I,K,ROMFXK=   3  9   .093
CLCON,CLCONN=  1.732   .000
   100.0   1   1    1.732     2     .024  .025  .030  .630  .901  .878  .998
I, NCHAR, TYP,TVAL,RMMDOT,ROMX,ROMT =  169 M      80.00  132.18   36.09   10.26
I, NCHAR, TYP,TVAL,RMMDOT,ROMX,ROMT =  263 M      80.00  134.01   62.18   16.13
I, NCHAR, TYP,TVAL,RMMDOT,ROMX,ROMT =  367 M      80.00  133.26   47.93   12.98
I,ROMFX1, ROMFX2, ROMFX3 =   1   .056   .026  1.913
I, NCHAR, TYP,TVAL,RMMDOT,ROMX,ROMT =  468 M      80.00  132.78   41.86   11.60
I, NCHAR, TYP,TVAL,RMMDOT,ROMX,ROMT =  565 M      80.00  133.87   54.60   14.46
I,K,ROMFXK=   2  4  1.159
I,K,ROMFXK=   2  5   .524
I, NCHAR, TYP,TVAL,RMMDOT,ROMX,ROMT =  669 M      80.00  132.18   38.95   10.93
I, NCHAR, TYP,TVAL,RMMDOT,ROMX,ROMT =  767 M      80.00  133.26   44.88   12.29
I, NCHAR, TYP,TVAL,RMMDOT,ROMX,ROMT =  866 M      80.00  133.63   51.22   13.71
I, NCHAR, TYP,TVAL,RMMDOT,ROMX,ROMT =  964 M      80.00  134.00   58.29   15.28
I,K,ROMFXK=   3  6   .357
I,K,ROMFXK=   3  7  1.943
I,K,ROMFXK=   3  8  1.251
```

```
I,K,ROMFXK=   3  9    .144
CLCON,CLCONN=   .922    .000
   100.0    1    2      .922      1      .137   .139   .154   .782   .946   .933   .999
   105.0 NO ACTIVE LOS
   110.0 NO ACTIVE LOS
   115.0 NO ACTIVE LOS
   120.0 NO ACTIVE LOS
1

               TOTAL TRANMITANCE FOR ALL SOURCES IS:   .1538E+00




                                END EOSAEL RUN
STOP 000
```

D-3 Example 3: Creating a New Cloud Using SUBA and SUBC

The following example is discussed in detail in section 5.4 in the main body of the report.

D-3.1 Input

```
WAVL      1.06
COMBIC
PHAS            1.0       5.0       6.0       0.0       9.0       1.0       0.0
FILE            9.0      his.18a1
NAME            0.0       0.0       0.0       0.0       0.0       0.0       0.0
         Testing L8A1 self-screening RP smoke grenades
MET1           90.0      2.00        2.      27.50     962.5    202.40      0.00
MUNT            1.       .794        0.        5.       95.        0.        1.
BURN          658.       0.0       0.0        0.        0.      120.   .008333
CLOU            3.       0.0       0.0       0.0       0.0       0.0       0.0
SUBA            1.     0.050       0.0       1.0       1.0       5.0       0.0
SUBC            7.       0.0       0.0       0.0       1.0       0.0       0.0
SUBA            2.     0.925       0.0       2.0       1.0       5.0       0.0
SUBC            0.       0.0       0.0       0.0       1.0       0.0       0.0
SUBA            3.     0.025       0.0       1.0       21.       5.0       0.0
SUBC            0.       0.0       0.0       0.0       1.0       0.0       0.0
DONE            0.0       0.0       0.0       0.0       0.0       0.0       0.0
END
CONTINUE
WAVL      1.06
COMBIC
PHAS            2.0       5.0       6.0      12.0       9.0       0.0       1.0
FILE            9.0      his.18a1
NAME
         Testing L8A1 self-screening RP smoke grenades
ORIG            0.0       0.0       0.0      90.0     265.0       0.0       0.0
SLOC            1.0       1.0       0.0     300.0       0.0       0.0       2.0
SLOC            1.0       1.0       0.0     300.0       5.0       0.0       2.0
SLOC            1.0       1.0       0.0     300.0      10.0       0.0       2.0
OLOC            1.0      10.0     100.0       2.0       0.0     300.0       0.0
TLOC            1.0      10.0    -100.0       2.0       1.0       0.0       0.0
LIST            2.0       0.0     300.0       5.0
DONE            0.0       0.0       0.0       0.0       0.0       0.0       0.0
END
STOP
```

D-3.2 Output

```
*****************************************************************************
  WARNING - THIS LIBRARY CONTAINS TECHNICAL DATA WHOSE EXPORT IS RESTRICTED
  BY THE ARMS EXPORT CONTROL ACT (TITLE 22, U.S.C., SEC 2751 ET SEQ.) OR
  EXECUTIVE ORDER 12470.  VIOLATION OF THESE EXPORT LAWS ARE SUBJECT TO
                  SEVERE CRIMINAL PENALTIES.
*****************************************************************************


1




                  *********************************
                  *                               *
                  *    ELECTRO-OPTICAL SYSTEMS    *
                  *                               *
                  *  ATMOSPHERIC EFFECTS LIBRARY  *
                  *                               *
                  *    NOT FOR OPERATIONAL USE    *
                  *                               *
                  * EOSAEL87 REV 2.1   02/23/90   *
                  *                               *
                  *********************************



WAVL      1.06
 NOTE: THAT THE ABOVE CARD WAS MODIFIED FOR CONSISTENCY TO:
WAVL       .1060E+01 .1060E+01 .0000E+00



                                     BEGINNING           ENDING

            WAVENUMBER (CM**-1)       9433.963           9433.963

            WAVELENGTH (MICROMETERS)     1.060              1.060

            FREQUENCY (GHZ)         283018.875         283018.875



         **** EOSAEL WARNING ****
 VISIBILITY AND EXTINCTION = 0.0, VISIBILITY CHANGED TO 10.0 KM
```

VISIBILITY
10.00 KM

1

```
*********************************
*                               *
*        C O M B I C            *
*                               *
*COMBINED OBSCURATION MODEL FOR*
* BATTLEFIELD-INDUCED AEROSOLS *
*   NOT FOR OPERATIONAL USE     *
*                               *
* EOSAEL87 REV 2.3   12/12/90  *
*                               *
*********************************
```

1

```
                 *****************
                 *               *
                 *    COMBIC     *
                 *    PHASE 1    *
                 *               *
                 *****************
```

COMBIC WARNING: FILE(his.18a1)
WILL BE OVER WRITTEN

COMBIC CLOUD HISTORY ON UNIT 9 OPENED TO: his.18a1

1

METEOROLOGICAL CONDITIONS

REFERENCE HEIGHT 10.00 METERS WIND SPEED 2.00 METERS/SEC TEMPERATURE 27.49 DEG C

SURFACE ROUGHNESS .10000 METERS WIND DIRECTION 202.4 DEG WRT NORTH PRESSURE 963. MB

INVERSION HEIGHT 995. METERS PASQUILL CATEGORY 2 RELATIVE HUMIDITY 90.0 PERCENT

BOUNDARY LAYER PARAMETERS

FRICTION VELOCITY .213 M/SEC PASQUILL CLASS 1.60 AIR DENSITY 1110.4 G/M**3

1./MONIN-OBUKHOV LENGTH -.05987 M**-1 KAZANSKI-MONIN -.8109 MEAN STATIC SBAR (10-50M) -.000409 SEC**-2

SENSIBLE HEAT FLUX 49.7 WATT/M**2 COLD REGION FLAG 0 SURFACE BUOYANCY FLUX .0014 M**2/S**3

OMEGA .874 SBAR MODEL FLAG 0

DIFFUSION COEFFICIENTS

A COEFFICIENT .316 B COEFFICIENT .900 C COEFFICIENT .233 D COEFFICIENT .845

SURFACE CONDITIONS

SNOW COVER FLAG 0 SILT CONTENT 50.0 PERCENT SOD DEPTH .000 METERS

1 VERTICAL PROFILE MODEL

HEIGHT (M)	WINDSPEED (M/S)	ATMOSPHERIC TEMPERATURE CONSTANT SBAR MODEL (DEG K)	VARIABLE S MODEL (DEG K)	S, STATIC STABILITY PARAMETER	EDDY DISSIPATION RATE (M**2/S**3)
1.0	1.13	300.85	301.32	-.01228233	.01889
2.0	1.43	300.83	301.04	-.00505972	.00863
3.0	1.59	300.81	300.90	-.00293463	.00561
4.0	1.70	300.78	300.81	-.00197406	.00424
5.0	1.78	300.76	300.75	-.00144432	.00349
6.0	1.84	300.74	300.70	-.00111580	.00302
7.0	1.89	300.72	300.66	-.00089552	.00271
8.0	1.93	300.69	300.62	-.00073934	.00249
9.0	1.97	300.67	300.59	-.00062386	.00233

10.0	2.00	300.65	300.56	-.00053562	.00220
15.0	2.12	300.54	300.45	-.00029655	.00186
20.0	2.19	300.43	300.36	-.00019430	.00172
25.0	2.25	300.32	300.29	-.00013977	.00164
30.0	2.29	300.20	300.22	-.00010670	.00159
35.0	2.33	300.09	300.15	-.00008489	.00156
40.0	2.35	299.98	300.09	-.00006962	.00154
45.0	2.38	299.87	300.03	-.00005843	.00152
50.0	2.40	299.76	299.98	-.00004995	.00151
55.0	2.42	299.65	299.92	-.00004334	.00150
60.0	2.44	299.53	299.86	-.00003807	.00149
65.0	2.45	299.42	299.81	-.00003378	.00149
70.0	2.47	299.31	299.76	-.00003025	.00148
75.0	2.48	299.20	299.70	-.00002729	.00148
80.0	2.49	299.09	299.65	-.00002478	.00147
85.0	2.50	298.98	299.60	-.00002264	.00147
90.0	2.51	298.87	299.54	-.00002078	.00147
95.0	2.52	298.76	299.49	-.00001917	.00147
100.0	2.53	298.64	299.44	-.00001776	.00074
125.0	2.57	298.09	299.18	-.00001272	.00074
150.0	2.60	297.53	298.93	-.00000968	.00073
175.0	2.62	296.98	298.68	-.00000769	.00073
200.0	2.64	296.42	298.43	-.00000630	.00073
225.0	2.66	295.87	298.18	-.00000528	.00073
250.0	2.67	295.32	297.93	-.00000451	.00073
275.0	2.69	294.76	297.68	-.00000391	.00073
300.0	2.70	294.21	297.43	-.00000343	.00072
325.0	2.71	293.66	297.19	-.00000304	.00072
350.0	2.72	293.11	296.94	-.00000272	.00072
375.0	2.73	292.56	296.69	-.00000246	.00072
400.0	2.73	292.01	296.45	-.00000223	.00072
450.0	2.75	290.91	295.95	-.00000187	.00072
500.0	2.76	289.82	295.46	-.00000160	.00072
550.0	2.77	288.73	294.97	-.00000138	.00072
600.0	2.78	287.63	294.48	-.00000121	.00072
650.0	2.79	286.55	293.98	-.00000108	.00072
700.0	2.80	285.46	293.49	-.00000096	.00072
750.0	2.80	284.38	293.00	-.00000087	.00072
800.0	2.81	283.29	292.51	-.00000079	.00072
850.0	2.82	282.22	292.02	-.00000072	.00072
900.0	2.82	281.14	291.53	-.00000066	.00072
950.0	2.83	280.06	291.04	-.00000061	.00072
1000.0	2.83	278.99	290.55	-.00000056	.00072

1

MASS EXTINCTION COEFFICIENTS (M**2/GRAM)

OBSCURANT CODE	WAVELENGTH (MICROMETERS) .4-.7	.7-1.2	1.06	3.-5.	8.-12.	10.6	94 GHZ
1	3.2280	2.3638	2.1094	.4127	.3043	.2792	.0010
2	3.2280	2.3638	2.1094	.4127	.3043	.2792	.0010
3	2.1520	2.1368	2.0302	.2668	.0601	.0750	.0010
4	6.8510	4.5920	3.4970	.2450	.0200	.0180	.0010
5	3.2280	2.3638	2.1094	.4127	.3043	.2792	.0010
6	1.8600	1.6300	1.4000	1.7900	1.6800	1.6800	.0010
7	1.8600	1.6300	1.4000	1.7900	1.6800	1.6800	.0010
8	5.6500	4.0800	3.2500	.2450	.0230	.0270	.0010
9	.3200	.3000	.2900	.2700	.2500	.2500	.0010
10	.3200	.2900	.2600	.2700	.2600	.2400	.0010
11	.0350	.0360	.0370	.0350	.0380	.0360	.0010
12	1.5000	1.4600	1.4200	.7500	.3200	.3000	.0010
13	.0010	.0010	.0010	.0010	.0010	.0010	.0004
14	6.1000	3.7500	2.9400	1.3500	1.0100	1.0000	.0020
15	6.8510	4.5920	1.4300	.0540	.0200	.0180	.0010
16	5.3700	2.9000	2.1000	.0900	.0900	.0700	.0010
17	6.2000	3.5000	2.5000	.2300	.0500	.0480	.0010
18	3.3300	2.7500	2.6600	.2600	.3200	.2300	.0010
19	1.3000	1.7400	1.7000	.0800	.1600	.3800	.0010
20	.0000	.0000	.0000	.0000	.0000	.0000	.0000
21	.0000	.0000	.0000	.0000	.0000	.0000	.0000
22	.0000	.0000	.0000	.0000	.0000	.0000	.0000
23	.0000	.0000	.0000	.0000	.0000	.0000	.0000
24	.0000	.0000	.0000	.0000	.0000	.0000	.0000
25	.0000	.0000	.0000	.0000	.0000	.0000	.0000
26	.0000	.0000	.0000	.0000	.0000	.0000	.0000
27	.0000	.0000	.0000	.0000	.0000	.0000	.0000
28	.0000	.0000	.0000	.0000	.0000	.0000	.0000
29	.0000	.0000	.0000	.0000	.0000	.0000	.0000
30	.0000	.0000	.0000	.0000	.0000	.0000	.0000

1

CLOUD HISTORY, FILE NAME = COMHIS

HISTORY FILE SOURCE # 1 CONTAINS 3 SUBCLOUDS, TOTAL 2684.72 GRAMS OBSCURANT

XN NO. OF SOURCES	FILL WEIGHT (LB, GAL OR LB TNT)	MENU SELECTION TYPE	OBSCURANT TYPE CODE	EFFICIENCY (PERCENT)	YIELD FACTOR	NUMBER OF SUBMUNITIONS
1.00	.794	0.	5.	95.0	7.847	1.00

BURN DURATION (SEC)	BURN RATE COEFFICIENTS B1	B2	B3	B4	B5	B6
658.00	.0000	.0000	.0000	.0000	120.0000	.0083

SMOULDERING TIME (SEC)	SMOULDERING COEFFICIENT CSMLD
.00	.0000

1

PROCESSING SUBCLOUD 1

SUBCLOUD # 1 HISTORY FILE SOURCE # 1

MASS FRACTION	DEBRIS CARBON (G/G OBSC)	PLUME (1=PUFF, 2=PLUME)	CLOUD RISE MODEL (1=RISE, 2= NO RISE, >2=STEM)	EXTINCTION COEFFICIENT CODE	BALLISTIC SUBCLOUD (1=Y, 0=N)
.925000	.000	2.	1.	5.	0.

INITIAL OBSCURANT RADII (M) DOWNWIND	CROSSWIND	VERTICAL	BUOYANCY RADIUS(M)	INITIAL CLOUD TEMP(DEG K)	THERMAL PRODUCTION COEF (CAL/G)	UPWARD VELOCITY (M/S)
17.54	17.54	3.00	2.43	303.68	9318.31	.65

HEIGHT OF BURST (M)	FALL VELOCITY (M/S)	EVAPORATION/DEPOSITION FD (LONG-TERM)	DELTA (S**-1)	REFL. COEF.	MOMENTUM RADIUS (M)	HORIZONTAL VELOCITY (M/S)
.0	.000	1.000000	.00000	1.0000	.00	.59

MASS PRODUCTION PROFILE

TIME T AFTER IGNITION (SEC)	MASS PRODUCED UP UNTIL TIME T (G)	MASS STILL AIRBORNE BY TIME T (G)
11.942	236.2	236.2
23.884	450.0	450.0
35.826	643.6	643.6
47.768	818.9	818.9
59.710	977.5	977.5
71.652	1121.1	1121.1
83.593	1251.1	1251.1
95.535	1368.8	1368.8
107.477	1475.4	1475.4
119.419	1571.9	1571.9
131.361	1659.2	1659.2
143.303	1738.2	1738.2
155.245	1809.8	1809.8
167.187	1874.6	1874.6
179.129	1933.2	1933.2
191.071	1986.3	1986.3
203.013	2034.4	2034.4
214.955	2077.9	2077.9
226.897	2117.3	2117.3
238.838	2152.9	2152.9
250.780	2185.2	2185.2
262.722	2214.4	2214.4
274.664	2240.9	2240.9
286.606	2264.8	2264.8
298.548	2286.5	2286.5
310.490	2306.1	2306.1
322.432	2323.9	2323.9
334.374	2340.0	2340.0
346.316	2354.6	2354.6
358.258	2367.7	2367.7
370.200	2379.7	2379.7
382.142	2390.5	2390.5
394.083	2400.3	2400.3
406.025	2409.1	2409.1
417.967	2417.1	2417.1
429.909	2424.4	2424.4
441.851	2431.0	2431.0
453.793	2436.9	2436.9
465.735	2442.3	2442.3
477.677	2447.2	2447.2
489.619	2451.6	2451.6

501.561	2455.6	2455.6
513.503	2459.2	2459.2
525.445	2462.4	2462.4
537.387	2465.4	2465.4
549.328	2468.1	2468.1
561.270	2470.5	2470.5
573.212	2472.7	2472.7
585.154	2474.7	2474.7
597.096	2476.5	2476.5
609.038	2478.1	2478.1
620.980	2479.6	2479.6
632.922	2481.0	2481.0
644.864	2482.2	2482.2
656.806	2483.3	2483.3
668.748	2483.4	2483.4
680.690	2483.4	2483.4
692.632	2483.4	2483.4

SUBCLOUD TRAJECTORY

DOWNWIND DISTANCE (M)	TIME (SEC)	CENTROID HEIGHT (M)	GAUSSIAN CLOUD STD. DEVIATIONS (M) SIGMAX	SIGMAY	SIGMAZ	PEAK CLOUD TEMP. (DEG K)	MEAN CLOUD TEMP. (DEG K)	AIR TEMP. (DEG K)	AIR DENSITY (G/M**3)	CENTROID OR CM VELOCITY VERT. (M/S)	HOR. (M/S)	CM HEIGHT (M)	EFFECTIVE BUOYANCY RADIUS (M)
.10	.16	.10	8.16	8.22	1.45	307.19	303.59	301.23	1109.39	.62	.62	1.3	2.468
1.00	1.36	.75	8.16	8.61	2.10	305.67	302.89	301.07	1109.90	.46	.88	2.0	2.714
2.00	2.39	1.18	8.16	8.97	2.48	304.69	302.46	300.99	1110.13	.37	1.06	2.5	2.893
4.00	4.11	1.74	8.16	9.61	3.02	303.66	302.01	300.92	1110.31	.29	1.25	3.2	3.188
6.00	5.64	2.14	8.16	10.21	3.46	303.11	301.76	300.87	1110.42	.25	1.36	3.8	3.441
10.00	8.43	2.78	8.16	11.34	4.25	302.48	301.47	300.81	1110.53	.21	1.49	4.7	3.874
16.00	12.24	3.13	8.16	12.68	5.11	301.63	301.07	300.78	1110.57	.14	1.62	5.4	4.125
25.00	17.61	3.13	8.16	14.37	6.10	301.20	300.92	300.77	1110.59	.14	1.68	6.2	4.125
36.00	23.97	3.13	8.16	16.40	7.27	300.96	300.82	300.73	1110.63	.14	1.73	7.1	4.125
49.85	31.76	3.13	8.16	18.92	8.70	300.83	300.76	300.69	1110.66	.14	1.78	8.2	4.125
55.98	35.12	3.13	8.16	20.02	9.31	300.74	300.70	300.65	1110.67	.14	1.83	8.7	4.125
62.87	38.81	3.13	8.16	21.25	10.00	300.69	300.67	300.63	1110.66	.15	1.87	9.2	4.125
70.60	42.89	3.13	8.16	22.62	10.76	300.65	300.64	300.62	1110.66	.15	1.90	9.8	4.125
79.29	47.40	3.13	8.16	24.15	11.60	300.63	300.62	300.60	1110.64	.15	1.93	10.5	4.125
89.05	52.39	3.13	8.16	25.86	12.53	300.61	300.60	300.58	1110.62	.15	1.95	11.2	4.125
100.00	57.93	3.13	8.16	27.76	13.57	300.59	300.58	300.57	1110.60	.15	1.98	12.0	4.125
112.30	64.08	3.13	8.16	29.88	14.71	300.57	300.56	300.55	1110.57	.15	2.00	12.9	4.125
126.12	70.91	3.13	8.16	32.24	15.97	300.55	300.55	300.53	1110.53	.15	2.02	14.0	4.125
141.64	78.49	3.13	8.16	34.86	17.37	300.53	300.52	300.50	1110.48	.15	2.04	15.1	4.125

159.06	86.93	3.13	8.16	37.79	18.92	300.50	300.50	300.48	1110.42	.15	2.07	16.3	4.125
178.63	96.30	3.13	8.16	41.04	20.63	300.48	300.48	300.46	1110.35	.14	2.09	17.6	4.125
200.61	106.72	3.13	8.16	44.66	22.52	300.46	300.46	300.43	1110.27	.14	2.11	19.2	4.125
225.28	118.30	3.13	8.16	48.69	24.60	300.43	300.43	300.41	1110.17	.14	2.13	20.8	4.125
253.00	131.18	3.13	8.16	53.17	26.91	300.41	300.41	300.38	1110.06	.14	2.15	22.6	4.125
284.13	145.50	3.13	8.16	58.15	29.46	300.38	300.38	300.35	1109.94	.14	2.17	24.7	4.125
319.08	161.43	3.13	8.16	63.69	32.27	300.35	300.35	300.32	1109.79	.14	2.19	26.9	4.125
358.34	179.15	3.13	8.16	69.84	35.38	300.32	300.32	300.29	1109.63	.14	2.22	29.4	4.125
402.42	198.86	3.13	8.16	76.68	38.81	300.29	300.29	300.26	1109.44	.14	2.24	32.1	4.125
451.93	220.79	3.13	8.16	84.29	42.60	300.26	300.26	300.22	1109.23	.14	2.26	35.2	4.125
507.53	245.20	3.13	8.16	92.74	46.79	300.22	300.22	300.18	1108.99	.14	2.28	38.5	4.125
569.97	272.36	3.13	8.16	102.13	51.40	300.18	300.18	300.14	1108.72	.14	2.30	42.2	4.125
640.09	302.61	3.13	8.16	112.56	56.50	300.14	300.14	300.10	1108.42	.13	2.32	46.2	4.125
718.83	336.28	3.13	8.16	124.15	62.13	300.10	300.10	300.05	1108.08	.13	2.34	50.7	4.125
807.27	373.78	3.13	8.16	137.02	68.34	300.05	300.05	300.00	1107.71	.13	2.36	55.7	4.125
906.58	415.55	3.13	8.16	151.32	75.19	300.00	300.00	299.94	1107.29	.13	2.38	61.1	4.125
1018.12	462.09	3.13	8.16	167.20	82.75	299.94	299.94	299.88	1106.82	.13	2.40	67.2	4.125
1143.37	513.94	3.13	8.16	184.83	91.10	299.88	299.88	299.82	1106.31	.13	2.42	73.8	4.125
1284.04	571.73	3.13	8.16	204.42	100.31	299.81	299.81	299.74	1105.73	.13	2.43	81.2	4.125
1442.01	636.15	3.13	8.16	226.17	110.47	299.74	299.74	299.67	1105.10	.13	2.45	89.3	4.125
1619.41	707.97	3.13	8.16	250.33	121.68	299.66	299.66	299.58	1104.39	.12	2.47	98.2	4.125
1818.64	788.07	3.13	8.16	277.15	134.05	299.57	299.57	299.49	1103.61	.12	2.49	108.1	4.125
2042.38	877.39	3.13	8.16	306.93	147.69	299.48	299.48	299.39	1102.74	.12	2.50	119.0	4.125
2293.64	977.05	3.13	8.16	339.99	162.75	299.38	299.38	299.27	1101.78	.12	2.52	131.0	4.125
2575.82	1088.23	3.13	8.16	376.71	179.36	299.26	299.26	299.15	1100.73	.12	2.54	144.3	4.125
2892.71	1212.30	3.13	8.16	417.47	197.68	299.14	299.14	299.02	1099.56	.12	2.55	158.9	4.125
3248.59	1350.78	3.13	8.16	462.73	217.90	299.00	299.00	298.87	1098.26	.12	2.57	175.0	4.125
3648.25	1505.37	3.13	8.16	512.98	240.21	298.85	298.85	298.71	1096.83	.12	2.59	192.8	4.125
4097.08	1677.97	3.13	8.16	568.77	264.81	298.69	298.69	298.53	1095.26	.11	2.60	212.4	4.125
4601.13	1870.70	3.13	8.16	630.71	291.95	298.51	298.51	298.33	1093.52	.11	2.62	234.1	4.125
5167.19	2085.96	3.13	8.16	699.47	321.90	298.31	298.31	298.11	1091.60	.11	2.63	258.0	4.125
5802.88	2326.40	3.13	8.16	775.80	354.93	298.09	298.09	297.88	1089.48	.11	2.64	284.3	4.125
6516.79	2595.02	3.13	8.16	860.55	391.37	297.86	297.86	297.62	1087.14	.11	2.66	313.4	4.125
7318.52	2895.16	3.13	8.16	954.63	431.56	297.59	297.59	297.33	1084.57	.11	2.67	345.5	4.125
8218.89	3230.57	3.13	8.16	1059.08	475.90	297.30	297.30	297.01	1081.72	.11	2.68	380.9	4.125
9230.02	3605.44	3.13	8.16	1175.03	524.82	296.98	296.98	296.66	1078.59	.10	2.70	419.9	4.125
10365.55	4024.47	3.13	8.16	1303.75	578.78	296.63	296.63	296.27	1075.15	.10	2.71	462.9	4.125
11640.78	4492.93	3.13	8.16	1446.64	638.30	296.24	296.24	295.85	1071.35	.10	2.72	510.4	4.125
13072.90	5016.70	3.13	8.16	1605.27	703.95	295.81	295.81	295.38	1067.16	.10	2.73	562.8	4.125
14681.20	5602.40	3.13	8.16	1781.37	776.38	295.34	295.34	294.87	1062.55	.10	2.75	620.6	4.125
16487.37	6257.42	3.13	8.16	1976.86	856.27	294.82	294.82	294.30	1057.48	.10	2.76	684.3	4.125

1

PROCESSING SUBCLOUD 2

SUBCLOUD # 2 HISTORY FILE SOURCE # 1

MASS FRACTION	DEBRIS CARBON (G/G OBSC)	PLUME (1=PUFF, 2=PLUME)	CLOUD RISE MODEL (1=RISE, 2= NO RISE, >2=STEM)	EXTINCTION COEFFICIENT CODE	BALLISTIC SUBCLOUD (1=Y, 0=N)
.050000	.000	1.	1.	5.	0.

INITIAL OBSCURANT RADII (M)			BUOYANCY	INITIAL CLOUD	THERMAL PRODUCTION	UPWARD VELOCITY
DOWNWIND	CROSSWIND	VERTICAL	RADIUS(M)	TEMP(DEG K)	COEF (CAL/G)	(M/S)
3.32	3.32	2.49	1.16	433.30	9318.31	1.62

HEIGHT OF BURST (M)	FALL VELOCITY (M/S)	EVAPORATION/DEPOSITION FD (LONG-TERM)	DELTA (S**-1)	REFL. COEF.	MOMENTUM RADIUS (M)	HORIZONTAL VELOCITY (M/S)
7.0	.000	1.000000	.00000	1.0000	.00	.94

INITIAL MASS IN THIS PUFF = 134.2 GM

SUBCLOUD TRAJECTORY

DOWNWIND DISTANCE (M)	TIME (SEC)	CENTROID HEIGHT (M)	GAUSSIAN CLOUD STD. DEVIATIONS (M)			PEAK CLOUD TEMP. (DEG K)	MEAN CLOUD TEMP. (DEG K)	AIR TEMP. (DEG K)	AIR DENSITY (G/M**3)	CENTROID OR CM VELOCITY		CM HEIGHT (M)	EFFECTIVE BUOYANCY RADIUS (M)
			SIGMAX	SIGMAY	SIGMAZ					VERT. (M/S)	HOR. (M/S)		
.10	.09	7.15	1.59	1.59	1.20	925.79	412.00	300.73	1110.48	1.65	1.16	7.2	1.195
1.00	.69	8.11	1.91	1.88	1.44	463.96	349.96	300.70	1110.48	1.50	1.68	8.1	1.432
2.00	1.26	8.92	2.20	2.16	1.66	392.13	331.61	300.68	1110.47	1.33	1.81	9.0	1.632
4.00	2.33	10.21	2.73	2.65	2.03	346.28	317.37	300.64	1110.44	1.11	1.91	10.3	1.953
6.00	3.36	11.28	3.21	3.10	2.36	329.56	311.56	300.61	1110.39	.97	1.96	11.4	2.218
10.00	5.37	13.05	4.10	3.92	2.94	316.18	306.63	300.58	1110.32	.80	2.02	13.1	2.655
16.00	8.31	15.17	5.32	5.04	3.72	309.08	303.89	300.53	1110.20	.66	2.06	15.4	3.182
25.00	12.63	17.73	7.02	6.60	4.76	305.21	302.36	300.49	1110.06	.54	2.11	17.8	3.817

36.00	17.80	20.29	8.96	8.38	5.90	303.34	301.59	300.44	1109.86	.46	2.14	20.7	4.452
49.85	24.21	22.99	11.27	10.50	7.23	302.26	301.14	300.40	1109.69	.39	2.17	23.1	5.125
55.98	27.03	24.06	12.26	11.40	7.79	301.97	301.02	300.39	1109.62	.37	2.19	24.2	5.392
62.87	30.17	25.19	13.36	12.40	8.41	301.73	300.91	300.37	1109.53	.35	2.20	25.4	5.674
70.60	33.68	26.39	14.57	13.50	9.08	301.51	300.82	300.36	1109.43	.33	2.21	26.6	5.973
79.29	37.60	27.66	15.90	14.72	9.81	301.33	300.73	300.34	1109.34	.31	2.22	27.9	6.290
89.05	41.97	28.45	17.30	15.98	10.53	300.83	300.51	300.33	1109.29	.01	2.24	28.6	6.489
100.00	46.83	28.45	18.72	17.26	11.19	300.58	300.42	300.33	1109.29	.01	2.25	28.6	6.489
112.30	52.27	28.45	20.30	18.69	11.92	300.45	300.37	300.33	1109.28	.02	2.26	28.7	6.489
126.12	58.37	28.45	22.06	20.27	12.74	300.39	300.35	300.33	1109.27	.02	2.27	28.9	6.489
141.64	65.20	28.45	24.02	22.03	13.64	300.36	300.34	300.32	1109.26	.03	2.27	29.1	6.489
159.06	72.86	28.45	26.20	24.00	14.64	300.34	300.33	300.32	1109.25	.04	2.27	29.4	6.489
178.63	81.45	28.45	28.63	26.18	15.75	300.33	300.32	300.32	1109.22	.04	2.28	29.7	6.489
200.61	91.08	28.45	31.32	28.60	16.98	300.32	300.32	300.31	1109.20	.05	2.28	30.2	6.489
225.28	101.89	28.45	34.32	31.30	18.35	300.31	300.31	300.31	1109.16	.05	2.28	30.8	6.489
253.00	114.00	28.45	37.65	34.30	19.86	300.31	300.31	300.30	1109.11	.06	2.29	31.5	6.489
284.13	127.58	28.45	41.35	37.63	21.53	300.30	300.30	300.29	1109.06	.06	2.29	32.4	6.489
319.08	142.80	28.45	45.47	41.34	23.37	300.29	300.29	300.28	1108.99	.07	2.30	33.5	6.489
358.34	159.85	28.45	50.04	45.46	25.42	300.28	300.28	300.26	1108.90	.07	2.30	34.7	6.489
402.42	178.95	28.45	55.12	50.03	27.68	300.26	300.26	300.25	1108.80	.08	2.31	36.1	6.489
451.93	200.33	28.45	60.77	55.12	30.18	300.25	300.25	300.23	1108.69	.08	2.32	37.8	6.489
507.53	224.26	28.45	67.04	60.76	32.94	300.23	300.23	300.21	1108.56	.08	2.32	39.7	6.489
569.97	251.03	28.45	74.00	67.04	35.99	300.21	300.21	300.19	1108.40	.08	2.33	41.8	6.489
640.09	280.98	28.45	81.74	74.01	39.36	300.19	300.19	300.16	1108.23	.08	2.34	44.3	6.489
718.83	314.46	28.45	90.33	81.75	43.08	300.16	300.16	300.13	1108.02	.08	2.35	47.0	6.489
807.27	351.88	28.45	99.87	90.35	47.20	300.13	300.13	300.10	1107.80	.08	2.36	50.1	6.489
906.58	393.71	28.45	110.47	99.89	51.74	300.10	300.10	300.07	1107.54	.08	2.37	53.5	6.489
1018.12	440.44	28.45	122.24	110.50	56.76	300.06	300.06	300.03	1107.25	.08	2.39	57.3	6.489
1143.37	492.65	28.45	135.31	122.27	62.30	300.02	300.02	299.99	1106.93	.08	2.40	61.6	6.489
1284.04	550.96	28.45	149.82	135.35	68.41	299.98	299.98	299.94	1106.56	.08	2.41	66.3	6.489
1442.01	616.08	28.45	165.93	149.87	75.16	299.93	299.93	299.89	1106.16	.08	2.43	71.6	6.489
1619.41	688.81	28.45	183.82	165.99	82.62	299.88	299.88	299.83	1105.71	.08	2.44	77.4	6.489
1818.64	770.02	28.45	203.68	183.89	90.84	299.82	299.82	299.77	1105.20	.08	2.45	83.8	6.489
2042.38	860.70	28.45	225.74	203.77	99.92	299.76	299.76	299.70	1104.64	.08	2.47	91.0	6.489
2293.64	961.94	28.45	250.22	225.83	109.94	299.69	299.69	299.62	1104.02	.08	2.48	98.9	6.489
2575.82	1074.99	28.45	277.41	250.33	120.99	299.62	299.62	299.54	1103.33	.08	2.50	107.6	6.489
2892.71	1201.23	28.45	307.59	277.53	133.19	299.53	299.53	299.45	1102.56	.08	2.51	117.3	6.489
3248.59	1342.18	28.45	341.09	307.73	146.65	299.44	299.44	299.35	1101.71	.08	2.52	128.0	6.489
3648.25	1499.58	28.45	378.29	341.26	161.51	299.34	299.34	299.24	1100.77	.07	2.54	139.8	6.489
4097.08	1675.36	28.45	419.59	378.48	177.89	299.23	299.23	299.12	1099.73	.07	2.55	152.8	6.489
4601.13	1871.67	28.45	465.44	419.80	195.98	299.11	299.11	298.99	1098.58	.07	2.57	167.2	6.489
5167.19	2090.93	28.45	516.34	465.67	215.93	298.98	298.98	298.85	1097.31	.07	2.58	183.0	6.489
5802.88	2335.84	28.45	572.84	516.60	237.94	298.83	298.83	298.69	1095.90	.07	2.60	200.6	6.489
6516.79	2609.44	28.45	635.57	573.14	262.22	298.67	298.67	298.51	1094.35	.07	2.61	219.9	6.489
7318.52	2915.10	28.45	705.20	635.90	289.01	298.49	298.49	298.32	1092.64	.07	2.62	241.2	6.489
8218.89	3256.61	28.45	782.51	705.57	318.57	298.30	298.30	298.10	1090.74	.07	2.64	264.8	6.489
9230.02	3638.24	28.45	868.32	782.92	351.17	298.08	298.08	297.87	1088.66	.07	2.65	290.8	6.489
10365.55	4064.71	28.45	963.59	868.79	387.14	297.85	297.85	297.61	1086.35	.07	2.66	319.5	6.489

11640.78	4541.37	28.45	1069.35	964.11	426.82	297.59	297.59	297.33	1083.81	.07	2.68	351.1	6.489
13072.90	5074.17	28.45	1186.74	1069.92	470.60	297.30	297.30	297.02	1081.01	.07	2.69	386.0	6.489
14681.20	5669.78	28.45	1317.07	1187.39	518.88	296.99	296.99	296.67	1077.93	.06	2.70	424.5	6.489
16487.37	6335.68	28.45	1461.74	1317.79	572.15	296.64	296.64	296.29	1074.53	.06	2.71	467.0	6.489

1

PROCESSING SUBCLOUD 3

SUBCLOUD # 3 HISTORY FILE SOURCE # 1

MASS FRACTION	DEBRIS CARBON (G/G OBSC)	PLUME (1=PUFF, 2=PLUME)	CLOUD RISE MODEL (1=RISE, 2= NO RISE, >2=STEM)	EXTINCTION COEFFICIENT CODE	BALLISTIC SUBCLOUD (1=Y, 0=N)
.025000	.000	1.	12.	5.	0.

INITIAL OBSCURANT RADII (M)			BUOYANCY	INITIAL CLOUD	THERMAL PRODUCTION	UPWARD VELOCITY
DOWNWIND	CROSSWIND	VERTICAL	RADIUS(M)	TEMP(DEG K)	COEF (CAL/G)	(M/S)
3.32	3.32	2.49	.00	.00	9318.31	.00

HEIGHT OF BURST (M)	FALL VELOCITY (M/S)	EVAPORATION/DEPOSITION FD (LONG-TERM)	DELTA (S**-1)	REFL. COEF.	MOMENTUM RADIUS (M)	HORIZONTAL VELOCITY (M/S)
.0	.000	1.000000	.00000	1.0000	.00	.00

INITIAL MASS IN THIS PUFF = 67.1 GM

SUBCLOUD TRAJECTORY

DOWNWIND		CENTROID	GAUSSIAN CLOUD		PEAK CLOUD	MEAN CLOUD	AIR	AIR	CENTROID OR CM VELOCITY		CM	EFFECTIVE BUOYANCY
DISTANCE	TIME	HEIGHT	STD. DEVIATIONS (M)		TEMP.	TEMP.	TEMP.	DENSITY	VERT.	HOR.	HEIGHT	RADIUS

(M)	(SEC)	(M)	SIGMAX	SIGMAY	SIGMAZ	(DEG K)	(DEG K)	(DEG K)	(G/M**3)	(M/S)	(M/S)	(M)	(M)
.10	.14	3.22	1.01	5.92	2.34	300.46	300.46	300.46	1112.01	24.52	1.62	3.2	5.175
1.00	1.04	4.19	1.38	6.18	2.59	300.37	300.37	300.37	1112.22	1.09	1.71	4.2	6.028
2.00	1.90	4.96	1.69	6.46	2.82	300.32	300.32	300.32	1112.31	.91	1.77	5.0	6.724
4.00	3.38	6.03	2.14	6.96	3.21	300.26	300.26	300.26	1112.39	.72	1.84	6.0	7.791
6.00	4.76	6.88	2.51	7.44	3.53	300.22	300.22	300.22	1112.42	.62	1.88	6.9	8.680
10.00	7.28	8.24	3.14	8.36	4.08	300.17	300.17	300.17	1112.44	.54	1.94	8.2	10.195
16.00	10.82	9.73	3.88	9.59	4.85	300.12	300.12	300.12	1112.43	.42	1.99	9.7	12.126
25.00	15.92	11.30	4.77	11.21	5.96	300.08	300.08	300.08	1112.38	.31	2.04	11.3	14.659
36.00	21.92	12.87	5.73	13.09	7.17	300.04	300.04	300.04	1112.32	.26	2.07	12.9	17.448
49.85	29.22	14.66	6.86	15.39	8.50	300.00	300.00	300.00	1112.24	.24	2.11	14.7	20.693
55.98	32.42	15.40	7.34	16.40	9.06	299.99	299.99	299.99	1112.20	.23	2.12	15.4	22.074
62.87	35.92	16.20	7.85	17.51	9.62	299.98	299.98	299.98	1112.15	.23	2.14	16.2	23.547
70.60	39.82	16.99	8.40	18.74	10.15	299.96	299.96	299.96	1112.10	.20	2.15	17.0	25.066
79.29	44.22	17.69	8.95	20.09	10.56	299.95	299.95	299.95	1112.06	.16	2.16	17.7	26.550
89.05	49.02	18.31	9.50	21.55	10.90	299.94	299.94	299.94	1112.02	.13	2.17	18.3	28.022
100.00	54.32	19.01	10.12	23.16	11.26	299.93	299.93	299.93	1111.97	.13	2.18	19.0	29.628
112.30	60.22	19.77	10.79	24.96	11.65	299.91	299.91	299.91	1111.92	.13	2.19	19.8	31.391
126.12	67.02	20.66	11.57	27.02	12.08	299.90	299.90	299.90	1111.86	.13	2.20	20.7	33.390
141.64	74.22	21.77	12.20	29.21	12.52	299.88	299.88	299.88	1111.79	.15	2.21	21.8	35.298
159.06	82.42	23.14	12.81	31.70	12.99	299.86	299.86	299.86	1111.69	.17	2.23	23.1	37.315
178.63	91.62	24.67	13.49	34.49	13.48	299.84	299.84	299.84	1111.58	.17	2.24	24.7	39.528
200.61	101.82	26.35	14.24	37.58	13.98	299.82	299.82	299.82	1111.45	.17	2.26	26.4	41.921
225.28	113.22	28.22	15.07	41.02	14.49	299.79	299.79	299.79	1111.31	.16	2.28	28.2	44.524
253.00	125.82	30.27	16.00	44.81	15.01	299.76	299.76	299.76	1111.15	.16	2.29	30.3	47.319
284.13	140.02	32.56	17.03	49.07	15.53	299.73	299.73	299.73	1110.97	.16	2.31	32.6	50.372
319.08	155.82	35.09	18.18	53.81	16.04	299.70	299.70	299.70	1110.77	.16	2.33	35.1	53.657
358.34	173.22	37.85	19.44	59.00	16.53	299.67	299.67	299.67	1110.55	.16	2.34	37.8	57.147
402.42	192.82	40.93	20.86	64.84	17.00	299.63	299.63	299.63	1110.30	.16	2.36	40.9	60.932
451.93	214.62	44.33	22.42	71.31	17.44	299.59	299.59	299.59	1110.02	.16	2.38	44.3	64.975
507.53	238.82	48.07	24.15	78.47	17.84	299.55	299.55	299.55	1109.70	.15	2.39	48.1	69.273
569.97	266.02	52.24	26.07	86.49	18.19	299.50	299.50	299.50	1109.35	.15	2.41	52.2	73.887
640.09	296.52	56.87	28.22	95.45	18.49	299.45	299.45	299.45	1108.96	.15	2.43	56.9	78.812
718.83	330.02	61.91	30.56	105.27	18.71	299.39	299.39	299.39	1108.53	.15	2.44	61.9	83.942
807.27	367.52	67.49	33.16	116.21	18.85	299.33	299.33	299.33	1108.05	.15	2.46	67.5	89.370
906.58	409.02	73.61	36.01	128.28	18.90	299.26	299.26	299.26	1107.52	.15	2.48	73.6	95.022
1018.12	456.02	80.47	39.22	141.89	18.86	299.19	299.19	299.19	1106.92	.15	2.49	80.5	101.015
1143.37	508.02	87.98	42.73	156.89	18.70	299.11	299.11	299.11	1106.27	.14	2.51	88.0	107.178
1284.04	565.52	96.21	46.58	173.41	18.42	299.03	299.03	299.03	1105.55	.14	2.52	96.2	113.467
1442.01	630.52	105.41	50.89	192.00	18.00	298.93	298.93	298.93	1104.74	.14	2.54	105.4	119.974
1619.41	702.52	115.49	55.62	212.50	17.44	298.83	298.83	298.83	1103.85	.14	2.56	115.5	126.480
1818.64	783.52	126.71	60.89	235.46	16.71	298.71	298.71	298.71	1102.86	.14	2.57	126.7	132.993
2042.38	872.52	138.90	66.62	260.56	15.84	298.59	298.59	298.59	1101.78	.14	2.59	138.9	139.212
2293.64	973.52	152.58	73.05	288.91	14.78	298.45	298.45	298.45	1100.56	.14	2.60	152.6	145.194
2575.82	1084.52	167.45	80.04	319.91	13.57	298.30	298.30	298.30	1099.24	.13	2.61	167.4	150.507
2892.71	1209.52	184.00	87.82	354.64	12.21	298.13	298.13	298.13	1097.77	.13	2.63	184.0	155.102
3248.59	1348.52	202.19	96.38	393.04	10.77	297.95	297.95	297.95	1096.16	.13	2.64	202.2	158.768

3648.25	1504.52	222.36	105.88	435.91	9.37	297.75	297.75	297.75	1094.36	.13	2.66	222.4	161.870
4097.08	1677.52	244.46	116.28	483.18	8.30	297.53	297.53	297.53	1092.40	.13	2.67	244.5	166.007
4601.13	1871.52	268.95	127.81	535.87	8.04	297.29	297.29	297.29	1090.22	.13	2.68	268.9	175.483
5167.19	2087.52	295.87	140.50	594.19	9.06	297.02	297.02	297.02	1087.82	.12	2.70	295.9	195.018
5802.88	2329.52	325.67	154.53	659.13	11.40	296.72	296.72	296.72	1085.17	.12	2.71	325.7	224.949
6516.79	2599.52	358.49	170.00	731.13	14.81	296.40	296.40	296.40	1082.26	.12	2.72	358.5	262.233
7318.52	2901.52	394.74	187.08	811.15	19.08	296.04	296.04	296.04	1079.04	.12	2.73	394.7	304.941
8218.89	3238.52	434.67	205.90	899.86	24.11	295.65	295.65	295.65	1075.50	.12	2.74	434.7	352.279
9230.02	3615.52	478.76	226.68	998.44	29.87	295.21	295.21	295.21	1071.60	.12	2.75	478.8	404.405
10365.55	4036.52	527.35	249.59	1107.77	36.37	294.73	294.73	294.73	1067.31	.12	2.77	527.4	461.560
11640.78	4507.52	581.00	274.87	1229.24	43.65	294.20	294.20	294.20	1062.58	.11	2.78	581.0	524.355
13072.90	5034.52	640.22	302.79	1364.20	51.76	293.62	293.62	293.62	1057.37	.11	2.79	640.2	593.394
14681.20	5622.52	705.41	302.79	1513.70	60.74	292.98	292.98	292.98	1051.65	.11	2.80	705.4	593.394
16487.37	6281.52	777.50	302.79	1680.06	70.62	292.27	292.27	292.27	1045.34	.11	2.81	777.5	593.394

TOTAL TRANMITANCE FOR ALL SOURCES IS: .0000E+00

```
WAVL      1.06
 NOTE: THAT THE ABOVE CARD WAS MODIFIED FOR CONSISTENCY TO:
WAVL       .1060E+01 .1060E+01 .0000E+00
```

	BEGINNING	ENDING
WAVENUMBER (CM**-1)	9433.963	9433.963
WAVELENGTH (MICROMETERS)	1.060	1.060
FREQUENCY (GHZ)	283018.875	283018.875

**** EOSAEL WARNING ****
VISIBILITY AND EXTINCTION = 0.0, VISIBILITY CHANGED TO 10.0 KM

VISIBILITY
10.00 KM

RUN NUMBER 2
1

****
* *
* COMBIC *
* PHASE 2 *
* *
****

PHAS .2000E+01 .5000E+01 .6000E+01 .1200E+02 .9000E+01 .0000E+00 .1000E+01
FILE 9.0 his.18a1

COMBIC CLOUD HISTORY ON UNIT 9 OPENED TO: his.18a1
NAME
Testing L8A1 self-screening RP smoke grenades
ORIG 0.0 0.0 0.0 90.0 265.0 0.0 0.0
1

METEOROLOGICAL CONDITIONS FROM HISTORY FILE

WINDSPEED (10 M) = 2.0 M/S WIND DIRECTION = 202.4 DEG WRT N
RELATIVE HUMIDITY = 90.0 PERCENT PASQUILL CATEGORY = B (1.60)
AIR TEMPERATURE = 300.6 DEG K AIR PRESSURE = 963. MB
SURFACE ROUGHNESS = .1000 M AIR DENSITY = 1110. G/M**3

MASS EXTINCTION COEFFICIENTS FROM HISTORY FILE (M**2/GRAM)

OBSCURANT CODE	WAVELENGTH (MICROMETERS) .4-.7	.7-1.2	1.06	3.-5.	8.-12.	10.6	94 GHZ
1	3.2280	2.3638	2.1094	.4127	.3043	.2792	.0010
2	3.2280	2.3638	2.1094	.4127	.3043	.2792	.0010
3	2.1520	2.1368	2.0302	.2668	.0601	.0750	.0010
4	6.8510	4.5920	3.4970	.2450	.0200	.0180	.0010
5	3.2280	2.3638	2.1094	.4127	.3043	.2792	.0010
6	1.8600	1.6300	1.4000	1.7900	1.6800	1.6800	.0010
7	1.8600	1.6300	1.4000	1.7900	1.6800	1.6800	.0010
8	5.6500	4.0800	3.2500	.2450	.0230	.0270	.0010
9	.3200	.3000	.2900	.2700	.2500	.2500	.0010
10	.3200	.2900	.2600	.2700	.2600	.2400	.0010
11	.0350	.0360	.0370	.0350	.0380	.0360	.0010
12	1.5000	1.4600	1.4200	.7500	.3200	.3000	.0010
13	.0010	.0010	.0010	.0010	.0010	.0010	.0004
14	6.1000	3.7500	2.9400	1.3500	1.0100	1.0000	.0020
15	6.8510	4.5920	1.4300	.0540	.0200	.0180	.0010
16	5.3700	2.9000	2.1000	.0900	.0900	.0700	.0010
17	6.2000	3.5000	2.5000	.2300	.0500	.0480	.0010
18	3.3300	2.7500	2.6600	.2600	.3200	.2300	.0010
19	1.3000	1.7400	1.7000	.0800	.1600	.3800	.0010
20	.0000	.0000	.0000	.0000	.0000	.0000	.0000
21	.0000	.0000	.0000	.0000	.0000	.0000	.0000
22	.0000	.0000	.0000	.0000	.0000	.0000	.0000
23	.0000	.0000	.0000	.0000	.0000	.0000	.0000
24	.0000	.0000	.0000	.0000	.0000	.0000	.0000
25	.0000	.0000	.0000	.0000	.0000	.0000	.0000
26	.0000	.0000	.0000	.0000	.0000	.0000	.0000
27	.0000	.0000	.0000	.0000	.0000	.0000	.0000
28	.0000	.0000	.0000	.0000	.0000	.0000	.0000
29	.0000	.0000	.0000	.0000	.0000	.0000	.0000
30	.0000	.0000	.0000	.0000	.0000	.0000	.0000

1

HISTORY FILE CONTAINS INFORMATION ON 1 SOURCES

SOURCE ID	NUMBER OF SUBCLOUDS	XN SCALE FACTOR	FILL WEIGHT	MENU NUMBER	OBSC TYPE	EFFICIENCY PERCENT	YIELD FACTOR	NUMBER OF SUB-MUNITIONS
1	3	1.00	.79	0.	5.	95.00	7.85	1.00

SOURCE ID	BURN DURATION (SEC)	VEHICLE SPEED (M/S)	VEHICLE DIRECTION DEG	BARRAGE ROUNDS PER SEC	BARRAGE DURATION (SEC)	BARRAGE IMPACT X (M)	BARRAGE REGION Y (M)	HIGH-EXP SOIL TYPE	HIGH-EXP DOB (M)
1	658.	.0	0.	.0	0.	0.	0.	.0	.00

WIND DIRECTION ALTERED TO 265.0 DEG WRT N

SLOC	1.0	1.0	0.0	300.0	0.0	0.0	2.0

SOURCES ADDED

SOURCE UNIT	ID	XN SCALING	ACTIVE TIME LIMIT BEGIN	ACTIVE TIME LIMIT END	POSITION (ORIGINAL SYSTEM) X	Y	Z	POSITION (ROTATED SYSTEM) X	Y	Z	MOVING SOURCE SPEED	DIRECTION
1	1	1.000	.00	300.00	.0	.0	2.0	.0	.0	2.0	.00	-359.8
SLOC		1.0	1.0	0.0	300.0	5.0	0.0	2.0				
2	1	1.000	.00	300.00	5.0	.0	2.0	5.0	-.4	2.0	.00	-359.8
SLOC		1.0	1.0	0.0	300.0	10.0	0.0	2.0				
3	1	1.000	.00	300.00	10.0	.0	2.0	10.0	-.9	2.0	.00	-359.8
OLOC		1.0	10.0	100.0	2.0	0.0	300.0	0.0				
TLOC		1.0	10.0	-100.0	2.0	1.0	0.0	0.0				

NEW OR ALTERED LINES OF SIGHT

OBS NO.	TGT NO.	ORIGINAL SYSTEM OBSERVER (M) X	Y	Z	TARGET (M) X	Y	Z	ROTATED SYSTEM OBSERVER (M) X	Y	Z	TARGET (M) X	Y	Z	TIME (SEC) START	END
1	1	10.0	100.0	2.0	10.0	-100.0	2.0	18.7	98.7	2.0	1.2	-100.5	2.0	.0	300.0
LIST		2.0	0.0	300.0	5.0										
DONE		0.0	0.0	0.0	0.0	0.0	0.0	0.0							

1

TIME (SEC)	OBS NO.	TARG NO.	SUBCLOUD CL (G/M**2)	CLOUD NUMBER	TRANSMISSION .4-.7	.7-1.2	1.06	3.-5.	8.-12.	10.6	94 GHZ	PATH-LENGTH METERS	MAX. CONTRIBUTION TO CLOUD X	Y	Z	SIGX	SIGY	SIGZ	WBAR
			1.151	3								58.1	11.1	-.9	2.6	.0	8.7	2.2	6.47E+00
			.481	2								63.0	9.6	-.4	3.4	.0	9.8	3.2	4.22E+00
			.031	2								19.8	11.4	-.4	11.1	2.6	7.5	3.6	6.71E+01
			.317	1								67.8	9.6	.0	4.1	.0	11.2	4.2	3.75E+00
5.0	1	1	1.980	3	.002	.009	.015	.442	.547	.575	.998								
			2.031	3								60.1	11.2	-.9	2.8	.0	8.7	2.2	1.18E+01
			.860	2								66.0	9.6	-.4	3.9	.0	9.8	3.2	8.14E+00
			.552	1								72.0	9.6	.0	4.8	.0	11.2	4.2	7.17E+00

			.016	1								24.3	14.6	.0	13.5	3.7	9.3	4.7	6.72E+01
10.0	1	1	3.459	3	.000	.000	.001	.240	.349	.381	.997								
			2.166	3								60.8	11.2	-.9	2.9	.0	8.7	2.2	1.27E+01
			1.182	2								67.1	9.6	-.4	4.1	.0	9.8	3.2	1.15E+01
			.769	1								73.5	9.6	.0	5.0	.0	11.2	4.2	1.04E+01
15.0	1	1	4.117	3	.000	.000	.000	.183	.286	.317	.996								
			2.020	3								61.1	11.2	-.9	2.8	.0	8.7	2.2	1.18E+01
			1.172	2								67.6	9.6	-.4	4.0	.0	9.8	3.2	1.14E+01
			.908	1								74.2	9.6	.0	5.2	.0	11.2	4.2	1.27E+01
20.0	1	1	4.100	3	.000	.000	.000	.184	.287	.318	.996								
			1.998	3								61.3	11.2	-.9	2.8	.0	8.7	2.2	1.17E+01
			1.146	2								68.0	9.6	-.4	4.0	.0	9.8	3.2	1.11E+01
			.868	1								74.6	9.6	.0	5.1	.0	11.2	4.2	1.20E+01
25.0	1	1	4.011	3	.000	.000	.000	.191	.295	.326	.996								
			1.866	3								61.5	11.2	-.9	2.8	.0	8.7	2.2	1.09E+01
			1.115	2								68.2	9.6	-.4	4.0	.0	9.8	3.2	1.08E+01
			.851	1								74.9	9.6	.0	5.1	.0	11.2	4.2	1.17E+01
30.0	1	1	3.832	3	.000	.000	.000	.206	.312	.343	.996								
			1.841	3								61.6	11.2	-.9	2.8	.0	8.7	2.2	1.07E+01
			1.057	2								68.4	9.6	-.4	4.0	.0	9.8	3.2	1.02E+01
			.805	1								75.2	9.6	.0	5.1	.0	11.2	4.2	1.10E+01
35.0	1	1	3.702	3	.000	.000	.000	.217	.324	.356	.996								
			1.767	3								61.6	11.2	-.9	2.8	.0	8.7	2.2	1.03E+01
			1.033	2								68.5	9.6	-.4	4.0	.0	9.8	3.2	9.92E+00
			.791	1								75.3	9.6	.0	5.0	.0	11.2	4.2	1.08E+01
40.0	1	1	3.591	3	.000	.000	.001	.227	.335	.367	.996								
			1.682	3								61.7	11.2	-.9	2.8	.0	8.7	2.2	9.74E+00
			.967	2								68.6	9.6	-.4	3.9	.0	9.8	3.2	9.24E+00
			.766	1								75.5	9.6	.0	5.0	.0	11.2	4.2	1.04E+01
45.0	1	1	3.415	3	.000	.000	.001	.244	.354	.385	.997								
			1.651	3								61.7	11.2	-.9	2.8	.0	8.7	2.2	9.55E+00
			.956	2								68.6	9.6	-.4	3.9	.0	9.8	3.2	9.11E+00
			.735	1								75.5	9.6	.0	5.0	.0	11.2	4.2	9.87E+00
50.0	1	1	3.341	3	.000	.000	.001	.252	.362	.393	.997								
			1.536	3								61.7	11.2	-.9	2.7	.0	8.7	2.2	8.85E+00
			.918	2								68.7	9.6	-.4	3.9	.0	9.8	3.2	8.73E+00
			.720	1								75.6	9.6	.0	5.0	.0	11.2	4.2	9.64E+00
55.0	1	1	3.173	3	.000	.001	.001	.270	.381	.412	.997								
			1.532	3								61.8	11.2	-.9	2.7	.0	8.7	2.2	8.82E+00
			.883	2								68.7	9.6	-.4	3.9	.0	9.8	3.2	8.37E+00
			.681	1								75.6	9.6	.0	4.9	.0	11.2	4.2	9.05E+00
60.0	1	1	3.096	3	.000	.001	.001	.279	.390	.421	.997								
			1.442	3								61.8	11.2	-.9	2.7	.0	8.7	2.2	8.28E+00
			.858	2								68.7	9.6	-.4	3.9	.0	9.8	3.2	8.12E+00
			.667	1								75.6	9.6	.0	4.9	.0	11.2	4.2	8.84E+00
65.0	1	1	2.968	3	.000	.001	.002	.294	.405	.437	.997								
			1.401	3								61.8	11.2	-.9	2.7	.0	8.7	2.2	8.03E+00
			.808	2								68.7	9.6	-.4	3.9	.0	9.8	3.2	7.61E+00

			.631	1								75.6	9.6	.0	4.9	.0	11.2	4.2	8.32E+00
70.0	1	1	2.840	3	.000	.001	.003	.310	.421	.452	.997								
			1.361	3								61.8	11.2	-.9	2.7	.0	8.7	2.2	7.79E+00
			.793	2								68.7	9.6	-.4	3.9	.0	9.8	3.2	7.45E+00
			.617	1								75.6	9.6	.0	4.8	.0	11.2	4.2	8.11E+00
75.0	1	1	2.771	3	.000	.001	.003	.319	.430	.461	.997								
			1.277	3								61.7	11.2	-.9	2.7	.0	8.7	2.2	7.29E+00
			.754	2								68.7	9.6	-.4	3.8	.0	9.8	3.2	7.01E+00
			.604	1								75.6	9.6	.0	4.8	.0	11.2	4.2	7.92E+00
80.0	1	1	2.635	3	.000	.002	.004	.337	.448	.479	.997								
			1.262	3								61.7	11.2	-.9	2.7	.0	8.7	2.2	7.20E+00
			.742	2								68.6	9.6	-.4	3.8	.0	9.8	3.2	6.87E+00
			.570	1								75.5	9.6	.0	4.8	.0	11.2	4.2	7.43E+00
85.0	1	1	2.574	3	.000	.002	.004	.346	.457	.487	.997								
			1.173	3								61.7	11.2	-.9	2.7	.0	8.7	2.2	6.67E+00
			.723	2								68.6	9.6	-.4	3.8	.0	9.8	3.2	6.67E+00
			.558	1								75.5	9.6	.0	4.8	.0	11.2	4.2	7.26E+00
90.0	1	1	2.454	3	.000	.003	.006	.363	.474	.504	.998								
			1.163	3								61.7	11.2	-.9	2.7	.0	8.7	2.2	6.62E+00
			.690	2								68.6	9.6	-.4	3.7	.0	9.8	3.2	6.31E+00
			.525	1								75.5	9.6	.0	4.7	.0	11.2	4.2	6.79E+00
95.0	1	1	2.379	3	.000	.004	.007	.375	.485	.515	.998								
			1.109	3								61.7	11.2	-.9	2.6	.0	8.7	2.2	6.30E+00
			.675	2								68.6	9.6	-.4	3.7	.0	9.8	3.2	6.14E+00
			.515	1								75.4	9.6	.0	4.7	.0	11.2	4.2	6.65E+00
100.0	1	1	2.299	3	.001	.004	.008	.387	.497	.526	.998								
			1.059	3								61.7	11.2	-.9	2.6	.0	8.7	2.2	6.01E+00
			.636	2								68.5	9.6	-.4	3.6	.0	9.8	3.2	5.74E+00
			.497	1								75.4	9.6	.0	4.7	.0	11.2	4.2	6.37E+00
105.0	1	1	2.193	3	.001	.006	.010	.404	.513	.542	.998								
			1.036	3								61.6	11.2	-.9	2.6	.0	8.7	2.2	5.87E+00
			.628	2								68.5	9.6	-.4	3.6	.0	9.8	3.2	5.66E+00
			.482	1								75.4	9.6	.0	4.6	.0	11.2	4.2	6.12E+00
110.0	1	1	2.146	3	.001	.006	.011	.412	.520	.549	.998								
			.964	3								61.6	11.2	-.9	2.6	.0	8.7	2.2	5.45E+00
			.602	2								68.5	9.6	-.4	3.6	.0	9.8	3.2	5.39E+00
			.474	1								75.3	9.6	.0	4.6	.0	11.2	4.2	5.98E+00
115.0	1	1	2.040	3	.001	.008	.014	.431	.538	.566	.998								
			.959	3								61.6	11.2	-.9	2.6	.0	8.7	2.2	5.42E+00
			.584	2								68.4	9.6	-.4	3.6	.0	9.8	3.2	5.21E+00
			.451	1								75.3	9.6	.0	4.5	.0	11.2	4.2	5.63E+00
120.0	1	1	1.994	3	.002	.009	.015	.439	.545	.573	.998								
			.898	3								61.6	11.2	-.9	2.6	.0	8.7	2.2	5.07E+00
			.568	2								68.4	9.6	-.4	3.5	.0	9.8	3.2	5.05E+00
			.443	1								75.2	9.6	.0	4.5	.0	11.2	4.2	5.50E+00
125.0	1	1	1.909	3	.002	.011	.018	.455	.559	.587	.998								
			.877	3								61.6	11.2	-.9	2.6	.0	8.7	2.2	4.94E+00
			.538	2								68.4	9.6	-.4	3.5	.0	9.8	3.2	4.75E+00

			.419	1								75.2	9.6	.0	4.4	.0	11.2	4.2	5.16E+00
130.0	1	1	1.834	3	.003	.013	.021	.469	.572	.599	.998								
			.848	3								61.5	11.2	-.9	2.6	.0	8.7	2.2	4.78E+00
			.527	2								68.3	9.6	-.4	3.5	.0	9.8	3.2	4.65E+00
			.413	1								75.1	9.6	.0	4.4	.0	11.2	4.2	5.06E+00
135.0	1	1	1.788	3	.003	.015	.023	.478	.580	.607	.998								
			.797	3								61.5	11.2	-.9	2.6	.0	8.7	2.2	4.48E+00
			.495	2								68.3	9.6	-.4	3.4	.0	9.8	3.2	4.34E+00
			.403	1								75.1	9.6	.0	4.3	.0	11.2	4.2	4.92E+00
140.0	1	1	1.695	3	.004	.018	.028	.497	.597	.623	.998								
			.785	3								61.5	11.2	-.9	2.6	.0	8.7	2.2	4.41E+00
			.489	2								68.3	9.6	-.4	3.4	.0	9.8	3.2	4.28E+00
			.384	1								75.1	9.6	.0	4.3	.0	11.2	4.2	4.65E+00
145.0	1	1	1.658	3	.005	.020	.030	.504	.604	.629	.998								
			.726	3								61.5	11.2	-.9	2.6	.0	8.7	2.2	4.07E+00
			.474	2								68.2	9.6	-.4	3.4	.0	9.8	3.2	4.14E+00
			.377	1								75.0	9.6	.0	4.3	.0	11.2	4.2	4.55E+00
150.0	1	1	1.576	3	.006	.024	.036	.522	.619	.644	.998								
			.724	3								61.5	11.2	-.9	2.6	.0	8.7	2.2	4.07E+00
			.452	2								68.2	9.6	-.4	3.4	.0	9.8	3.2	3.93E+00
			.357	1								75.0	9.6	.0	4.2	.0	11.2	4.2	4.27E+00
155.0	1	1	1.532	3	.007	.027	.039	.531	.627	.652	.998								
			.685	3								61.4	11.2	-.9	2.5	.0	8.7	2.2	3.84E+00
			.440	2								68.2	9.6	-.4	3.4	.0	9.8	3.2	3.82E+00
			.350	1								74.9	9.6	.0	4.2	.0	11.2	4.2	4.18E+00
160.0	1	1	1.475	3	.009	.031	.045	.544	.638	.662	.999								
			.658	3								61.4	11.2	-.9	2.5	.0	8.7	2.2	3.69E+00
			.413	2								68.1	9.6	-.4	3.3	.0	9.8	3.2	3.57E+00
			.335	1								74.9	9.6	.0	4.1	.0	11.2	4.2	3.98E+00
165.0	1	1	1.405	3	.011	.036	.052	.560	.652	.675	.999								
			.641	3								61.4	11.2	-.9	2.5	.0	8.7	2.2	3.59E+00
			.407	2								68.1	9.6	-.4	3.3	.0	9.8	3.2	3.51E+00
			.324	1								74.8	9.6	.0	4.1	.0	11.2	4.2	3.84E+00
170.0	1	1	1.372	3	.012	.039	.055	.568	.659	.682	.999								
			.597	3								61.4	11.2	-.9	2.5	.0	8.7	2.2	3.34E+00
			.386	2								68.1	9.6	-.4	3.3	.0	9.8	3.2	3.33E+00
			.318	1								74.8	9.6	.0	4.1	.0	11.2	4.2	3.75E+00
175.0	1	1	1.301	3	.015	.046	.064	.584	.673	.695	.999								
			.593	3								61.4	11.2	-.9	2.5	.0	8.7	2.2	3.32E+00
			.375	2								68.1	9.6	-.4	3.3	.0	9.8	3.2	3.23E+00
			.300	1								74.7	9.6	.0	4.0	.0	11.2	4.2	3.53E+00
180.0	1	1	1.268	3	.017	.050	.069	.592	.680	.702	.999								
			.552	3								61.3	11.2	-.9	2.5	.0	8.7	2.2	3.09E+00
			.365	2								68.0	9.6	-.4	3.3	.0	9.8	3.2	3.13E+00
			.294	1								74.7	9.6	.0	4.0	.0	11.2	4.2	3.45E+00
185.0	1	1	1.211	3	.020	.057	.078	.607	.692	.713	.999								
			.542	3								61.3	11.2	-.9	2.5	.0	8.7	2.2	3.03E+00
			.344	2								68.0	9.6	-.4	3.3	.0	9.8	3.2	2.95E+00

			.276	1								74.7	9.6	.0	4.0	.0	11.2	4.2	3.22E+00
190.0	1	1	1.163	3	.023	.064	.086	.619	.702	.723	.999								
			.521	3								61.3	11.2	-.9	2.5	.0	8.7	2.2	2.91E+00
			.337	2								68.0	9.6	-.4	3.3	.0	9.8	3.2	2.88E+00
			.272	1								74.6	9.6	.0	4.0	.0	11.2	4.2	3.16E+00
195.0	1	1	1.130	3	.026	.069	.092	.627	.709	.730	.999								
			.492	3								61.3	11.2	-.9	2.5	.0	8.7	2.2	2.75E+00
			.314	2								67.9	9.6	-.4	3.2	.0	9.8	3.2	2.68E+00
			.263	1								74.6	9.6	.0	3.9	.0	11.2	4.2	3.06E+00
200.0	1	1	1.069	3	.032	.080	.105	.643	.722	.742	.999								
			.483	3								61.3	11.2	-.9	2.5	.0	8.7	2.2	2.70E+00
			.310	2								67.9	9.6	-.4	3.2	.0	9.8	3.2	2.64E+00
			.251	1								74.5	9.6	.0	3.9	.0	11.2	4.2	2.90E+00
205.0	1	1	1.045	3	.034	.085	.110	.650	.728	.747	.999								
			.446	3								61.2	11.2	-.9	2.5	.0	8.7	2.2	2.49E+00
			.299	2								67.9	9.6	-.4	3.2	.0	9.8	3.2	2.54E+00
			.245	1								74.5	9.6	.0	3.9	.0	11.2	4.2	2.84E+00
210.0	1	1	.991	3	.041	.096	.124	.664	.740	.758	.999								
			.446	3								61.2	11.2	-.9	2.5	.0	8.7	2.2	2.49E+00
			.286	2								67.8	9.6	-.4	3.2	.0	9.8	3.2	2.43E+00
			.231	1								74.5	9.6	.0	3.8	.0	11.2	4.2	2.66E+00
215.0	1	1	.964	3	.045	.102	.131	.672	.746	.764	.999								
			.420	3								61.2	11.2	-.9	2.5	.0	8.7	2.2	2.34E+00
			.278	2								67.8	9.6	-.4	3.2	.0	9.8	3.2	2.36E+00
			.226	1								74.4	9.6	.0	3.8	.0	11.2	4.2	2.60E+00
220.0	1	1	.924	3	.051	.113	.142	.683	.755	.773	.999								
			.405	3								61.2	11.2	-.9	2.5	.0	8.7	2.2	2.26E+00
			.261	2								67.8	9.6	-.4	3.2	.0	9.8	3.2	2.20E+00
			.214	1								74.4	9.6	.0	3.8	.0	11.2	4.2	2.46E+00
225.0	1	1	.880	3	.058	.125	.156	.695	.765	.782	.999								
			.394	3								61.2	11.2	-.9	2.5	.0	8.7	2.2	2.19E+00
			.256	2								67.8	9.6	-.4	3.2	.0	9.8	3.2	2.16E+00
			.209	1								74.3	9.6	.0	3.8	.0	11.2	4.2	2.39E+00
230.0	1	1	.859	3	.063	.131	.163	.702	.770	.787	.999								
			.368	3								61.1	11.2	-.9	2.5	.0	8.7	2.2	2.05E+00
			.241	2								67.7	9.6	-.4	3.1	.0	9.8	3.2	2.04E+00
			.204	1								74.3	9.6	.0	3.8	.0	11.2	4.2	2.33E+00
235.0	1	1	.813	3	.072	.146	.180	.715	.781	.797	.999								
			.364	3								61.1	11.2	-.9	2.5	.0	8.7	2.2	2.02E+00
			.236	2								67.7	9.6	-.4	3.1	.0	9.8	3.2	1.99E+00
			.192	1								74.3	9.6	.0	3.7	.0	11.2	4.2	2.19E+00
240.0	1	1	.792	3	.078	.154	.188	.721	.786	.802	.999								
			.339	3								61.1	11.2	-.9	2.5	.0	8.7	2.2	1.88E+00
			.229	2								67.7	9.6	-.4	3.1	.0	9.8	3.2	1.93E+00
			.188	1								74.2	9.6	.0	3.7	.0	11.2	4.2	2.14E+00
245.0	1	1	.755	3	.087	.168	.203	.732	.795	.810	.999								
			.334	3								61.1	11.2	-.9	2.5	.0	8.7	2.2	1.86E+00
			.216	2								67.6	9.6	-.4	3.1	.0	9.8	3.2	1.82E+00

			.176	1									74.2	9.6	.0	3.7	.0	11.2	4.2	2.00E+00
250.0	1	1	.726	3	.096	.180	.216	.741	.802	.816	.999									
			.320	3									61.1	11.2	-.9	2.4	.0	8.7	2.2	1.77E+00
			.210	2									67.6	9.6	-.4	3.1	.0	9.8	3.2	1.77E+00
			.173	1									74.2	9.6	.0	3.7	.0	11.2	4.2	1.96E+00
255.0	1	1	.703	3	.103	.190	.227	.748	.807	.822	.999									
			.304	3									61.1	11.2	-.9	2.4	.0	8.7	2.2	1.68E+00
			.196	2									67.6	9.6	-.4	3.1	.0	9.8	3.2	1.65E+00
			.166	1									74.1	9.6	.0	3.7	.0	11.2	4.2	1.88E+00
260.0	1	1	.666	3	.117	.207	.245	.760	.817	.830	.999									

1

TIME	OBS	TARG	SUBCLOUD CL	CLOUD NUMBER	TRANSMISSION							PATH-LENGTH	MAX. CONTRIBUTION TO CLOUD					
(SEC)	NO.	NO.	(G/M**2)		.4-.7	.7-1.2	1.06	3.-5.	8.-12.	10.6	94 GHZ	METERS	X	Y	Z	SIGX	SIGY	SIGZ	WBAR
			.298	3								61.0	11.2	-.9	2.4	.0	8.7	2.2	1.65E+00
			.193	2								67.6	9.6	-.4	3.1	.0	9.8	3.2	1.62E+00
			.159	1								74.1	9.6	.0	3.7	.0	11.2	4.2	1.79E+00
265.0	1	1	.650	3	.123	.215	.254	.765	.821	.834	.999									
SUBCLOUD		8 REMOVED																		
SUBCLOUD		5 REMOVED																		
SUBCLOUD		2 REMOVED																		
			.276	3								61.0	11.2	-.9	2.4	.0	8.7	2.2	1.53E+00
			.185	2								67.5	9.6	-.4	3.1	.0	9.8	3.2	1.55E+00
			.155	1								74.1	9.6	.0	3.7	.0	11.2	4.2	1.75E+00
270.0	1	1	.616	3	.137	.233	.273	.775	.829	.842	.999									
			.275	3								61.0	11.2	-.9	2.4	.0	8.7	2.2	1.52E+00
			.178	2								67.5	9.6	-.4	3.1	.0	9.8	3.2	1.49E+00
			.146	1								74.0	9.6	.0	3.6	.0	11.2	4.2	1.64E+00
275.0	1	1	.599	3	.145	.243	.283	.781	.833	.846	.999									
			.258	3								61.0	11.2	-.9	2.4	.0	8.7	2.2	1.43E+00
			.173	2								67.5	9.6	-.4	3.1	.0	9.8	3.2	1.45E+00
			.143	1								74.0	9.6	.0	3.6	.0	11.2	4.2	1.60E+00
280.0	1	1	.574	3	.157	.258	.298	.789	.840	.852	.999									
			.250	3								61.0	11.2	-.9	2.4	.0	8.7	2.2	1.38E+00
			.163	2								67.5	9.6	-.4	3.0	.0	9.8	3.2	1.36E+00
			.134	1								74.0	9.6	.0	3.6	.0	11.2	4.2	1.51E+00
285.0	1	1	.547	3	.171	.274	.315	.798	.847	.858	.999									
			.243	3								61.0	11.2	-.9	2.4	.0	8.7	2.2	1.34E+00
			.160	2								67.4	9.6	-.4	3.0	.0	9.8	3.2	1.33E+00
			.131	1								73.9	9.6	.0	3.6	.0	11.2	4.2	1.47E+00
290.0	1	1	.533	3	.179	.283	.325	.802	.850	.862	.999									
			.227	3								61.0	11.2	-.9	2.4	.0	8.7	2.2	1.25E+00
			.150	2								67.4	9.6	-.4	3.0	.0	9.8	3.2	1.25E+00
			.128	1								73.9	9.6	.0	3.6	.0	11.2	4.2	1.43E+00
295.0	1	1	.505	3	.196	.303	.345	.812	.858	.868	.999									
			.224	3								60.9	11.2	-.9	2.4	.0	8.7	2.2	1.24E+00
			.147	2								67.4	9.6	-.4	3.0	.0	9.8	3.2	1.22E+00
			.120	1								73.9	9.6	.0	3.6	.0	11.2	4.2	1.35E+00

```
   300.0   1   1     .492     3     .204  .313  .354  .816  .861  .872 1.000
1


               TOTAL TRANMITANCE FOR ALL SOURCES IS:   .3542E+00









                                END EOSAEL RUN
STOP 000
```

Bibliography

Abramowitz, M., and I. Stegun, 1964: *Handbook of Mathematical Functions*, p 913. Dover Publishing, New York.

Alexander, MAJ A., D. Brown, and D. Mott, 1984: *Feasibility Study for Remote Debris Sensor*. FJSRL-TR-84-0001, U.S. Air Force Frank J. Seiler Research Laboratory, USAF Academy.

AMC, 1967: *Engineering Design Handbook, Military Pyrotechnics, Part I*, pages 5–26. AMCP-706-185, U.S. Army Materiel Command, Washington, DC (AD 817071).

Ayres, S. D., and Larry Baca, 1987: "Changes in the Burn Rate Coefficients of COMBIC." In *Proc. Eighth Annual EOSAEL/TWI Conference*, vol. 1, pp 53–62, U.S. Army Atmospheric Sciences Laboratory.

Ayres, S. D., and P. H. Randolph, 1990: "Orthographic versus Perspective LOS for Battlefield Obscurants." In *Proc. Eleventh Annual EOSAEL/TWI Conference*, p 341. U.S. Army Atmospheric Sciences Laboratory, PSL-90/99.

Ayres, S. D., Maluka Munoz, and Edward Spitznagel, 1988: "A Statistical Evaluation of the COMBIC Model." In *Proc. Ninth Annual EOSAEL/TWI Conference*, pp 543–562. U.S. Army Atmospheric Sciences Laboratory.

Ayres, S. D., 1985: "COMBIC Validation." In *Proc. Sixth Annual EOSAEL/TWI Conference*, pp 269–288. U.S. Army Atmospheric Sciences Laboratory.

Ayres, S. D., 1986: "COMBIC Validation—Part II." In *Proceedings of the Smoke Symposium X, DRCPM-SMK-T-001-78*. OPM Smoke/Obscurants (ATTN: AMCPM-SMK-T).

Ayres, S. D., M. Munoz, D. W. Hoock, and E. Spitznagel, 1991: "Statistical Evaluation of the COMBIC Model." Draft, U.S. Army Atmospheric Sciences Laboratory.

Baer, L., and G. O. Rubel, August 1984: "Smoke Yield Factor for HC, WP and PEG200." Letter report to R. Sutherland, U.S. Army Atmospheric Sciences Laboratory.

Baer, L., August 1984: "Efficiency of the M1 and M2 HC Canister." Letter reports to R. Sutherland, U.S. Army Atmospheric Sciences Laboratory.

Baer, L. E., July 1984: "Data Sheet for Smoke Pots and Generator." Letter reports to R. Sutherland, U.S. Army Atmospheric Sciences Laboratory.

Batchelor, G. K., 1954: "Heat Conduction and Buoyancy Effects in Fluids." *J. R. Meteorol. Soc.* **80**:339–358.

Battelle Columbus Laboratory, 1979: *Large Area Screening Systems (LASS) Program, Battel Columbus*. ARCSL-TR-79034, U.S. Army Chemical Research and Development Center (ADB037399).

Berk, A., L. S. Bernstein, and D. C. Robertson, *MODTRAN: A Moderate Resolution Model for LOWTRAN 7*. GL-TR-89-0122, Air Force Geophysics Laboratory.

Bowman, E., J. Steedman, D. Keefer, W. Farmer, and L. Pinson, 1979: *Smoke Week II, Electro-Optical (EO) Systems Performance in Characterized Obscured Environments, Eglin Air Force Base*. OPM Smoke / Obscurants.

Briggs, A., 1969: *Plume Rise, AEC Critical Review Series*. TID-25075, National Technical Information Service, U.S. Department of Commerce.

Bromley, D., 1982: "Smoke Yield Factor for HC, WP and PEG200." Private communication to D. Hoock, U.S. Army Atmospheric Sciences Laboratory.

Brown, R. A., 1981: "Modeling the Geostrophic Drag Coefficient for AIDJEX." *J. Geophys. Res.* **86**:1989–1994.

Bruce, C., 1984: private communication to R. Gomez and R. Sutherland, U.S. Army Atmospheric Sciences Laboratory.

Cichowicz, J. 1983: *Programmatic Life Cycle Environmental Assessment for Smoke Obscurants*. ARCSL-TR-83007, U.S. Army Chemical Research and Development Center.

Danard, M., 1984: *Proposed Bulk Mesoscale Models for the Atmospheric Boundary Layer*. Contract Report DAA07-83-C0126, U.S. Army Atmospheric Sciences Laboratory.

DARCOM Pamphlet, 1981: *Complete Round Charts, Change I*. DARCOM Pamphet P-700-3-3, Department of the Army, Washington, DC.

Dolce, T., and D. Metz, 1977: *An Analysis of the Smoke Cloud Data from the August 1975 Jefferson Proving Ground Smoke Test*. Technical Report 201, U.S. Army Materiel Systems Analysis Activity.

Duncan, L. D., 1981: *Electro-Optical Systems Atmospheric Effects Library EOSAEL 80, Volume I—Technical Documentation*. ASL-TR-0072, U.S. Army Atmospheric Sciences Laboratory.

Duncan, L. D., 1982: *EOSAEL 82, Transmission Through Battlefield Aerosols*. ASL-TR-0122, U.S. Army Atmospheric Sciences Laboratory.

Dyck, R. I., and J. Stukel, 1976: "Fugitive Dust Emission from Trucks on Unpaved Roads." *Environ. Sci. Technol.* **10**:1046–1048.

Ebersole, J., 1982: *Source Characteristics of Inventory and Developmental Smokes: Survey and Recommendations*. OMI-82-011, Optimetrics Inc., report for U.S. Army Atmospheric Sciences Laboratory.

Frickel, R. H., G. Rubel, and E. Steubing, 1979: "Relative Humidity Dependence of the Infrared Extinction by Aerosol Clouds of Phosphoric Acid." In *Proceedings of the Smoke Symposium III, DRCPM-SMK-T-001*. OPM Smoke / Obscurants.

Gould, K. E., 1981: *High Explosive Field Tests*. DNA 6187F, Defense Nuclear Agency, Washington, DC.

Hanel, G., 1976: "The Properties of Atmospheric Particulates as Functions of the Relative Humidity at Thermodynamic Equilibrium with the Surrounding Moist Air." In *Advances in Geophysics*, Academic Press, New York.

Hanna, S. R., G. A. Briggs, and R. P. Hosker, 1982: *Handbook on Atmospheric Diffusion, US Dept of Energy*. National Technical Information Center, U.S. Department of Commerce, DOE / TIC-11223 edition.

Hansen, F. V., and R. Pena, 1990: *Investigation of Variance of Wing Direction Fluctuations*. Internal report, U.S. Army Atmospheric Sciences Laboratory.

Hansen, F. V., and R. Pena, 1990: *Siroccos, Sigmas, and Stability*. Internal report, U.S. Army Atmospheric Sciences Laboratory.

Hansen, F. V., 1979: *Engineering Estimates for the Calculation of Atmospheric Dispersion Coefficients*. Internal report, U.S. Army Atmospheric Sciences Laboratory.

Hansen, F. V., 1990: *Weighted Lagrangian Dispersion Lengths for the Gaussian Diffusion*. Internal report, U.S. Army Atmospheric Sciences Laboratory.

Hoock, Donald W., 1986: "Comparisons of Data with COMBIC Model Assumptions." In *Proc. Sixth Annual EOSAEL/TWI Conference*. U.S. Army Atmospheric Sciences Laboratory.

Hoock, Donald W., and R. Sutherland, 1982: "Extending Methodologies for Realistic Dust and Smoke Modeling." In *Proceedings of the Smoke Symposium VI, DRCPM-SMK-T-001-82*. OPM Smoke / Obscurants (ATTN: AMCPM-SMK-T).

Hoock, Donald W., R. Sutherland, and D. Clayton, 1984: *Combined Obscuration Model for Battlefield Induced Contaminants*. TR-0160-11, U.S. Army Atmospheric Sciences Laboratory.

Hoult, D. P., J. A. Fay, and J. J. Forney, 1969: "A Theory of Plume Rise Compared with Field Observations." *J. Air Pollut. Con. Assoc.* **19**:585–590.

Huang, K. H., and W. Frost, November 1985: "Development of an Improved Monte Carlo Dispersion (MoCaPD) Model and Initial Application in Sensitivity Studies of Optical Systems in a Smoke Obscured Field." In *Proc. Fifth Annual EOSAEL/TWI Conference*, pp 108–118. U.S. Army Atmospheric Sciences Laboratory.

Irwin, S., 1979: "Estimating Plume Dispersion—A Recommended Generalized Scheme." In *4th Symposium on Turbulence, Diffusion and Air Pollution*, Boston, MA, Am. Meteorol. Soc.

Kennedy, B. W., 1980: *Dusty Infrared Test-II (DIRT-II) Program*. ASL-TR-0058, U.S. Army Atmospheric Sciences Laboratory.

Khanna, R. D., D. Hoock, and R. Sutherland, November 1984: "Extinction Properties of Battlefield Smoke Clouds: Some Theoretical and Experimental Results." In *Proc. Fifth Annual EOSAEL/TWI Conference*. U.S. Army Atmospheric Sciences Laboratory.

Lawrence, F. A., Tamra L. Kite, Daniel R. Fuller, and Terri L. Wood, 1984: *Validation of Electro-Optical Systems Atmospheric Effects Models: COMBIC*. DAAD07-82-C-0009, Physical Sciences Laboratory.

Long, K., J. Mason, and B. Durst, 1984: *Results of Fort Carson, Colorado Terrain Dust Obscuration Tests using Explosives*. EL-84-6, U.S. Army Engineer Waterways Experiment Station.

Maddix, M., B. L. Williams, and S. Brazelton, 1982: *A Survey of Extinction Coefficients Available for Various Transient Aerosols and Selection of Extinction Coefficients for BELDWSS Modeling of Transient Aerosols*. RG-82-1, U.S. Army Missile Command.

Matise, B., 1984: *Effects of a Cold Environment and Snow on Obscuration*. Optimetrics Inc.

Milham, M., and D. Anderson, 1983: *Obscuration Sciences Smoke Data Compendium: Standard Smokes*. ARCSL-TR-82024, U.S. Army Chemical Research and Development Center.

Milham, M. E., D. Anderson, and G. O. Rubel, 1982: *Time Dependent Extinction of Phosphorus-Derived Smoke*. ARCSL-TR-82083, U.S. Army Chemical Research and Development Center (ATTN: SMCCR-SPS-IR).

Morton, B. R., G. Taylor, and J. S. Turner, 1956: "Turbulent Gravitational Convection from Maintained and Point Sources." In *Proc. R. Soc. London Ser. A* **134**:1–23.

Muhly, R. L., 1983: *Programmatic Life Cycle Environmental Assessment for Smoke/Obscurants, Volume 1, Fog Oil, Diesel Fuels and Polyethylene Glycol (PEG 200)*. ARCSL-EA-83001, U.S. Army Chemical Research and Development Center.

Nelson, G., and W. Farmer, 1981: *Smoke Week III, Electro-Optical (EO) Systems Performance in Characterized Obscured Environments, Eglin Air Force Base*. OPM Smoke / Obscurants (Attn: AMCPM-SMK-T).

Pasquill, F., 1961: "The Estimation of the Dispersion of Windborne Material." *Meteorol. Mag.*, **1063**:38–49.

Pasquill, F., 1974: *Atmospheric Diffusion*. John Wiley and Sons, NY.

Pennsyle, R., 1982: *Modeling Bulk-Filled WP Smoke Munitions*. ARCSL-TR-81099, U.S. Army Chemical Research and Development Center.

Pennsyle, R., September 1982: "Smoke Munition Characterization Data." Letter reports to R. Sutherland, U.S. Army Atmospheric Sciences Laboratory.

Pinnick, R. G., and S. G. Jennings, 1980: *Relationships Between Radiative Properties and Mass Content of Phosphoric Acid, HC, Petroleum Oil and Sulfuric Acid Military Smokes*. ASL-TR-0052, U.S. Army Atmospheric Sciences Laboratory.

Pinnick, R. G., G. Fernandez, and B. Hinds, 1982: "Explosion Debris Particle Size Measurements in DIRT-III." In *Proceedings of the Smoke SymposiumVI, DRCPM-SMK-T-001-82*. OPM Smoke / Obscurants.

Pinnick, R. G., G. Fernandez, and B. Hinds, 1983: "Explosion Debris Particle Size Measurements." *Appl. Opt.* **22**:95–102.

Pinnick, R. G., 1982: *Vehicular Dust and Fire Products Particle Size and Concentration Measurements in BIC-1 and BIC-2*. Internal report, U.S. Army Atmospheric Sciences Laboratory.

Richards, J. M., 1963: "Experiments on Motion of Isolated Cylindrical Thermals through Unstratified Surroundings." *Int. J. Air Water Pollut.* **17**:17–34.

Rubel, G. O., 1978: *Predicting the Droplet Size and Yield Factors of a Phosphorus Smoke as a Function of Droplet Composition and Ambient Relative Humidity Under Tactical Conditions*. ARCSL-TR-78057, U.S. Army Chemical Research and Development Center.

Rubel, G., 1981: *A Semiquantitative Model for the Prediction of the Persistency of Multicomponent Oil Smokes*. ARCSL-TR-81019, U.S. Army Chemical Research and Development Center.

Rubel, G. O., 1981: *An Improved Thermodynamic Model for Phosphorus Smokes*. ARCSL-TR-80060, U.S. Army Chemical Research and Development Center.

Rubel, G. O., 1983: *Physical Constants of Standard Military Smokes*. ARCSL-TR-83025, U.S. Army Chemical Research and Development Center.

Sauter, D., and F. V. Hansen, 1990: *Relative Diffusion in the Surface Boundary Layer*. Internal report, U.S. Army Atmospheric Sciences Laboratory.

Seebaugh, R., and H. Linnerud, 1978: *Debris Environment Predictions for High Explosive Bursts*. SAI-79-861-WA, Science Applications Inc.

Shirkey, R. C., 1980: *Single Scattering Code AGAUSX: Theory, Applications Comparisons and Listing*. ASL-TR-0062, U.S. Army Atmospheric Sciences Laboratory.

Smith, F. B., 1979: "The Relation Betweeen Pasquill Stability P and Kazanski-Monin Stability K (in Neutral and Unstable Conditions)." *Atmos. Environ*. **13**:879–881.

Smoke and Aerosol Working Group, 1979: *Joint Munitions Effectiveness Manual: Summary of Smoke Obscuration Data*. JTCG / ME-79-2, JTCG / ME-SAWG.

Spitznagel, Edward, and S. D. Ayres, 1988: "A Methodology for the Evaluation of COMBIC." In *Proc. Ninth Annual EOSAEL/TWI Conference*, pp 533–542. U.S. Army Atmospheric Sciences Laboratory.

Sutherland, R. A., and W. D. Bach, November 1984: "Significance of Sensible Heat Flux, Surface Roughness and Windspeed in Determining Atmospheric Stability." In *Proc. EOSAEL 84 Workshop*, pp 53–62. U.S. Army Atmospheric Sciences Laboratory.

Sutherland, R. A., 1981: *Determination and Use of the Hanel Growth Factor for Modeling Hygroscopic Aerosols*. Internal report (ATTN: SLCAS-AR-M), U.S. Army Atmospheric Sciences Laboratory.

Sutherland, R. A., and D. W. Hoock, January 1982: "An Improved Smoke Obscuration Model Act II: Part I Theory." ASL-TR-0103, U.S. Army Atmospheric Sciences Laboratory.

Sutherland, R., 1983: "Tables of U.S. Army and Threat Smoke Munitions Characteristics." (Unpublished.)

Tarnove, T. L., and M.G. Gordon, 1983: *Mechanical Smoke Generating Systems; Smoke Liquids; and an Analysis of the Dependence of the Screening Length on the Physical Properties of the Smoke Liquid*. ARCSL-TR-82010, U.S. Army Chemical Research and Development Center.

Tarnove, T. L., 1981: *Studies of the Chemistry of the Formation of Phosphorus Derived Smokes and Their Implications for Phosphorus Smoke Munitions*. ARCSL-TR-80049, U.S. Army Chemical Research and Development Center.

Taylor, G. I., 1945: *Dynamics of a Mass of Hot Gas Rising in the Air*. USAEC Report MDDC-919 (LADC-276), Los Alamos Scientific Laboratory.

Thompson, J., and J. DeVore, 1982: *ASL-Dust, Version II: A Tactical Battlefield Dust Cloud and Propagation Code*. Kaman Tempo Report KT-82-007, U.S. Army Atmospheric Sciences Laboratory.

Thompson, J., 1979: *Models for Munition Dust Clouds*. ASL-CR-79-00005-2, U.S. Army Atmospheric Sciences Laboratory.

Thompson, J., 1980: *ASL-Dust: A Tactical Battlefield Dust Cloud and Propagation Code, 2 volumes*. ASL-CR-80-0143-1,2, U.S. Army Atmospheric Sciences Laboratory.

Thompson, J. H., 1980a: *Fire Plumes Modeling Progress Report*. GE-TEMPO Report, Contract DAAD07-80-C-0072, U.S. Army Atmospheric Sciences Laboratory.

Turner, J. S., 1962: "The Starting Plume in Neutral Surroundings." *J. Fluid Mech.* **13**:356–368.

Turner, S., 1969: "Buoyant Plumes and Thermals." *Ann. Rev. Fluid Mech.* **1**:29–44.

U.S. Army Dugway Proving Ground, 1977: *Basic Smoke Characterization Test*. DPG-TP-77-311, TECOM Project 7-CO-RD7-DPI-001.

U.S. Army Dugway Proving Ground, 1978: *Final Test Report on Smoke Week II at Eglin AFB, FL*. DPG-FR-78-317 (ADB031193).

U.S. Army Dugway Proving Ground, 1978: *Inventory Smoke Munition Test (PHASE IIA)*. DPG-FR-77-314, OPM for Smoke / Obscurants.

U.S. Army Field Manual, 1967: *Chemical Reference Handbook*. FM-3-6, Department of the Army, Washington, DC.

U.S. Army Technical Manual, 1967: *Chemical Weapons and Munitions*. TM-43-0001026-2, Department of the Army, Washington, DC.

Weil, J. C., 1982: "Source Buoyancy Effects in Boundary Layer Diffusion." In *Proceedings of the Workshop on the Parmeterization of Mixed Layer Diffusion*, R. Cionco, editor. U.S. Army Atmospheric Sciences Laboratory.

Wentsel, R. S., R. Pennsyle, and T. M. Mann, 1984: "Field Measurement of EA5763 Deposition from the XM76 and XM52". In *Proceedings of the Smoke Symposium VIII, DRCPM-SMK-T-001-82*. OPM Smoke / Obscurants.

Woolf, H. M., 1968: *On the Computation of Solar Elevation Angle and the Determination of Sunrise and Sunset Tables*. ESSA Weather Bureau, National Meteorological Center, Hillcrest Heights, MD.

Yon, L., R. S. Wentsel, and J. M. Bane, 1983: *Programmatic Life Cycle Environmental Assessment for Smoke/Obscurants, Volume 2, Red, White and Plasticized White Phosphorus*. ARCSL-EA-83004, U.S. Army Chemical Research and Development Center.

Distribution

Admnstr
Defns Techl Info Ctr
Attn DTIC-OCP
8725 John J Kingman Rd Ste 0944
FT Belvoir VA 22060-6218

Defns Mapping Agency
Attn R Klotz
4211 Briars Rd
Olney MD 20832-1814

Defns Mapping Agency
Attn L-41 B Hagan
Attn L-41 D Morgan
Attn L-41 F Mueller
3200 S 2nd Stret
ST Louis MO 63118

Defns Mapping Agency
Attn L-A1 B Tallman
3200 2nd Stret
ST Louis MO 63116

Mil Asst for Env Sci
Ofc of the Undersec of Defns for Rsrch & Engrg R&AT E LS
Pentagon Rm 3D129
Washington DC 20301-3080

Ofc of the Secy of Defns
Attn OUSD(A&T)/ODDR&E(R) R J Trew
3080 Defense Pentagon
Washington DC 20301-7100

AMC OMP/746 TS
Attn A Chasko
PO Box 310
High Rolls NM 88325

AMCOM MRDEC
Attn AMSMI-RD W C McCorkle
Redstone Arsenal AL 35898-5240

ARL Chemical Biology Nuc Effects Div
Attn AMSRL-SL-CO
Aberdeen Proving Ground MD 21005-5423

Army Corps of Engrs Engr Topographics Lab
Attn CETEC-TR-G P F Krause
7701 Telegraph Rd
Alexandria VA 22315-3864

Army Field Artillery School
Attn ATSF-TSM-TA
FT Sill OK 73503-5000

Army Infantry
Attn ATSH-CD-CS-OR E Dutoit
FT Benning GA 30905-5090

Army Materiel Sys Analysis Activity
Attn AMXSY-CS Bradley
Aberdeen Proving Ground MD 21005-5071

CBIAC
Attn J Rosser
PO Box 196 Gunpowder Br
Aberdeen Proving Ground MD 21010-0196

Dir for MANPRINT
Ofc of the Deputy Chief of Staff for Prsnnl
Attn J Hiller
The Pentagon Rm 2C733
Washington DC 20301-0300

Kwajalein Missile Range
Attn Meteorologist in Charge
PO Box 57
APO San Francisco CA 96555

Natl Ground Intllgnc Ctr Army Foreign Sci Tech Ctr
Attn CM
220 7th Stret NE
Charlottesville VA 22901-5396

Natl Security Agency
Attn W21 Longbothum
9800 Savage Rd
FT George G Meade MD 20755-6000

Pac Mis Test Ctr Geophysics Div
Attn Code 3250 Battalino
Point Mugu CA 93042-5000

Redstone Scientific Info Ctr
Attn AMSMI-RD-CS-R
Bldg 4484
Redstone Arsenal AL 35898

Science & Technology
101 Research Dr
Hampton VA 23666-1340

Distribution (cont'd)

SMC/CZA
2435 Vela Way Ste 1613
El Segundo CA 90245-5500

US Army Aviation and Missile Command
Attn AMSMI-RD-WS-PL G Lill Jr
Bldg 7804
Redstone Arsenal AL 35898-5000

US Army Combined Arms Combat
Attn ATZL-CAW
FT Leavenworth KS 66027-5300

US Army CRREL
Attn CRREL-GP F Scott
Attn CRREL-GP J Koenig
Attn CRREL-GP R Detsch
Attn CRREL-RG Boyne
72 Lyme Rd
Hanover NH 03755-1290

US Army Dugway Proving Ground
Attn STEDP 3
Attn STEDP-MT-DA-L-3
Attn STEDP-MT-M Bowers
Dugway UT 84022-5000

US Army Info Sys Engrg Cmnd
Attn AMSEL-IE-TD F Jenia
FT Huachuca AZ 85613-5300

US Army Natick RDEC Acting Techl Dir
Attn SBCN-T P Brandler
Natick MA 01760-5002

US Army OEC
Attn CSTE EFS
4501 Ford Ave Park Center IV
Alexandria VA 22302-1458

US Army Simulation, Train, & Instrmntn Cmnd
Attn J Stahl
12350 Research Parkway
Orlando FL 32826-3726

US Army Soldier & Biol Chem Cmnd Dir of Rsrch & Techlgy Dirctrt
Attn SMCCR-RS I G Resnick
Aberdeen Proving Ground MD 21010-5423

US Army Spc Technology Rsrch Ofc
Attn Brathwaite
5321 Riggs Rd
Gaithersburg MD 20882

US Army Tank-Automtv Cmnd Rsrch, Dev, & Engrg Ctr
Attn AMSTA-TR J Chapin
Warren MI 48397-5000

US Army Topo Engrg Ctr
Attn CETEC-ZC
FT Belvoir VA 22060-5546

US Army TRADOC Anlys Cmnd—WSMR
Attn ATRC-WSS-R
White Sands Missile Range NM 88002

US Army Train & Doctrine Cmnd
Battle Lab Integration & Techl Dirctrt
Attn ATCD-B J A Klevecz
FT Monroe VA 23651-5850

US Army White Sands Missile Range
Attn STEWS-IM-ITZ Techl Lib Br
White Sands Missile Range NM 88002-5501

US Military AcademyMathematical Sci Ctr of Excellence
Attn MDN-A LTC M D Phillips
Dept of Mathematical Sci Thayer Hall
West Point NY 10996-1786

USATRADOC
Attn ATCD-FA
FT Monroe VA 23651-5170

Nav Air War Cen Wpn Div
Attn CMD 420000D C0245 A Shlanta
1 Admin Cir
China Lake CA 93555-6001

Nav Rsrch Lab
Attn Code 4110 Ruhnke
Washington DC 20375-5000

Nav Rsrch Lab
Attn Code 8150/SFA J Buisson
4555 Overlook Dr SW
Washington DC 20375-5354

Distribution (cont'd)

Nav Surface Warfare Ctr
Attn Code B07 J Pennella
Attn Code K12 E Swift
17320 Dahlgren Rd Bldg 1470 Rm 1101
Dahlgren VA 22448-5100

Naval Surface Weapons Ctr
Attn Code G63
Dahlgren VA 22448-5000

Ofc of Nav Rsrch
Attn ONR 331 H Pilloff
800 N Quincy Stret
Arlington VA 22217

AFCCC/DOC
Attn Glauber
151 Patton Ave Rm 120
Asheville NC 28801-5002

AFSPC/DRFN
Attn CAPT R Koon
150 Vandenberg Stret Ste 1105
Peterson AFB CO 80914-45900

Air Force
Attn Weather Techl Lib
151 Patton Ave Rm 120
Asheville NC 28801-5002

Air Force Research Laboratory
Attn Battlespace Environment Division
29 Randolph Rd
Hanscom AFB MA 01731

Air Force Research Laboratory
Attn USBL P Tattelman
29 Randolph Rd
Hanscom AFB MA 01731

Air Force Research Laboratory
Attn IFOIL
26 Electronic Parkway
Rome NY 13441-4514

ASC OL/YUH
Attn JDAM-PIP LT V Jolley
102 W D Ave
Eglin AFB FL 32542

DOT AFSPC/DRFN
Attn H Skalski
150 Vandenberg Stret
Peterson AFB CO 80914

Holloman AFB
Attn K Wernie
1644 Vandergrift Rd
Holloman AFB NM 88330-7850

Phillips Lab Atmospheric Sci Div
Geophysics Dirctrt
Attn PL-LYP Chisholm
Attn PL/LYP 3
Attn PL/LYP
Kirtland AFB NM 87118-6008

TAC/DOWP
Langley AFB VA 23665-5524

USAF Rome Lab Tech
Attn Corridor W Ste 262 RL SUL
26 Electr Pkwy Bldg 106
Griffiss AFB NY 13441-4514

Los Alamos Natl Lab
Attn M Mosier
PO Box 1663 Mail Stop P364
Los Alamos NM 87545

DARPA
Attn S Welby
3701 N Fairfax Dr
Arlington VA 22203-1714

NASA Marshal Spc Flt Ctr Atmos Sci Div
Attn Code ED 41 1
Attn Code ED-41
Huntsville AL 35812

NIST
Attn MS 847.5 M Weiss
Attn R/E/SE J Kunches
325 Broadway
Boulder CO 80303

Distribution (cont'd)

Applied Rsrch Lab Univ of Texas
Attn B Renfro
Attn J Saunders
Attn R Mach
PO Box 8029
Austin TX 78713-8029

Stanford Univ
Attn HEPL/GP-B D Lawrence
Attn HEPL/GP-B T Walter
Stanford CA 94305-4085

Aerospace
Attn J Langer
Attn M Dickerson
PO Box 92957 M4/954
Los Angeles CA 90009

ARINC
Attn P Mendoza
4055 Hancock Stret
San Diego CA 92110

Ashtech Inc
Attn S Gourevitch
1177 Kifer Rd
Sunnyvale CA 94086

BD Systems
Attn J Butts
385 Van Ness Ave #200
Torrance CA 90501

Dept of Commerce Ctr Mountain Administration
Attn Spprt Ctr Library R51
325 S Broadway
Boulder CO 80303

Hewlett-Packard Co
Attn J Kusters
5301 Stevens Creed Blvd
Santa Clara CA 95052

Hicks & Associates Inc
Attn G Singley III
1710 Goodrich Dr Ste 1300
McLean VA 22102

Hughes
Attn S Peck
Attn R Malla
800 Apollo Ave PO Box 902
El Segundo CA 90245

Intermetrics Inc
Attn J McGowan
615 Hope Rd Bldg 4 2nd floor
Eatontown NJ 07724

ITT Aerospace
Attn MS 2511 R Peller
Attn MS 8528 H Rawicz
Attn MS 8538 L Doyle
100 Kingsland Rd
Clifton NJ 07014

KERNCO
Attn R Kern
28 Harbor Stret
Danvers MA 01923

Lockheed Martin
Attn B Marquis
1250 Academy Park Loop #101
Colorado Springs CO 80912

LORAL
Attn B Mathon
700 N Frederick Pike
Gaithersburg MD 20879

LORAL Federal Systems
Attn J Kane
Attn M Baker
9970 Federal Dr
Colorado Springs CO 80921

Natl Ctr for Atmospheric Research
Attn NCAR Library Serials
PO Box 3000
Boulder CO 80307-3000

Natl Ground Intelligence Ctr
Attn IANG-TSC J Breeden
220 Seventh Street NE
Charlottesville VA 22902

Distribution (cont'd)

NCSU
Attn J Davis
PO Box 8208
Raleigh NC 27650-8208

Ontar Corporation
9 Village Way
North Andover MA 01845-2000

Overlook Systems
Attn D Brown
Attn T Ocvirk
1150 Academy Park Loop Ste 114
Colorado Springs CO 80910

Pacific Missile Test Ctr Geophysics Div
Attn Code 3250
Point Mugu CA 93042-5000

PAQ Commctn
Attn Q Hua
607 Shetland Ct
Milpitas CA 95035

Rockwell CACD
Attn L Burns
400 Collins Rd NE
Cedar Rapids IA 52398

Rockwell Collins
Attn C Masko
Cedar Rapids IA 52498

Rockwell DA85
Attn W Emmer
12214 Lakewood Blvd
Downey CA 92104

Rockwell Space Ops Co
Attn AFMC SSSG DET2 / NOSO / Rockwell R Smetek
Attn B Carlson
442 Discoverer Ave Ste 38
Falcon AFB CO 80912-4438

Rockwell Space Systems Div
Attn Mailcode 841-DA49 D McMurray
12214 Lakewood Blvd
Downey CA 90241

Stanford Telecom
Attn B F Smith
1221 Crossman Ave
Sunnyvale CA 94088

Trimble Nav
Attn P Turney
585 N Mary
Sunnyvale CA 94086

US Army Rsrch Lab
Attn AMSRL-CI-EA J Cogan
Attn AMSRL-CI-EW D Hoock
Attn AMSRL-SL-EM R Sutherland
Attn AMSRL-SL-EM S Ayres
Battlefield Envir Dir
White Sands Missile Range NM 88002-5001

US Army Rsrch LabBattlefield Envir Dirctrt
Attn AMSRL-BE B Sauter
Attn AMSRL-BE D Knapp
White Sands Missile Range NM 88002-5501

Director
US Army Rsrch Ofc
Attn AMSRL-RO-D JCI Chang
Attn AMSRL-RO-EN W D Bach
PO Box 12211
Research Triangle Park NC 27709

US Army Rsrch Lab
Attn AMSRL-DD J M Miller
Attn AMSRL-CI-AI-R Mail & Records Mgmt
Attn AMSRL-CI-AP Techl Pub (3 copies)
Attn AMSRL-CI-LL Techl Lib (3 copies)
Attn AMSRL-IS-EM D Garvey
Attn AMSRL-IS-EP A Wetmore (20 copies)
Attn AMSRL-IS-EP P Gillespie
Attn AMSRL-SE-EE Z G Sztankay
Adelphi MD 20783-1197

REPORT DOCUMENTATION PAGE

Form Approved
OMB No. 0704-0188

1. AGENCY USE ONLY *(Leave blank)*	2. REPORT DATE	3. REPORT TYPE AND DATES COVERED
	August 2000	Final, 1990 to 1995

4. TITLE AND SUBTITLE COMBIC, Combined Obscuration Model for Battlefield Induced Contaminants:
Volume 1—Technical Documentation and Users Guide

5. FUNDING NUMBERS
DA PR: N / A
PE: N / A

6. AUTHOR(S) Alan Wetmore and Scarlett D. Ayres

7. PERFORMING ORGANIZATION NAME(S) AND ADDRESS(ES)
U.S. Army Research Laboratory
Attn: AMSRL-CI-EE email: awetmore@arl.mil
2800 Powder Mill Road
Adelphi, MD 20783-1197

8. PERFORMING ORGANIZATION REPORT NUMBER
ARL-TR-1831-1

9. SPONSORING/MONITORING AGENCY NAME(S) AND ADDRESS(ES)
U.S. Army Research Laboratory
2800 Powder Mill Road
Adelphi, MD 20783-1197

10. SPONSORING/MONITORING AGENCY REPORT NUMBER

11. SUPPLEMENTARY NOTES
ARL PR: N / A
AMS code: N / A

12a. DISTRIBUTION/AVAILABILITY STATEMENT Approved for public release; distribution unlimited.

12b. DISTRIBUTION CODE

13. ABSTRACT *(Maximum 200 words)*

Airborne dust, smoke, and debris can significantly degrade a battlefield environment and affect electro-optical systems. The most direct effect of these combat-induced aerosols on a propagating electromagnetic signal is to remove energy (reduce transmission) through absorption and scattering. Reduced transmission through inventory smokes and dust is generally most significant at visual and infrared wavelengths and less severe at millimeter wavelengths.

Obscurant concentrations can change rapidly in a combat environment. Once generated, an aerosol cloud moves with the wind, undergoes thermally buoyant rise, and expands in the atmospheric turbulence. Thus, prevailing winds, aerosol generation factors, and the geometry of targets, observers, and aerosol clouds are important in determining transmission.

The Combined Obscuration Model for Battlefield Induced Contaminants (COMBIC) predicts time and spatial variations in transmission through dust and debris raised by high-energy explosives and by vehicular movement; smoke from phosphorus and hexachloroethane munitions; smoke from diesel oil fires; generator-disseminated fog oil and diesel fuel; and other screening aerosols from sources defined by inputs. COMBIC has been designed primarily for large scenarios where many different obscuration sources are present and where many observer-target lines of sight (LOS) must be treated simultaneously.

This document has been developed to provide both a technical description of the physics used in the COMBIC model and to serve as an operations guide for users of the COMBIC software.

14. SUBJECT TERMS	15. NUMBER OF PAGES
Smoke, model, dispersion, obscuration	148
	16. PRICE CODE

17. SECURITY CLASSIFICATION OF REPORT	18. SECURITY CLASSIFICATION OF THIS PAGE	19. SECURITY CLASSIFICATION OF ABSTRACT	20. LIMITATION OF ABSTRACT
Unclassified	Unclassified	Unclassified	UL

NSN 7540-01-280-5500

Standard Form 298 (Rev. 2-89)
Prescribed by ANSI Std. Z39-18
298-102